PB82-198508

Outdoor Smog Chamber Experiments to Test Photochemical Models

North Carolina Univ. at Chapel Hill

Prepared for

Environmental Sciences Research Lab.
Research Triangle Park, NC

Apr 82

U.S. Department of Commerce
National Technical Information Service
NTIS

PB82-198508

EPA-600/3-82-016A
April 1982

OUTDOOR SMOG CHAMBER EXPERIMENTS TO TEST PHOTOCHEMICAL MODELS

by

H. E. Jeffries
R. M. Kamens
K. G. Sexton
A. A. Gerhardt

Department of Environmental Sciences and Engineering
School of Public Health
University of North Carolina
Chapel Hill, N.C. 27514
919-966-5451

Cooperative Agreement No. 805843

Project Officer

Marcia C. Dodge
Atmospheric Chemistry and Physics Division
Enivronmental Sciences Research Laboratory
Research Triangle Park, North Carolina 27711

ENVIRONMENTAL SCIENCES RESEARCH LABORATORY
OFFICE OF RESEARCH AND DEVELOPMENT
U.S. ENVIRONMENTAL PROTECTION AGENCY
RESEARCH TRIANGLE PARK, NORTH CAROLINA 27711

REPRODUCED BY
NATIONAL TECHNICAL
INFORMATION SERVICE
U.S. DEPARTMENT OF COMMERCE
SPRINGFIELD, VA 22161

TECHNICAL REPORT DATA

(Please read Instructions on the reverse before completing)

1. REPORT NO. EPA-600/3-82-016A	2. ORD Report	3. RECIPIENT'S ACCESSION NO. PB82 198508
4. TITLE AND SUBTITLE OUTDOOR SMOG CHAMBER EXPERIMENTS TO TEST PHOTOCHEMICAL MODELS		5. REPORT DATE April 1982 6. PERFORMING ORGANIZATION CODE
7. AUTHOR(S) H. E. Jeffries, R. M. Kamens, K. G. Sexton, and A.A. Gerhardt		8. PERFORMING ORGANIZATION REPORT NO.
9. PERFORMING ORGANIZATION NAME AND ADDRESS University of North Carolina School of Public Health Chapel Hill, North Carolina 27514		10. PROGRAM ELEMENT NO. CDWA1A/01 - 0311 (FY-82) 11. CONTRACT/GRANT NO. Cooperative Agreement 805843
12. SPONSORING AGENCY NAME AND ADDRESS Environmental Sciences Research Laboratory-RTP, NC Office of Research and Development U.S. Environmental Protection Agency Research Triangle Park, North Carolina 27711		13. TYPE OF REPORT AND PERIOD COVERED Final (5/78 - 5/81) 14. SPONSORING AGENCY CODE EPA/600/09

15. SUPPLEMENTARY NOTES

16. ABSTRACT

The smog chamber facility of the University of North Carolina was used in a study to provide experimental data for developing and testing kinetic mechanisms of photochemical smog formation. The smog chamber, located outdoors in rural North Carolina, is an A-frame structure covered with Teflon film. Because the chamber is partitioned into two sections, each with a volume of 156 m^3, two experiments can be conducted simultaneously. The dual chamber is operated under natural conditions of solar radiation, temperature, and relative humidity. In this study, 115 dual all-day experiments were conducted using NO_x and a variety of organic species. The organic compounds investigated included various paraffins, olefins, aromatics and oxygenates, both singly and in mixtures of two or more components. In this report the data collected over the three-year period of the study are described. The experimental procedures and analytical methods used in this study and the limitations and uncertainties of the data are discussed. Guidance for modeling of the data is also given, including a detailed discussion of how to estimate photolytic rate constants from the available UV and total solar radiation data and how to treat such chamber artifacts as dilution, wall sources and losses of pollutants, and reactivity of the background air.

17. KEY WORDS AND DOCUMENT ANALYSIS

a. DESCRIPTORS	b. IDENTIFIERS/OPEN ENDED TERMS	c. COSATI Field/Group

18. DISTRIBUTION STATEMENT RELEASE TO PUBLIC	19. SECURITY CLASS *(This Report)* UNCLASSIFIED	21. NO. OF PAGES 280
	20. SECURITY CLASS *(This page)* UNCLASSIFIED	22. PRICE

EPA Form 2220-1 (Rev. 4-77) PREVIOUS EDITION IS OBSOLETE

DISCLAIMER

This report has been reviewed by the Environmental Sciences Research Laboratory, U.S. Environmental Protection Agency, and approved for publication. Approval does not signify that the contents necessarily reflect the views and policies of the U.S. Environmental Protection Agency, nor does mention of trade names or commercial products constitute endorsement or recommendation for use.

ABSTRACT

From 1977 to 1981 the University of North Carolina Dual Outdoor Smog Chamber was used to conduct experiments of interest to researchers developing mathematical models of photochemical kinetic processes. These data were supplied to three model developing groups as soon as they became available.

The purpose of this report is to make the experimental data available to researchers and model developers. To provide maximum access to the data, they are being supplied in four forms: 1) a computer magnetic tape containing all data from 115 dual all day experiments; 2) a set of microfiche of listings and plots of the entire data set; 3) summary hourly listing and plots of ten key runs included in the report; and 4) a collection of plots illustrating interesting aspects of the data set included in the report. Tables giving key characteristics of the 115 runs are included in report to aid in selection.

Guidance and documentation of chamber experiments are included. Because of its importance, a detailed discussion of the calculation of photolytic rates is given. Other subjects discussed include: dilution rates; wall loss reactions; wall sources; background air reactivity; and temperature and water vapor measurements. Data quality is also discussed and illustrated.

CONTENTS

Abstract iii
Figures vi
Tables xiii
Acknowledgements xvi

1. Background and Purpose 1
2. Introduction to the UNC Chamber Data 2
    Conventions 2
    Examples of Outdoor Runs 3
        August 8, 1977
            side-to-side matched propylene experiment
        July 17, 1980
            side-to-side different concentration isoprene experiment
3. Overview of Total Dataset 13
    Numbers and types of runs
4. Guidance for Modeling UNC Dataset 29
    Treatment of light data 29
    Dilution rates 68
    Ozone wall losses 72
    NO_x wall losses 74
    Walls as source of radicals 78
    Background air reactivity 83
    OH monitors 92
    Temperature data 93
    Water vapor data 94
5. Guidance on Data Quality 96
    Comments about specific methods 96
    Comments about chamber reproducibility 103
6. Condensed Data Set for Ten Key Runs 110
    Plots and hourly data listings
7. Illustrations of Significant Features in the Dataset . . . 179

References 211

Appendices

A. Chamber and Facility Description 213
B. Measurement Techniques Used During This Project 227
C. Magnetic Tape Format 260
D. Microfiche Format 263

Preceding page blank

TYPING GUIDE SHEET

FIGURES

1 Example of a matched propylene experiment in UNC dual outdoor smog chamber: nitrogen compounds and ozone data. Solid lines are for the RED chamber and dashed lines are for the BLUE chamber. Data shown as symbols only measured on RED side. 4

2 Meteorological variables for matched propylene experiment: ambient total solar radiation, chamber air temperature, and chamber dewpoint (water vapor content). 4

3 Carbon compound reactants and products for matched propylene experiment. 6

4 Nitrogen balance for RED side of propylene experiment. Each line represents the sum of all of the species below it. Dashed line accounts for dilution only. 8

5 Carbon balance for RED side of propylene experiment. Each line represents the sum of all of the species below it. Dashed line accounts for dilution only. 8

6 Example of a differential isoprene concentration experiment in UNC dual outdoor smog chamber: nitrogen compounds and ozone data. Solid lines are for the RED chamber and dashed lines are for the BLUE chamber. The maximum ozone concentration in the BLUE side was 1.29 ppm. 10

7 Carbon compound reactants and products for isoprene experiment. Trichloroethylene is used as OH tracer. 11

8 Meteorological variables for isoprene experiment: ambient total solar radiation and chamber air temperature, ambient ultraviolet radiation and chamber dewpoint (both sides). 12

9 Examples of total solar radiation rating scale used in summary tables. 26

10 Calculated photolysis rates at chamber site. 36

11 Calculated photolysis rates at chamber site. 37

12 Calculated photolysis rates at chamber site. 38

13 Calculated photolysis rates at chamber site. 39

14 Ultraviolet and total solar radiation for selected clear days in June of each year 1975 to 1980. 41

15 Estimated average ultraviolet and total solar radiation for selected clear days in June of each year 1975 to 1980. TSR instrument was damaged in 1979. 42

16 Theoretical formaldehyde and nitrogen dioxide photolysis rate. 44

17 Comparison of UV and TSR for selected clear days. 45

18 Specific photolysis rate for nitrogen dioxide and incident total solar radiation and ultraviolet radiation as a function of time for September 19, 1974. 48

19 Comparisons of radiometer and actinometer measurements for September 19, 1974. 49

20 Experimental nitrogen dioxide photolysis (kl) and UV measurements of Stedman, Harvey, and Dickerson (1977). 50

21 Specific photolysis rate for nitrogen dioxide and incident total solar radiation and ultraviolet radiation as a function of time for August 6, 1976. 51

22 Specific photolysis rate for nitrogen dioxide and incident total solar radiation and ultraviolet radiation as a function of time for October 8, 1976. 52

23 Specific photolysis rate for nitrogen dioxide and incident total solar radiation and ultraviolet radiation as a function of time for November 18, 1976. 53

24 Specific photolysis rate for nitrogen dioxide and incident total solar radiation and ultraviolet radiation as a function of time for December 3, 1976. 54

25 Comparison of UV and TSR radiometer measurements for selected days. 55

26 Comparison of UV radiometer and actinometer measurements for selected days. 56

27 Comparison of TSR radiometer and actinometer measurements for selected days. 57

28 Zenith spectral distribution (6 view) outside and inside UNC outdoor smog chamber at 1400-1500 EDT. 62

29 Comparison of theoretical calculated and rate empirically calculated nitrogen dioxide photolysis at UNC chamber. 67

30 Chamber dilution process: measurements of carbon tetrachloride in the chamber (top figure) and chamber air temperature (bottom figure) in a nighttime experiment. 70

31 Illustration of ozone wall loss and dilution in a nighttime experiment. Ozone injected for first 120 minutes. 73

32 Illustration of probable nitrogen wall loss. Measured nitrogen balance (top figure), model predicted nitrogen balance (middle figure) showing predicted nitric acid on walls (WHNO3), and a comparison of experimental data (dashed lines and symbols) and model predictions (solid lines) in the bottom figure. 75

33 Chamber measurements for a nighttime experiment (top figure). Ozone injected into both chambers for first 51 minutes. Model predictions using six step mechanism (bottom figure). 76

34 Effect of adding HONO to SAI model of UNC smog chamber run. 79

35 Comparison of background air and two hydrocarbon mixture levels in UNC chamber. 84

36 Nitrogen dioxide oxidation experiment with background air. 87

37 Nitric oxide oxidation experiment with background air. 87

38 Nitrogen dioxide oxidation experiment. Solid lines are for background air. Dashed lines are for 50 ppm carbon monoxide added. 89

39 Background air reactivity experiment. 90

40 Chamber and ambient air temperature. 94

41 Conversion of dewpoint temperature to water vapor mixing ratio. 95

42 Maximum sensitivity of Carle Chromatograph. 100

43 Similar chemical conditions in both halves of UNC chamber, 1973-77, RED side, BLUE side. 104

44 Similar chemical conditions in both halves of UNC chamber, 1977-79, RED side, BLUE side. 105

45 Similar chemical conditions in both halves of UNC chamber, 1979-80, RED side, BLUE side. 106

46 Approximately similar initial condition propylene experiments in UNC chamber over two year period. 107

47 Approximately similar initial condition ethylene experiments in UNC chamber over two year period. 108

48 Duplicate propylene experiment one year apart. 109

49 Nitrogen and Ozone Data. 113

50 Carbon Reactant and Product Data. 114

51 Total Solar Radiation, Dewpoint, and Temperature Data. 115

52 Nitrogen and Ozone Data. 120

53 Carbon Reactant and Product Data. 121

54 Total Solar Radiation and Temperature Data. 122

55 Nitrogen Balance. Dashed line accounts for dilution only. Each line represents the sum of all species below it. 123

56 Carbon Balance. Dashed line accounts for dilution only. Each line represents the sum of all species below it. 124

57 Nitrogen and Ozone Data, both chamber sides. 129

58 Nitrogen, Ozone, and Hydrocarbon, n-butane side only. 130

59 Nitrogen, Ozone, and Hydrocarbon n-pentane side only. 131

60 Total Solar Radiation and Temperature Data. TSR magnitude not valid. 132

61 Ultraviolet Radiation and Dewpoint Data. 133

62 Nitrogen and Ozone Data. 138

63 Carbon Reactant and Product Data. 139

64 Total Solar Radiation and Temperature. 140

65 Nitrogen and Ozone Data. 145

66 Nitrogen, Ozone, and Carbon Data, formaldehyde only. 146

67 Total Solar Radiation, Temperature and Dewpoint Data. 147

68 Nitrogen and Ozone Data. 151

69 Nitrogen, Ozone, and Carbon Data, formaldehyde only. 152

70 Total Solar Radiation, Temperature and Dewpoint Data. 153

71 Nitrogen and Ozone Data. 157

72 Total Solar Radiation and Temperature Data. 158

73 Nitrogen and Ozone Data. 162

74 Total Solar Radiation and Temperature Data. 163

75 Ultraviolet Radiation and Dewpoint Data (+, Blue). 164

76 Nitrogen and Ozone Data. 168

77 Total Solar Radiation and Temperature Data. 169

78 Ultraviolet Radiation and Dewpoint Data (+, Blue). 170

79 Nitrogen/Ozone Data. 174

80 Total Solar Radiation and Temperature Data. 175

81 Ultraviolet Radiation and Dewpoint Data (+, Blue). 176

82 Four 1979 n-butane-NOx experiments in UNC chamber. 180

83 N-pentane and n-octane experiments in UNC chamber. 181

84 Alkyl nitrate chromatogram from October 9, 1979 n-pentane, n-butane experiment. 183

85 Three 2,3-dimethylbutane-NOx experiments in UNC chamber. 184

86 MEK and acetone experiments in UNC chamber. 188

87 Five formaldehyde-NOx experiments in UNC chamber. 189

88 Data for July 18, 1977 formaldehyde/acetaldehyde experiment in UNC chamber. 191

89 1979 aromatic experiments in UNC chamber. 193

90 Example of static and dynamic HC mix experiment in UNC chamber continued. 196

91 Illustration of effect of addition of initial formaldehyde (0.6 ppm) to a propylene/NOx experiment in UNC chamber. 199

92 Illustration of effect of addition of initial acetaldehyde (1.8 ppmC) to propylene/NOx experiment in UNC chamber. 201

93 Illustration of effect of addition of initial carbon monoxide (41 and 12 ppm) to propylene/NOx experiment in UNC chamber. 202

94 Chamber data and model predictions for wet/dry runs. 206

95 Chamber data for series of wet/dry experiments. 209

TABLES

1 Distribution of runs by year....................13

2 Distribution of runs by month....................13

3 Compounds used in Smog Chamber Runs....................14

4 Chronological Summary Listing of UNC Dataset....................15

5 Chronological Summary Listing of Formaldehyde Runs....................18

6 Chronological Summary Listing of Acetaldehyde Runs....................19

7 Chronological Summary Listing of Ethylene Runs....................20

8 Chronological Summary Listing of Propylene Only Runs....................21

9 Chronological Summary Listing of Propylene Runs....................22

10 Chronological Summary Listing of n-Butane Runs....................23

11 Chronological Summary Listing of Aromatic Runs....................24

12 Chronological Summary Listing of Isoprene/ a-Pinene Runs....................25

13 Calculated Actinic Flux at the Earth's Surface....................32

14 Absorption Cross Sections..... 33

15 Quantum Yields of Photolytic Species....................34

16 Photolytic Rates at Selected Zenith Angles....................35

17 Least Squares Regression Slopes for Chemical Actinometer and Total Solar Radiation....60

18 Comparison of Regression Slopes with and without Clouds....................61

19 Ratio of NO_2 Photolysis Inside and Outside UNC Chamber 64

20 1980 Dilution Rates of UNC Chamber 71

21 Nighttime Ozone-Nitrogen Dioxide Mechanism 73

22 Effects of Initial HONO on UNC Propylene Model Predictions 80

23 Initial HONO Assumed by SAI for Selected UNC Chamber Runs 81

24 Gas Chromatographic Analysis of UNC Background Air by RTI 85

25 Simple Mechanism to Account for Chamber Reactivity 90

26 Completeness, Accuracy,and Precision Goals 102

27 Initial Conditions for Selected Runs 111

28 Hourly Values of Continuous Data for August 8, 1977 116

29 Concentrations of Selected Species for August 8, 1977 117

30 Concentrations of Selected Species for August 8, 1977 118

31 Hourly Values of Continuous Data for October 22, 1977 125

32 Concentrations of Selected Species for October 22, 1977 126

33 Hourly Values of Continuous Data for October 9, 1979 134

34 Concentrations of Selected Species for October 9, 1979 135

35 Concentrations of Selected Species for October 9, 1979 136

36 Hourly Values of Continuous Data for October 12, 1978 142

37 Concentrations of Selected Species for October 12, 1978 143

38 Hourly Values of Continuous Data for August 5, 1979 148

39 Concentrations of Selected Species for August 5, 1979 149

40 Hourly Values of Continuous Data for August 1, 1979 154

41 Concentrations of Selected Species for August 1, 1979 155

42 Hourly Values of Continuous Data for June 13, 1979 159

43 Concentrations of Selected Species for June 13, 1979 160

44 Hourly Values of Continuous Data for August 8, 1980 165

45 Concentrations of Selected Species for August 8, 1980 166

46 Hourly Values of Continuous Data for July 30, 1980 171

47 Concentrations of Selected Species for July 30, 1980 172

48 Hourly Values of Continuous Data for June 23, 1980 177

49 Concentrations of Selected Species for June 23, 1980 178

50 Afternoon Carbon Balances for 1979 Paraffin-NO_x Experiments in UNC Chamber 186

51 Product Concentrations from Toluene and O-xylene NO_x Systems August 15, 1979 194

52 Critical Data for Humid vs. Dry Runs 204

ACKNOWLEDGEMENTS

The authors gratefully acknowledge the assistance of several people in performing the work described herein. Douglas Case was a key individual in performing all the data processing. He was responsible for plot generation, for listings, and for the magnetic tape production. Doug was assisted by Kathleen Bernier and Jeff L. Hoffner. Jeffrey Liotta wrote the computer programs for processing. Kenneth Crossen wrote the computer programs for data collection and transfer.

Edward Cole, Maurice Jackson, Gary Howe, Jeff Taylor, Todd Sobol and earlier Russ Weiner, performed a significant number of the experimental runs and maintained the site equipment.

Gary Whitten and James Killus of System Applications, Inc. and Marcia Dodge of EPA provided significant discussion and suggestions for experimental conditions.

Donna Simmons' word processing expertise proved invaluable in compiling this report.

SECTION 1

BACKGROUND AND PURPOSE

BACKGROUND

During the period 1977 to 1981 the University of North Carolina Outdoor Dual Smog Chamber was used to conduct experiments of immediate interest to researchers developing mathematical models of photochemical kinetic processes. In these experiments reactant and product concentrations were measured as functions of time in chemical systems that were designed to elucidate selected aspects of the suspected mechanisms. The outdoor chamber conditions of light, temperature, and humidity were similar to those of the urban environment where the chemical transformation models would be applied.

These data were supplied to model developers as soon as they became available. Timely external feedback and internal modelling work conducted by the UNC research group often resulted in a dynamically evolving experimental design. A hierarchical process in which the expected products of a parent organic compound were used as the initial reactant in a side-by-side experiment proved revealing.

PURPOSE

The purpose of this report is to make the experimental data generated in this project available to researchers and model developers as an aid in further development and testing of chemical transformation models. To provide maximum access to the the data, they are supplied in four forms: 1) a computer readable magnetic tape containing all data from 115 dual all day experiments; 2) a set of microfiche of listings and plots of the entire dataset for those who want noncomputer access to the dataset; 3) summary hourly listings and detailed plots of ten key runs (see Chapter 6); and 4) a collection of plots illustrating interesting aspects of the dataset (see Chapter 7). Guidance on parameter choices for modelling is also included.

Copies of the magnetic tape and microfiche are available from either the National Technical Information Service, Springfield, VA or the principal author for handling and distribution costs.

SECTION 2

INTRODUCTION TO UNC CHAMBER DATA

Descriptions of the chamber, facility, experimental methods, and procedures are given in Appendix A.

CONVENTIONS

A number of conventions adopted for data presentations, standard styles, and other information useful in interpreting the experimental results are listed below.

-All times in data are Eastern Daylight (Savings) Time.

-"Concentration" units are usually parts per million (volume/volume), parts per million Carbon, or occasionally parts per billion.

-The two 153 m^3 halves or sides of the chamber are called RED and BLUE.

-The date of the run in combination with the chamber side is used to identify the experiment.

-RED side data are always shown as solid-lines and the BLUE side data are shown as dashed-lines when both chamber sides are shown in one plot.

-On each side, the continuous instrument data density is every 8 minutes. The data points are offset by 4 minutes between the two sides.

-On each side, the gas chromatographic data in plots are shown as different symbols, usually every 30 minutes. Keys to symbols appear on plots.

-Total solar radiation and UV radiation have a data density of 4 minutes.

-TSR and UV units are cal/cm^2/min (langley/min) and (1.0E-3 cal)/cm^2/min.

-Total solar and UV radiation data are taken at a height of 25 feet outside of the chamber.

-Temperature data plotted are for chamber air temperature (inside chamber). Occasionally both chamber and outside ambient temperature will be shown.

-Dewpoint data are for chamber air. Until 1979 only one side was monitored for dewpoint. In 1979 and 1980 both sides were monitored and are shown as two symbols in plots.

-The chemiluminescent NO_x analyzer in the NO_2 mode responds 100% to PAN; it exhibits no response for nitric acid. Therefore afternoon chemiluminescent NO_2 data are actually NO_2+PAN data.

-Manual Saltzman NO_2 data are occasionally used to show afternoon NO_2 concentrations.

EXAMPLES OF OUTDOOR RUNS

The usual experiment in the UNC chamber is designed to have the same oxides of nitrogen (NO_x) conditions (the same nitric oxide (NO) and nitrogen dioxide (NO_2) concentrations) on the two sides of the chamber. The variable factor in the run is therefore the hydrocarbon (HC).

On the two sides, the hydrocarbon identity can be different, the HC concentration can be different, or both HC identity and HC concentration can be different. The first example experiment is called a matched condition experiment in which both the HC identity and HC concentration are the same on the two sides. This type of experiment demonstrates, among other things, the reproducibility of the two chamber sides. The second example experiment demonstrates the effect of HC concentration at constant NO_x.

August 8, 1977 Experiment

It usually requires a minimum of three plots to present the significant data for an experiment.

On one plot, the NO, NO_2, and O_3 concentrations for each side of the chamber are shown. Peroxyacetylnitrate (PAN), nitric acid (HNO_3) and Saltzman NO_2 data are usually shown on the same plot. Figure 1 shows such a data plot for the August 8, 1977 matched propylene (C_3H_6) experiment. In this experiment, the NO injections into the chamber halves occurred before 0500 EDT and were essentially identical. Thermal oxidation of high concentrations of NO during injection results in some NO_2 appearing as shown between 0500 and 0600 EDT. At 0600 EDT, NO_2 was injected so as to establish a concentration of about 20% of the total NO_x. The resulting NO_x concentration on the two sides is matched to within 2 ppb (BLUE chamber higher). The rest of Figure 1 will be described below.

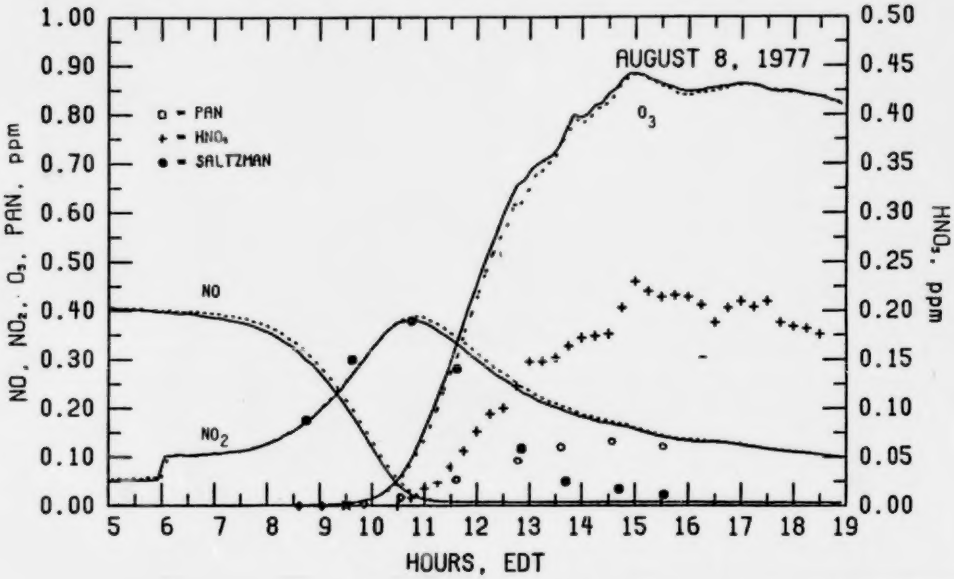

Figure 1. Example of a matched propylene experiment in UNC dual outdoor smog chamber: nitrogen compounds and ozone data. Solid lines are for the RED chamber and dashed lines are for the BLUE chamber. Data shown as symbols only measured on RED side.

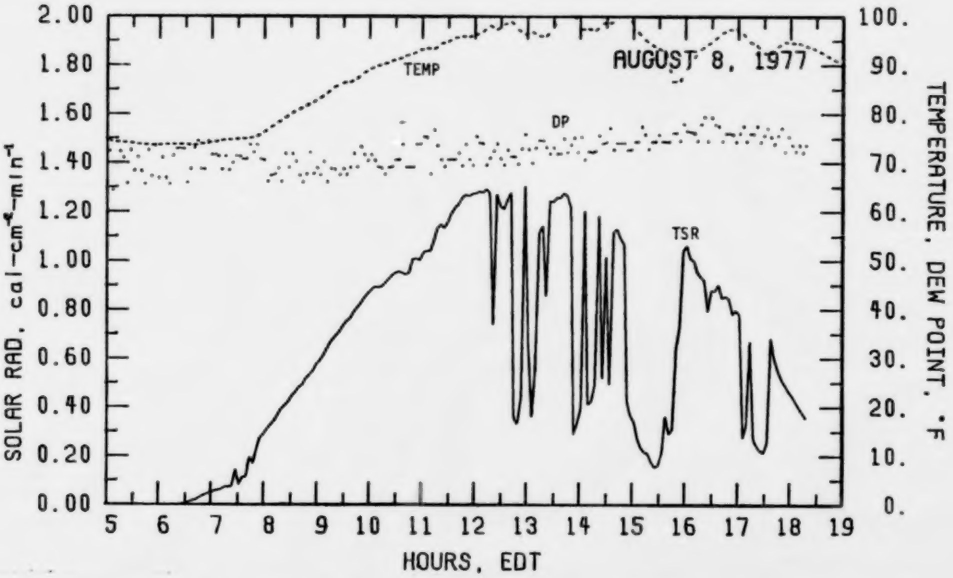

Figure 2. Meteorological variables for matched propylene experiment: ambient total solar radiation, chamber air temperature, and chamber dewpoint (water vapor content).

A second plot is used to show the total solar radiation (TSR), the chamber air temperature, and the chamber dewpoint. These characterize the physical conditions under which the experiment occurred and the data for August 8, 1977 are shown in Figure 2. In Figure 2, the TSR curve shows that: sunrise occurred about 0630 EDT; for about an hour the sky conditions were not entirely clear; after this period the morning was very clear; partly cloudy conditions began to occur at 1220 EDT; a heavy overcast lasting more than one hour occurred at mid-afternoon and was followed by more than one hour of nearly clear skies; finally sunset occured after 1900 EDT.

The chamber air temperature curve in Figure 2 shows that the minimum temperature occurred just before sunrise (74 F, 23.3 C) and rose to a maximum, near 1400 EDT of about 101 F (38.3 C). The maixmum ambient temperature was about 95 F (35 C) on this day. Notice that the chamber temperature fluctuated with changes in solar radiation and dropped about 12 F (6.6 C) during the heavy overcast. This drop in temperature and the heavy overcast in TSR was caused by a small summer thunderstorm.

The dots in Figure 2 are four-minute values for dewpoint. The early instrument used was very noisy; a line faired through the points is probably a good representation of the dewpoint. The air was initially near saturation because of overnight cooling. Throughout the day there was a small rise in dewpoint; this is probably due to the high temperatures evaporating all of the condensed water from the interior surfaces, cracks, and areas of the chamber.

A third plot is used to show the organic initial reactants and products in the run. For this experiment, the initial reactant was propylene and the primary carbon containing products are: formaldehyde (HCHO), acetaldehyde (CH_3CHO), PAN ($CH_3C(O)O_2NO_2$), carbon monoxide (CO) and carbon dioxide (CO_2). Figure 3 shows the concentrations of the measured species. These were determined by automated gas sample valve injections into gas chromatographs alternately sampling from the two sides. Smooth lines have been drawn through the points. As the C_3H_6 is disappearing due to reaction, the aldehydes are increasing. When the C_3H_6 is nearly consumed, aldehydes reach a maximum and then they too begin to be consumed. It can be seen that the BLUE chamber had slightly less propylene injected initially (1.49 vs. 1.52 ppmC). Referring to Figure 1, this difference in initial C_3H_6 results in the BLUE side being slightly slower in reaching NO to NO_2 crossover and NO_2 maximum.

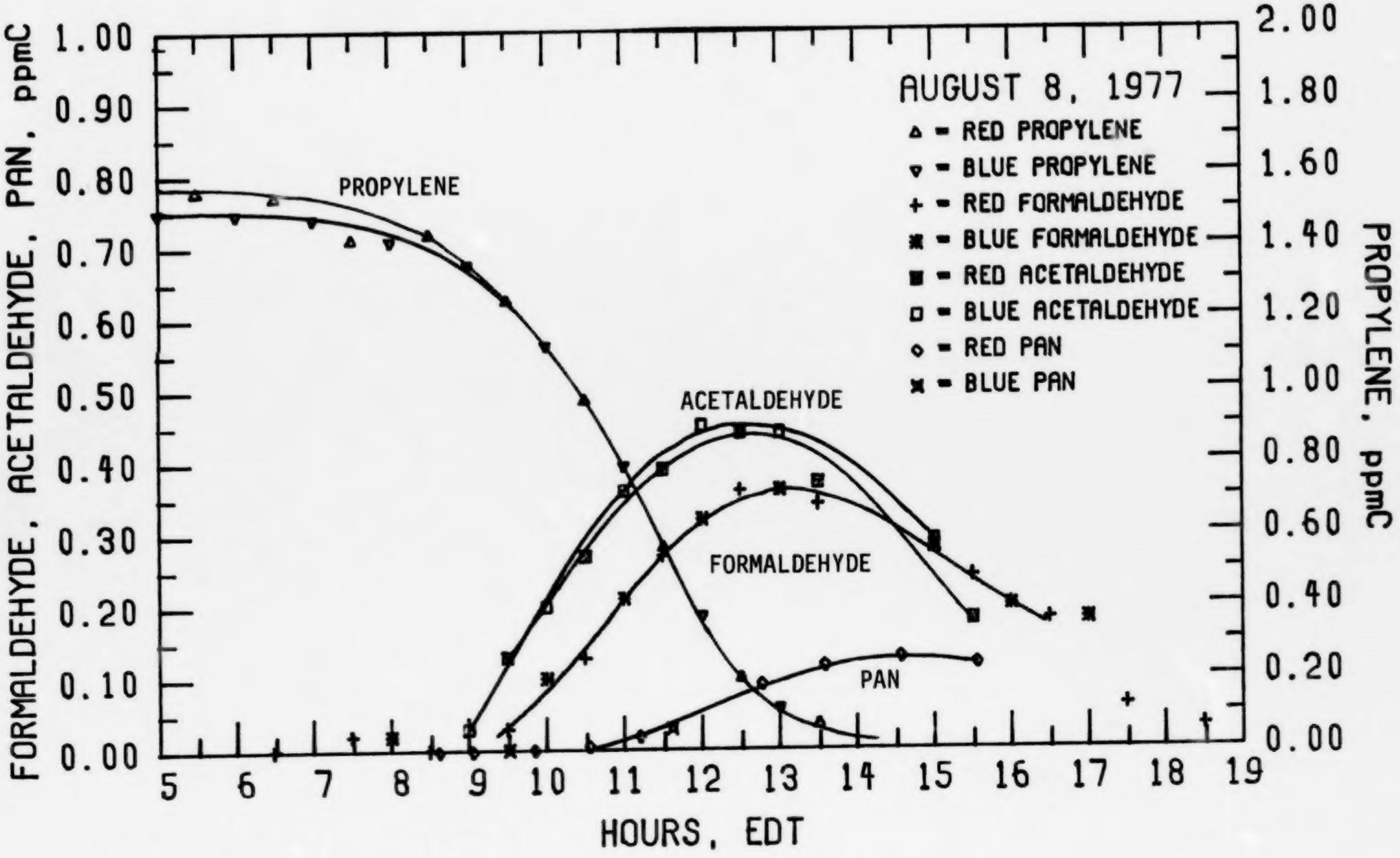

Figure 3. Carbon compound reactants and products for matched propylene experiment.

In Figure 1, the manual Saltzman NO_2 data (which were taken only on one side) show that the chemiluminescent meter is accurate in NO_2 measurements until PAN formation begins. After the NO_2 maximum, the sum of the Saltzman NO_2 data and the gas chromatographic PAN data equal the chemiluminescent NO_2 data. Nitric acid data were only taken on one side because of the instrumental technique used. It is clear that the chemiluminescent NO_2 data do not include HNO_3

The O_3 formation process was essentially constant until about 1245 EDT, the time that the first clouds appeared. After this the O_3 formation rate fluctuated with increases and decreases in solar radiation. By the time the large dip in TSR occurred at about 1500 EDT, the run was actually over (i.e. there was no NO_x left).

Figures 4 and 5 show nitrogen and carbon balance plots constructed from the data in Figures 1 and 3. These data are for the RED side only. The dashed line on the top represents the effects of dilution only. Each line in these figures represents the sum of all of the species below it.

In Figure 4, the NO_2 disappeared to form PAN and HNO_3. It is evident, however, that about 20% of the nitrogen was not measured. Kinetic models suggest that this unmeasured nitrogen was the result of N_2O_5 hydrolysis with water on the walls to form HNO_3 which then remained on the walls (see later discussion in Chapter 7).

In Figure 5, the lost propylene appeared as acetaldehyde and formaldehyde. These, in turn, were converted to PAN and CO. One measured CH_3CHO or HCHO point (1030 EDT) is evidently too large, since the sum of the products exceeds the initial carbon corrected for dilution. As the experiment proceeded, the amount of carbon accounted for decreased. Kinetics models suggest that the unmeasured carbon is CO_2, primarily from $CH_3C(O)$ decomposition after NO oxidation. Carbon dioxide is not measured because of the large ambient background level (320 ppm). Carbon monoxide is measured. Carbon monoxide has a background concentration of about 0.3 ppm; in Figure 5 only the experimentally produced CO is shown.

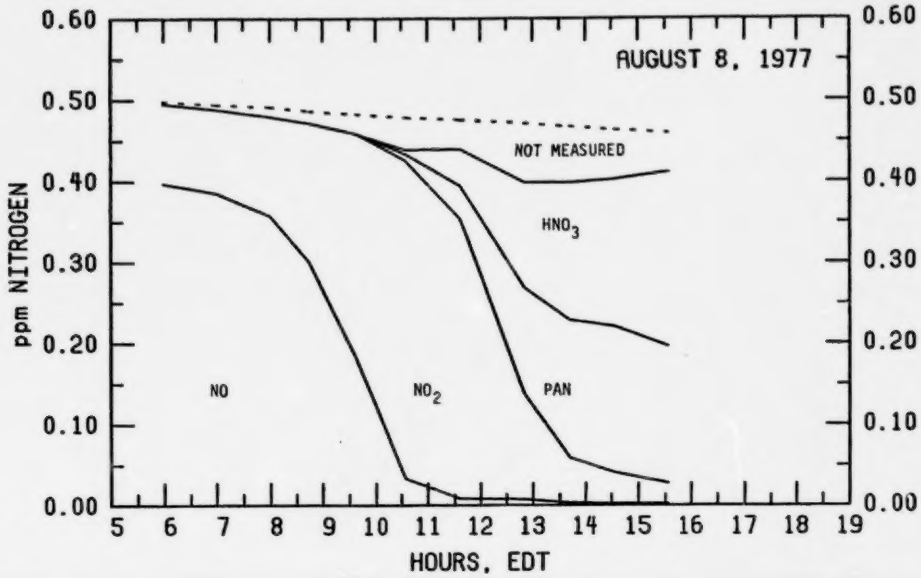

Figure 4. Nitrogen balance for RED side of propylene experiment. Each line represents the sum of all of the species below it. Dashed line accounts for dilution only.

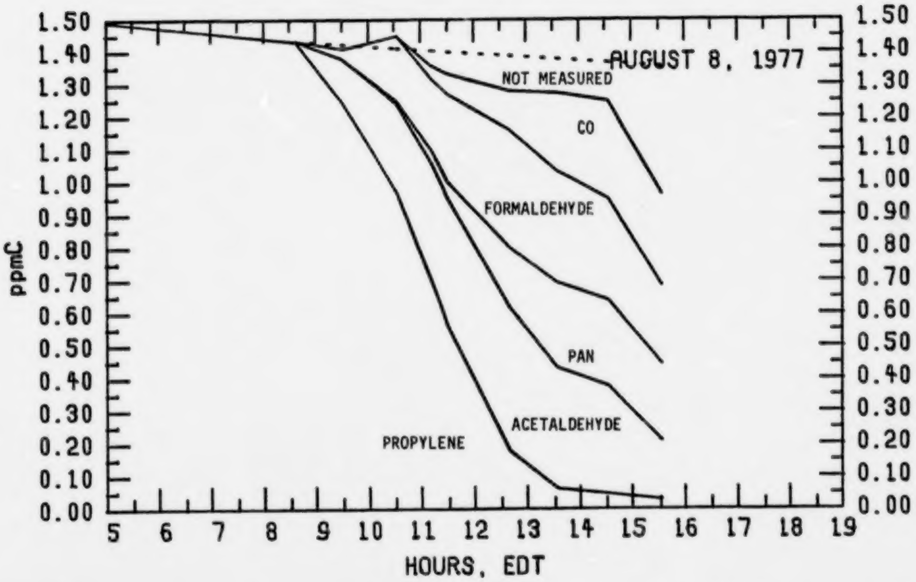

Figure 5. Carbon balance for RED side of propylene experiment. Each line represents the sum of all of the species below it. Dashed line accounts for dilution only.

July 17, 1980 Experiment

This experiment was a differential isoprene concentration run. That is, theinitial NO_2 concentration was the same on both sides of the chamber but the initial isoprene concentrations differed by a factor of about 2.5. Such an experiment is a good basis for testing model mechanisms since the same assumptions must be made for both sides and the model must predict the two sides simultaneously. Thus the same photolytic rates, the same temperature effects, and the same chemical assumptions would have to be used to model each side.

Six plots are used to show the results of the run. Figure 6 shows the NO, NO_2, PAN, and O_3 data. The NO_x injections occurred before 0500 EDT and again they were within a ppb of being identical. It is evident from the figure, however, that the chemistry in the BLUE chamber proceeded much faster. The ozone production rate was much faster and the maximum exceeded one ppm. The maximum ozone in the RED side had just been reached when ozone and NO_x data collection ceased for instrument calibration just before the operators went home; they were placed back on line at 1730 EDT.

Figure 7 shows the hydrocarbon related data: isoprene, methylacrolein (MACR), and formaldehyde on the two sides of the chamber. On both sides of the chamber isoprene disappears very rapidly to form MACR and other products. These in turn react rapidly to form formaldehyde, PAN, and other products. Once the isoprene is consumed, MACR reaches a maximum and then it is consumed. Because of the high temperature, the PAN formed is not very stable and when the source of methylperoxy radicals (MACR) is reduced, the PAN decays. Similar processes occur at quite different rates on the two sides of the chamber, however. A new modeling aid available in several of the 1980 runs was the inclusion of an OH tracer, trichloroethylene, at ppb levels. The concentration history of this tracer is shown in Figure 7; it was included only in the BLUE side.

Figure 8 shows the total solar radiation, temperature, ultraviolet radiation, and dewpoint. The latter data were acquired with an improved dewpoint instrument from both sides of the chamber. A drying process was instituted in 1979 to remove water vapor from the chamber after filling; therefore the absolute humidity in the chamber does not rise during the day. The two chambers had slightly different amounts of water vapor.

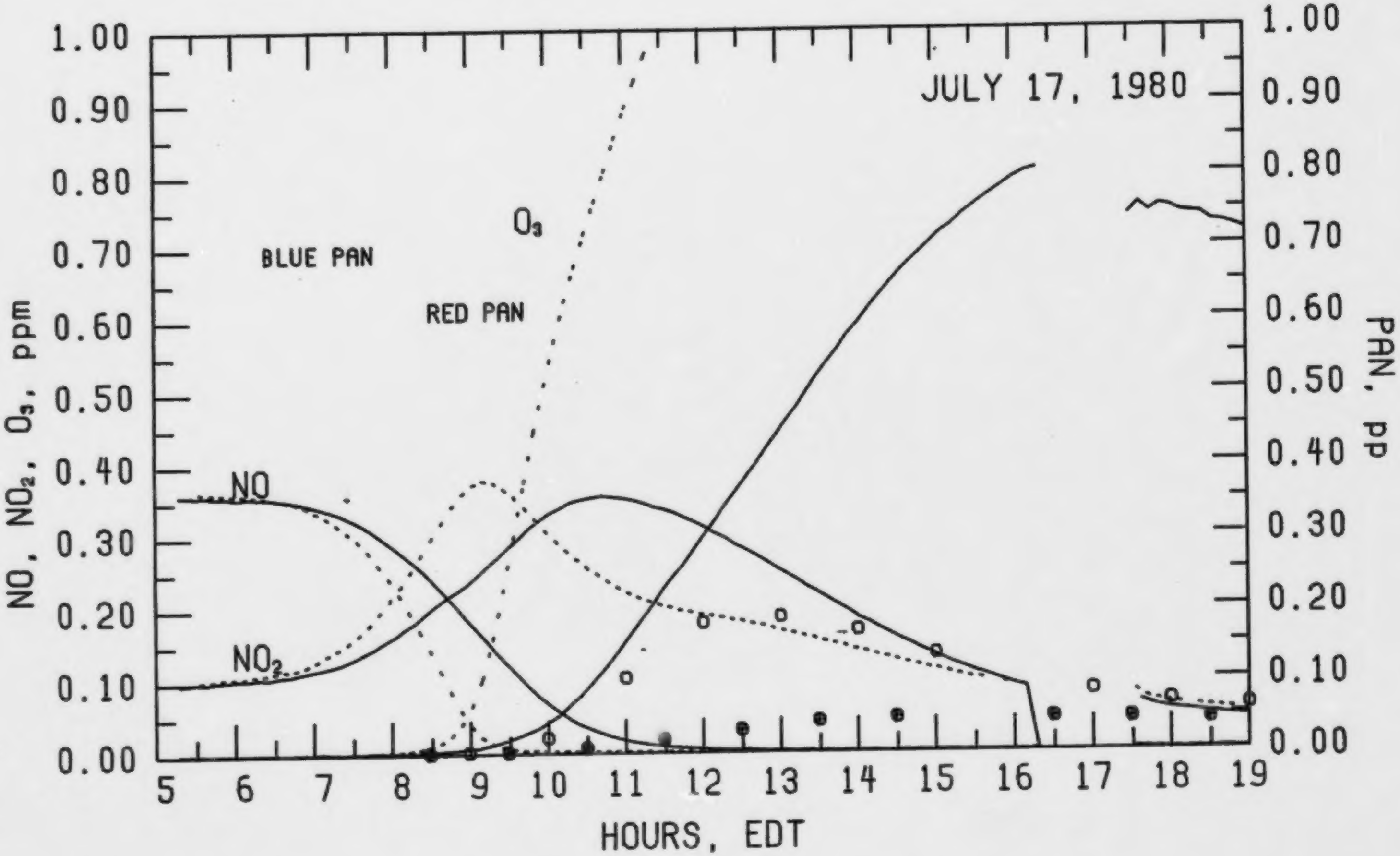

Figure 6. Example of a differential isoprene concentration experiment in UNC dual outdoor smog chamber: nitrogen compounds and ozone data. Solid lines are for the RED chamber and dashed lines are for the BLUE chamber. The maximum ozone concentration in the BLUE side was 1.29 ppm.

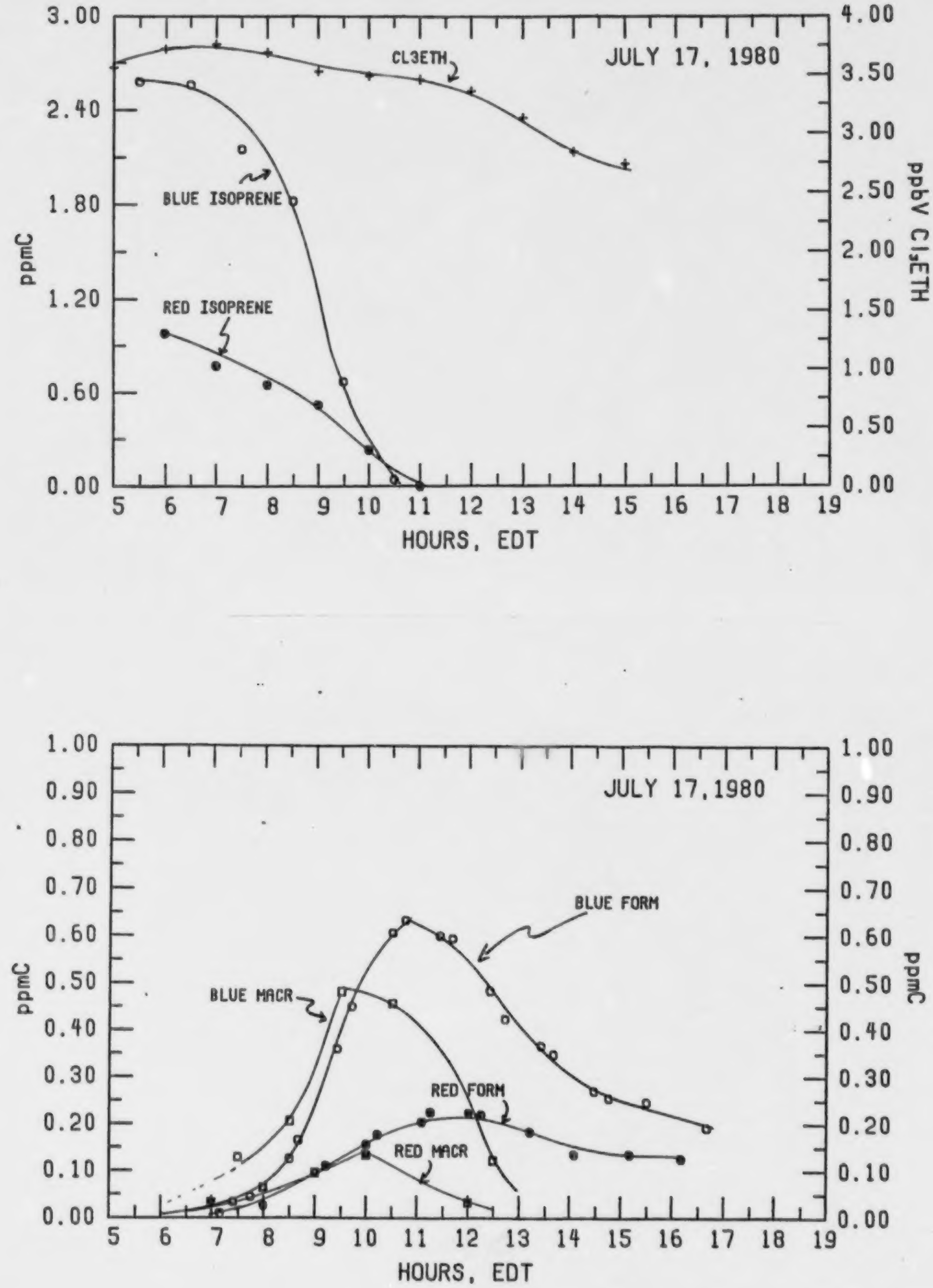

Figure 7. Carbon compound reactants and products for isoprene experiment. Trichloroethylene is used as OH tracer.

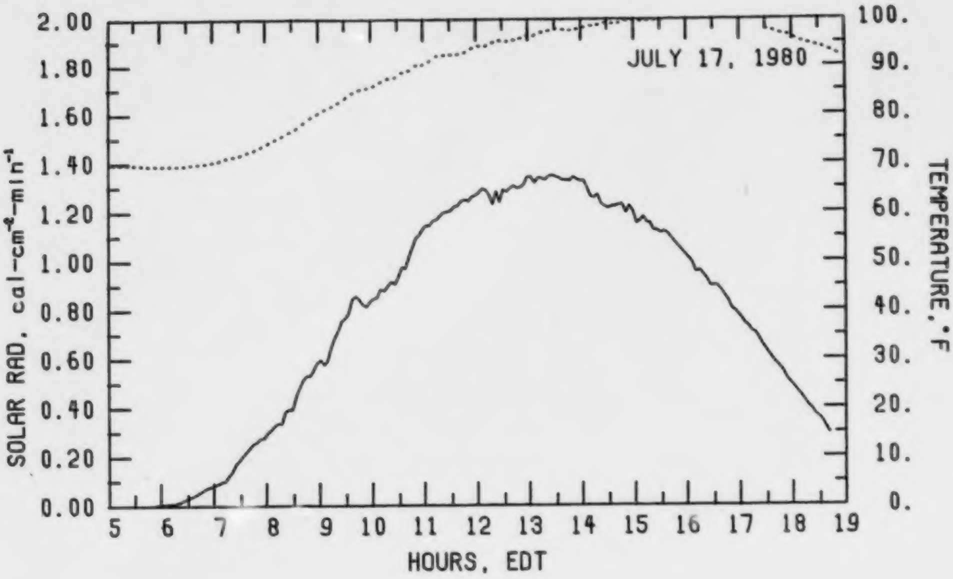

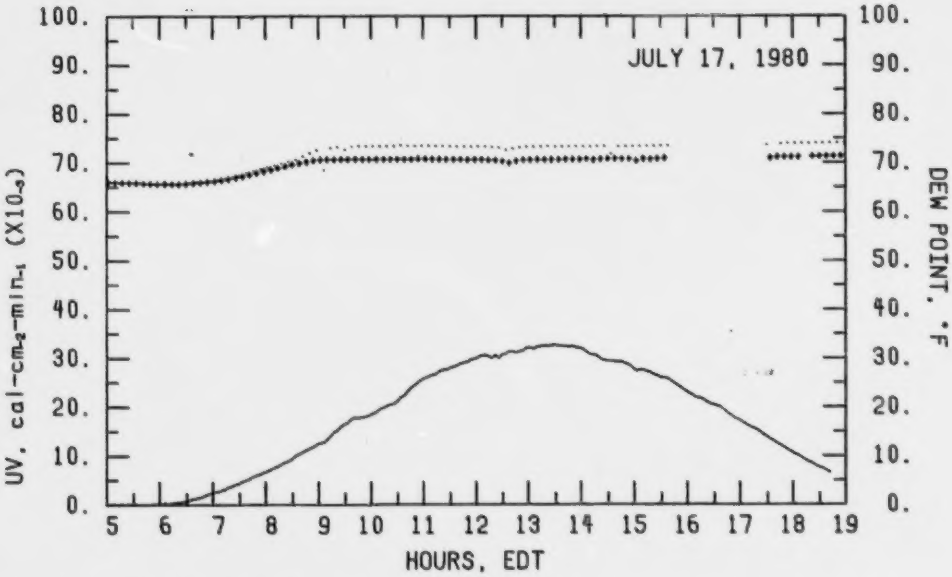

Figure 8. Meteorological variables for isoprene experiment: ambient total solar radiation and chamber air temperature, ambient ultraviolet radiation and chamber dewpoint (both sides).

SECTION 3

OVERVIEW OF TOTAL DATASET

The purpose of this section is to present a survey of the dataset and to provide an index for finding runs of interest.

The yearly distribution of runs is shown in Table 1. The months represented and the number of runs in each month are shown in Table 2. Table 3 lists the organic compounds and mixtures included in this dataset. Nineteen single compounds and 18 mixtures were used in the chamber runs.

Table 4 lists important characteristics of the entire dataset in chronological order. Most of the information in the table is self-explanatory; the sun numbers, however, are subjective values assigned by visually examining the total solar and UV radiation plots. Examples of TSR plots and their assigned numbers are given in Figure 9. Tables 5 to 12 are for selected compounds abstracted from Table 4. These allow certain conditions to be found more easily.

Table 1. Distribution of Runs by Year

Year	No. Runs	
1977	17	
1978	46	
1979	29	
1980	23	
	115	Total

Table 2. Distribution of Runs by Month

Month	No. Runs	
Jan	3	
Feb	1	
Mar	2	
Apr	0	
May	3	
Jun	19	
Jul	20	
Aug	30	
Sep	10	
Oct	19	
Nov	6	
Dec	2	
	115	Total

Table 3 Compounds Used in Smog Chamber Runs

Single Compounds

Formaldehyde
Acetaldehyde
Biacetyl
Methyl-glyoxal
Benzaldehyde
Methyl-ethyl-ketone
Acetone

Ethylene
Propylene
Isoprene
a-pinene

Butane
Pentane
Dimethylpentane
Octane

Butyl nitrate

Toluene
o-Xylene

CO

Mixtures

Formaldehyde/MEK
Formaldehyde/Acetone
Formaldehyde/Benzaldehyde
Formaldehyde/CO

Ethylene/Formaldehyde
Ethylene/Acetaldehyde
Ethylene/Trichloroethylene
Ethylene/trans-2-butene
Ethylene/CO
Propylene/Formaldehyde
Propylene/Acetaldehyde
Propylene/CO
Propylene/Toluene
Propylene/Butane

Toluene/Benzaldehyde
Toluene/CO

A-Pinene/Isoprene

Urban Mix

Table 4. Chronological Summary Listing of UNC Dataset

DATE	COMPOUND	CONC	NO	NO2	O3M	COMPOUND	CONC	NO	NO2	O3M	TINIT	TMAX	SUN
770518	ACETALDHYDE	1.87	0.287	0.072	0.937	FORMALDHYDE	1.10	0.287	0.070	0.744	60.0	96.0	8
770603	PROPYL/FORM	2.34	0.286	0.065	0.886	PROPYLENE	1.69	0.289	0.056	0.943	53.9	82.0	7
770720	FORMALDHYDE	1.21	0.398	0.141	0.653	ACETALDHYDE	1.00	0.394	0.141	0.711	72.0	102.0	7
770729	FORMALDHYDE	1.16	0.361	0.165	0.593	FORMALDHYDE	2.20	0.358	0.171	1.030	54.3	91.6	5
770727	FORMALDHYDE	1.00	0.388	0.164	0.588	ACETALDHYDE	0.55	0.389	0.161	0.441	60.8	91.1	?
770808	PROPYLENE	1.54	0.394	0.105	0.884	PROPYLENE	1.50	0.397	0.104	0.882	73.8	100.5	5
770914	FORMALDHYDE	1.05	0.293	0.104	0.621	FORMALDHYDE	1.20	0.007	0.002	0.336	65.0	92.0	4
770918	FORMALDHYDE	1.00	0.297	0.085	0.641	FORMALDHYDE	0.68	0.300	0.086	0.435	67.2	92.7	5
771012	PROPYLENE	3.56	0.380	0.125	0.237	PROPYLENE	1.72	0.373	0.128	0.058	56.7	59.3	4
771018	ETHYLENE	3.84	0.383	0.111	0.916	ETHYLENE	1.88	0.375	0.109	0.462	29.0	68.0	6
771022	PROPYLENE	3.69	0.406	0.112	0.701	BUTANE	8.10	0.411	0.114	0.001	33.1	75.4	6
771024	PROPYLENE	3.69	0.388	0.129	0.633	BUTANE	8.00	0.360	0.130	0.002	50.1	71.1	5
771109	PROPYLENE	3.77	0.387	0.142	0.682	PROPYLENE	1.92	0.397	0.143	0.411	47.3	77.4	7
771112	ETHYLENE	2.00	0.390	0.113	0.054	ACETALDHYDE	1.72	0.358	0.113	0.026	25.2	52.5	6
771119	ETHYLENE	3.78	0.417	0.034	0.034	ACETALDHYDE	3.82	0.416	0.416	0.028	28.0	64.0	7
771120	ETHYLENE	4.37	0.416	0.030	0.754	ACETALDHYDE	3.92	0.837	0.044	0.062	27.0	64.0	8
771226	PROPYLENE	2.96	0.281	0.118	0.384	ACETALDHYDE	3.82	0.290	0.117	0.039	25.0	35.0	9
780110	PROPYLENE	3.25	0.323	0.139	0.000	ETHYLENE	4.35	0.344	0.138	0.000	8.5	30.5	8
780128	PROPYLENE	3.25	0.401	0.099	0.545	NONE	0000	00000	00000	00000	19.1	41.0	6
780129	PROPYLENE	3.20	0.393	0.084	0.467	NONE	0000	00000	00000	00000	8.2	37.5	6
780227	PROPYLENE	3.95	0.371	0.125	0.594	ACETALDHYDE	1.90	0.268	0.086	0.148	16.5	50.0	7
780306	PROPYLENE	3.77	0.394	0.117	0.647	ACETALDHYDE	1.80	0.291	0.083	0.259	27.4	61.4	5
780331	PROPYLENE	3.82	0.392	0.091	0.819	ACETALDHYDE	2.00	0.327	0.066	0.521	33.0	80.0	6
780616	ETHYLENE	3.95	0.423	0.211	1.100	PROPYLENE	2.00	0.429	0.211	1.020	56.0	90.0	7
780618	BUTANE/PROP	3.02	0.268	0.086	0.702	URBAN MIX	3.28	0.269	0.085	0.821	90.7	93.1	7
780621	URBAN MIX	1.85	0.291	0.066	0.313	BUTANE/PROP	2.12	0.293	0.060	0.321	62.1	94.0	6
780701	ETHYLENE	1.45	0.679	0.208	00000	PROPYLENE	1.51	0.612	0.323	0.000	69.1	91.7	7
780721	BUTANE	7.30	0.189	0.054	0.767	BUTANE	15.7	0.186	0.056	0.986	61.5	97.0	8
780722	BUTANE	8.34	0.432	0.116	0.163	BUTANE	17.5	0.436	0.121	0.785	62.0	100.0	8
780724	PROPYLENE	2.97	0.775	0.184	1.20	PROPYLENE	1.47	0.778	0.174	0.278	74.2	100.6	7
780727	BUTANE	13.5	0.189	0.077	0.719	BUTANE	13.2	0.385	0.124	0.391	67.5	92.4	5
780730	ETHYLENE	1.32	0.396	0.078	0.789	PROPYLENE	1.25	0.399	0.084	0.838	67.5	98.9	6
780805	PROPYLENE	0.83	0.196	0.052	0.617	PROPYLENE	1.55	0.423	0.145	0.770	64.4	90.6	4
780806	PROPYLENE	1.69	0.420	0.141	0.515	ETHYLENE	2.59	0.418	0.151	1.100	72.6	90.9	4
780808	ACETALDHYDE	0.91	0.421	0.095	0.512	ACETALDHYDE	4.00	0.424	0.103	1.100	71.1	95.6	4
780811	BACKGROUND	0000	0.000	0.005	0.076	BACKGROUND	0000	0.000	0.004	0.077	68.4	90.8	5
780814	BACKGROUND	0000	0.509	0.013	00002	CO	49.2	0.513	0.020	0.017	67.1	96.7	6
780815	PROPYLENE	1.45	0.434	0.109	0.910	ETHYLENE	1.58	0.430	0.133	0.940	69.9	95.2	7

---

a) hydrocarbon concentrations are in ppmC; all other species in ppmV
b) TINIT minimum morning temperature; TMAX maximum temperature during run
c) SUN values are subjective solar radiation quality estimates on scale of 1 - 10 (10 highest)
examples of solar radiation curves given in 3.1

Table 4. Chronological Summary (continued)

DATE	COMPOUND	CONC	NO	NO2	O3M	COMPOUND	CONC	NO	NO2	O3M	TINIT	TMAX	SUN
780816	PROPYLENE	1.56	0.606	0.081	0.729	TOLUENE	3.93	0.603	0.088	0.267	69.5	96.8	7
780817	ACETALDHYDE	0.96	0.614	0.087	00000	ACETALDHYDE	4.00	0.609	0.091	00000	71.0	99.2	6
780818	PROPYLENE	0.74	0.380	0.115	0.407	PROPYLENE	2.88	0.375	0.116	1.400	66.6	97.2	8
780821	ETHYLENE	1.39	0.797	0.181	0.035	PROPYLENE	1.28	0.798	0.183	0.096	61.8	88.9	9
780823	ETHYLENE	2.93	0.412	0.095	1.110	ETHYLENE	2.97	0.417	0.104	1.130	54.3	92.6	8
780824	BUTANE	58.0	0.468	0.107	1.140	BUTANE	56.3	0.751	0.152	0.989	57.1	96.4	9
780825	BUTANE	13.2	0.415	0.103	0.191	BUTANE	26.6	0.412	0.106	0.796	64.2	98.3	7
780908	FORMALDHYDE	3.25	0.817	0.151	1.280	FORMALDHYDE	0.90	0.761	0.155	0.020	65.0	93.1	4
780914	TOLUENE	2.24	0.234	0.058	0.308	ETHYLENE	0.97	0.232	0.062	0.612	60.9	82.3	5
780915	ETHYLENE	2.98	0.407	0.119	0.710	FORMALDHYDE	2.00	0.211	0.057	0.550	60.8	81.3	3
780918	ETHYLENE	2.98	0.399	0.104	00000	TOLUENE	4.21	0.390	0.106	00000	67.6	95.2	5
780919	ETHYLENE	1.88	0.568	0.120	1.030	FORMALDHYDE	2.00	0.576	0.114	1.160	68.5	97.1	7
780921	ETHYLENE	1.93	0.192	0.066	0.810	FORMALDHYDE	1.97	0.190	0.067	0.742	63.0	87.2	5
781003	ETHYLENE	0.98	0.359	0.138	0.025	BUTANE/PROP	1.50	0.354	0.138	0.409	47.7	79.7	6
781012	ETHY/ACETAL	1.46	0.364	0.115	0.260	PROPYLENE	1.33	0.364	0.115	0.461	41.8	82.0	9
781013	ACETALDHYDE	0.92	0.378	0.115	0.084	ACETALDHYDE	2.02	0.770	0.136	0.149	48.3	81.6	4
781017	PROPYLENE	1.35	0.371	0.125	0.097	ETHYLENE	2.74	0.366	0.125	0.440	40.1	63.0	5
781018	ETHYLENE	3.12	0.343	0.113	0.709	PROPYLENE	1.52	0.340	0.116	0.281	32.4	67.2	9
781020	PROPYLENE	1.39	0.336	0.124	0.341	PROPYLENE	3.65	0.329	0.128	0.727	42.6	72.3	7
781021	PROPYLENE	3.50	0.397	0.100	0.670	PROPYLENE	3.54	0.395	0.100	0.744	34.5	75.2	10
781022	PROPYLENE	1.40	0.379	0.111	0.353	PROPYLENE	1.40	0.373	0.114	0.341	38.7	79.3	10
781025	ETHY/ACETAL	1.26	0.341	0.103	0.147	PROPYLENE	1.22	0.338	0.104	0.230	29.6	72.7	9
781029	PROPYLENE	1.35	0.374	0.124	0.222	PROPYLENE	3.68	0.370	0.125	0.659	52.3	72.7	5
781102	PROPYLENE	3.52	0.433	0.120	0.734	PROPYLENE	1.41	0.430	0.120	0.241	37.2	72.3	8
781107	PROPYLENE	1.37	0.301	0.140	0.348	ETHYLENE	2.67	0.295	0.146	0.153	44.1	76.7	5
790521	ACETALDHYDE	2.81	0.004	0.000	0.074	ACETALDHYDE	0.83	0.004	0.000	0.067	53.0	70.8	0
790531	PROPYLENE	2.70	0.388	0.103	0.994	PROP/CO	52.7	0.396	0.106	1.020	69.1	81.7	5
790601	PROPYLENE	1.52	0.402	0.133	0.940	PROPYLENE	1.52	0.402	0.135	0.942	67.5	82.6	5
790602	PROPYLENE	1.55	0.171	0.045	0.798	PROP/CO	42.2	0.171	0.044	0.826	63.7	85.6	7
790612	PROPYLENE	0.83	0.257	0.243	0.438	PROP/ACETAL	1.33	0.254	0.240	0.747	49.5	79.4	7
790613	PROPYLENE	2.81	0.367	0.085	1.08	PROP/ACETAL	5.89	0.360	0.083	0.826	52.0	81.4	7
790614	PROPYLENE	1.82	0.364	0.087	0.880	PROP/TOLUEN	4.81	0.356	0.087	0.732	55.1	79.0	7
790620	BUTANE	6.23	0.135	0.052	0.248	M-E-KETONE	6.00	0.133	0.049	0.549	58.1	78.7	6
790627	BENZALD	5.85	0.269	0.068	0.034	TOLUENE	15.5	0.266	0.067	0.399	55.2	77.2	6
790629	PROPYLENE	3.83	0.369	0.090	0.968	PROPYLENE	3.78	0.369	0.083	0.966	58.8	79.2	6
790721	ACETALDHYDE	2.00	0.001	0.008	0.365	ACETALDHYDE	2.0	0.001	0.014	0.461	78.6	96.4	4
790729	PROPYLENE	1.99	0.422	0.503	0.974	PROP/CO	13.8	0.423	0.505	0.999	77.0	101.4	5
790730	FORMALD/CO	17.8	0.223	0.065	0.713	FORMALDHYDE	2.00	0.227	0.065	0.660	78.8	95.8	7
790731	FORMALDHYDE	1.43	0.407	0.106	0.293	PROPYLENE	5.13	0.407	0.106	0.682	74.7	104.8	7
790801	ACETALDHYDE	1.91	0.274	0.075	0.682	FORMALDHYDE	1.00	0.277	0.076	0.529	79.0	104.6	8
790802	PROPYLENE	1.49	0.151	0.054	0.788	FORMALDHYDE	1.01	0.157	0.048	0.606	78.0	102.8	7
790804	ETHYLENE	0.88	0.167	0.060	0.729	FORMALDHYDE	0.56	0.170	0.060	0.378	73.4	100.7	6
790805	ETHYLENE	4.11	0.503	0.135	1.290	FORMALDHYDE	1.20	0.407	0.132	0.506	74.0	102.7	0
790813	PROPYLENE	4.39	0.399	0.097	0.696	PROPYLENE	0.57	0.149	0.039	0.367	59.7	92.2	7
790815	OXLYENE	4.99	0.240	0.082	0.514	TOLUENE	5.20	0.236	0.084	0.402			5
790816	PROPYLENE	1.42	0.314	0.129	0.688	ETHY/ACETAL	1.47	0.314	0.122	0.540	57.1	83.6	9
790907	ETHY/FORMAL	1.34	0.413	0.134	0.617	ETHY/FORMAL	1.30	0.412	0.137	0.541	70.0	95.4	

Table 4. Chronological Summary (continued)

DATE	COMPOUND	CONC	NO	NO2	O3M	COMPOUND	CONC	NO	NO2	O3M	TINIT	TMAX	SUN
791009	BUTANE	14.3	0.171	0.036	0.191	PENTANE	14.2	0.171	0.036	0.183	54.5	84.7	8
791018	DIMEBUTANE	15.9	0.142	0.060	0.236	BUTANE	13.8	0.141	0.060	0.208	48.7	80.5	7
791020	DIMEBUTANE	12.1	0.163	0.061	0.562	M-E-KETONE	13.5	0.162	0.061	0.216	57.5	86.9	5
791024	PROPYLENE	3.55	0.337	0.119	0.568	PROPYLENE	3.54	0.330	0.116	0.557	36.6	66.4	8
791014	PROPYLENE	2.92	0.416	0.087	0.717	PROPYLENE	2.94	0.415	0.087	0.646	33.4	64.4	9
791211	DIMEBUTANE	12.5	0.173	0.066	0.066	ACETONE	14.1	0.176	0.066	0.018	28.4	66.8	9
800604	ACETALDHYDE	4.80	0.130	0.046	0.232	M-E-KETONE	3.80	0.131	0.045	0.671	66.3	90.9	9
800612	BUTYL NITRA	10.9	0.169	0.052	0.319	NONE	0000	00000	00000	00000	56.5	84.2	7
800614	A-PIN/ISOPR	3.15	0.182	0.028	0.465	A-PINENE	1.70	0.182	0.030	0.519	48.9	90.4	8
800615	A-PINENE	1.22	0.169	0.044	0.280	A-PINENE	0.80	0.177	0.042	0.147	59.8	96.0	6
800617	ISOPRENE	0.50	0.142	0.050	0.354	ISOPRENE	1.40	0.075	0.023	0.405	64.5	85.9	5
800620	ISOPRENE	0.50	0.377	0.100	0.088	NONE	0.000	00000	00000	00000	59.8	90.4	7
800621	A-PINENE	1.97	0.394	0.105	0.222	NONE	0000	00000	00000	00000	57.7	85.6	6
800708	ETHYLENE	2.10	0.374	0.380	0.632	ETHYL/CCL3	3.23	0.374	0.380	0.039	65.0	93.8	5
800709	BIACETYL	1.70	0.356	0.390	1.06	ME-GLYOXAL	1.50	0.361	0.390	1.110	67.1	96.7	5
800715	A-PINENE	1.04	0.154	0.030	0.209	A-PINENE	2.68	0.157	0.031	0.470	62.1	94.8	6
800716	ISOPRENE	4.01	0.148	0.038	0.661	ISOPRENE	1.97	0.149	0.039	0.836	69.3	100.9	9
800717	ISOPRENE	2.58	0.358	0.102	0.806	ISOPRENE	0.98	0.363	0.103	1.290	69.4	100.3	9
800725	A-PINENE	1.02	0.207	0.040	0.377	A-PINENE	0.94	0.205	0.047	0.331	62.7	94.3	7
800730	TOLUENE	3.78	0.156	0.023	0.273	OXYLENE	2.23	0.155	0.023	0.554	66.9	98.6	7
800801	ETHY/T2BUTE	0.68	0.296	0.237	0.255	ETHY/T2BUTE	0.71	0.295	0.256	0.254	68.2	102.8	9
800808	ACETALDHYDE	1.90	0.322	0.097	1.040	BIACETYL	0.85	0.330	0.089	0.780	70.4	99.7	10
800809	ACETONE	40.0	0.361	0.117	1.020	FORM/ACETON	37.4	0.360	0.107	1.170	69.3	99.4	7
800811	TOLUENE	3.18	0.224	0.081	0.383	BZALD/TOLUE	4.29	0.229	0.089	0.357	72.1	99.5	4
800812	FORMALDHYDE	0.84	0.371	0.110	0.396	BZALD/FORM	2.55	0.370	0.114	0.451	70.8	98.4	4
800813	M-E-KETONE	22.5	0.379	0.153	1.310	FORM/M-E-KE	19.4	0.199	0.054	1.120	67.8	97.0	8
800814	ETHY/T2BUTE	1.19	0.386	0.084	0.862	ETHY/T2BUTE	1.25	0.384	0.082	0.919	64.8	100.8	6
800826	ETHYL/CCL3	1.99	0.406	0.066	0.801	ETHYL/CCL3	1.00	0.392	0.072	0.360	56.4	95.5	8
800827	TOLUENE/CO	102	0.387	0.095	0.735	PROPYL/CO	102	0.387	0.104	1.04	56.6	95.5	8

Table 5. Chronological Summary Listing of Formaldehyde Runs

DATE	COMPOUND	CONC	NO	NO2	O3M	COMPOUND	CONC	NO	NO2	O3M	TINIT	TMAX	SUN
770518	ACETALDHYDE	1.87	0.287	0.072	0.937	FORMALDHYDE	1.10	0.287	0.070	0.744	60.0	96.0	8
770720	FORMALDHYDE	1.21	0.398	0.141	0.653	ACETALDHYDE	1.0	0.394	0.141	0.711	72.0	102.0	7
770729	FORMALDHYDE	1.16	0.361	0.165	0.593	FORMALDHYDE	2.20	0.358	0.171	01.03	54.3	91.6	5
770727	FORMALDHYDE	1.0	0.388	0.164	0.588	ACETALDHYDE	.55	0.389	0.161	0.441	60.8	91.1	?
770914	FORMALDHYDE	1.05	0.293	0.104	0.621	FORMALDHYDE	1.20	0.007	0.002	0.336	65.0	92.0	4
770918	FORMALDHYDE	1.0	0.297	0.085	0.641	FORMALDHYDE	.68	0.300	0.086	0.435	67.2	92.7	5
780908	FORMALDHYDE	3.25	0.817	0.151	01.28	FORMALDHYDE	.90	0.761	0.155	0 .02	65.0	93.1	4
780915	ETHYLENE	2.98	0.407	0.119	0.710	FORMALDHYDE	2.0	0.211	0.057	0.550	60.8	81.3	3
780919	ETHYLENE	1.88	0.568	0.120	01.03	FORMALDHYDE	2.0	0.576	0.114	01.16	68.5	97.1	7
780921	ETHYLENE	1.93	0.192	0.066	0.810	FORMALDHYDE	1.97	0.190	0.067	0.742	63.0	87.2	5
790730	FORMALD/CO	17.8	0.223	0.065	0.713	FORMALDHYDE	2.00	0.227	0.065	0.660	78.8	95.8	7
790731	FORMALDHYDE	1.43	0.407	0.106	0.293	PROPYLENE	5.13	0.407	0.106	0.682	74.7	104.8	7
790801	ACETALDHYDE	1.91	0.274	0.075	0.682	FORMALDHYDE	1.00	0.277	0.076	0.529	79.0	104.6	8
790802	PROPYLENE	1.49	0.151	0.054	0.788	FORMALDHYDE	1.01	0.157	0.048	0.606	78.0	102.8	7
790804	ETHYLENE	.877	0.167	0.060	0.729	FORMALDHYDE	.564	0.170	0.060	0.378	73.4	100.7	6
790805	ETHYLENE	4.11	0.503	0.135	01.29	FORMALDHYDE	1.20	0.407	0.132	0.506	74.0	102.7	0
800812	FORMALDHYDE	.841	0.371	0.110	0.396	BZALD/FORM	2.55	0.370	0.114	0.451	70.8	98.4	4

Table 6. Chronological Listing of Acetaldehyde Runs

DATE	COMPOUND	CONC	NO	NO2	O3M	COMPOUND	CONC	NO	NO2	O3M	TINIT	TMAX	SUN
770518	ACETALDHYDE	1.87	0.287	0.072	0.937	FORMALDHYDE	1.10	0.287	0.070	0.744	60.0	96.0	8
770720	FORMALDHYDE	1.21	0.398	0.141	0.653	ACETALDHYDE	1.0	0.394	0.141	0.711	72.0	102.0	7
770727	FORMALDHYDE	1.0	0.388	0.164	0.588	ACETALDHYDE	.55	0.389	0.161	0.441	60.8	91.1	?
771112	ETHYLENE	2.0	0.390	0.113	0.054	ACETALDHYDE	1.72	0.358	0.113	0.026	25.2	52.5	6
771119	ETHYLENE	3.78	0.417	0.034	0.034	ACETALDHYDE	3.82	0.416	0.416	0.028	28.0	64.0	7
771120	ETHYLENE	4.37	0.416	0.030	0.754	ACETALDHYDE	3.92	0.837	0.044	0.062	27.0	64.0	8
771226	PROPYLENE	2.96	0.281	0.118	0.384	ACETALDHYDE	3.82	0.290	0.117	0.039	25.0	35.0	9
780227	PROPYLENE	3.95	0.371	0.125	0.594	ACETALDHYDE	1.90	0.268	0.086	0.148	16.5	50.0	7
780306	PROPYLENE	3.77	0.394	0.117	0.647	ACETALDHYDE	1.80	0.291	0.083	0.259	27.4	61.4	5
780331	PROPYLENE	3.82	0.392	0.091	0.819	ACETALDHYDE	2.0	0.327	0.066	0.521	33.0	80.0	6
780808	ACETALDHYDE	.91	0.421	0.095	0.512	ACETALDHYDE	4.0	0.424	0.103	01.10	71.1	95.6	4
780817	ACFTALDHYDE	.96	0.614	0.087	00000	ACETALDHYDE	4.0	0.609	0.091	00000	71.0	99.2	6
781013	ACETALDHYDE	.92	0.378	0.115	0.084	ACETALDHYDE	2.02	0.770	0.136	0.149	48.3	81.6	4
790521	ACETALDHYDE	2.81	0.004	0.000	0.074	ACETALDHYDE	.834	0.004	0.000	0.067	53.0	70.8	0
790721	ACETALDHYDE	2.0	0.001	0.008	0.365	ACETALDHYDE	2.0	0.001	0.014	0.461	78.6	96.4	4
790801	ACETALDHYDE	1.91	0.274	0.075	0.682	FORMALDHYDE	1.00	0.277	0.076	0.529	79.0	104.6	8
800604	ACETALDHYDE	4.80	0.130	0.046	0.232	M-E-KETONE	3.80	0.131	0.045	0.671	66.3	90.9	9
800808	ACETALDHYDE	1.90	0.322	0.097	01.04	BIACETYL	.85	0.330	0.089	0.780	70.4	99.7	10

Table 7. Chronological Listing of Ethylene Runs

DATE	COMPOUND	CONC	NO	NO2	O3M	COMPOUND	CONC	NO	NO2	O3M	TINIT	TMAX	SUN
771018	ETHYLENE	3.84	0.383	0.111	0.916	ETHYLENE	1.88	0.375	0.109	0.462	29.0	68.0	6
771112	ETHYLENE	2.0	0.390	0.113	0.054	ACETALDHYDE	1.72	0.358	0.113	0.026	25.2	52.5	6
771119	ETHYLENE	3.78	0.417	0.034	0.034	ACETALDHYDE	3.82	0.416	0.416	0.028	28.0	64.0	7
771120	ETHYLENE	4.37	0.416	0.030	0.754	ACETALDHYDE	3.92	0.837	0.044	0.062	27.0	64.0	8
780110	PROPYLENE	3.25	0.323	0.139	0.000	ETHYLENE	4.35	0.344	0.138	0.000	8.5	30.5	8
780616	ETHYLENE	3.95	0.423	0.211	1.10	PROPYLENE	2.0	0.429	0.211	1.02	56.0	90.0	7
780701	ETHYLENE	1.45	0.679	0.208	00000	PROPYLENE	1.51	0.612	0.323	00000	69.1	91.7	7
780730	ETHYLENE	1.32	0.396	0.078	0.789	PROPYLENE	1.25	0.399	0.084	0.838	67.5	98.9	6
780806	PROPYLENE	1.69	0.420	0.141	0.515	ETHYLENE	2.59	0.418	0.151	1.10	72.6	90.9	4
780815	PROPYLENE	1.45	0.434	0.109	0.910	ETHYLENE	1.58	0.430	0.133	0.940	69.9	95.2	7
780821	ETHYLENE	1.39	0.797	0.181	0.035	PROPYLENE	1.28	0.798	0.183	0.096	61.8	88.9	9
780823	ETHYLENE	2.93	0.412	0.095	1.11	ETHYLENE	2.97	0.417	0.104	1.13	54.3	92.6	8
780914	TOLUENE	2.24	0.234	0.058	0.308	ETHYLENE	.97	0.232	0.062	0.612	60.9	82.3	5
780915	ETHYLENE	2.98	0.407	0.119	0.710	FORMALDHYDE	2.0	0.211	0.057	0.550	60.8	81.3	3
780918	ETHYLENE	2.98	0.399	0.104	00000	TOLUENE	4.21	0.390	0.106	00000	67.6	95.2	5
780919	ETHYLENE	1.88	0.568	0.120	1.03	FORMALDHYDE	2.0	0.576	0.114	1.16	68.5	97.1	7
780921	ETHYLENE	1.93	0.192	0.066	0.810	FORMALDHYDE	1.97	0.190	0.067	0.742	63.0	87.2	5
781003	ETHYLENE	.977	0.359	0.138	0.025	BUTANE/PROP	1.50	0.354	0.138	0.409	47.7	79.7	6
781107	PROPYLENE	1.37	0.301	0.140	0.348	ETHYLENE	2.67	0.295	0.146	0.153	44.1	76.7	5
781017	PROPYLENE	1.35	0.371	0.125	0.097	ETHYLENE	2.74	0.366	0.125	0.440	40.1	63.0	5
781018	ETHYLENE	3.12	0.343	0.113	0.709	PROPYLENE	1.52	0.340	0.116	0.281	32.4	67.2	9
790804	ETHYLENE	.877	0.167	0.060	0.729	FORMALDHYDE	.564	0.170	0.060	0.378	73.4	100.7	6
790805	ETHYLENE	4.11	0.503	0.135	1.29	FORMALDHYDE	1.20	0.407	0.132	0.506	74.0	102.7	0
800708	ETHYLENE	2.10	0.374	0.380	0.632	ETHYL/CCL3	3.23	0.374	0.380	0.039	65.0	93.8	5

Table 8. Chronological Listing of Propylene -only Runs

DATE	COMPOUND	CONC	NO	NO2	O3M	COMPOUND	CONC	NO	NO2	O3M	TINIT	TMAX	SUN
770808	PROPYLENE	1.54	0.394	0.105	0.884	PROPYLENE	1.50	0.397	0.104	0.882	73.8	100.5	5
771012	PROPYLENE	3.56	0.380	0.125	0.237	PROPYLENE	1.72	0.373	0.128	0.058	56.7	59.3	4
771109	PROPYLENE	3.77	0.387	0.142	0.682	PROPYLENE	1.92	0.397	0.143	0.411	47.3	77.4	7
780724	PROPYLENE	2.97	0.775	0.184	01.20	PROPYLENE	1.47	0.778	0.174	0.278	74.2	100.6	7
780805	PROPYLENE	.83	0.196	0.052	0.617	PROPYLENE	1.55	0.423	0.145	0.770	64.4	90.6	4
780818	PROPYLENE	.74	0.380	0.115	0.407	PROPYLENE	2.88	0.375	0.116	0 1.4	66.6	97.2	8
781029	PROPYLENE	1.35	0.374	0.124	0.222	PROPYLENE	3.68	0.370	0.125	0.659	52.3	72.7	5
781102	PROPYLENE	3.52	0.433	0.120	0.734	PROPYLENE	1.41	0.430	0.120	0.241	37.2	72.3	8
781020	PROPYLENE	1.39	0.336	0.124	0.341	PROPYLENE	3.65	0.329	0.128	0.727	42.6	72.3	7
781021	PROPYLENE	3.50	0.397	0.100	0.670	PROPYLENE	3.54	0.395	0.100	0.744	34.5	75.2	10
781022	PROPYLENE	1.40	0.379	0.111	0.353	PROPYLENE	1.40	0.373	0.114	0.341	38.7	79.3	10
790813	PROPYLENE	4.39	0.399	0.097	0.696	PROPYLENE	.574	0.149	0.039	0.367	59.7	92.2	7
790601	PROPYLENE	1.52	0.402	0.133	0.940	PROPYLENE	1.52	0.402	0.135	0.942	67.5	82.6	5
790629	PROPYLENE	3.83	0.369	0.090	0.968	PROPYLENE	3.78	0.369	0.083	0.966	58.8	79.2	6
791024	PROPYLENE	3.55	0.337	0.119	0.568	PROPYLENE	3.54	0.330	0.116	0.557	36.6	66.4	8
791014	PROPYLENE	2.92	0.416	0.087	0.717	PROPYLENE	2.94	0.415	0.087	0.646	33.4	64.4	9

Table 9. Chronological Listing of Propylene Runs

DATE	COMPOUND	CONC	NO	NO2	O3M	COMPOUND	CONC	NO	NO2	O3M	TINIT	TMAX	SUN
770603	PROPYL/FORM	2.34	0.286	0.065	0.886	PROPYLENE	1.69	0.289	0.056	0.943	53.9	82.0	7
770808	PROPYLENE	1.54	0.394	0.105	0.884	PROPYLENE	1.50	0.397	0.104	0.882	73.8	100.5	5
771012	PROPYLENE	3.56	0.380	0.125	0.237	PROPYLENE	1.72	0.373	0.128	0.058	56.7	59.3	4
771022	PROPYLENE	3.69	0.406	0.112	0.701	BUTANE	8.10	0.411	0.114	0.001	33.1	75.4	6
771024	PROPYLENE	3.69	0.388	0.129	0.633	BUTANE	8.0	0.360	0.130	0.002	50.1	71.1	5
771109	PROPYLENE	3.77	0.387	0.142	0.682	PROPYLENE	1.92	0.397	0.143	0.411	47.3	77.4	7
771226	PROPYLENE	2.96	0.281	0.118	0.384	ACETALDHYDE	3.82	0.290	0.117	0.039	25.0	35.0	9
780110	PROPYLENE	3.25	0.323	0.139	0.000	ETHYLENE	4.35	0.344	0.138	0.000	8.5	30.5	8
780128	PROPYLENE	3.25	0.401	0.099	0.545	NONE	0000	00000	00000	00000	19.1	41.0	6
780129	PROPYLENE	3.20	0.393	0.084	0.467	NONE	0000	00000	00000	00000	8.2	37.5	6
780227	PROPYLENE	3.95	0.371	0.125	0.594	ACETALDHYDE	1.90	0.268	0.086	0.148	16.5	50.0	7
780306	PROPYLENE	3.77	0.394	0.117	0.647	ACETALDHYDE	1.80	0.291	0.083	0.259	27.4	61.4	5
780331	PROPYLENE	3.82	0.392	0.091	0.819	ACETALDHYDE	2.0	0.327	0.066	0.521	33.0	80.0	6
780616	ETHYLENE	3.95	0.423	0.211	01.10	PROPYLENE	2.0	0.429	0.211	01.02	56.0	90.0	7
780701	ETHYLENE	1.45	0.679	0.208	00000	PROPYLENE	1.51	0.612	0.323	00000	69.1	91.7	7
780724	PROPYLENE	2.97	0.775	0.184	01.20	PROPYLENE	1.47	0.778	0.174	0.278	74.2	100.6	7
780730	ETHYLENE	1.32	0.396	0.078	0.789	PROPYLENE	1.25	0.399	0.084	0.838	67.5	98.9	6
780805	PROPYLENE	.83	0.196	0.052	0.617	PROPYLENE	1.55	0.423	0.145	0.770	64.4	90.6	4
780806	PROPYLENE	1.69	0.420	0.141	0.515	ETHYLENE	2.59	0.418	0.151	01.10	72.6	90.9	4
780815	PROPYLENE	1.45	0.434	0.109	0.910	ETHYLENE	1.58	0.430	0.133	0.940	69.9	95.2	7
780816	PROPYLENE	1.56	0.606	0.081	0.729	TOLULENE	3.93	0.603	0.088	0.267	69.5	96.8	7
780818	PROPYLENE	.74	0.380	0.115	0.407	PROPYLENE	2.88	0.375	0.116	0 1.4	66.6	97.2	8
780821	ETHYLENE	1.39	0.797	0.181	0.035	PROPYLENE	1.28	0.798	0.183	0.096	61.8	88.9	9
781012	ETHY/ACETAL	1.46	0.364	0.115	0.260	PROPYLENE	1.33	0.364	0.115	0.461	41.8	82.0	9
781029	PROPYLENE	1.35	0.374	0.124	0.222	PROPYLENE	3.68	0.370	0.125	0.659	52.3	72.7	5
781102	PROPYLENE	3.52	0.433	0.120	0.734	PROPYLENE	1.41	0.430	0.120	0.241	37.2	72.3	8
781107	PROPYLENE	1.37	0.301	0.140	0.348	ETHYLENE	2.67	0.295	0.146	0.153	44.1	76.7	5
790612	PROPYLENE	.833	0.257	0.243	0.438	PROP/ACETAL	1.33	0.254	0.240	0.747	49.5	79.4	7
790613	PROPYLENE	2.81	0.367	0.085	01.08	PROP/ACETAL	5.89	0.360	0.083	0.826	52.0	81.4	7
781017	PROPYLENE	1.35	0.371	0.125	0.097	ETHYLENE	2.74	0.366	0.125	0.440	40.1	63.0	5
781018	ETHYLENE	3.12	0.343	0.113	0.709	PROPYLENE	1.52	0.340	0.116	0.281	32.4	67.2	9
781020	PROPYLENE	1.39	0.336	0.124	0.341	PROPYLENE	3.65	0.329	0.128	0.727	42.6	72.3	7
781021	PROPYLENE	3.50	0.397	0.100	0.670	PROPYLENE	3.54	0.395	0.100	0.744	34.5	75.2	10
781022	PROPYLENE	1.40	0.379	0.111	0.353	PROPYLENE	1.40	0.373	0.114	0.341	38.7	79.3	10
781025	ETHY/ACETAL	1.26	0.341	0.103	0.147	PROPYLENE	1.22	0.338	0.104	0.230	29.6	72.7	9
790813	PROPYLENE	4.39	0.399	0.097	0.696	PROPYLENE	.574	0.149	0.039	0.367	59.7	92.2	7
790614	PROPYLENE	1.82	0.364	0.087	0.880	PROP/TOLUEN	4.81	0.356	0.087	0.732	55.1	79.0	7
790531	PROPYLENE	2.70	0.388	0.103	0.994	PROP/CO	52.7	0.396	0.106	01.02	69.1	81.7	5
790601	PROPYLENE	1.52	0.402	0.133	0.940	PROPYLENE	1.52	0.402	0.135	0.942	67.5	82.6	5
790602	PROPYLENE	1.55	0.171	0.045	0.798	PROP/CO	42.2	0.171	0.044	0.826	63.7	85.6	7
790629	PROPYLENE	3.83	0.369	0.090	0.968	PROPYLENE	3.78	0.369	0.083	0.966	58.8	79.2	6
790729	PROPYLENE	1.99	0.422	0.503	0.974	PROP/CO	13.8	0.423	0.505	0.999	77.0	101.4	5
790731	FORMALDHYDE	1.43	0.407	0.106	0.293	PROPYLENE	5.13	0.407	0.106	0.682	74.7	104.8	7
790802	PROPYLENE	1.49	0.151	0.054	0.788	FORMALDHYDE	1.01	0.157	0.048	0.606	78.0	102.8	7
790816	PROPYLENE	1.42	0.314	0.129	0.688	ETHY/ACETAL	1.47	0.314	0.122	0.540	57.1	83.6	9
791024	PROPYLENE	3.55	0.337	0.119	0.568	PROPYLENE	3.54	0.330	0.116	0.557	36.6	66.4	8
791014	PROPYLENE	2.92	0.416	0.087	0.717	PROPYLENE	2.94	0.415	0.087	0.646	33.4	64.4	9

Table 10. Chronological Listing of N-butane Runs

DATE	COMPOUND	CONC	NO	NO2	O3M	COMPOUND	CONC	NO	NO2	O3M	TINIT	TMAX	SUN
771022	PROPYLENE	3.69	0.406	0.112	0.701	BUTANE	8.10	0.411	0.114	0.001	33.1	75.4	6
771024	PROPYLENE	3.69	0.388	0.129	0.633	BUTANE	8.0	0.360	0.130	0.002	50.1	71.1	5
780721	BUTANE	7.30	0.189	0.054	0.767	BUTANE	15.7	0.186	0.056	0.986	61.5	97.0	8
780722	BUTANE	8.34	0.432	0.116	0.163	BUTANE	17.5	0.436	0.121	0.785	6.2	100.0	8
780727	BUTANE	13.5	0.189	0.077	0.719	BUTANE	13.2	0.385	0.124	0.391	67.5	92.4	5
780824	BUTANE	58.0	0.468	0.107	01.14	BUTANE	56.3	0.751	0.152	0.989	57.1	96.4	9
780825	BUTANE	13.2	0.415	0.103	0.191	BUTANE	26.6	0.412	0.106	0.796	64.2	98.3	7
790620	BUTANE	6.23	0.135	0.052	0.248	M-E-KETONE	6.00	0.133	0.049	0.549	58.1	78.7	6
791009	BUTANE	14.3	0.171	0.036	0.191	PENTANE	14.2	0.171	0.036	0.183	54.5	84.7	8
791018	DIMEBUTANE	15.9	0.142	0.060	0.236	BUTANE	13.8	0.141	0.060	0.208	48.7	80.5	7

Table 11. Chronological Listing of Aromatic Runs

DATE	COMPOUND	CONC	NO	NO2	O3M	COMPOUND	CONC	NO	NO2	O3M	TINIT	TMAX	SUN
780816	PROPYLENE	1.56	0.606	0.081	0.729	TOLUENE	3.93	0.603	0.088	0.267	69.5	96.8	7
780914	TOLUENE	2.24	0.234	0.058	0.308	ETHYLENE	0.97	0.232	0.062	0.612	60.9	82.3	5
780918	ETHYLENE	2.98	0.399	0.104	00000	TOLUENE	4.21	0.390	0.106	00000	67.6	95.2	5
790627	BENZALD	5.85	0.269	0.068	0.034	TOLUENE	15.5	0.266	0.067	0.399	55.2	77.2	6
790815	OXLYENE	4.99	0.240	0.082	0.514	TOLUENE	5.20	0.236	0.084	0.402			5
800730	TOLUENE	3.78	0.156	0.023	0.273	OXYLENE	2.23	0.155	0.023	0.554	66.9	98.6	7
800811	TOLUENE	3.18	0.224	0.081	0.383	BZALD/TOLUE	4.29	0.229	0.089	0.357	72.1	99.5	4

Table 12. Chronological Summary Listing of Isoprene/a-Pinene Runs

DATE	COMPOUND	CONC	NO	NO2	O3M	COMPOUND	CONC	NO	NO2	O3M	TINIT	TMAX	SUN
800617	ISOPRENE	.50	0.142	0.050	0.354	ISOPRENE	1.40	0.075	0.023	0.405	64.5	85.9	5
800620	ISOPRENE	.50	0.377	0.100	0.088	NONE	.000	00000	00000	00000	59.8	90.4	7
800716	ISOPRENE	4.01	0.148	0.038	0.661	ISOPRENE	1.97	0.149	0.039	0.836	69.3	100.9	9
800717	ISOPRENE	2.58	0.358	0.102	0.806	ISOPRENE	.98	0.363	0.103	01.29	69.4	100.3	9
800614	A-PIN/ISOPR	3.15	0.182	0.028	0.465	A-PINENE	1.70	0.182	0.030	0.519	48.9	90.4	8
800615	A-PINENE	1.22	0.169	0.044	0.280	A-PINENE	.80	0.177	0.042	0.147	59.8	96.0	6
800621	A-PINENE	1.97	0.394	0.105	0.222	NONE	0000	00000	00000	00000	57.7	85.6	6
800715	A-PINENE	1.04	0.154	0.030	0.209	A-PINENE	2.68	0.157	0.031	0.470	62.1	94.8	6
800725	A-PINENE	1.02	0.207	0.040	0.377	A-PINENE	.94	0.205	0.047	0.331	62.7	94.3	7

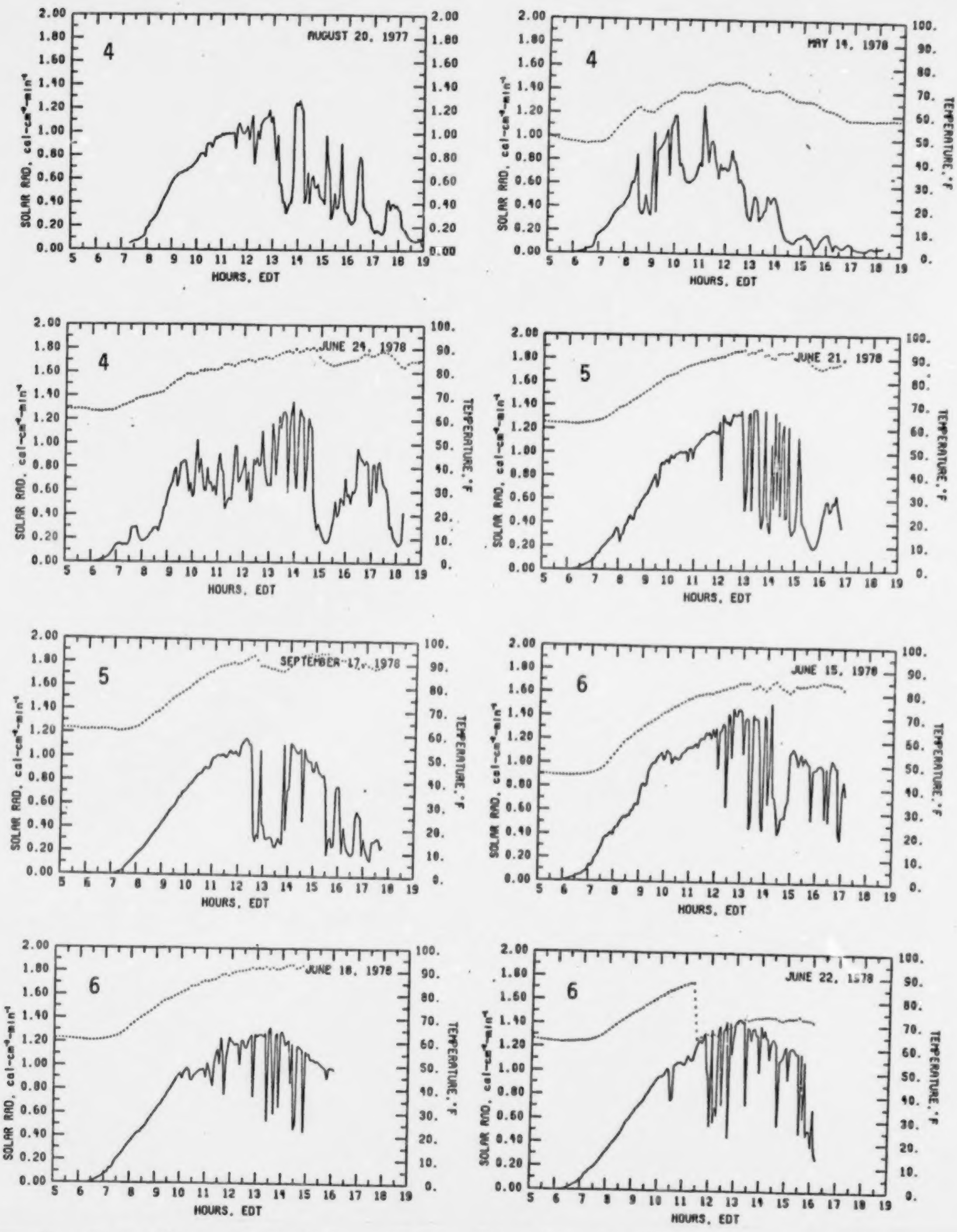

Figure 9. Examples of total solar radiation rating scale used in summary tables.

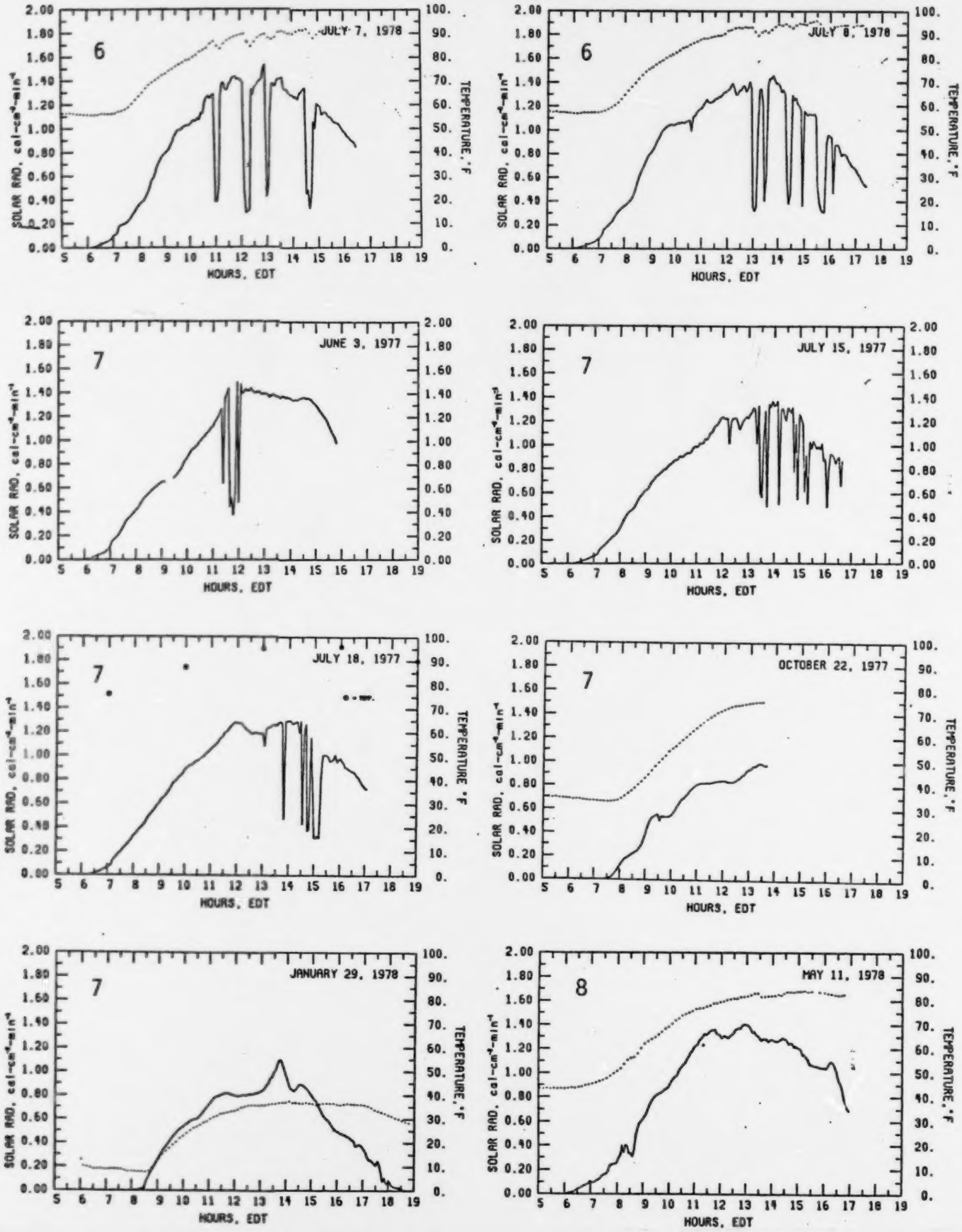

Figure 9. (cont) Examples of total solar radiation rating scale used in summary tables.

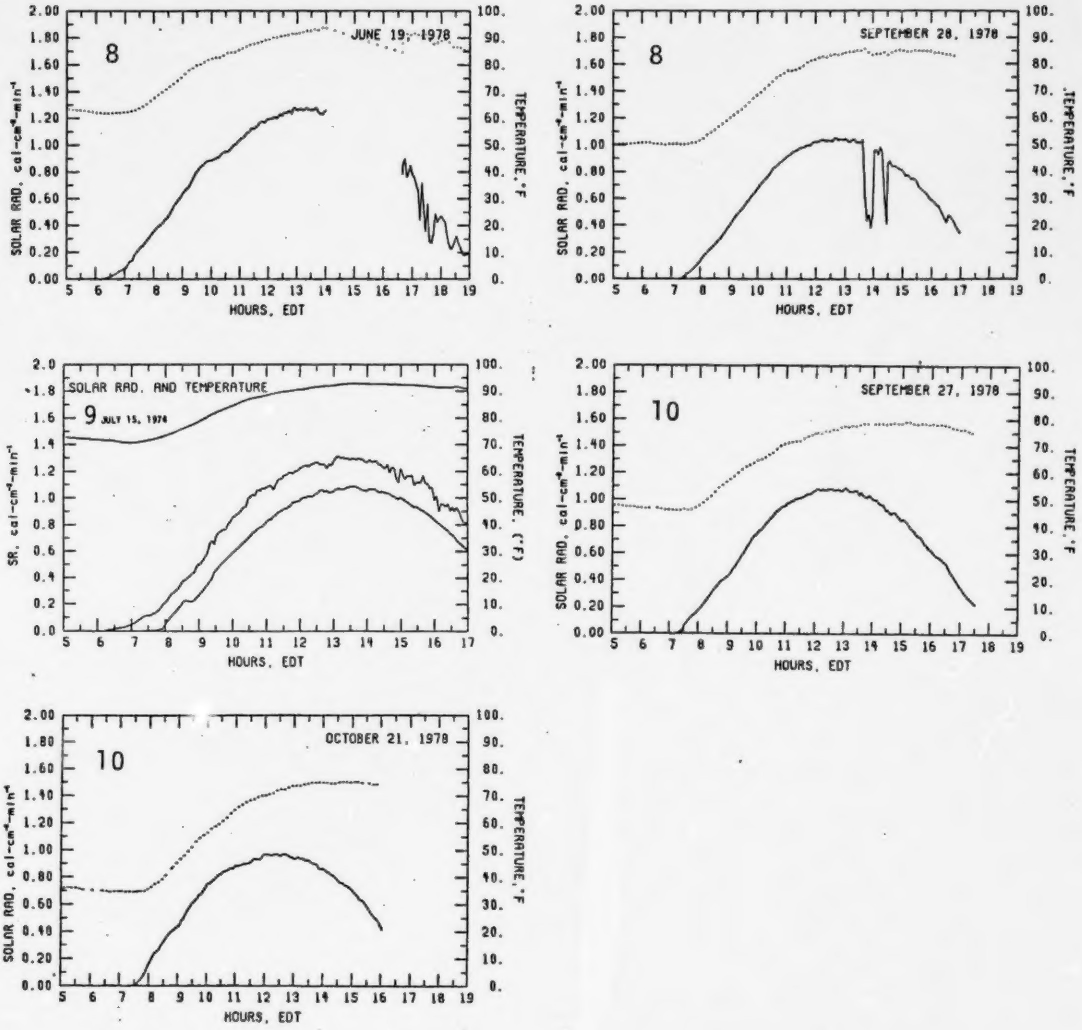

Figure 9. (cont) Examples of total solar radiation rating scale used in summary tables.

SECTION 4

GUIDANCE FOR MODELING UNC DATASET

TREATMENT OF LIGHT

The UNC smog chamber is located outdoors and is therefore exposed to ambient conditions of sunlight. These conditions include a certain degree of variablility both in intensity and spectral distribution; this may lead to some difficulty in modeling the experiments. The models, however, will be applied ultimately to urban environments that include similar sunlight conditions.

The purpose of this section is to provide information and guidance in estimating photolytic rates for the UNC chamber. The topics include theoretical calculation of rates, NO2 photolysis rates measured experimentally, empirical factors for using TSR, description of yearly variation in TSR and UV, and a description of a combination of methods used by Systems Applications, one of the frequent modelers of our data.

Theoretical Calculation of Photolytic Rate Constants: Theory, Assumptions, and Process

A computer model for calculating photolytic rate constants has been described and developed by Demerjian, Schere, and Peterson (1980). A version of this algorithm was modified by UNC for comparison of measured UV, measured TSR, and measured NO2 photolysis rates with theoretical estimates of diurnal photolytic rate constants. The theory and assumptions will be summarized and the calculation process described.

Theory. Photolytic rate constants are dependent upon three factors: actinic irradiance, absorption cross section, and the primary quantum yield. The latter two describe the efficiency with which a molecule absorbs light and dissociates. This efficiency varies over the wavelength range of absorption. Therefore the total photolyisis rate is estimated by integrating over the range of wavelengths of interest in the lower troposphere:

$$k(z)_i = \mathrm{Sum}_{w=290}^{800\ \mathrm{nm}} J(w,z)_i \times \mathrm{sigma}(w)_i \times \mathrm{phi}(w)_i$$

where J is the actinic (spherical) irradiance at wavelength w and zenith angle, z; sigma is the absorption cross section for the ith species; and phi is the primary quantum yield at each w. Absorption cross sections and quantum yields are from experimental determinations and sometimes large uncertainties occur for some species. Actinic irradiance estimates are based on results of a separate model of radiative transfer originally described by Dave(1972) and Braslau and Dave(1973,1973a).

Radiative Transfer and Actinic Flux. Demerjian calculated actinic flux at the earth's surface ("few meters") at various zenith angles, for wavelength intervals through the range of UV and visible solar spectrum. Actinic flux includes the light reflected from the earth's surface. The radiative transfer model calculates the incident irradiance at the surface.

Complete details of the radiative transfer model are given in the references of Braslau and Dave. The model includes the solar constant, the pressure height relation, molecular scattering, aerosol scattering and absorption, and absorption of ozone, water vapor, oxygen, and carbon dioxide. The model atmosphere is assumed to be cloudless, plane-parallel, and non-homogeneous. A monochromatic unidirectional solar flux is incident at the top with the bottom bounded by an idealized Lambert ground. The atmosphere is divided into a finite number of layers (up to 160). Demerjian used forty. At each level the attenuated direct solar flux and upward and downward diffuse components are calculated. Atmospheric aerosols are assumed spherical and homogeneous. Refractive index and size distribution are assumed. Aerosol size distribution and refractive index are assumed to be independent of height. Aerosol density can be varied with height (each layer) as well as ozone concentration.

Demerjian utilized the spherical flux or actinic flux (i.e. incident and reflected radiation from all directions: the sum of the downward and upward components). The model assumed an idealized Lambert ground whereby the incident radiation is reflected with isotropic intensity. The albedo selected by Demerjian represents man-made objects and ranges from 5 to 15 percent as a function of wavelength.

Aerosol and ozone concentrations and aerosol distribution were selected by Demerjian to represent general conditions in the continental U.S. but with emphasis on Los Angeles' atmosphere. The maximum aerosol density occurs with a 0.07 micrometer radius.

Demerjian points out that although this section of the model is computationally accurate (0.5%), uncertainties arise from uncertainties of the model input and the theoretical treatment of physical phenomenon such as the aerosol characteristics and optical properties. The solar constant and the surface albedo determine the upper and lower boundary conditions. The solar constant varies with the season +/- 3.4 percent. This is not built into the model by Demerjian. Wavelength dependence on the solar constant is uncertain (10%). Demerjian states that large errors may be observed at large zenith angles (near sunrise) since most of the actinic flux is due to multiple scattering.

Photolytic Rate Constant Calculation Process. The program utilizes precalculated actinic fluxes for 47 wavelength intervals (290 nm to 800 nm) and 10 zenith angles (0,10,20,30,40,50,60,70,78,86 degrees) stored as constants in the program. Absorption coefficients and quantum yields for six photolyzing species and eight reactions over the range of absorption wavelenghts for each molecular specie are also included as tables. Tables 13 to 15 list the data used in these calculations. Photolytic rate constants are calculated at the preselected solar zenith angles using the integrating scheme described above. This calculation actually needs to be performed only once and the resulting rates saved. The computed rates are shown in Table 16. Cubic splines are fitted to the rates as a function of zenith angles for each species; these then allow the calculation of a rate at any zenith angle for each species.

Location (longitude and latitude), date, and time are used in an algorithm for the equation of time to calculate zenith angles for each hour of the day of interest. The spline coefficients from above are used to calculate rate constants at each hour by knowing the zenith angle at that hour. This process, then, yields diurnal photolytic rate constants for a specific location and day.

Figures 10 to 13 present the calculated photolytic rate constants of four key species using this program run for the location of the UNC smog chamber for five times of the year showing the range and variation of predicted rates.

Table 13. Calculated Actinic Flux at the Earth's Surface as a Function of Wavelength and Zenith Angle within Specified Wavelength Intervals for Best Estimate Surface Albedos[a]

Wave-length (nm)	Exp	Actinic flux (photons cm^{-2} sec^{-1})									
		0°[b]	10°	20°	30°	40°	50°	60°	70°	78°	86°
290-295	14	0.001	0.001	--	--	--	--	--	--	--	--
295-300	14	0.041	0.038	0.030	0.019	0.009	0.003	--	--	--	--
300-305	14	0.398	0.381	0.331	0.255	0.167	0.084	0.027	0.004	0.001	--
305-310	14	1.41	1.37	1.25	1.05	0.800	0.513	0.244	0.064	0.011	0.002
310-315	14	3.14	3.10	2.91	2.58	2.13	1.56	0.922	0.357	0.090	0.009
315-320	14	4.35	4.31	4.10	3.74	3.21	2.52	1.67	0.793	0.264	0.030
320-325	14	5.48	5.41	5.19	4.80	4.23	3.43	2.43	1.29	0.502	0.073
325-330	14	7.89	7.79	7.51	7.01	6.27	5.21	3.83	2.17	0.928	0.167
330-335	14	8.35	8.25	7.98	7.50	6.76	5.72	4.30	2.54	1.15	0.241
335-340	14	8.24	8.16	7.91	7.46	6.78	5.79	4.43	2.69	1.25	0.282
340-345	14	8.89	8.80	8.54	8.09	7.38	6.36	4.93	3.04	1.44	0.333
345-350	14	8.87	8.79	8.54	8.11	7.43	6.44	5.04	3.15	1.51	0.352
350-355	14	10.05	9.96	9.70	9.22	8.48	7.39	5.83	3.69	1.77	0.414
355-360	14	9.26	9.18	8.94	8.52	7.86	6.88	5.47	3.50	1.69	0.391
360-365	14	10.25	10.16	9.91	9.46	8.76	7.71	6.17	3.99	1.94	0.444
365-370	15	1.26	1.25	1.22	1.17	1.08	0.958	0.772	0.505	0.247	0.055
370-375	15	1.14	1.13	1.10	1.06	0.983	0.873	0.708	0.467	0.230	0.051
375-380	15	1.27	1.26	1.23	1.18	1.10	0.983	0.802	0.535	0.265	0.058
380-385	15	1.05	1.04	1.02	0.980	0.917	0.820	0.673	0.453	0.226	0.049
385-390	15	1.15	1.15	1.12	1.08	1.01	0.909	0.750	0.510	0.257	0.054
390-395	15	1.19	1.18	1.16	1.11	1.05	0.943	0.783	0.537	0.273	0.057
395-400	15	1.44	1.43	1.40	1.35	1.28	1.15	0.962	0.666	0.341	0.070
400-405	15	1.73	1.72	1.69	1.63	1.53	1.39	1.16	0.809	0.418	0.085
405-410	15	1.94	1.93	1.90	1.83	1.73	1.57	1.32	0.926	0.482	0.097
410-415	15	2.05	2.04	2.00	1.93	1.83	1.66	1.41	0.993	0.522	0.104
415-420	15	2.08	2.07	2.03	1.96	1.86	1.70	1.44	1.03	0.543	0.107
420-430	15	4.08	4.06	3.99	3.87	3.67	3.36	2.87	2.07	1.11	0.216
430-440	15	4.20	4.18	4.11	3.99	3.80	3.49	3.01	2.19	1.20	0.229
440-450	15	4.87	4.85	4.77	4.64	4.43	4.09	3.54	2.61	1.45	0.272
450-460	15	5.55	5.51	5.43	5.27	5.03	4.64	4.02	2.99	1.67	0.312
460-470	15	5.68	5.65	5.57	5.42	5.17	4.79	4.17	3.12	1.77	0.325
470-480	15	5.82	5.79	5.70	5.55	5.31	4.91	4.32	3.26	1.87	0.341
480-490	15	5.78	5.75	5.67	5.53	5.29	4.93	4.33	3.29	1.90	0.339
490-500	15	5.79	5.76	5.68	5.54	5.31	4.96	4.37	3.34	1.95	0.344
500-510	15	5.99	5.96	5.87	5.71	5.47	5.09	4.47	3.41	1.99	0.340
510-520	15	5.88	5.86	5.77	5.62	5.38	5.02	4.43	3.40	2.00	0.340
520-530	15	5.98	5.95	5.87	5.72	5.48	5.11	4.52	3.47	2.04	0.336
530-540	15	5.98	5.95	5.87	5.72	5.48	5.12	4.52	3.48	2.05	0.326
540-550	15	5.88	5.85	5.77	5.62	5.40	5.04	4.46	3.44	2.03	0.317
550-560	15	5.94	5.91	5.83	5.68	5.44	5.08	4.49	3.46	2.04	0.312
560-570	15	5.99	5.96	5.88	5.73	5.49	5.13	4.54	3.50	2.06	0.306
570-580	15	6.12	6.09	6.00	5.85	5.61	5.24	4.63	3.57	2.10	0.301
580-600	16	1.25	1.24	1.22	1.19	1.14	1.07	0.951	0.737	0.439	0.064
600-620	16	1.26	1.26	1.24	1.21	1.16	1.08	0.963	0.748	0.448	0.065
620-640	16	1.27	1.26	1.24	1.17	1.10	1.10	0.980	0.771	0.473	0.074
640-660	16	1.30	1.30	1.28	1.25	1.20	1.13	1.01	0.803	0.502	0.086
660-680	16	1.33	1.33	1.31	1.28	1.23	1.16	1.04	0.828	0.527	0.096
680-700	16	1.33	1.32	1.30	1.27	1.23	1.16	1.04	0.839	0.541	0.104

[a] The second column (exp) lists the power of 10 by which all entries should be multiplied.

[b] Zenith angles.

Table 14. 10-nm Wavelength Integral Averaged Absorption Cross Section Data Used in the Photolytic Rate Constant Computations Presented in this Study

λ	Absorption cross section σ (10^{-20} cm^2 $molec^{-1}$) 10 nm integral averaged, centered about λ						
(nm)	NO_2	HONO	$HONO_2$	O_3	H_2CO	CH_3CHO	H_2O_2
290	8.52		0.634	162.	3.18	4.66	1.23
300	12.83		0.276	44.4	3.25	4.09	0.71
310	18.26	0.3	0.095	11.9	3.15	2.96	0.41
320	24.74	3.4	0.018	3.36	2.34	1.69	0.24
330	30.95	6.6		0.88	2.37	0.69	0.14
340	37.39	13.3		0.19	1.98	0.13	0.08
350	44.90	17.0		0.04	0.84		0.05
360	50.11	9.6			0.18		
370	54.05	17.2					
380	56.99	10.9					
390	58.22	2.3					
400	59.52						
410	58.03						
420	(54.52)[a]						
430	(51.46)[a]						
450				.020			
460				.036			
470				.054			
480				.075			
490				.096			
500				.131			
510				.174			
520				.220			
530				.276			
540				.331			
550				.378			
560				.454			
570				.509			
580				.493			
590				.515			
600				.552			
610				.498			
620				.417			
630				.361			
640				.318			
650				.269			
660				.217			
670				.179			
680				.152			
690				.126			
700				.098			
710				.081			
720				.068			
730				.056			
740				.048			
750				.041			

Table 15. 10 nm Wavelength Integral Averaged Quantum Yield Data Used in the Photolytic Rate Constant Computations Presented in this Study

	Quantum yields for photolytic processes 10 nm integral averaged, centered about λ												
λ (nm)	$NO_2[O(^3P)]$	HONO(OH)	$HONO_2(OH)$	$O_3[O(^3P)]^a$	$O_3[O(^1D)]$	$O_3[O_2(^1\Delta_g)]$	$H_2CO(H)$	$H_2CO(H_2)$	$CH_3CHO(CH_3)^b$		$CH_3CHO(CH_4)^b$		$H_2O_2(OH)$
									UL	LL	UL	LL	
290	1.0		1.0	0.0	1.0	1.0	.73	.28	.46	.38	.31	.10	1.0
300	1.0		1.0	0.0	1.0	1.0	.77	.23	.60	.33	.19	.05	1.0
310	1.0	1.0	1.0	1.0	.52	1.0	.75	.25	.72	.26	.09	.02	1.0
320	1.0	1.0	1.0	1.0	.01	1.0	.61	.39	.86	.17	0	0	1.0
330	1.0	1.0		1.0	0	1.0	.31	.59	.98	.05			1.0
340	1.0	1.0		1.0		1.0	.01	.42	1.00	0			1.0
350	1.0	1.0		1.0		1.0							1.0
360	1.0	1.0											
370	.99	1.0											
380	.97	1.0											
390	.91	1.0											
400	.65												
410	.22												
420	.02												
430	0												

[a] $O_3[O(^3P)]$ quantum yield in the 450–750 nm region equal 1.0.

[b] UL = upper limit; LL = lower limits. See text, Section IIIG.

Table 16.
Photolytic Rates at Selected Solar Zenith Angles
(min^{-1}, values have been multipled by 10^3)

Species	Zenith Angle (degrees)									
	0	10	20	30	40	50	60	70	78	86
NO_2	532.6	528.2	515.9	492.2	456.2	402.6	328.7	213.2	105.0	22.9
HONO	95.76	94.91	92.43	88.00	81.13	70.94	57.88	36.04	17.37	3.93
O_3[a]	31.00	30.79	30.11	28.82	27.01	24.69	21.16	15.82	19.33	1.51
O_3[b]	2.71	2.63	2.36	1.96	1.46	0.93	0.47	0.15	0.03	0.003
HCHO[c]	2.23	2.20	2.09	1.90	1.62	1.27	0.86	0.43	0.16	0.03
HCHO[d]	2.96	2.92	2.81	2.61	2.32	1.92	1.41	0.80	0.34	0.07
CH_3CHO	1.27	1.24	1.17	1.05	0.88	0.67	0.43	0.20	0.07	0.01
H_2O_2	0.54	0.53	0.50	0.46	0.40	0.32	0.23	0.12	0.05	0.01

a) $O_3 + h\nu \rightarrow O(^3P) + O_2$

b) $O_3 + h\nu \rightarrow O('D) + O_2$

c) $HCHO + h\nu \rightarrow HCO + H$

d) $HCHO + h\nu \rightarrow H_2 + CO$

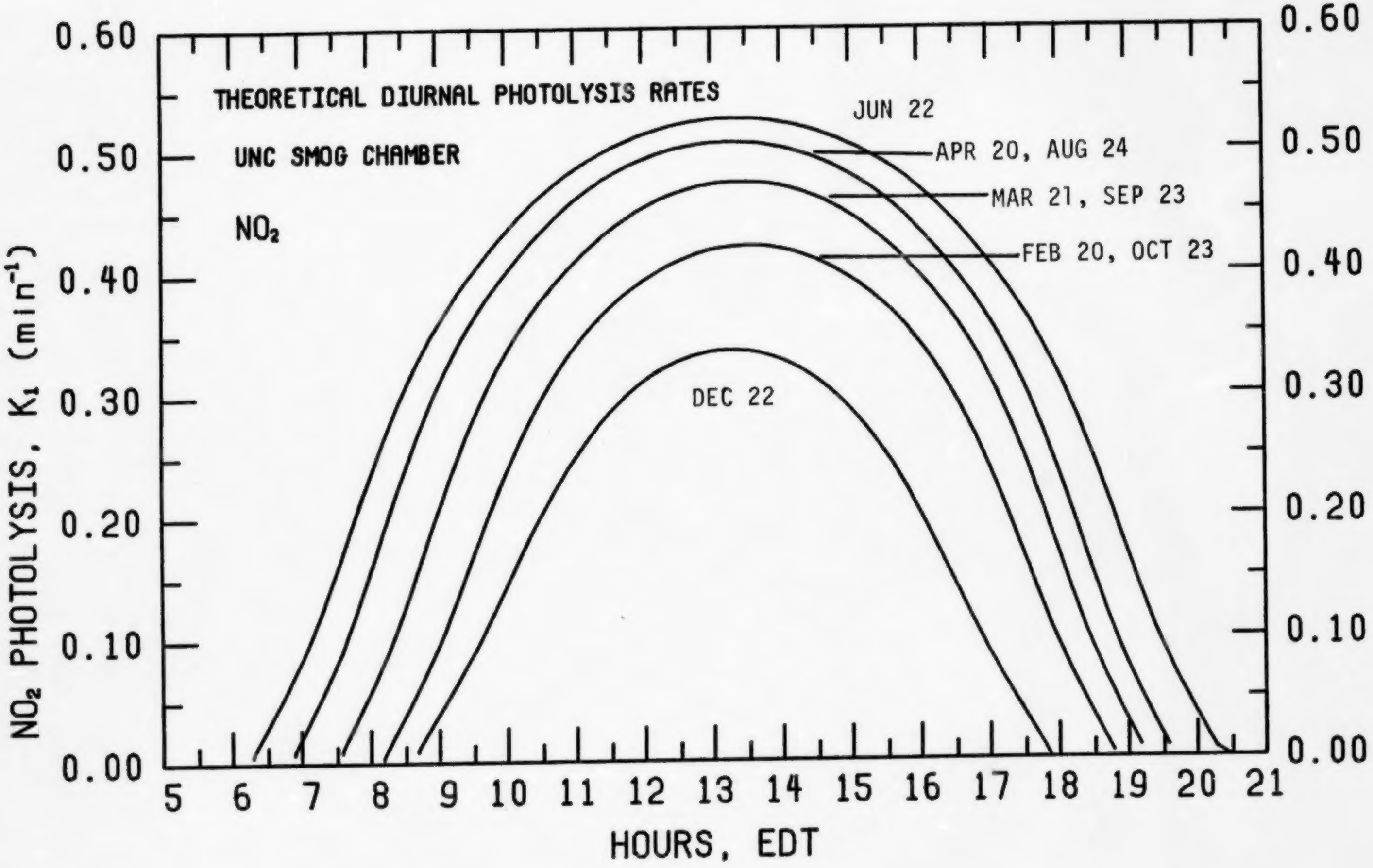

Figure 10. Calculated photolysis rates at chamber site.

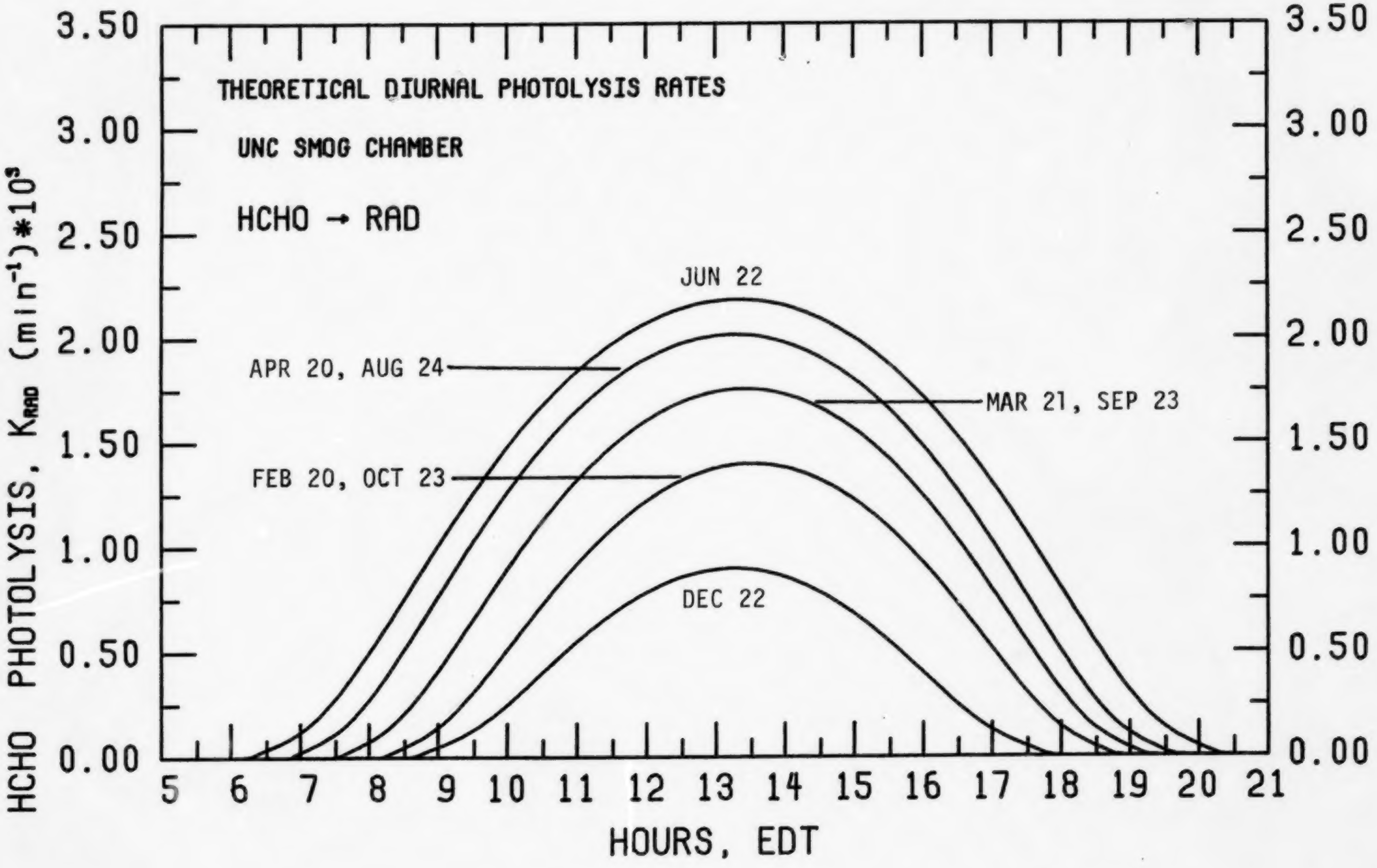

Figure 11. Calculated photolysis rates at chamber site.

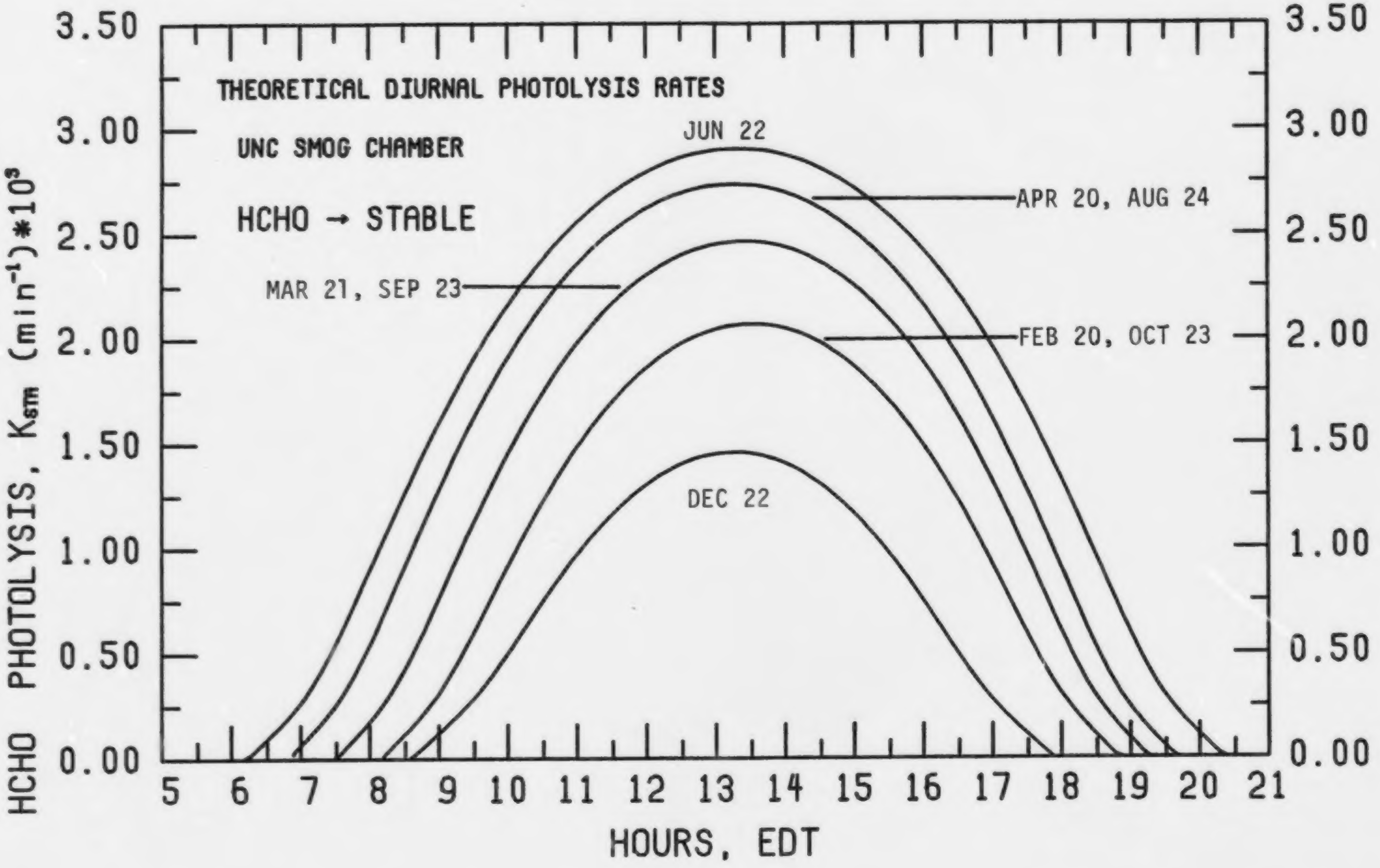

Figure 12. Calculated photolysis rates at chamber site.

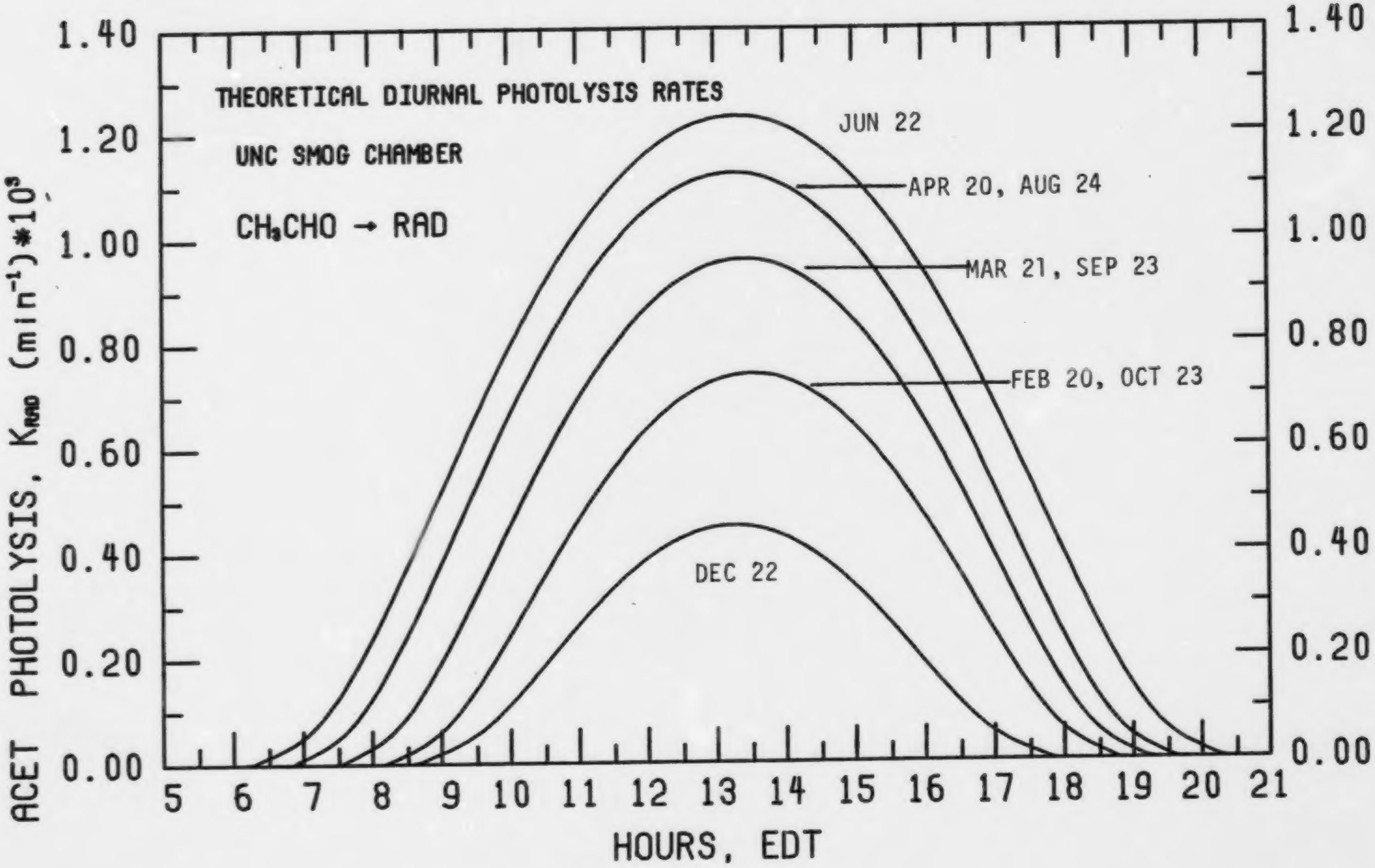

Figure 13. Calculated photolysis rates at chamber site.

Total Solar and Ultraviolet Radiation Measurements at the UNC Outdoor Smog Chamber

Total solar radiation (TSR) and the ultraviolet portion of the spectrum are routinely measured at the site of the UNC smog chamber facility using standard Eppley instruments mounted on a four meter tower. The characteristics of the instruments are given in Appendix A.

The Eppley black and white TSR radiometer was calibrated by Eppley Laboratory in 1972 and in 1980. The calibration changed by less than 2% in this eight year period. The Eppley UV radiometer was calibrated by Eppley Laboratory in 1972 and compared satisfactorily with another Eppley UV sensor in 1974 and in 1976.

An examination of our database has shown that there can be significant year-to-year variation in these measurements. To illustrate this variation several clear days in June for the years 1977 to 1980 were examined. Composite UV and TSR plots for these days are shown in Figure 14. Average lines were fitted to each year's data and these are shown in Figure 15. The 1979 TSR data are extremely anomalous; the sensor was damaged by water intrusion and the readings are suitable only for detecting clouds and not for measuring absolute intensity. The 1979 UV data, however, are valid.

The composite plots of Figure 15 show that the UV measurements exhibit significant year-to-year variation compared to TSR measurements. This is somewhat expected considering the spectral response of each instrument. The UV radiometer only responds to wavelengths between 295 and 385 nm while the TSR radiometer responses to those between 280 and 2800 nm. The UV measurement is approximately 4% of the TSR measurement. Factors that can effect the amount of UV radiation available at the earth's surface are: pathlength, scattering, absorption by ozone aloft, and atmospheric turbidity (water vapor, haze, dust, and aerosols).

UV radiation is scattered more than the visible and infrared, so that in the morning and evening when the air path is longer, there is less UV than at noon. A comparison of the absorption cross section for formaldehyde in Table 14 with the spectral response region of the UV sensor shows that they are somewhat similar, especially considering that the upper UV cut-off is achieved with a filter that begins to reduce the response at shorter wavelengths than the cutoff.

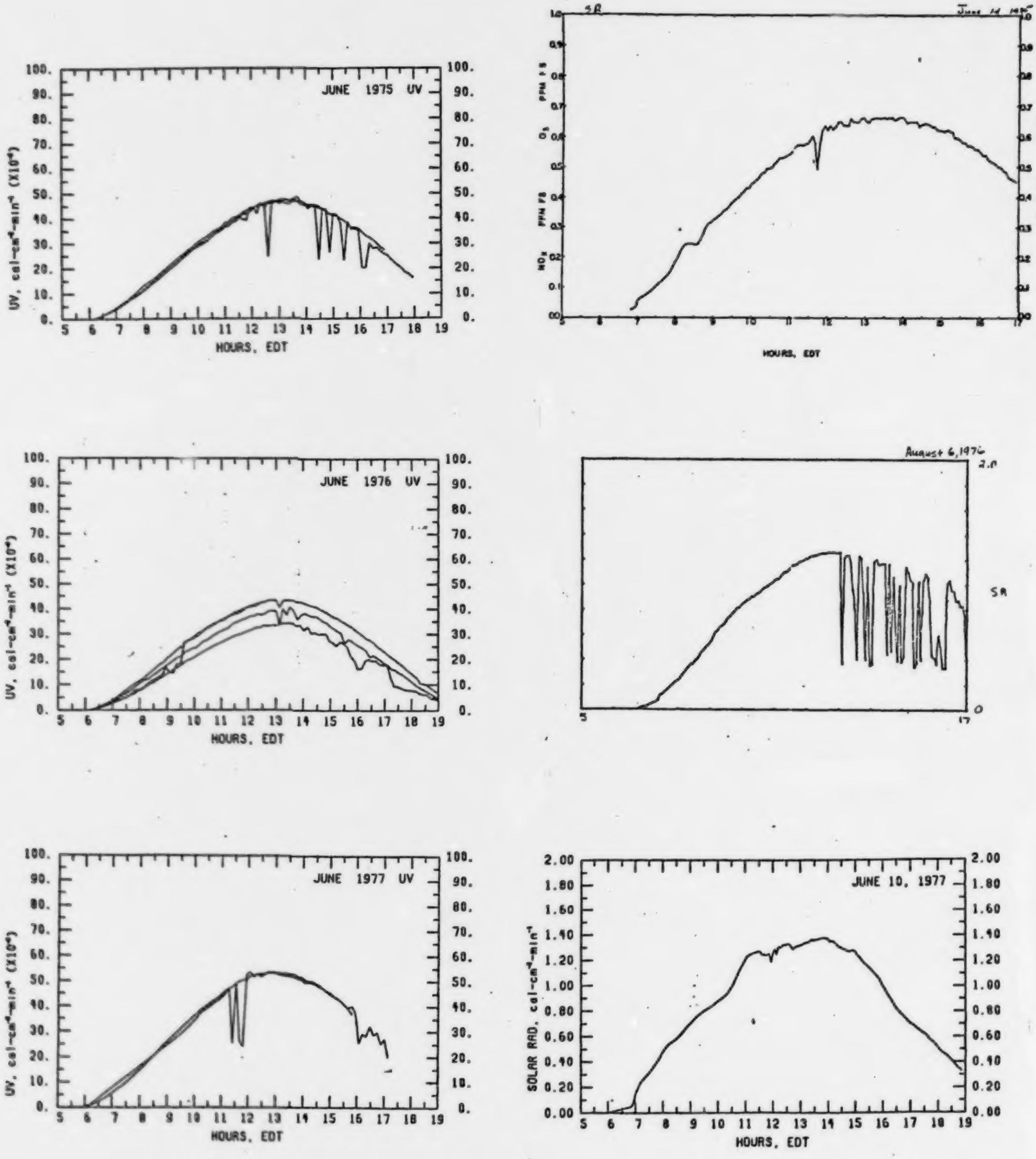

Figure 14. Ultraviolet and total solar radiation for selected clear days in June of each year 1975 to 1980.

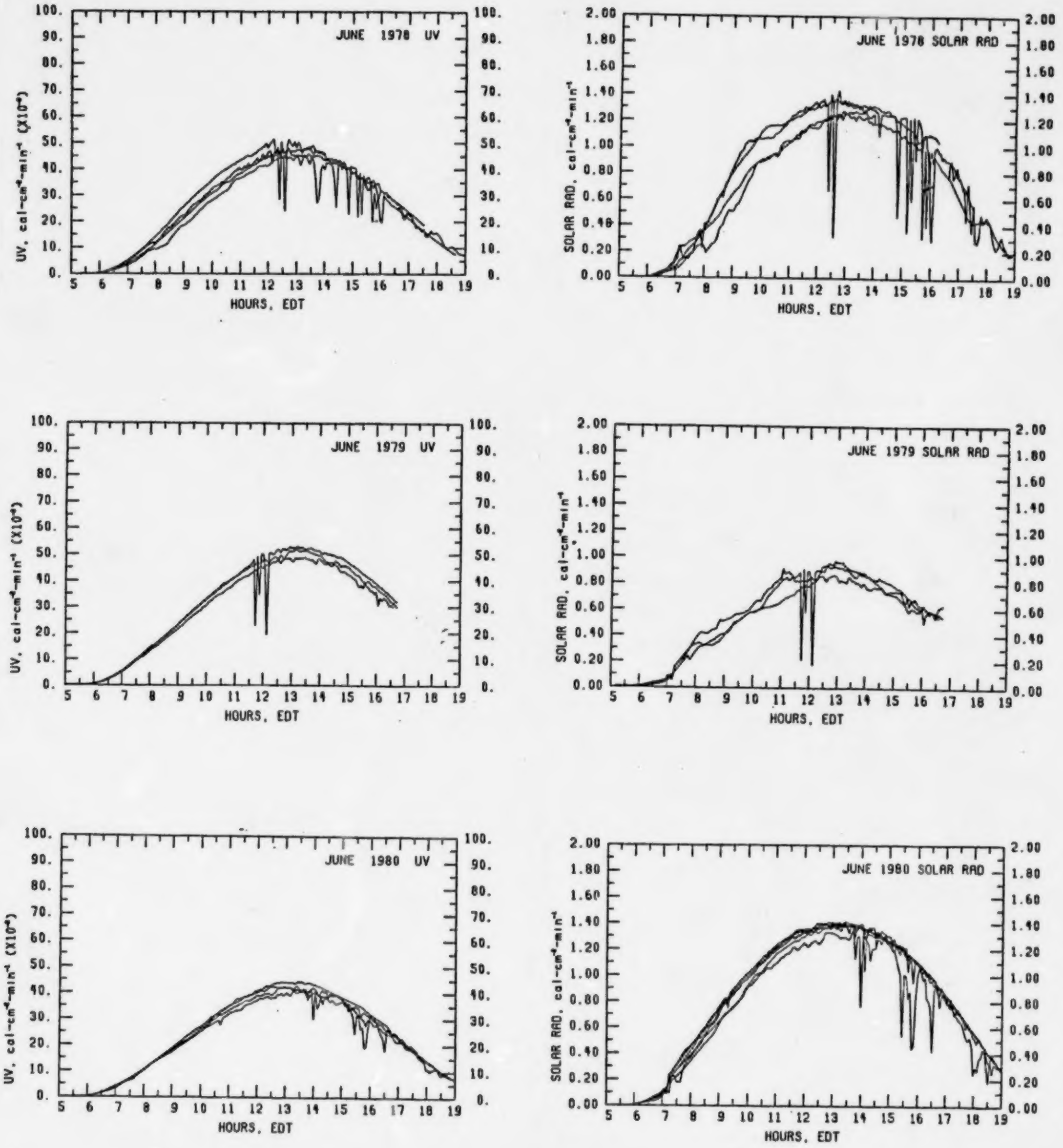

Figure 14. Ultraviolet and total solar radiation for selected clear days in June of each year 1975 to 1980 (continued).

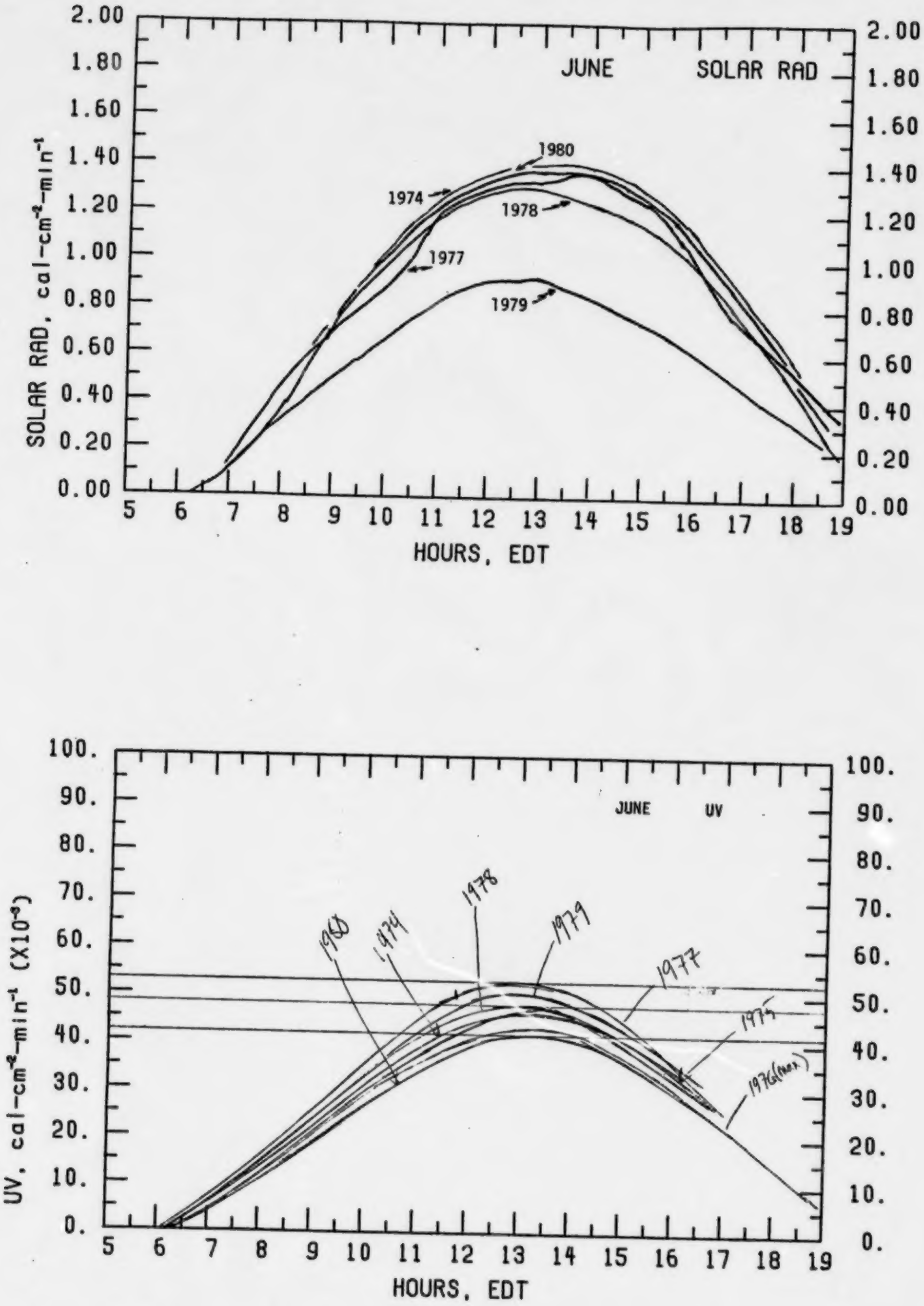

Figure 15. Estimated average ultraviolet and total solar radiation for selected clear days in June of each year 1975 to 1980. TSR instrument was damaged in 1979.

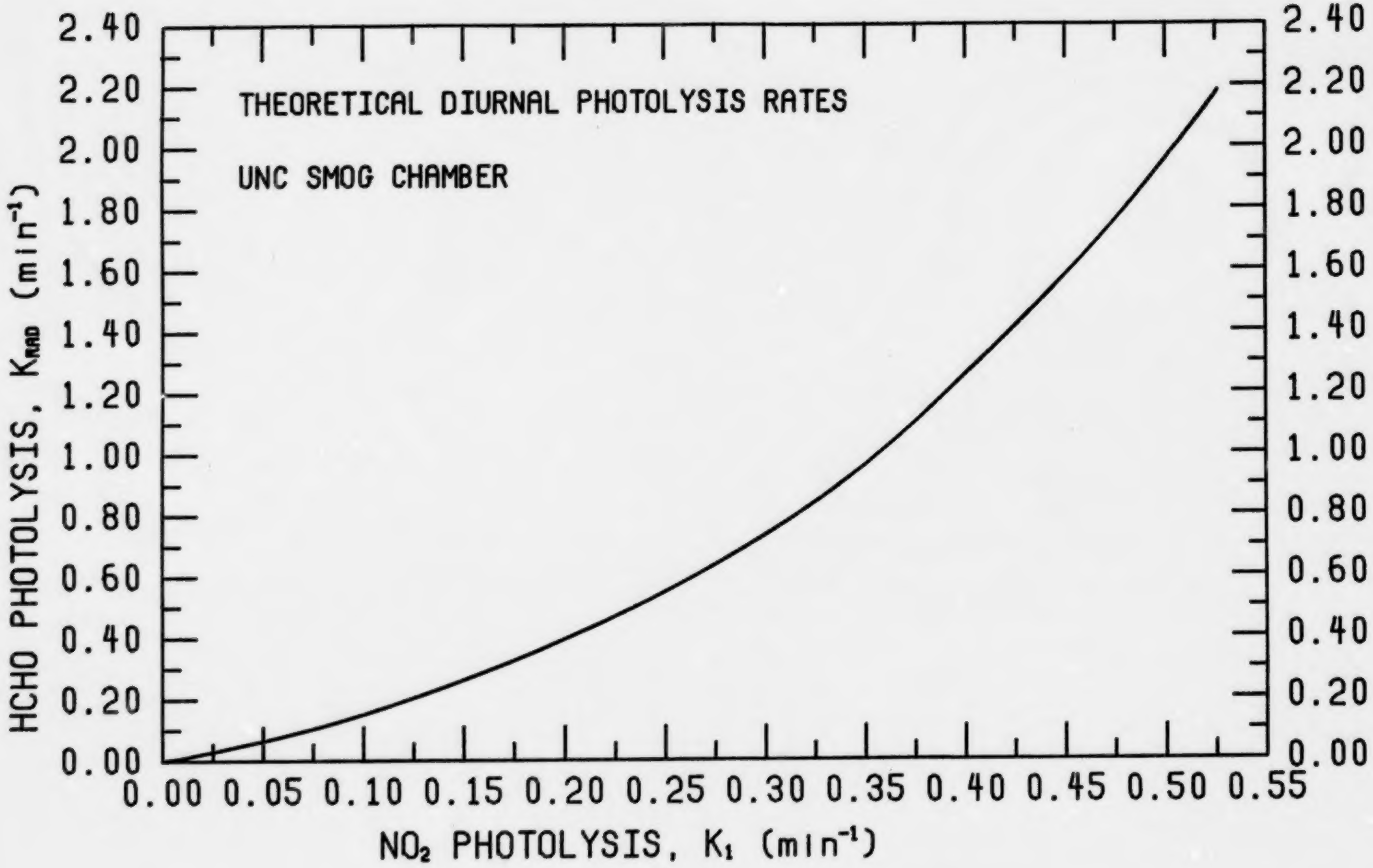

Figure 16. Theoretical formaldehyde and nitrogen dioxide photolysis rate.

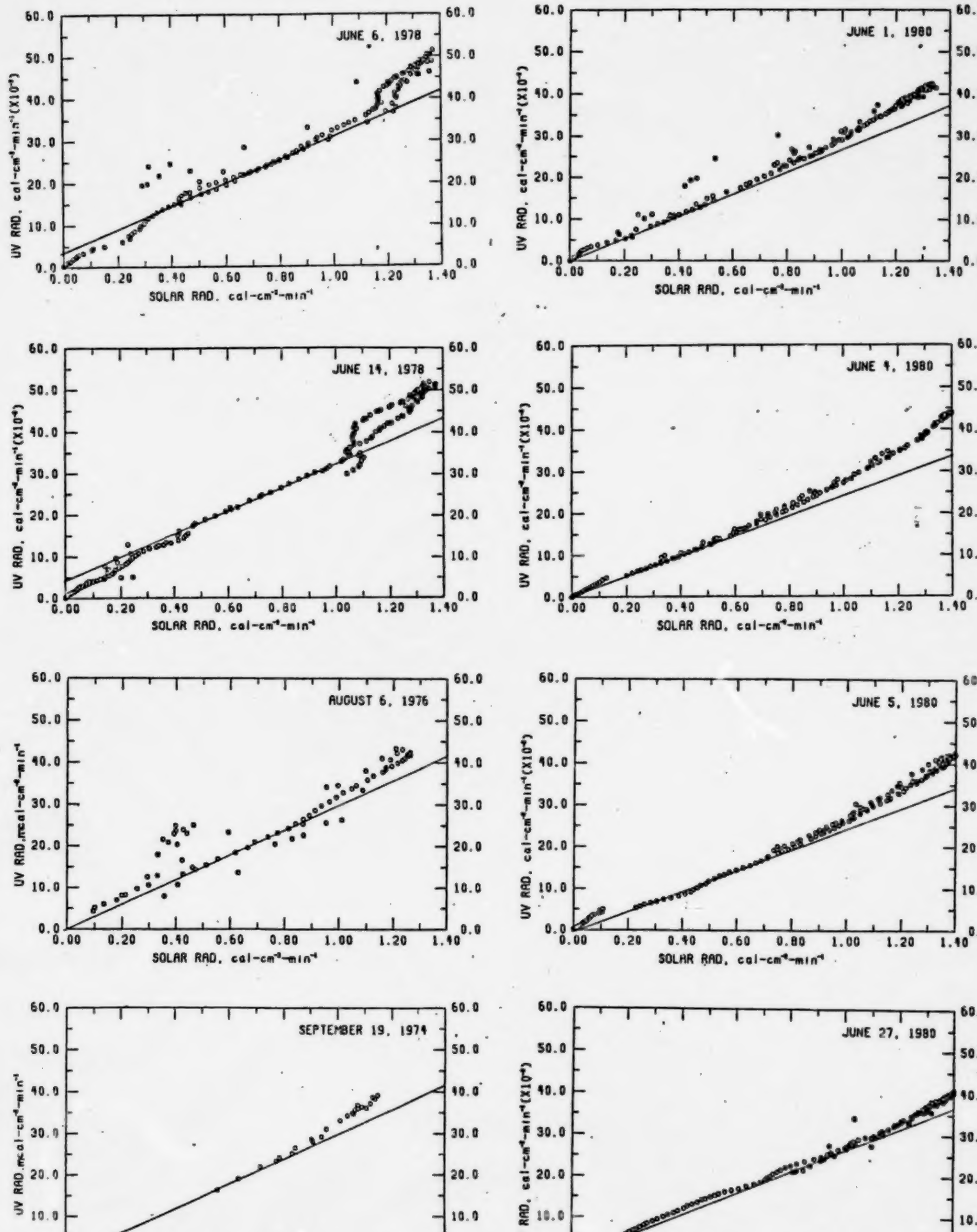

Figure 17. Comparison of UV and TSR for selected clear days.

The TSR radiometer's response includes all the wavelength region for NO_2 in Table 14. Because of these similaritiesbetween photolytic species and radiometer responses, the theoretical photolysis rates of the previous section can be used to illustrate the probable form of the relationship between the UV radiometer and the TSR radiometer by plotting the formaldehyde photolysis rate vs. the NO_2 photolysis rate; this is shown as Figure 16. Because of the difference in spectral response, it is expected that a plot of UV vs. TSR will exhibit upward curvature. This is indeed the case as shown in Figure 17 which includes the clear June days of Figure 14. These data suggest: that there is in general a curved relationship between UV and TSR measurements, that near noon there is substantially more UV, that for small clouds blocking the sun UV does not decrease as much as TSR (because of the larger scattering component in UV), and that thin clouds or haze can lead to rapid changes in one component and not the other (e.g. June 6 and 14, 1978).

Nitrogen Dioxide Photolysis Rate Measurements at the UNC Outdoor Smog Chamber

The NO_2 photolysis rate constant (k_1) has been measured both inside and outside of the UNC chamber. A spherical quartz continuous flow reactor (CSTR) was developed to expose NO_2 in N_2 to actinic light (Sickles and Jeffries, 1975, Saeger, 1977).

Photolysis Rate Over Grass. The first measurements of k_1 at the UNC chamber were made in 1974 and are shown in Figure 18 which also includes TSR and UV measurements. These measurements were taken at a height of 2 meters above grass near the chamber. For these September 19, 1974 measurements a black, light-proof bag was used to zero and check the actinometer system between each point of k_1 data shown in the figure.

Figure 19 shows k_1 vs. TSR, k_1 vs UV, and UV vs. TSR for this day. It is evident that the spherical quartz flask, above grass, measures a value that is linearly related to that measured by the Eppley black and white total solar radiation instrument, but is non-linearly related to the measurements produced by the Eppley UV instrument. The non-linear relationship between the Eppley UV and k_1 was also shown by Stedman et al. (1977) and is included herein as Figure 20. Stedman, not having a TSR radiometer, incorrectly concluded that it was the cosine response of the Eppley that was responsible for the curvature; the UV and TSR radiometers, however, have the same cosine response and they still show a similar curvature. As shown above, a more likely explanation is the spectral response differences between k_1 sensors and the UV sensor.

In 1976 a dual quartz flask actinometer system, one outside the chamber over grass, and one suspended in the center of one side of the chamber were used to more routinely monitor the NO photolysis rate. Some of the days with k_1 data are shown in Figures 21 to 24. Also included are TSR and UV measurements. The plot scales were selected to approximate normalized k_1 and UV with TSR at noon. The last three of these days also include k_1 measurements inside the chamber.

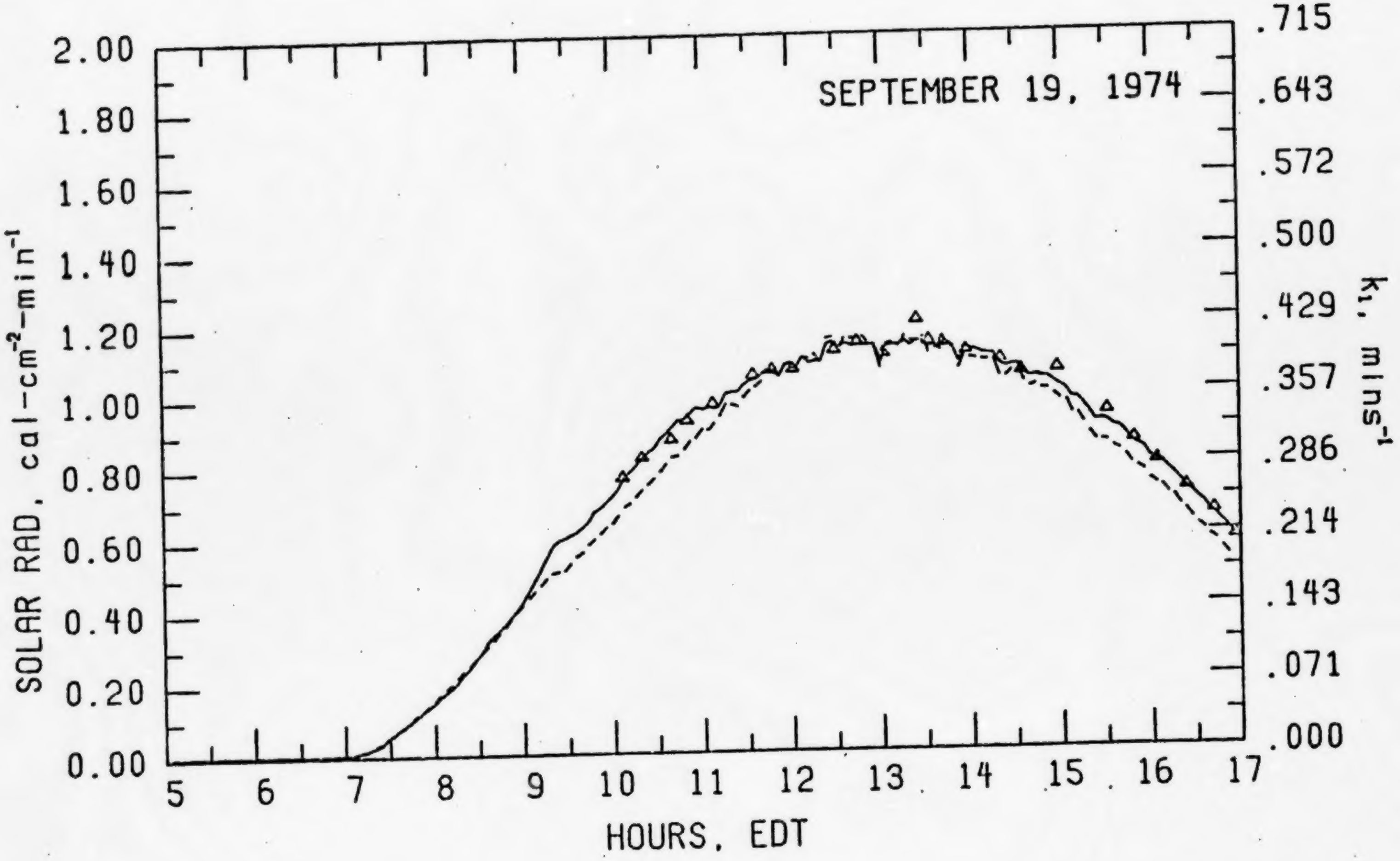

Figure 18. Specific photolysis rate for nitrogen dioxide and incident total solar radiation and ultraviolet radiation as a function of time for September 19, 1974. Solid line is total solar radiation; dashed line is ultraviolet radiation (full scale is 67.45 x 10-3 cal-cm-2-min) and Δ are k_1.

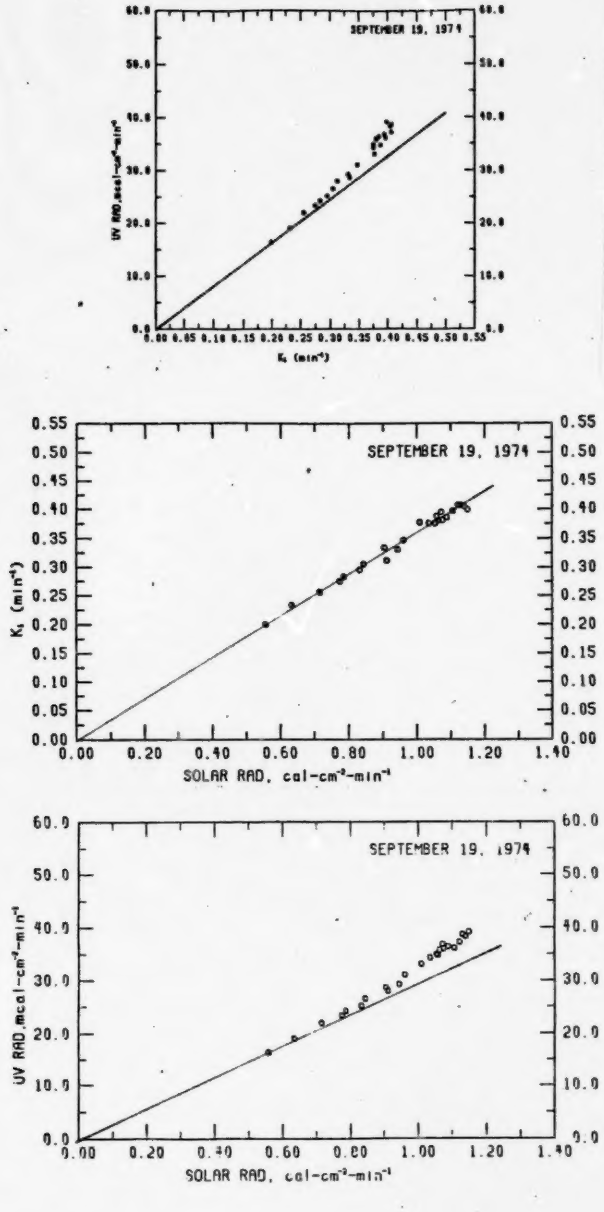

Figure 19. Comparisons of radiometer and actinometer measurements for September 19, 1974.

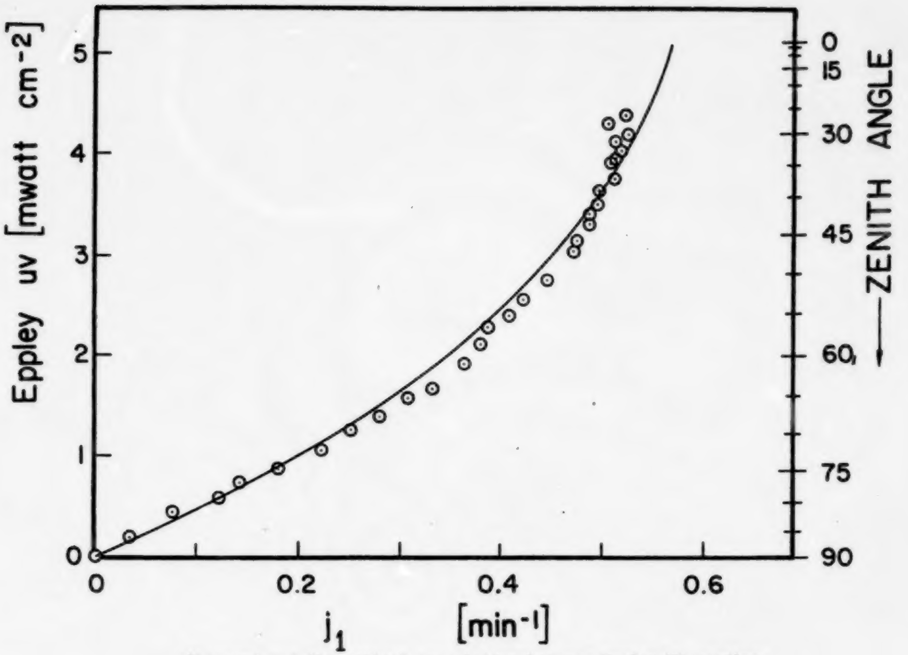

Observed and theoretical correlation between Eppley UV reading and directly measured J_1 for a clear sky. Data was taken between 12 noon and sunset in Ann Arbor, June 4, 1976. Eppley readings are given with the maximum zenith angle possible for that reading.

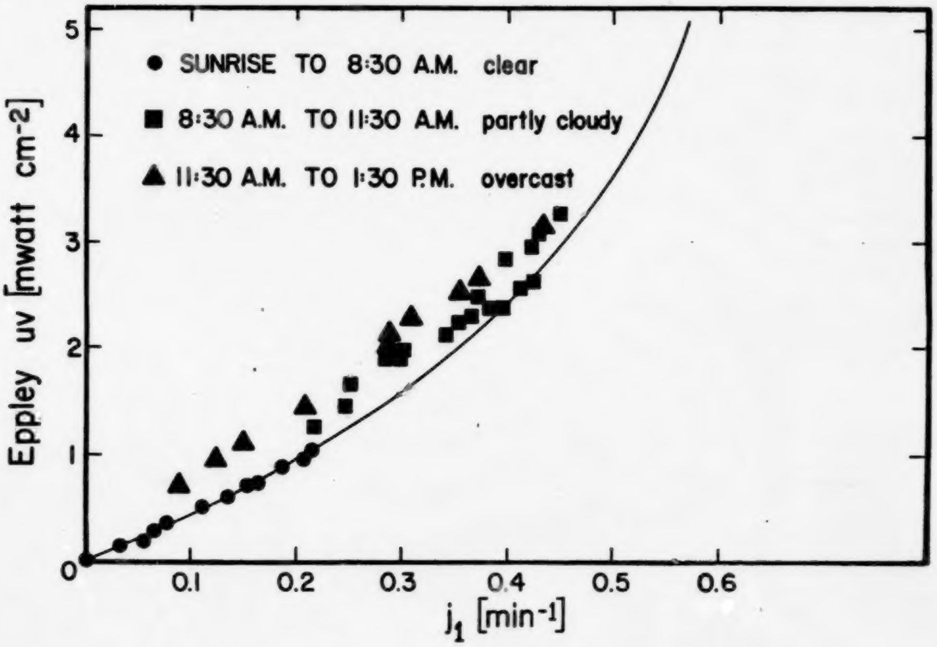

Observed correlation between Eppley and actinometer on May 28, 1976. The line is the theoretical prediction for a clear day from Figure 2.

Figure 20. Experimental nitrogen dioxide photolysis (k1) and UV measurements of Stedman, Harvey, and Dickerson (1977).

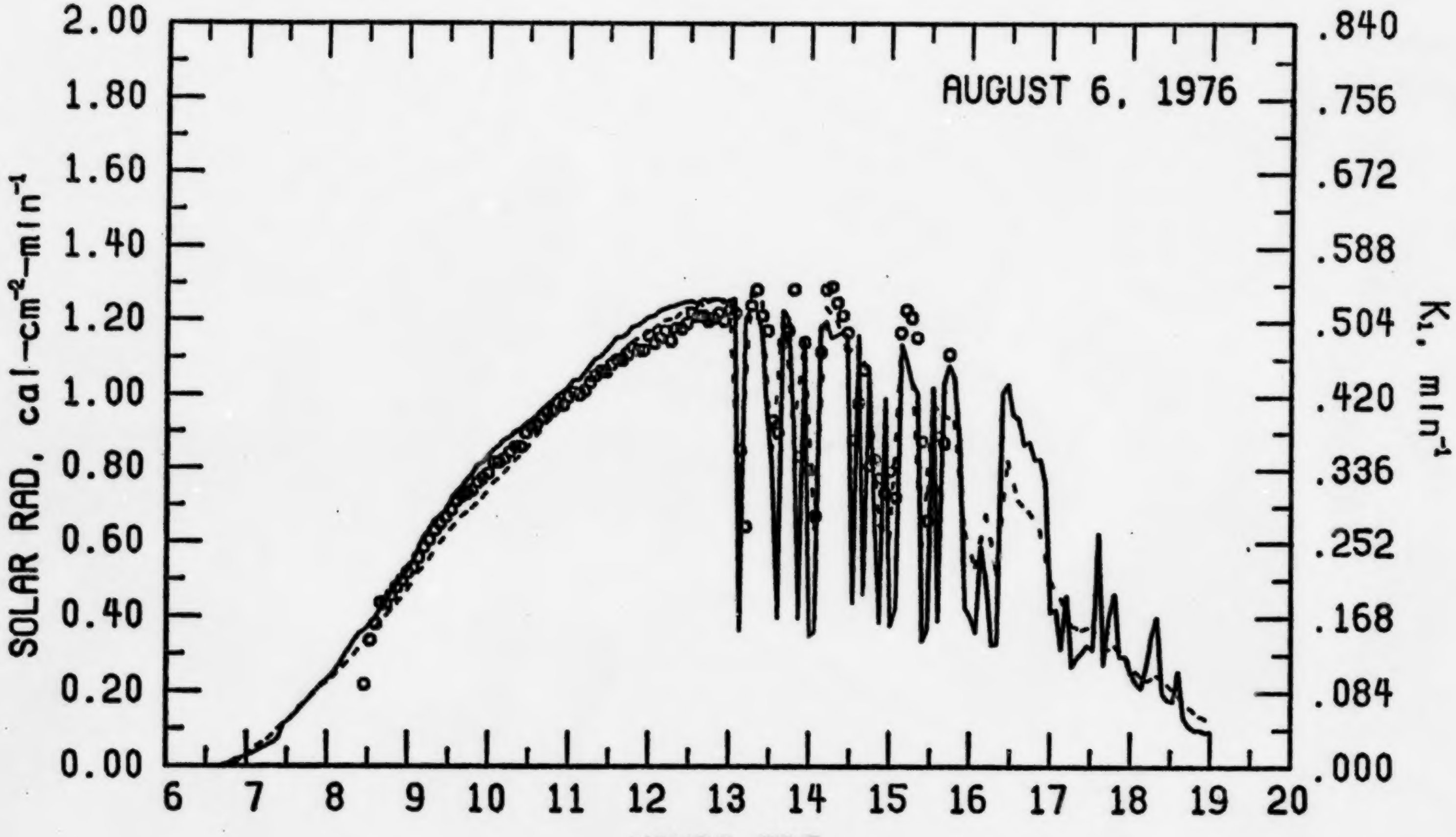

Figure 21. Specific photolysis rate of nitrogen dioxide and incident total solar radiation and ultraviolet radiation as a function of time for August 6, 1976. Solid line is total solar radiation; dashed line is ultraviolet radiation (full scale is 67.64 x 10^{-3} cal-cm^{-2}-min^{-1}); o are ambient k_1. Sky conditions were cloudy in afternoon.

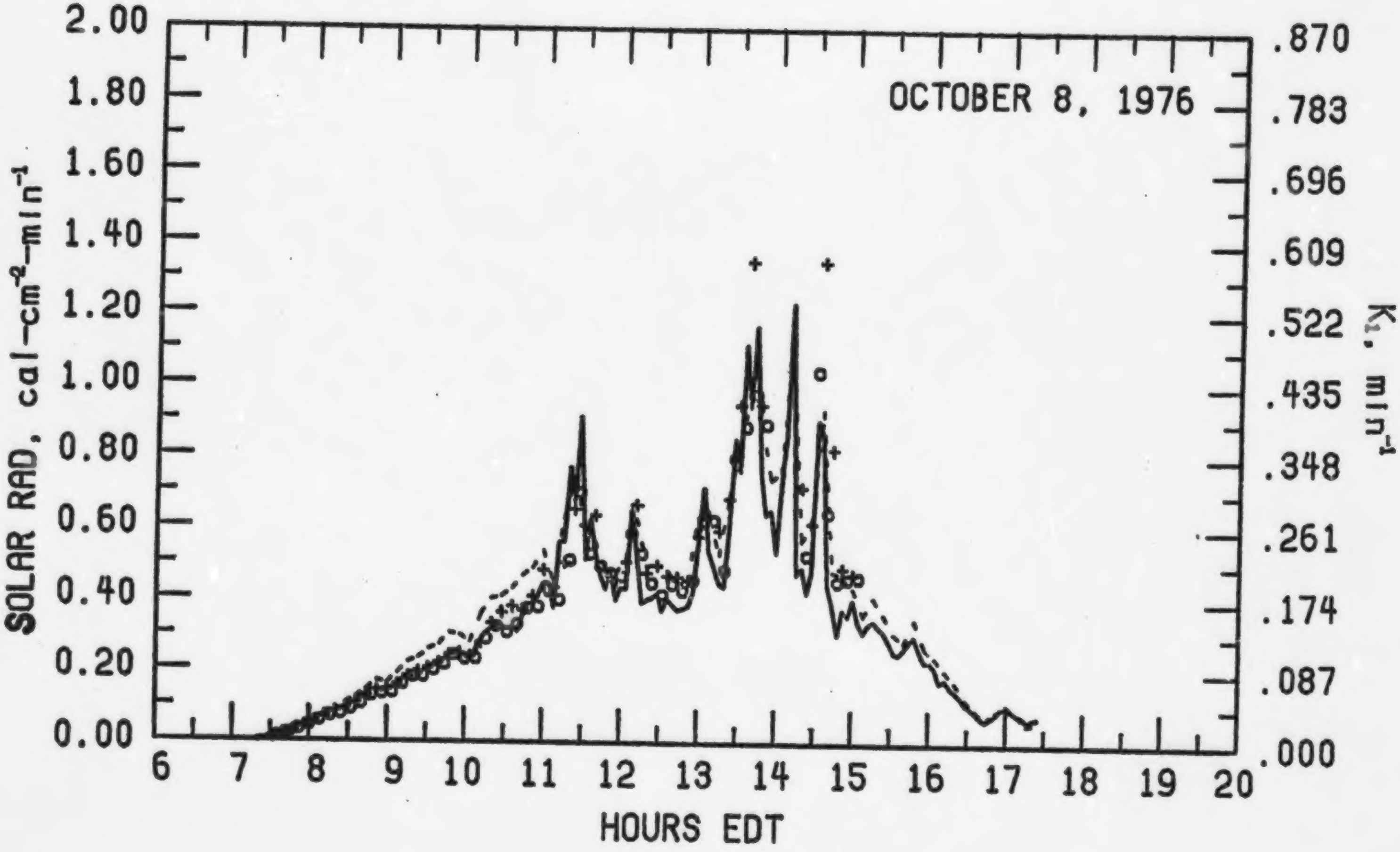

Figure 22. Specific photolysis rate of nitrogen dioxide and incident total solar radiation and ultraviolet radiation as a function of time for October 8, 1976. Solid line is total solar radiation; dashed line is ultraviolet radiation (full scale is 67.78 x 10-3 cal-cm^{-2}-min^{-1}); o are ambient k_1 + are k_1 inside the smog chamber. Sky conditions were overcast.

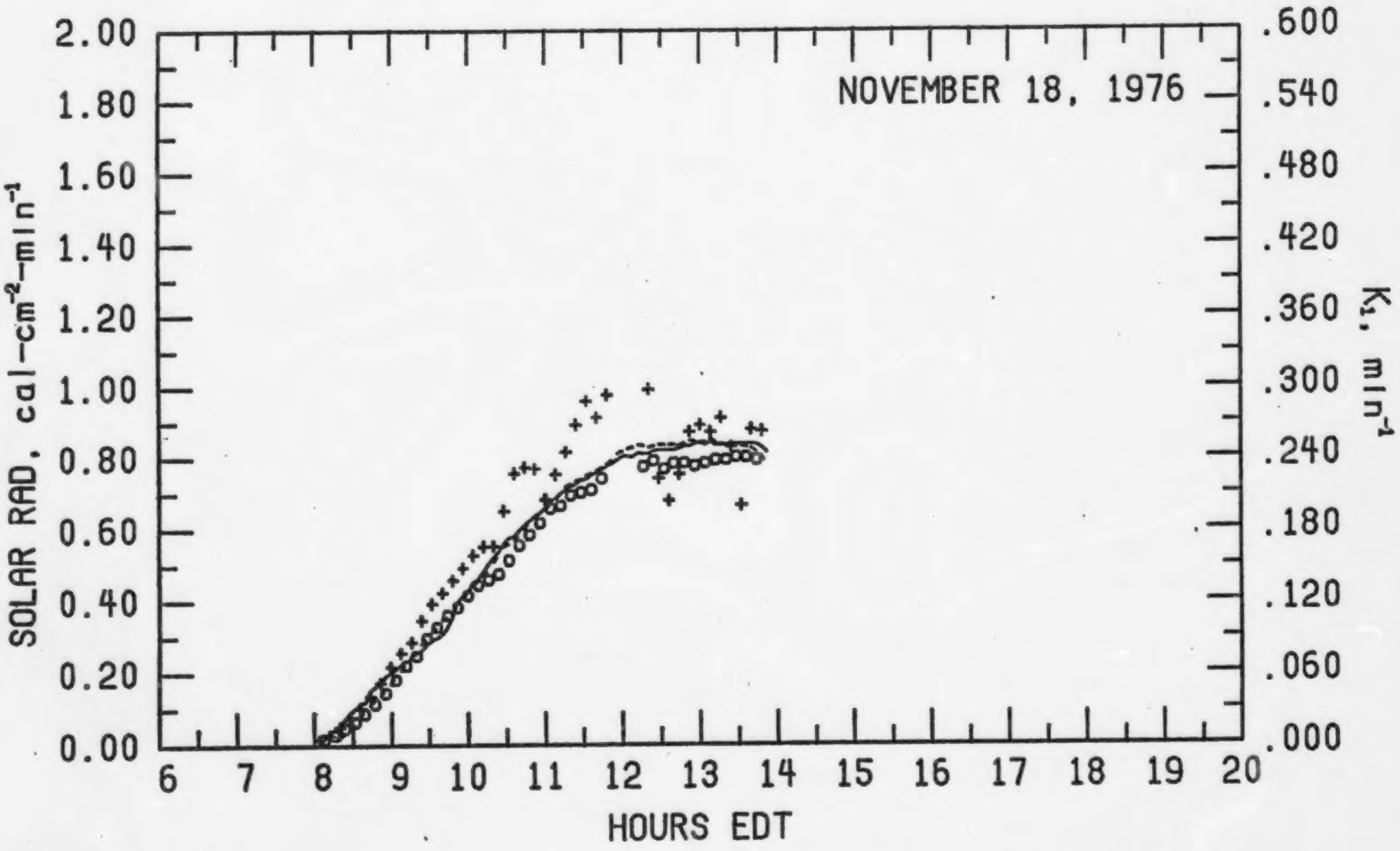

Figure 23. Specific photolysis rate of nitrogen dioxide and incident total solar radiation and ultraviolet radiation as a function of time for November 18, 1976. Solid line is total solar radiation; dashed line is ultraviolet radiation (full scale is 57.78×10^{-3} cal-cm^{-2}min^{-1}); o are ambient k_1 + are k_1 inside the smog chamber. Sky conditions were hazy.

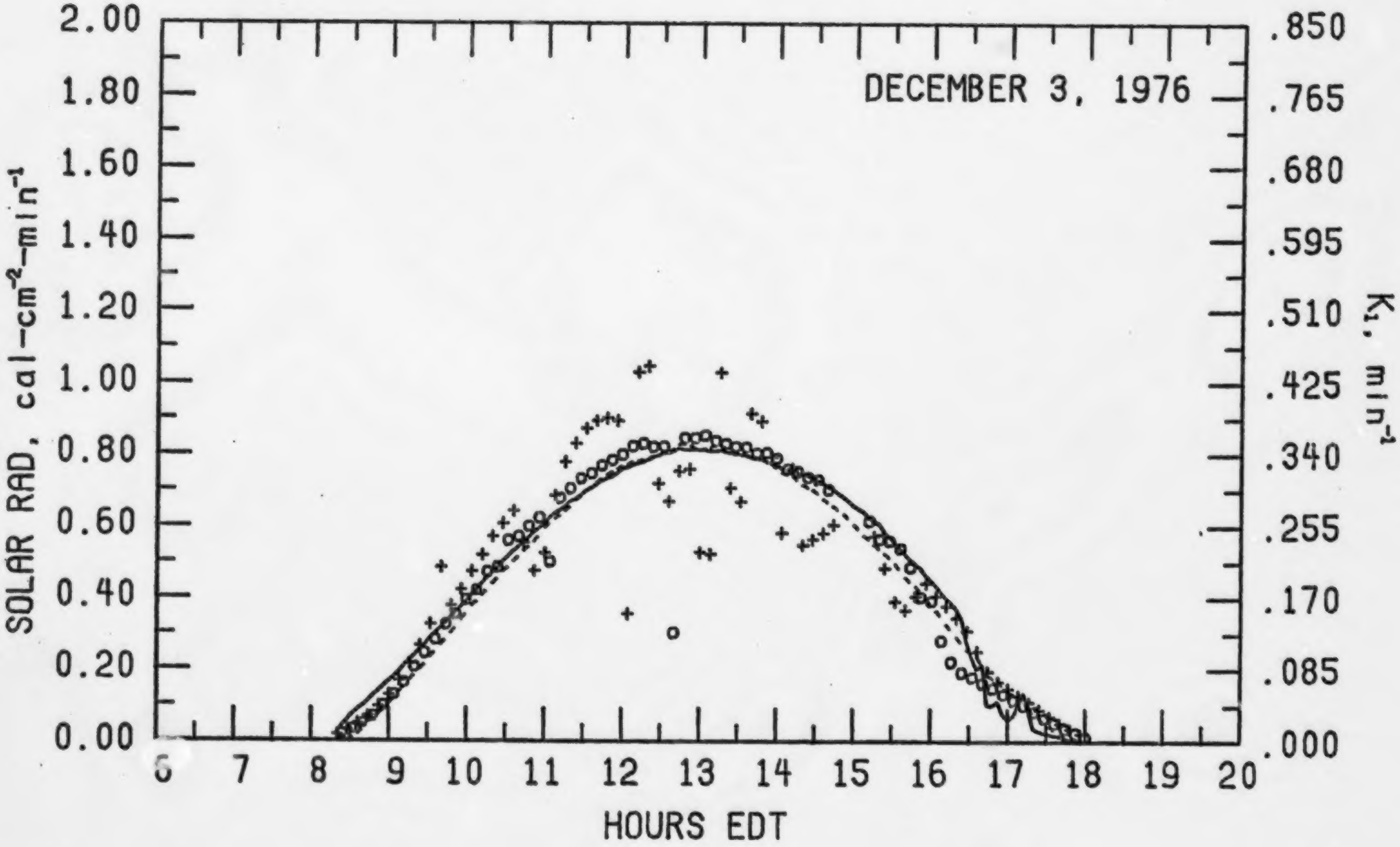

Figure 24. Specific photolysis rate of nitrogen dioxide and incident total solar radiation and ultraviolet radiation as a function of time for December 3, 1976. Solid line is total solar radiation; dashed line is ultraviolet radiation (full scale is 58.07 x 10-3 cal-cm-2-min-1); o are ambient k_1 + are k_1 inside the smog chamber. Sky conditions were generally clear.

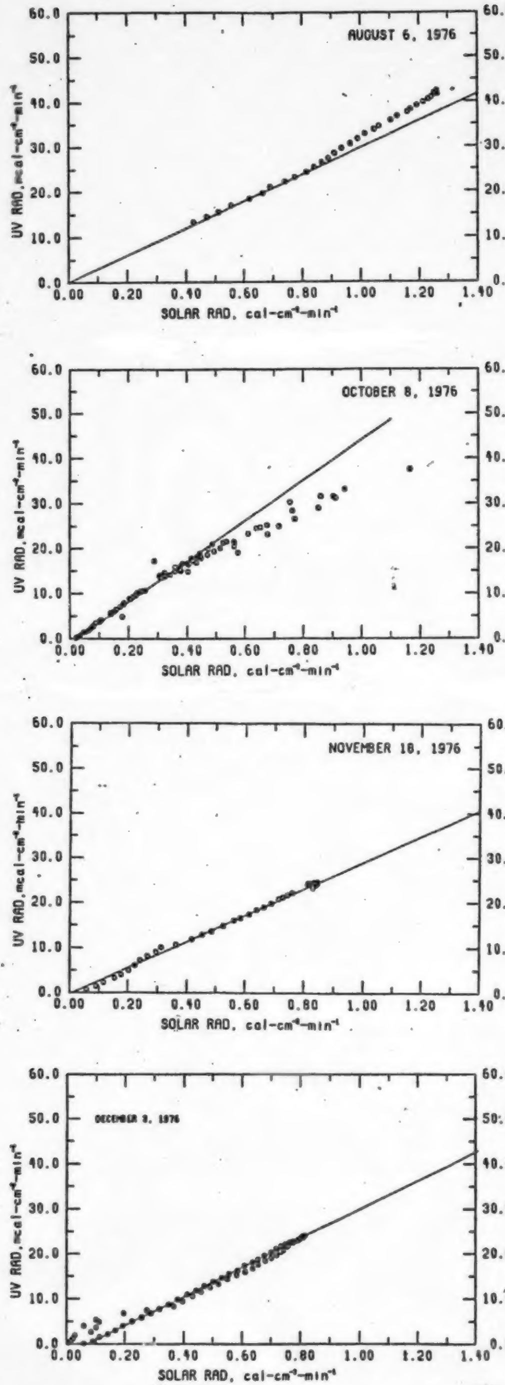

Figure 25. Comparison of UV and TSR radiometer measurements for selected days.

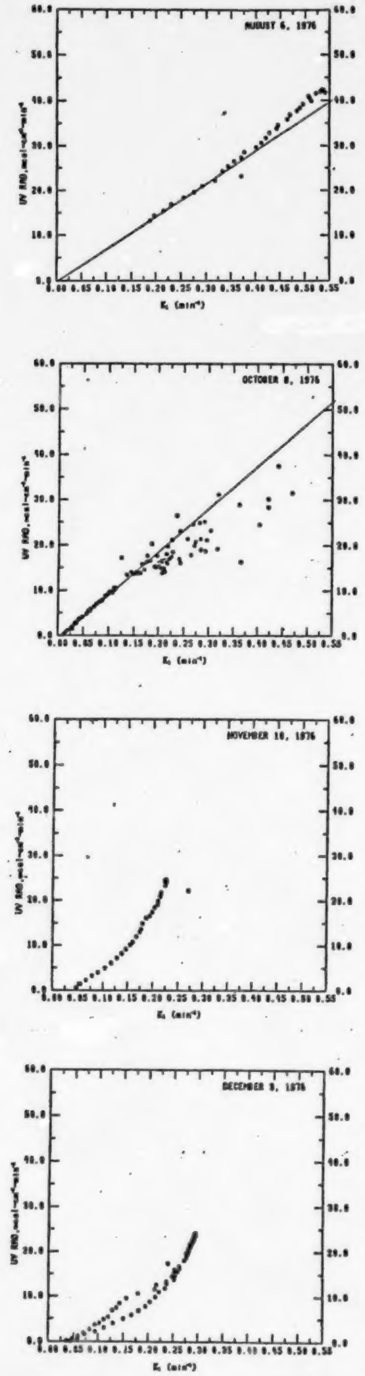

Figure 26. Comparison of UV radiometer and actinometer measurements for selected days.

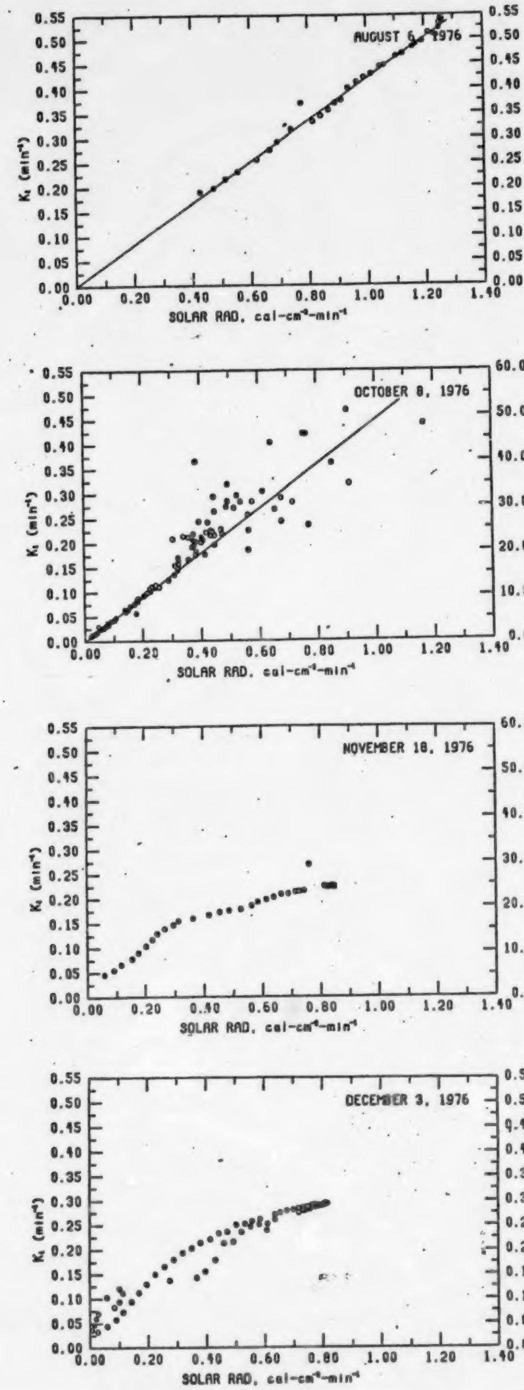

Figure 27. Comparison of TSR radiometer and actinometer measurements for selected days.

In the August 6 plot (Figure 21), the actinometer scale factor was not quite correct in that, in the period from 12 to 1300, it was not well matched with TSR. Nevertherless, the actinometer response did follow the dips in TSR caused by small clouds passing in front of the sun. Of interest is the actinometer's response inbetween these drops; the actinometer reads substaintially higher than TSR. The data density for UV is one half that of TSR and k_1. Still, it is evident at a few times in the choppiness that UV is higher than TSR. Because of the larger scattering for the shorter wavelengths, the relative UV radiation decrease by small clouds is not as great as the relative TSR radiation decrease (i.e. more UV penetrates into the shadow of the cloud).

October 8 and November 18 illustrate that heavy or thin clouds can selectively change the spectral distribution and since each sensor has a different spectral response, the comparison plots have different shapes. For example, the October 8 UV vs. k_1 plot (Fig. 26) has a downward curvature indicating attenuation of the shortest wavelengths compared to a clear day. The longer wavelengths that are not measured by the UV radiometer are mainly responsible for the NO_2 photolysis on this day. Since these longer wavelengths are measured by the TSR radiometer there is still a good linear relationship between k_1 and TSR (Figure 27) until the choppiness introduces time lag problems.

The November 18 data suggest the opposite of Oct. 8. The day appears clear in Figure 22; there are some indications of slow variations in TSR,however. The strong upward curvature of the UV vs. k_1 plot in Figure 26 and the downward curvature of the k_1 vs. TSR plot suggests that the middle of the UV spectrum was attenuated. That is, the wavelengths above the response of the UV radiometer that contribute to nitrogen dioxide photolysis were attenuated while the wavelengths above the response region of the actinometer were not attenuated and the TSR radiometer responds to these fully. The TSR intensity would be somewhat decreased because of the lost long wavelength UV.

The description of the day was hazy. Scattering by haze tends to make the sky white because longer wavelengths are scattered than by air alone. For air only, scattering is inversely proportional to wavelength to the fourth power, thus UV is most effected and visible is less effected. For haze, scattering is inversely proportional to wavelength to the first or second power, thus its effect is more in the visible region.

A least squares regression procedure was used to estimate the empirical factor needed to relate the nitrogen dioxide photolysis rate and the Epply total solar radiation measurement for each day. These regression slopes are given in Table 17. The combined factor is 0.406 min^{-1} /langley/min. Examination of the plots of k_1 suggests that clouds have greater impact on TSR measurements than they have on k_1 measurements and this tends to raise the scale factor. Therefore, the above regressions were repeated using only data with no clouds blocking the sun. These regression slopes are compared with the original slopes in Table 18. The fits are substantially improved and all slopes decreased. The clear sky factor is 0.401 min^{-1}/langley/min.

Photolysis rate inside chamber. Figure 24 shows two zenith spectral distributions, one outside the chamber and one inside the chamber. These were obtained with a spectral radiometer viewing the zenith (vertical) with a six degree apperature. That is, the instrument responded only to light coming straight down. These data illustrate the attenuation of the direct incoming radiation into the chamber even allowing for some internal chamber reflection straight down. The attenuation is relatively uniform with wavelength.

For a significant portion of the 1976 K1 study two actinometers were operated, one inside the chamber (suspended approximately in the center), and one outside over grass. Figures 22 and 23 showed examples of the two sets of measurements. As described in Appendix A, the chamber floor is designed to be reflective and although the Teflon side panels attenuate the direct incoming beam, the reflection increases the spherical (actinic) photon flux to above that for ambient conditions over grass.

Table 17. LIST OF DIURNAL SCALING FACTORS AND LEAST SQUARES REGRESSION SLOPES FOR SELECTED EXPERIMENTS

Date	Regression Slope min^{-1}/langley min^{-1} TSR	r^2
8/5/76	0.3763	0.9971
8/6/76	0.4166	0.9647
combined August	0.3962	0.9767
10/4/76	0.5242	0.9117
10/5/76	0.3579	0.8177
10/6/76	0.4503	0.9590
10/8/76	0.4190	0.9585
10/13/76	0.4922	0.9793
combined October	0.4412	0.9364
11/18/76	0.2846	0.9988
11/19/76	0.3810	0.9687
combined November	0.3394	0.9585
11/30/76	0.4008	0.9639
12/2/76	0.3907	0.9818
12/3/76	0.4201	0.9806
combined December	0.4051	0.9754
all days combined	0.4064	0.9563

Table 18. COMPARISON OF REGRESSION SLOPES + CORRELATION COEFFICIENTS COMPUTED WITH ALL DATA POINTS INCLUDED TO REGRESSION SLOPES + CORRELATION COEFFICIENTS COMPUTED AFTER ELIMINATING DATA POINTS COLLECTED WHILE PASSING CLOUDS WERE BLOCKING THE DIRECT SOLAR BEAM

DATE	Original Slope, min^{-1}/langley min^{-1}	r^2	Corrected Slope, min^{-1}/langley min^{-1}	r^2	% change
8/5/76	0.3763	0.9971	0.3749	0.9978	-0.372
8/6/76	0.4166	0.9647	0.4060	0.9992	-2.544
combined August	0.3962	0.9767	0.3888	0.9969	-1.868
10/4/76	0.5242	0.9117	0.5163	0.9966	-1.507
10/5/76	0.3579	0.9177	0.3444	0.9972	-3.772
10/6/76	0.4503	0.9590	0.4452	0.9972	-1.133
combined October	0.4412	0.9364	0.4463	0.9697	-1.156
all days	0.4064	.9563	0.4008	0.9768	-1.378

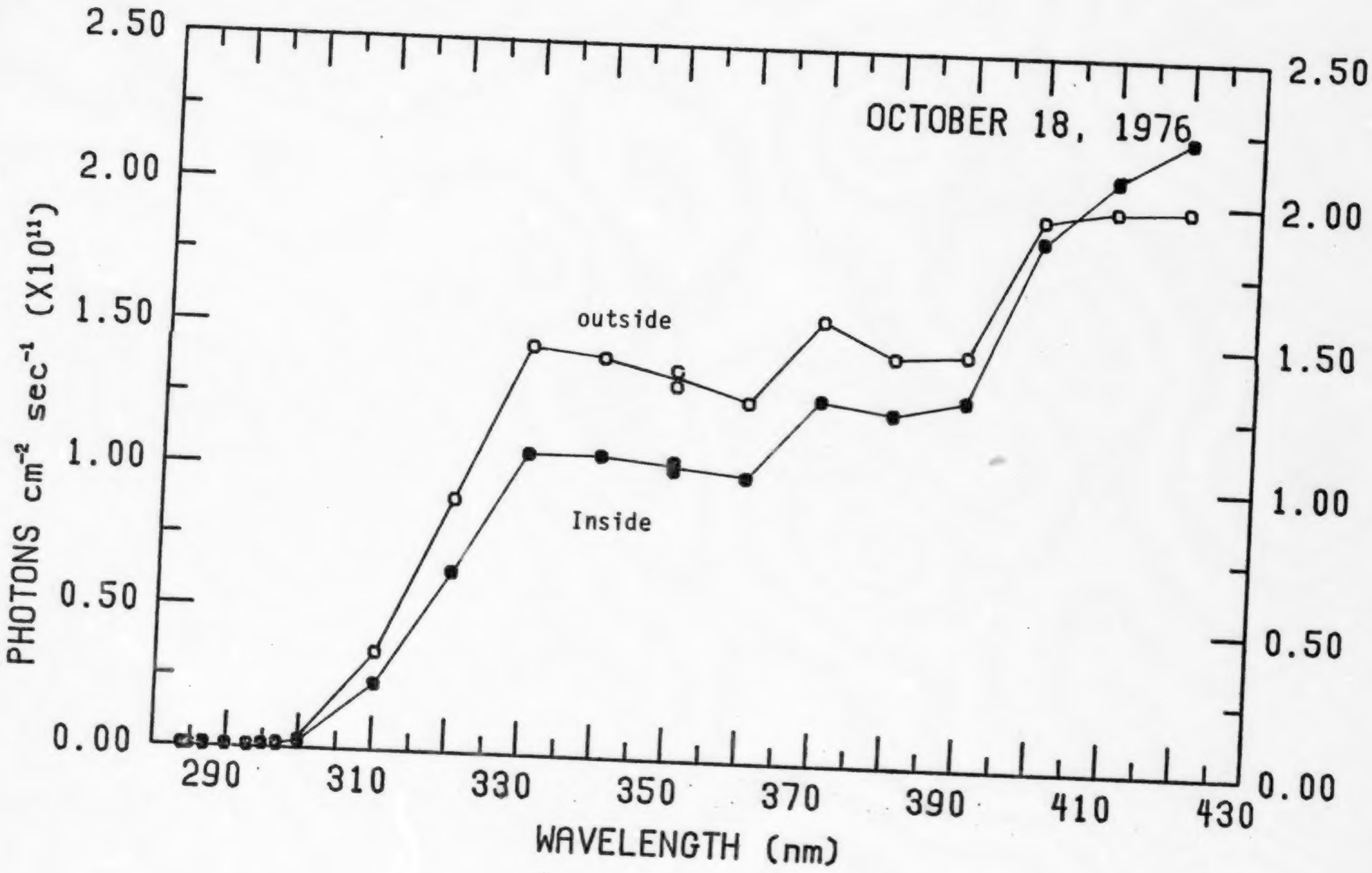

Figure 28. Zenith spectral distribution (6° view) outside and inside UNC outdoor smog chamber at 1400-1500 EDT.

A complicating factor in determining the chamber actinic intensity is that the chamber structural members cast shadows into the chamber volume (see chamber photograph in Appendix A). In the measurement of k_1 inside the chamber the quartz flask, therefore, is alternately in direct sunlight and in shadow with periods varying from half an hour to several hours. The shadowing of the actinometer lasts from four to ten minutes. Table 19 gives the average ratio of k_1 inside to k_1 outside for periods when the actinometer was in shadow and in direct beam. Also shown in the table are estimates of the ratio of inside to outside k_1 accounting for the fraction of the chamber in shadow. The shadowing of the chamber was estimated by using three dimensional projection techniques from the sun as a viewpoint.

Since the amount of reflection is partially a function of angle of incidence, the spherical intensity will probably vary with solar zenith angle. There is some evidence of this variation in the decreasing values between October and December in Table 19. Furthermore, inspection of Figures 22 and 23 suggest very little enhancement at the low solar altitudes (large zenith angles) of early morning and late afternoon.

Using the above information, SAI (Whitten et.al.,1980) developed a simple algorithm for estimating the ratio of inside to outside k_1 using the solar zenith angle. In this procedure it is assumed that the ambient k value as a function of time is known and that the solar zenith angle can be computed from location and date for any time of day. The algorithm is:

when $(90 > Z > 72)$: $k_1p = k_1$

when $(72 > Z > 44)$: $k_1p = k_1\ (0.85 + 0.486 \cos(Z))$

when $(44 > Z > 0)$: $k_1p = k_1\ (1.20)$

where Z = zenith angle

k_1p = inside chamber value

k_1 = outside ambient value

The 20% enhancement occurs with a zenith angle of less than 44 degrees; this value is the angle at noon near October 1. Therefore, days before October 1 will have a 20% enhancement for a period centered around noon, and days after October 1 will have less than a 20% enhancement at noon.

Table 19. GROUPED AVERAGE RATIOS OF k_1 INSIDE THE SMOG CHAMBER TO AMBIENT k_1 WHILE THE INSIDE ACTINOMETER WAS SHADED FROM THE DIRECT SOLAR BEAM, AND WHILE THE INSIDE ACTINOMETER WAS EXPOSED TO THE DIRECT SOLAR BEAM

Clear Days	Average Ratios			Weighted Average	
	Sensor in Shadow	Sensor not in Shadow	Average of All Points	25% shaded [a]	30% shaded [b]
October 13, 1976 Scaling Factor 0.451	1.0375	1.2390	1.1527	1.1886	1.1786
November 18, 1976 Scaling Factor 0.300	1.0205	1.2245	1.1617	1.1735	1.1633
December 3, 1976 Scaling Factor 0.425	0.8342	1.1692	1.053	1.0855	1.0687
Overcast Day					
October 8, 1976 Scaling Factor 0.435			1.0323		

[a] Overall ratio of k_1 inside the smog chamber to ambient k_1 assuming 25% of the smog chamber volume was shaded

[b] Overall ratio of k_1 inside the smog chamber to ambient k_1 assuming 30% of the smog chamber volume was shaded

Summary and Recommendations

Total solar radiation (TSR) and ultraviolet (UV), (295-385 nm) radiation exhibit not only day to day variables but also year to year trends that are probably climitologically related.

TSR data for 1979 are good only for indicating cloud cover and not for determining intensity because of a damaged sensor. UV data for 1979 are valid.

The UV sensor does not respond to the longer wavelengths contributing to NO_2 photolysis (K_1); as much as 25% of the photolysis can occur at wavelengths not measured by the UV sensor. The TSR sensor responds to all wavelengths that photolyze NO_2.

Because of sensor spectral responses and the increased scattering of UV at larger zenith angles, a plot of UV vs TSR is expected to show curvature with an increase in UV proportion occuring near noon. This occurs for clear days.

Likewise, a plot of UV vs. K_1 is expected to show a curvature because more short wavelength UV is available at small zenith angles and longer wavelength UV not measured by the UV sensor makes significant contribution to the K_1 measurement.

Plots of K_1 vs. TSR show a linear relationship and the TSR sensor responds to all NO_2 photolysis wavelengths.

A best clear sky estimate of the ratio of NO_2 photolysis rate to total solar radiation is 0.401 $min^{-1}/cal\text{-}cm^{-2}\text{-}min^{-1}$) with an r^2 of 0.977.

Days with small clouds have higher ratios, some as high as 0.450 $min^{-1}/cal\text{-}cm^{-2}\text{-}min^{-1}$).

Near the middle of the day the photolysis rate inside the chamber is higher than that above grass outside the chamber. The enhancement is 18-20% and probably depends upon zenith angle.

Recommendations for simple procedures

(In order of decreasing preference)

- For NO_2 photolysisrate:
  1) Scale TSR by 0.40 min^{-1}/langley/min;
  2) Scale UV using curved relationship;
  3) Use theory.
- For HCHO photolysis rate:
  1) Scale UV using linear relationship;
  2) Scale TSR using curved relationship;
  3) Use theory.
- Use SAI algorithm for chamber enhancement of rates

A comparison of nitrogen dioxide photolysis rates computed from theory (with best estimates albedo) and computed from the preferred empirical relationship for TSR is shown in Figure 29.

Best practice might be to use a combination of UV and TSR sensor comparison plots, spectral responses, and theory with estimated modified spectral input to estimate rates for all photolytic species.

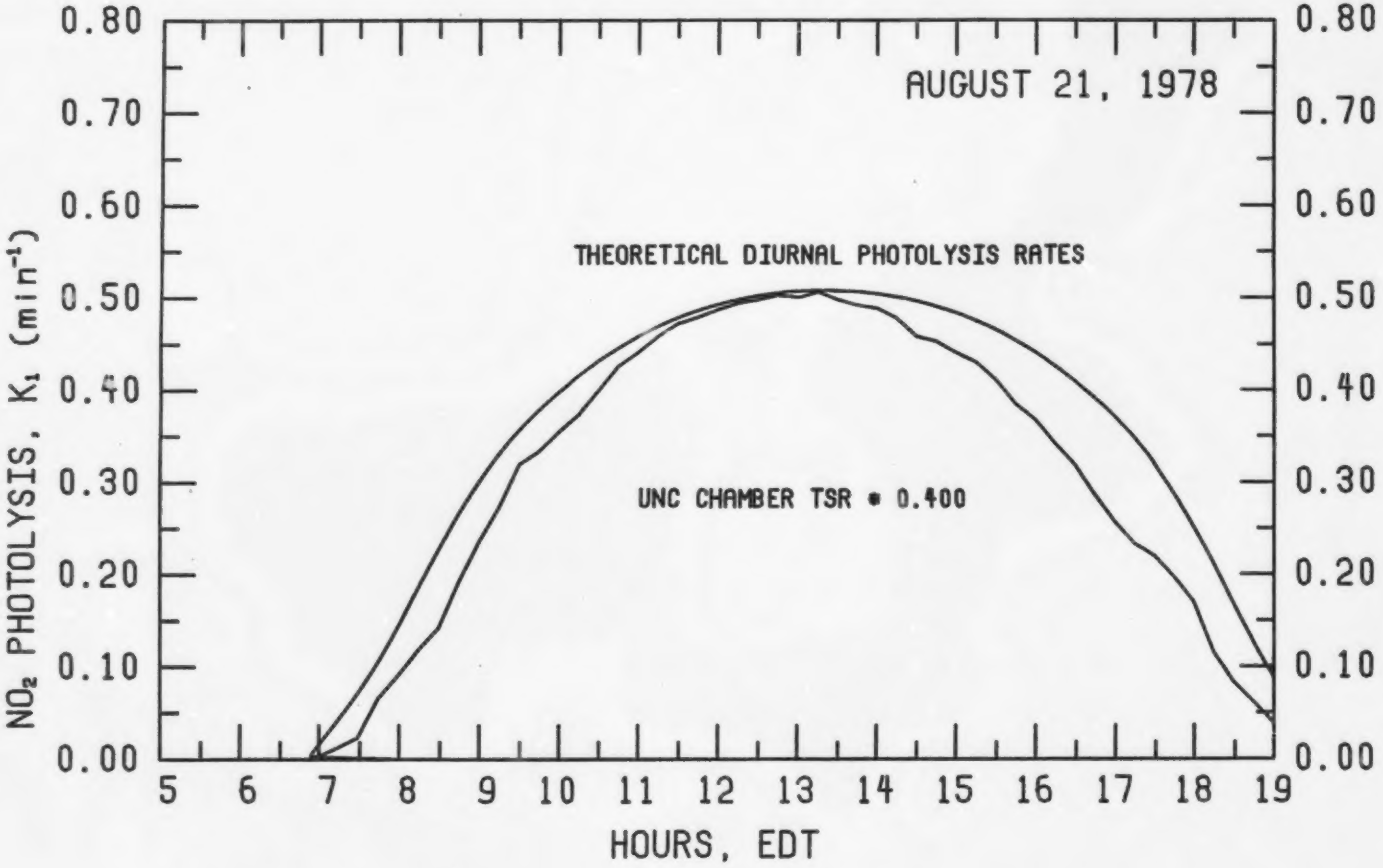

Figure 29. Comparison of theoretical calculated and empirically calculated nitrogen dioxide photolysis rate at UNC chamber.

DILUTION RATES

Explanation of the Dilution Process

There are three processes that cause chamber dilution: 1) sampling, 2) heating and cooling of the chamber, and 3) wind "pumping".

To sample the chamber, air is drawn from the chamber through a loop and returned to the chamber. Instruments sample air from the loop; the air drawn through the instruments is wasted. The total sample rate is estimated to be 5 liters/min. This corresponds to a dilution rate of $3 \times 10^{-5} min^{-1}$. Measured dilution rates are approximately $1.6 \times 10^{-4} min^{-1}$, about five times higher than the calculated value, corresponding to an exchange of about 25 liters/min in a volume of 153,000 liters. Losses of air in fan housings even though these are sealed with Teflon plates and gaskets may account for some of this loss.

The temperature usually rises during the first eight to nine hours after sunrise. Depending upon the cloud conditions, however, the temperature can increase, decrease, and increase again (see Figure 2, August 8, 1977). As the temperature rises, the volume and/or the pressure of the air in the chamber increases. This results in air and pollutants being expelled out of chamber cracks and fittings. Likewise, cooling of the chamber air results in external ambient air being drawn into the chamber. The former process is not experienced as dilution because the mixing ratio is not changed (loss of air and pollutant together) temperature in the sampling instruments. The cooling process is experienced as a dilution because the mixing ratio is changed by introduction of air only. For most of the run, temperature effects then contribute only a small amount to the dilution process.

The Teflon film walls of the chamber have some flexibility and the center of each panel can be moved up to two inches. Strong winds can cause the side panels to move in and out and thus "pump" the chamber by increasing and decreasing its volume. If this occurs very often throughout the day, the dilution rate can be substantially increased.

The combination of the above processes and their variations can result in dilution rates that vary over a range of 1 to $3 \times 10^{-4} min^{-1}$ (0.6-1.8%/hr).

Average Values

Until 1980 the chamber leak rate due to above processes was monitored during selected experiments in which high concentrations of CO or Freon were added to the chambers as inert gases. The rate of disappearance of these gases was taken to be the dilution rate. In 1973 and 1974 the rate could be approximated by a linear rate of 1%/hr. In 1975 it increased to 1.3%/hr because the chamber support structure needed repair and this caused additional stress on the Teflon wall panels creating more cracks. After rebuilding the entire chamber in 1976 a leak rate of 0.7% - 0.8% was observed. In general during 1977, 1978 and 1979 the Blue chamber dilution rate was approximately 0.8%/hr and the Red chamber was approximately 0.9%/hr.

Individual Values

In 1980 dilution was monitored more routinely by electron capture detection of CCl_4 and SF_6.
An example of monitoring the dilution rate by CCl_4 is shown in Figure 30 for the night of April 15-16. The lower plot shows that the chamber temperature was decreasing throughout the entire 400 minute period; as explained above, decreasing temperature is a major process for dilution. The rapid initial drop in temperature is reflected in the inital drop in CCl_4 concentration. Changes in rates of temperature decrease lead to changes in dilution rates. Using $k=(-1/t)*\ln(C/Co)$, the rates of dilution calculated from these data were (units min^{-1}): average=$3.6x10^{-4}$; minimum value=$2.2x10^{-4}$; maximum value=$5.3x10^{-4}$. The average value corresponds to an intake of approximately 50 liters/min by the cooling process.

A list of runs having daytime tracer data and daytime values estimated from these are given in Table 20.

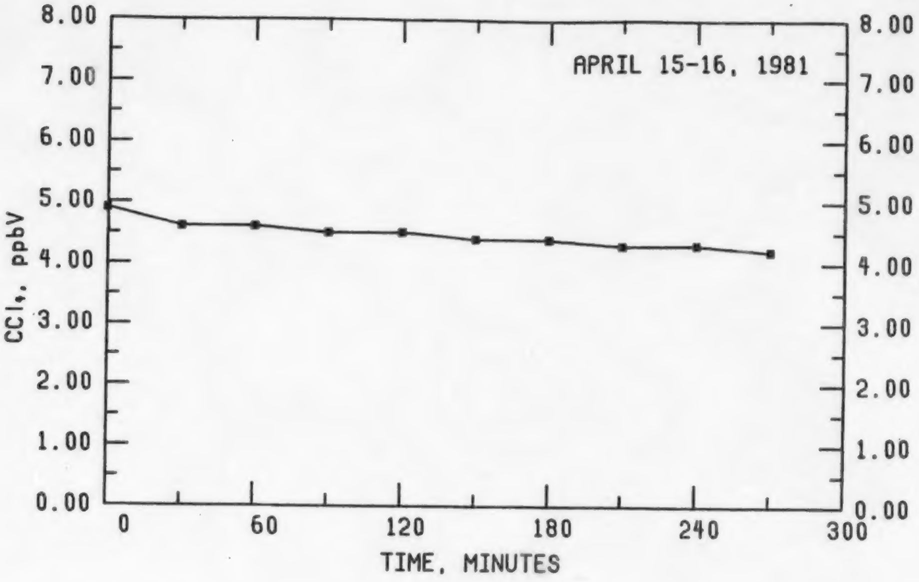

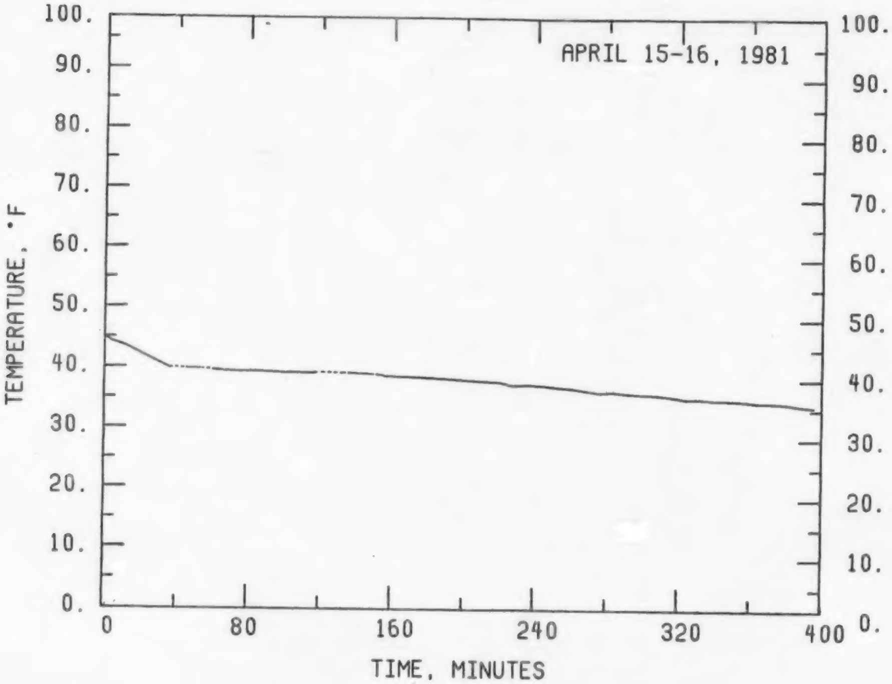

Figure 30. Chamber dilution process: measurements of carbon tetrachloride in the chamber (top figure) and chamber air temperature (bottom figure) in a nighttime experiment.

Table 20. 1980 Linear Dilution Rates* of UNC Chambers Due to Sample Losses and Leaks.

#	Date	B	R
1	August 1, 1980	0.7%/hr	1.1%/hr
2	August 14, 1980	-	1.75%/hr
3	August 26, 1980	1.72%/hr	1.89%/hr
4	August 27, 1980	1.76%/hr	1.83%/hr
5	July 31, 1980	1.25%	1.03%/hr
6	July 22, 1980	-	1.50%/hr
7	August 6, 1980	2.3%/hr**	1.30%/hr
8	August 30, 1980	-	0.95%/hr
9	September 1, 1980	-	1.30%/hr
10	September 3, 1980	-	0.80%/hr
11	September 7, 1980	-	1.32%/hr
12	September 8, 1980	-	0.92%/hr
13	September 15, 1980	0.82%/hr	0.87%/hr
14	September 22, 1980	-	1.19%/hr

*Dilution data taken by monitoring ppb levels of CCl_4 over 5-10 hours during the day light hours.

**Make up air valve may not have been completely shut off after early morning drying.

OZONE WALL LOSS

Ozone reacts with materials in the background air and with the surfaces of the chamber and is lost. During the daytime, O_3 is photolyzed as well. To characterize the former process, O_3 decay experiments have been performed at night. Figure 31 shows O_3 data for the same April 15-16, 1981 run that was used to illustrate the dilution. In this run O_3 was ramp-injected into the chamber for a period of 120 minutes and then allowed to dilute and decay. The concentration decreased from 0.622 ppm to 0.537 ppm in 280 minutes. This corresponds to an average loss rate of $5.3\times10^{-4}\mathrm{min}^{-1}$, but dilution was occurring at a rate of $3.6\times10^{-4}\mathrm{min}^{-1}$; therefore, O_3 was reacting with the walls at a rate of $1.7\times10^{-4}\mathrm{min}^{-1}$.

Figure 33 in the next section also shows ozone decay on the night of August 5-6, 1979. On this night, the temperature remained essentially constant and therefore the dilution process described in the previous section did not occur. The rate calculated for these conditions was $1.17\times10^{-4}\mathrm{min}^{-1}$, somewhat less than the above value.

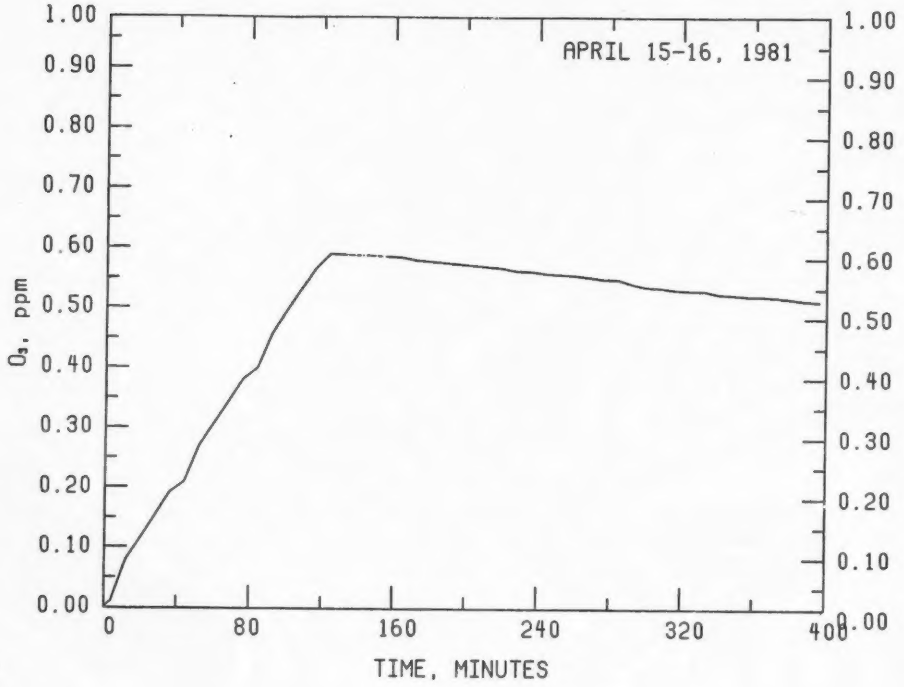

Figure 31. Illustration of ozone wall loss and dilution in a nighttime experiment. Ozone injected for first 120 minutes.

NOX WALL LOSSES

As shown in Figure 32, the August 8, 1977 nitrogen balance plot, not all of the initial nitrogen injected into the chamber can be accounted for by the gas phase measurements of the expected products: NO, NO_2, PAN, HNO_3, and alkylnitrates.

In performing a series of photochemical modelling tests of UNC chamber experiments, we have found that the best accounting of the lost nitrogen is the assumption that it is caused by the reaction

$$N_2O_5 + H_2O(\text{walls}) \rightarrow HNO_3(\text{walls})$$

The rate that best characterizes our propylene, ethylene, formaldehyde, acetaldehyde, and simple mixture experiments is $1.5\times10^{-5}\,\text{ppm}^{-1}\text{-min}^{-1}$, assuming that H_2O (wall) is directly proportional to the gaseous water vapor mixing ratio. (This value was also used by SAI in their modelling of UNC formaldehyde experiments, [Whitten et al, July 1980]).

Figure 32 shows the measured nitrogen balance, the model predicted nitrogen balance, and a comparison of experimental data and model predictions in a standard plot. This model used Reactions 3 to 6 in Table 21 to represent the N_2O_5 chemistry.

As a further test of this sequence, a special nighttime run was conducted in the two chambers. The run is shown in Figure 33. In the RED side of the chamber 0.38 ppm of NO_2 was injected into clean ambient air; the BLUE side of the chamber had only ambient air. Ozone was alternately injected into the two sides every two seconds at a rate of 0.21 ppm/hour for 51 minutes (total injection of 0.18 ppm in each side). In the RED side, the O_3 reacted with the NO_2; in the BLUE side, the O_3 reacted only with the walls.

A six step mechanism (Table 21) was used to simulate the results of the RED side for this experiment and the predictions are shown also in Figure 33. The agreement is nearly perfect.

It is recommended that the reaction

$$N_2O_5 + H_2O \rightarrow HNO_3 \text{ (walls)}$$

be included in models of UNC data with a rate constant of $1.5\times10^{-5}\,\text{ppm}^{-1}\text{-min}^{-1}$ and the H_2O concentration be determined from dewpoint data.

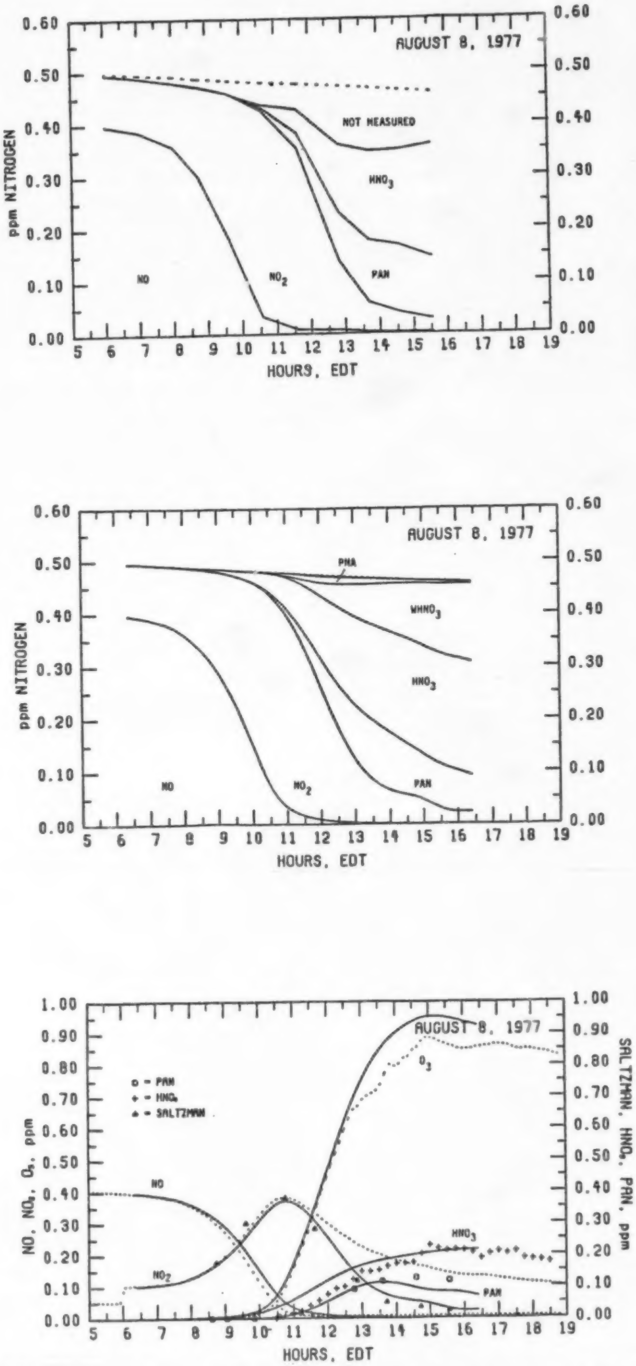

Figure 32. Illustration of probable nitrogen wall loss. Measured nitrogen balance (top figure), model predicted nitrogen balance (middle figure) showing predicted nitric acid on walls (WHNO3), and a comparison of experimental data (dashed lines and symbols) and model predictions (solid lines) in the bottom figure.

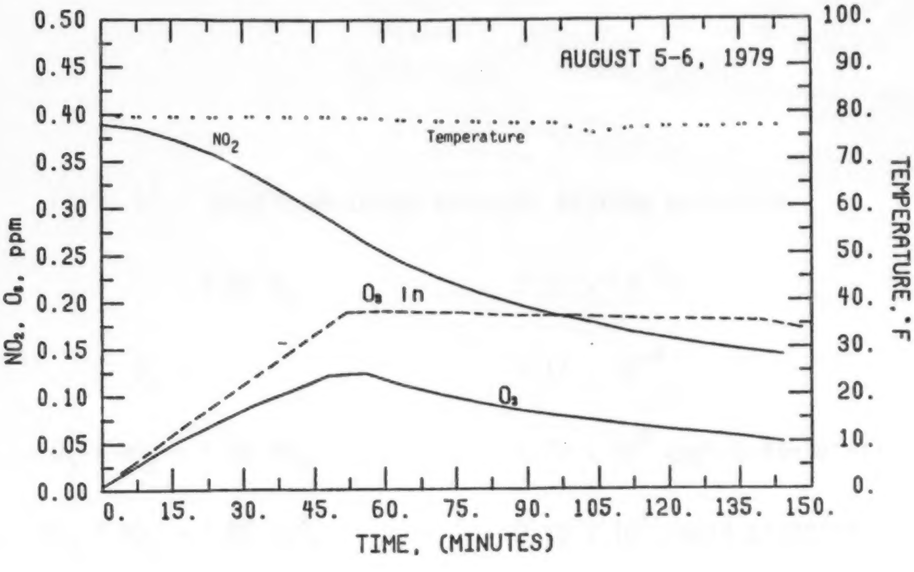

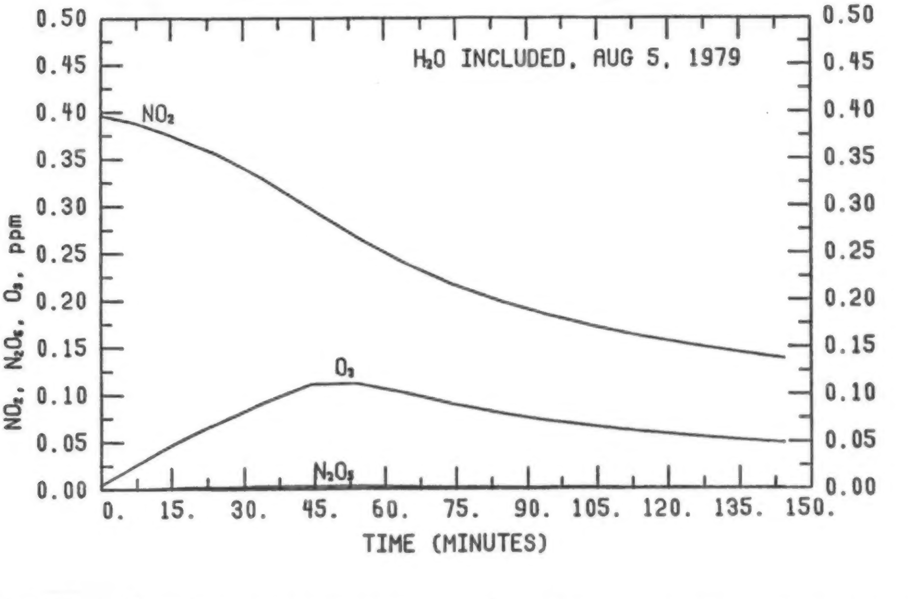

Figure 33. Chamber measurements for a nighttime experiment (top figure). Ozone injected into both chambers for first 51 minutes. Model predictions using six step mechanism (bottom figure).

WALLS AS SOURCES OF RADICALS

There are no direct methods for determining the extent to which walls of a smog chamber are sources of radicals. Therefore, the magnitudes of the processes have been inferred from model results. Unfortunately, the magnitude of wall radical sources needed to make the models work well varies with other assumptions in the model and consequently from one modeling group to another. Thus, whenever the model does not perform well, the modeller is tempted to add a wall source to improve the fit. Nevertheless, walls can be significant sources of radicals or serve as sites for processes that in turn are sources of radicals.

The most commonly invoked wall-related radical source in models is the presumably heterogeneous formation of nitrous acid (HONO) that probably occurs during NO and NO_2 injections. The revised homogeneous (gas-phase) chemistry of HONO formation and photolysis (Howard, 1977, Cox and Derwent, 1976, Stockwell and Calvert, 1978) has substantially lessened HONO's role in photolytic situations. Whitten et al., at SAI have demonstrated that the HONO daytime chemistry can be removed from the model provided HONO's role as an initial radical source is accounted for; Figure 34 illustrates SAI's models of August 8, 1977 with and without HONO.

During NOx injections, high concentrations (up to thousands of ppm) can occur during mixing for very short time periods; near surfaces with absorbed water this can lead to the possibility of forming HONO. These conditions are not likely to be very reproducible and thus some trial and error may be needed on each experiment to estimate the appropriate quantity to include in the initial conditions model. The sensitivity of the UNC propylene model to estimated initial HONO is shown in Table 22. Estimates of initial HONO used by SAI in modeling some of the UNC data are given in Table 23.

A simple way walls may be a source is for material adsorbed on the walls from a previous run to be released in the next run. The previous section demonstrated that nitrogen was sometimes lost, probably as HNO_3 to the walls. In another report UNC has shown that under a narrow range of environmental conditions this nitrogen on the walls has

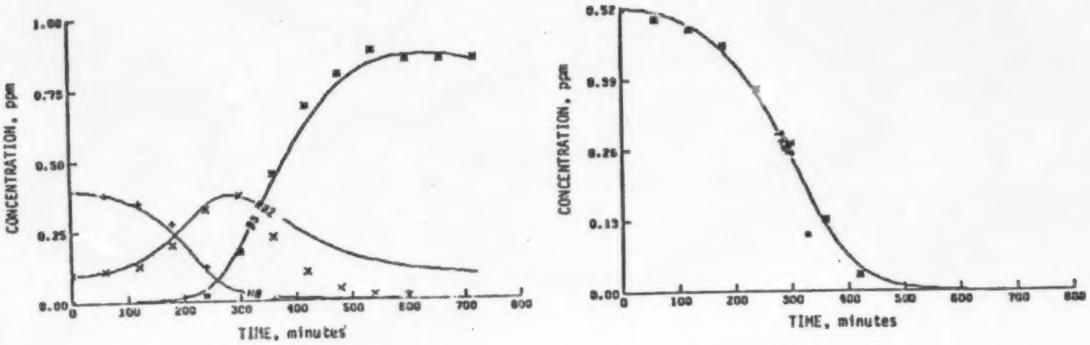

(a) NO_2, NO, and O_3

(b) Propylene

UNC propylene/NO_x measurements (8 August 1977) and explicit propylene mechanism predictions without HONO chemistry (an initial concentration of 1.5 ppb of radical source "RX" was included)

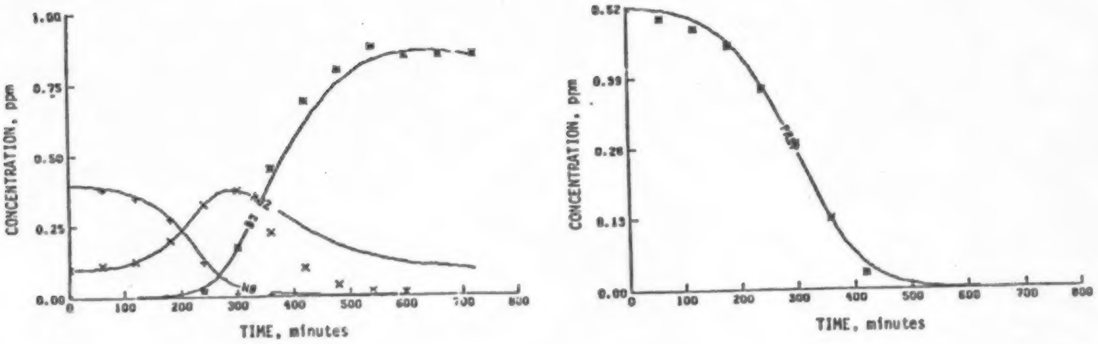

(a) NO_2, NO, and O_3

(b) Propylene

UNC propylene/NO_x measurements (8 August 1977) and explicit propylene mechanism predictions with HONO chemistry included (initial HONO concentration of 3 ppb)

Figure 34. Effect of adding HONO to SAI model of UNC smog chamber run.

Table 22. Effect of Initial Nitrous Acid Concentration Assumptions on UNC Propylene Model Predictions

Assumed Initial [HONO]ppb	October 22, 1977		August 8, 1977	
	Crossover min.	NO2 Max min.	Crossover min.	NO2 Max min.
0	162	220	217	291
1	152	216	200	279
2	145	213	187	273
3			177	262
5	125	192	162	246
10	103	180	126	222
Chamber results:	158	221	180	266

Table 23. Initial Nitrous Acid Concentrations Assumed by SAI for Selected Chamber Runs

Run Date	Compound	Conc, ppm	NOx, ppm	HONO,ppb
780805R	Propylene	0.83	0.25	8.0
780805B	Propylene	1.55	0.56	13.0
780821B	Propylene	1.28	0.98	10.0
781021B	Propylene	3.54	0.50	1.5
781021R	Propylene	3.50	0.50	2.0
780817B	Acetaldehyde	4.00	0.70	15.0
780817R	Acetaldehyde	0.96	0.70	15.0
790801R	Acetaldehyde	1.91	0.35	9.0
790801B	Formaldehyde	1.00	0.35	3.0
790802B	Formaldehyde	1.01	0.21	2.0
790804B	Formaldehyde	0.56	0.23	3.0
790805B	Formaldehyde	1.20	0.54	0.0
790730B	Formaldehyde	2.00	0.29	8.0
790730R	Formald/CO	2.00	0.29	6.0
790907R	Ethylene/Form	1.34	0.55	8.0
790907B	Ethylene/Form	1.30	0.55	2.0
EC-278				5.0
EC-279				9.0
EC-314				5.0

served as a source of NO_2 and HNO_3. The environmental conditions for this to occur are not those for runs suitable for modeling (e.g. heavy overcast in early morning) and therefore we do not believe this process is of any importance in modeling the experiments included herein.

Under near saturation conditions for water vapor, (cool morning temperature) formaldehyde injected into the chamber is adsorbed on the walls and then released as the temperature rises and the relative humidity falls. The majority of the formaldehyde experiments selected for inclusion in this report were "dried" experiments in which a refrigeration system was used to remove a large quantity of H_2O before the run began. Under these conditions, injected formaldehyde was not adsorbed on the walls.

Small quantities of formaldehyde and NO_2, however, may always be available from the walls; the next section provides suggestions for treating those low reactivity cases that may be influenced by these small quantities.

BACKGROUND AIR REACTIVITY

Background Concentrations

The site selection of the UNC smog chamber facility was substantially influenced by the need to locate in an area which would be reasonably free from anthropogenic emissions. After careful inspection of many possible sites, an area was selected which was located approximately 18 miles south of the University of North Carolina in one of the most rural counties in North Carolina. During the past 8 years background air quality has been measured by UNC and other research groups.

Carbon monoxide concentrations range from 0.2-0.4 ppm with an average value of ~0.33 ppm. Predawn NO_x values usually range from 3-12 ppb with NO_2 usually being more than half of the total NO_x. Background O_3 varies between 0.001 and 0.04 ppm. From late fall to early spring the O_3 background is usually 0.02 or higher and from late spring to early fall O_3 values are usually below 0.02 ppm. In 1973-74 nonmethane hydrocarbon data (NMHC) were taken with a conventional environmental nonmethane hydrocarbon monitor. Predawn NMHC concentrations ranged from 0.05-0.3 ppmC (after a correction factor of 1.6 was applied to the NMHC concentrations). A detailed gas chromatographic analysis by Research Triangle Institute (RTI) of early morning air inside the UNC chambers in 1975, however, indicated a total NMHC concentration of ~0.044 ppmC. The individual species are shown in Table 24 and these were mostly butanes and pentanes.

Since 1976 background chamber air was routinely measured by UNC on a C1-C10 automated gas chromatograph. This system can usually detect individual compounds as low as 0.01 ppmC. As an illustration, Figure 35 compares chamber background air during the spring of 1977 (in one side of the chamber) with 0.39 ppmC of the UNC eleven component mixture (which was injected in the other side of the chamber). It can be seen that there are only 3 or 4 small peaks in the background chamber air sample which might be distinguished from chromatographic baseline. These early morning analyses suggest that during most days the initial UNC chamber background is usually below 100 ppbC but on certain occasions it may have been as high as 200-300 ppbC.

Chamber and Air Reactivity

Smog chamber irradiations of background air have been conducted each data season over the past eight years. Generally

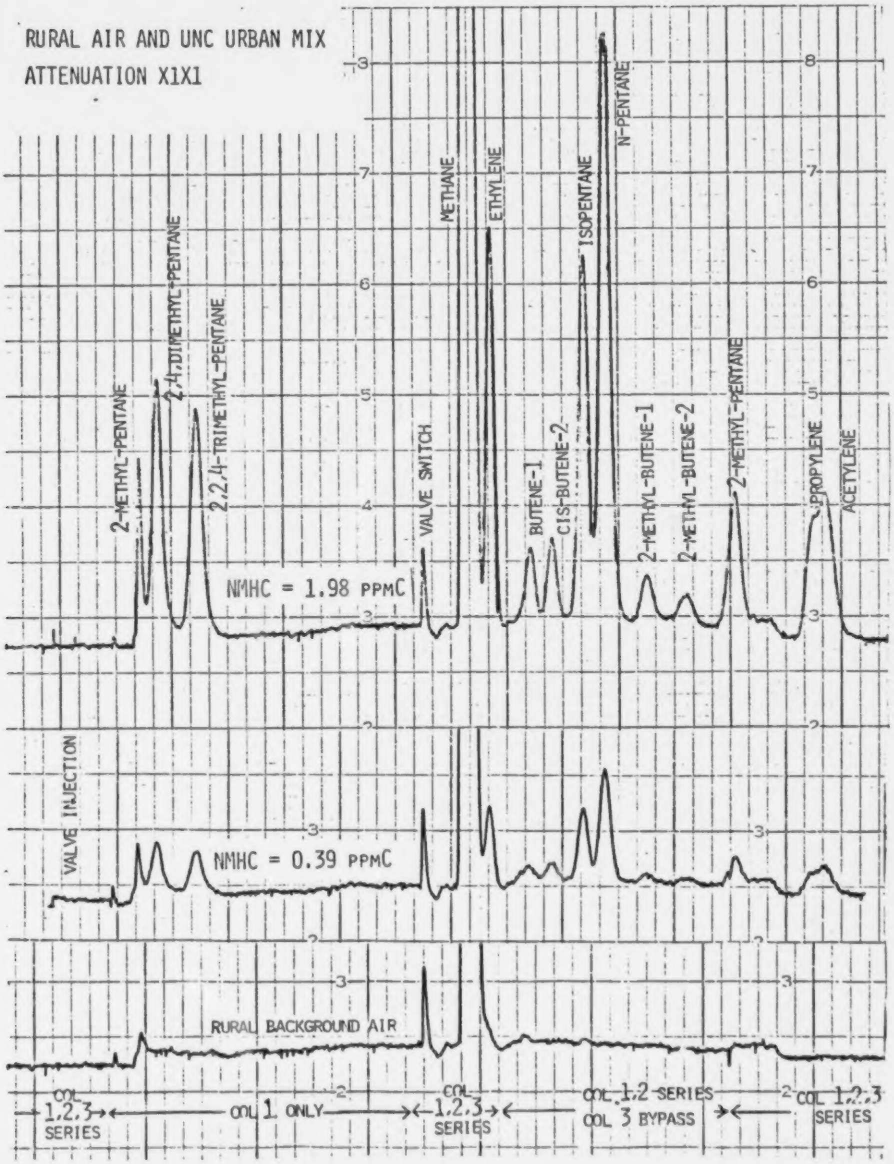

Figure 35. Comparison of background air and two hydrocarbon mixture levels in UNC chamber.

Table 24. Gas Chromatographic Analysis of UNC Chamber Background Air on November 5, 1976

Species	ppbV
ethane/ethylene	6
n-propane	2
propylene	1
acetylene	2
iso butane	1
n-butane	1
isopentane	1
n-pentane	1
total measured (C_2 to C_5) hydrocarbons	∿15

during these runs an increase of 10-20 ppb (over background) of NO_2 and almost no increase in NO have been observed. The background or NO-only runs for 1980 show ~0.05 ppmC increase in the region of the chromatogram where C_6's elute and no discernable C_2-C_5 aldehyde increase during the run. The amount of O_3 produced from the chambers with background air depends on the sunlight, temperature, humidity, and chamber run history. Background air systems can produce from 0.07 to 0.15 ppm O_3. An example of this type run is shown in Figure 36.

Another measure of background reactivity is the NO oxidation rate with background air. Nitric oxide oxidation tests are conducted by injecting 90% NO and 10% NO_2 into the chamber with background air. During the daytime the average rate of NO disappearance (uncorrected for dilution) was approximately 0.2 to 0.3 ppb/min for starting NO concentrations ranging from 0.45 to 0.65 ppm. For a system which started with 0.87 ppm NO an initial rate of 0.09 ppb/min was computed for the early morning (the theoretical thermal rate would be 0.06 ppb/min); this was followed by a midday rate of 0.31 ppb/min (thermal rate = 0.051 ppb/min) and an afternoon value of 0.24 ppb/min (thermal rate = 0.040 ppb/min). The rate of NO oxidation at lower initial NO concentrations is compared under both clear and overcast conditions in Figure 37. Although the NO oxidation for the clear day is slightly faster, the difference between these two days is not very large. This lends support to the idea that radical sources from the chamber air/walls are not very great under irradiation conditions. As would be expected these rates appear to be a function of light intensity, temperature and the amount of NO_2 available for photolysis.

In the August 14, 1978 NO oxidation run (Figure 38) at the 0.51 ppm level,the initial NO rate was 0.17 ppb/min (corrected for dilution) and the midday rate was 0.4 ppb/min. This is very similar to the above 1974 rates and demonstrates a degree of uniformity in chamber behavior over a span of four years. The August 14, 1978 experiment also included ~50 ppm CO on one side of the chamber run. The increase in NO oxidation rate under these conditions is significant and can be used by modellers to estimate the overall OH source strength in the chamber. A similar run, but at ~0.2 ppm NO_x, with and without CO is shown in Figure 39.

A simple mechanism to account for chamber reactivity that has been used by SAI in their Carbon Bond III mechanism modelling of the UNC mix experiments is shown in Table 25.

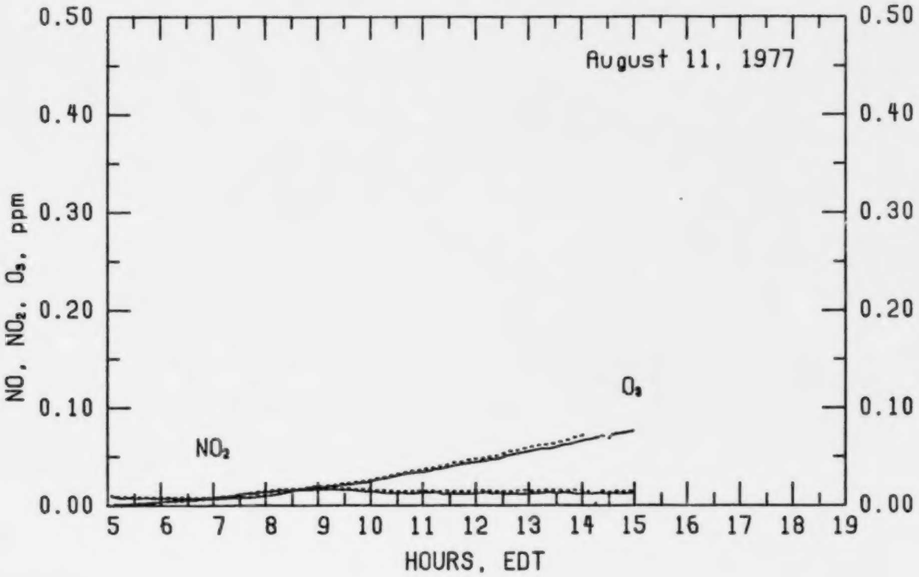

Figure 36. Nitrogen dioxide oxidation experiment with background air.

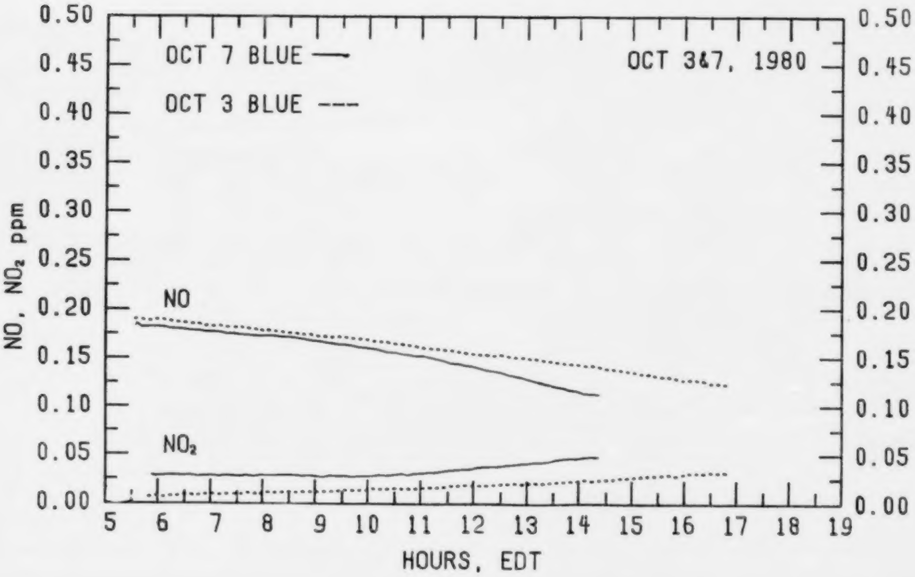

Figure 37. Nitric oxide oxidation experiment with background air.

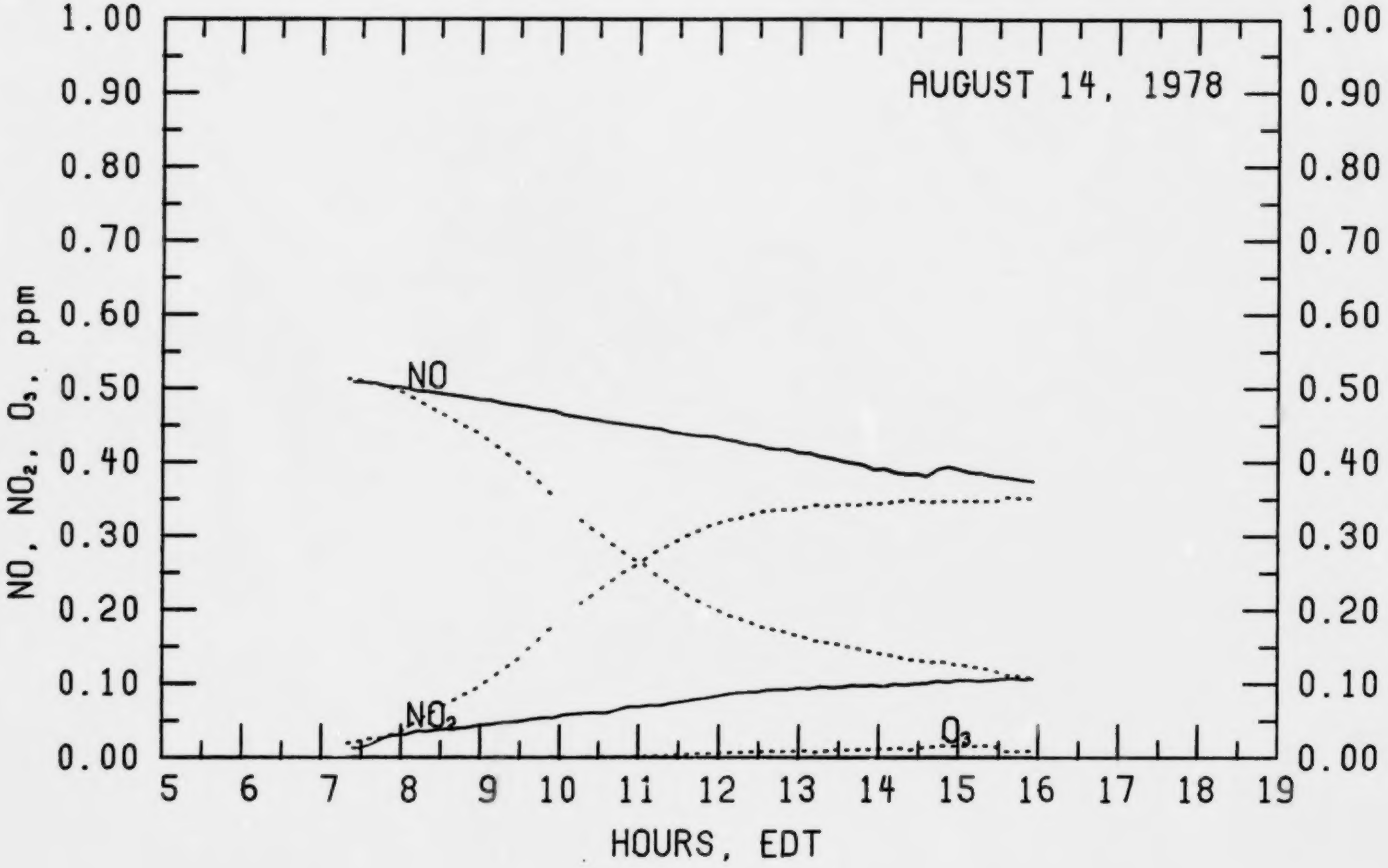

Figure 38. Nitrogen dioxide oxidation experiment. Solid lines are for background air. Dashed lines are for 50 ppm carbon monoxide added.

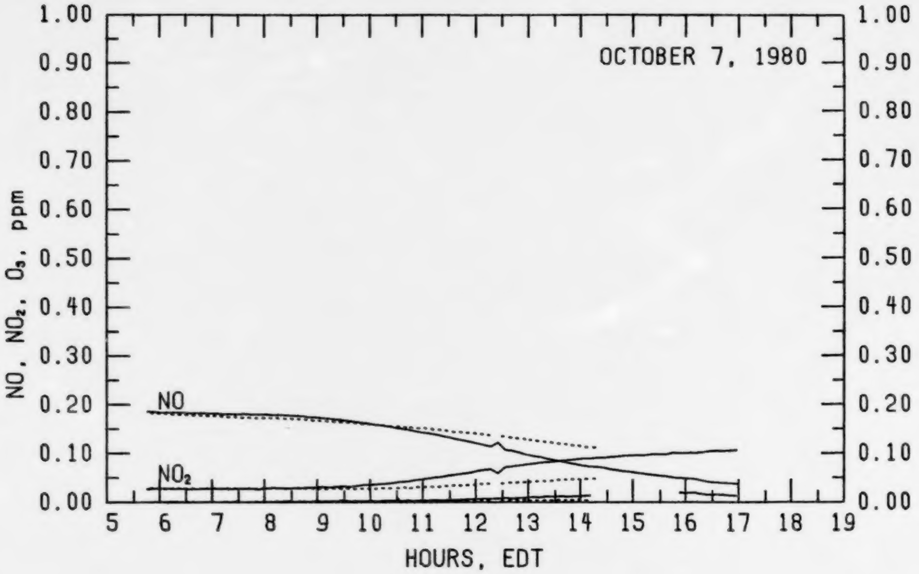

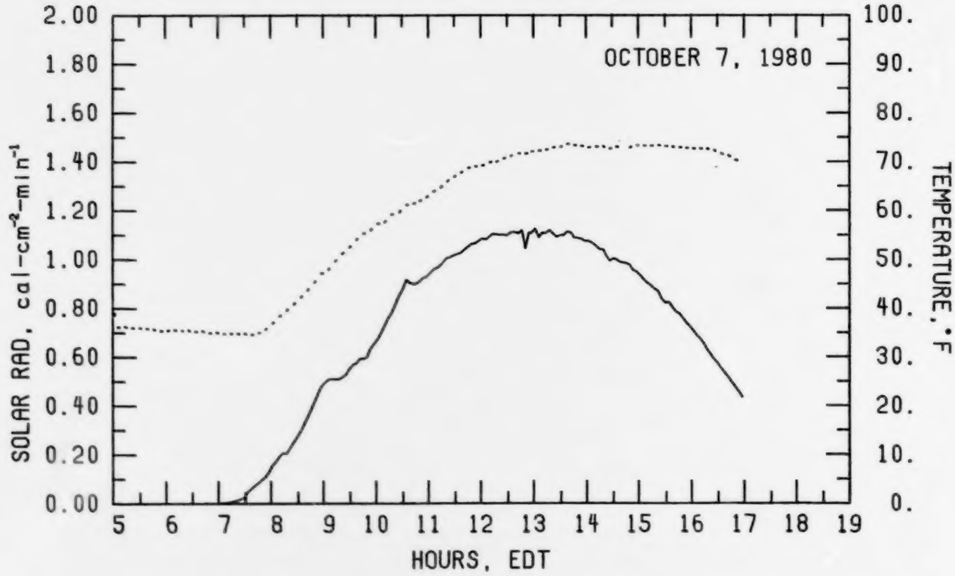

Figure 39.Background air reactivity experiment.

Table 25. Simple Mechanism to Account for Chamber Reactivity (after SAI)

OH	RO2	1000/ppm-min[a]
	HO2	1.5E-4*k1[b]
	NO2	5.0E-4*k1[c]

---

[a] equivilent to assuming ~0.30 ppmC background HC

[b] a total HCHO off-gassing from walls of ~0.025 ppm in 10 hrs

[c] total NO2 off-gassing from walls of ~0.075 ppm in 10 hrs

k_1 is the rate of NO2 photolysis

OH TRACERS

It was requested by SAI that UNC introduce ppb levels of trichloroethylene into some of the chamber runs so that its rate of disappearance could be used to monitor OH concentrations. Trichloroethylene was recommended because of its labile hydrogen (with correspondingly high OH attack rate of 3400 ppm^{-1}min^{-1}); the potential exists to measure this compound at very low concentrations. This would permit low levels of trichloroethylene to be introduced into smog chamber runs and its loss by OH reaction monitored at the same time. However since its concentration is very low it would not substantially contribute to any of the important smog reactions or represent even a minor path of OH loss. Separate experiments with initial high concentrations of trichloroethylene and NO_x were also run to assess the photochemical activity of trichloroethylene under irradiation conditions(July 8 and August 26, 1980).

Trichloroethylene was measured by electron capture and separated from other chlorinated hydrocarbons on a 2 foot x 1/8 inch ss column packed with 20% SP2100 + 1.5% carbowax 1500 on 80/100 Supelcoport. Usually experiments which had trichloroethylene also had ppb levels of carbon tetrachloride to monitor the dilution rate of the chamber. In the 1980 data set runs which had trace amounts of trichloroethylene are listed below.

July 15
July 17
August 1
August 8
August 9
August 11
August 12
August 13
August 14
August 27

TEMPERATURE DATA

The chamber air and ambient air temperatures are monitored with precision, linear thermistors. The chamber air temperature sensor is located in the sample intake manifold just below the chamber floor. In this position the sensor is aspirated by chamber air at a rate of 250 linear feet per minute, yet it is shielded from direct solar radiation and thus only responds to air temperature. There is only a fraction of a second lag-time between the air entering the manifold and reaching the sensor, so the air does not have time to cool off before it passes the sensor. The chamber is well mixed by the large mixing fans (see Appendix A) and temperature gradients within the chamber are less than 2 °F.

The ambient air temperature sensor is located under the chamber in the four foot space between the chamber floor and the ground and is subject to breezes and wind flow under the chamber but not any direct sun radiation. Since this sensor is not aspirated at a high flow rate with air that is exposed to direct sunlight, it may underestimate the ambient air temperature slighty.

Figure 40 shows a comparison of chamber and ambient air temperatures for October 22, 1977. Before sunrise, the chamber temperature is cooler than the ambient temperature. This is because the reflection floor of the chamber radiates heat better than the space under the chamber. After sunrise, the chamber air is warmer than the ambient air under the chamber by about 5 °F.

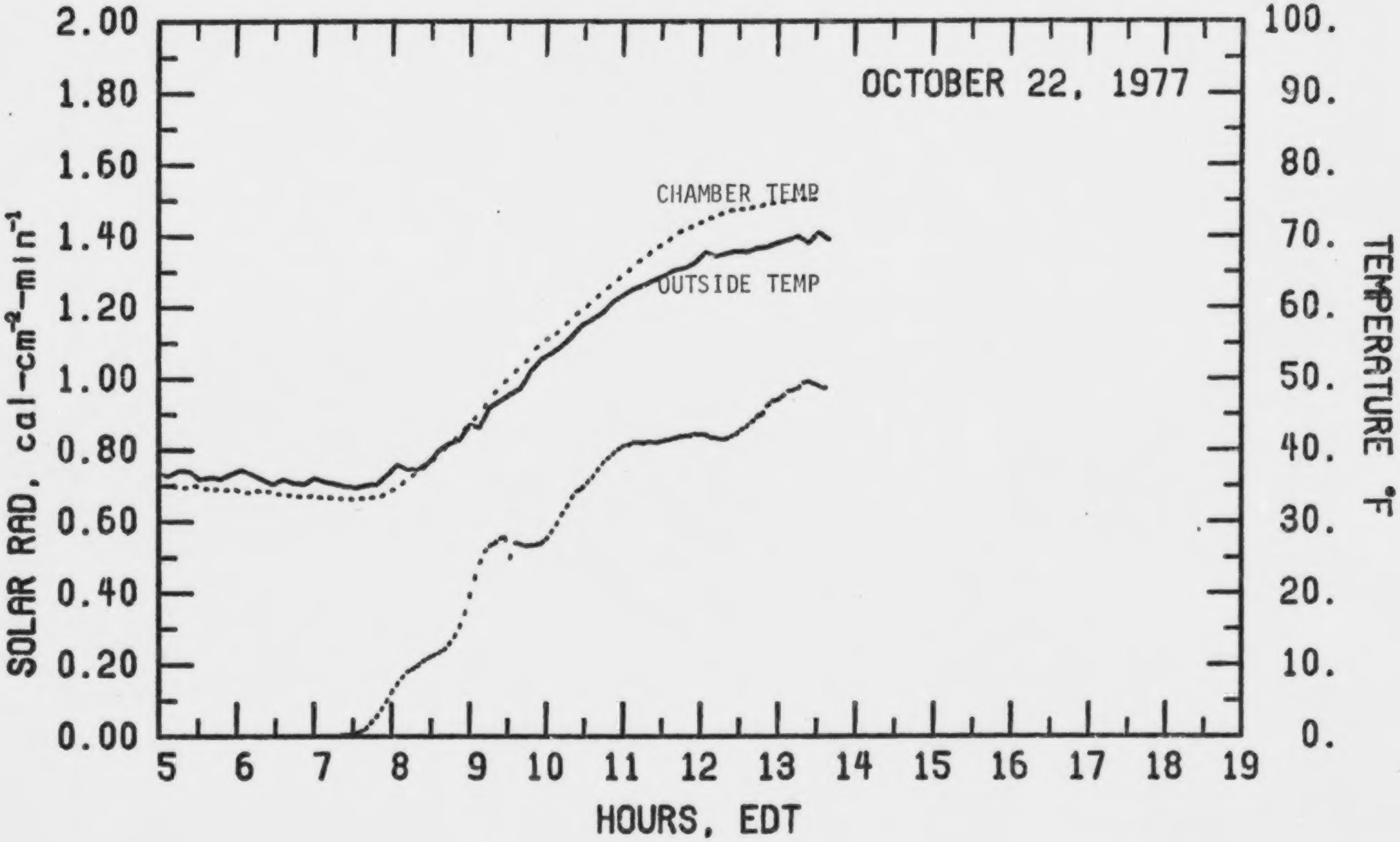

Figure 40. Chamber and ambient air temperature.

WATER VAPOR DATA

Description of How Obtained

If air is cooled at constant pressure a temperature will be reached at which the water vapor will condense; this temperature is called the dewpoint and is a direct measure of absolute humidity. The method in use at the chamber (EG&G 880) electrically cools a mirror until it just fogs over with water. The temperature that just maintains the fog thickness by cooling or not-cooling the mirror is the dewpoint.

Until 1979, the dewpoint meter was operated as supplied by the manufacturer; the results had not been entirely satisfactory and it had received frequent factory service. In 1979, a new circuit was installed by the factory. In addition, UNC built a special heated housing for the sensor that supplied external heat so that the sensor was always above the chamber dewpoint even in the air conditioned laboratory. These changes greatly improved the meter response and stability. It became possible to switch alternately between the two chamber sides every four minutes. See July 17, 1980 Figure 8.

Explanation of Rises in Chamber Dewpoint

The chamber is purged with background air from approximately 1900 until approximately 0400 EDT. During this time the air temperature is usually decreasing and the air often becomes saturated with water vapor. The surfaces of the chamber can collect an invisible film of water. Even if the air never cools to the dewpoint, significant quantities of water can accumulate on the chamber surfaces. During the daytime, as the ambient temperature rises, the relative humidity can decrease and the adsorbed water will evaporate. This raises the absolute humidity and increases the dewpoint. Once the adsorbed water has all evaporated, the dewpoint remains constant but the relative humidity can continue to decrease because the temperature is rising.

Conversion of Dewpoint to PPM

Figure 41 can be used as a quick method to convert chamber dewpoint into parts per million water vapor.

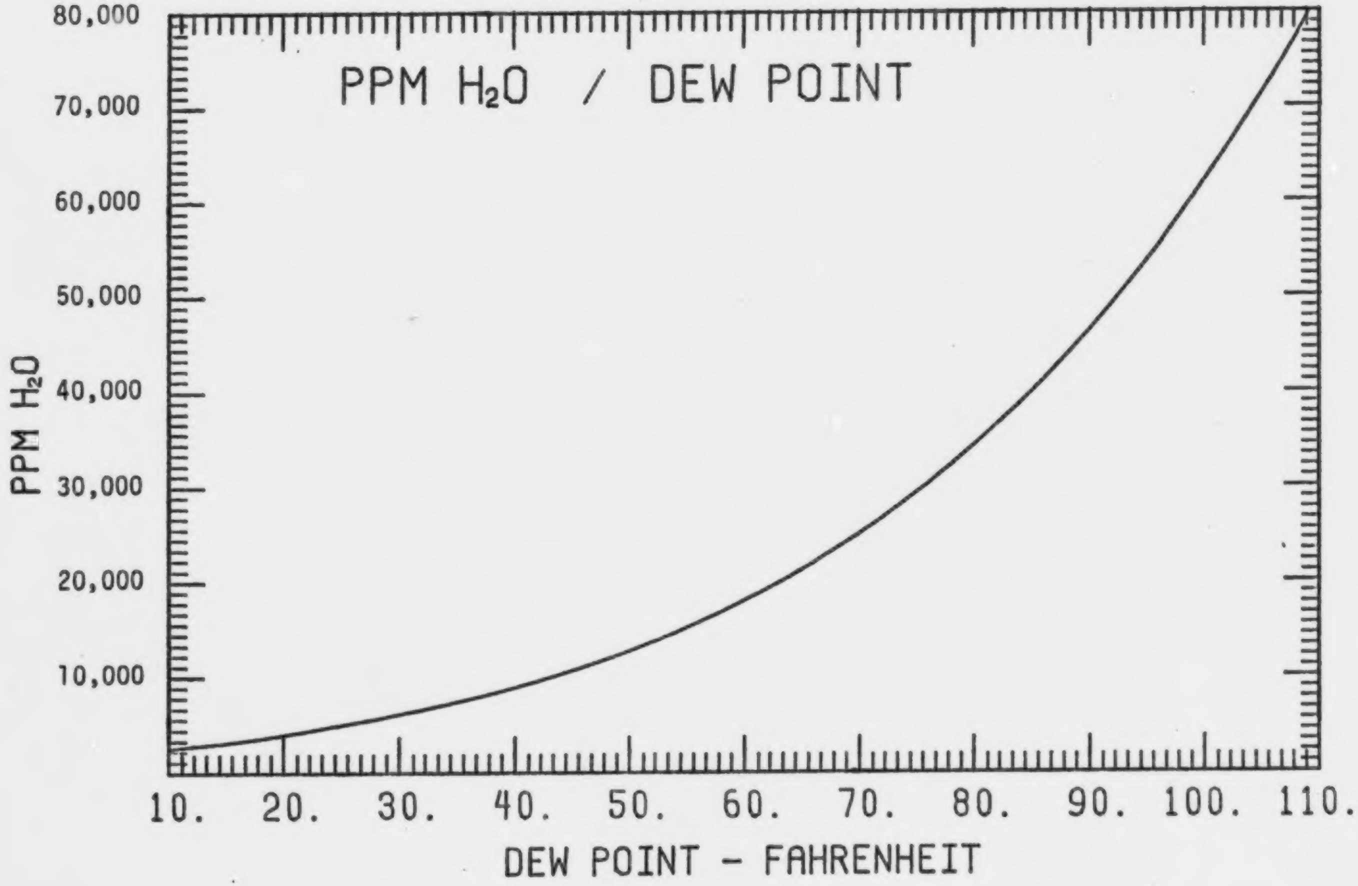

Figure 41. Conversion of dewpoint temperature to water vapor mixing ratio.

SECTION 5

GUIDANCE ON DATA QUALITY

COMMENTS ABOUT SPECIFIC METHODS

The following caveats should be remembered when examining the data:

1. Most of the methods (especially the instrument methods) exhibit very good precision and linearity, but require comparison of response to an external standard to establish accuracy. Since precision and linearity do not depend upon calibration, the relative magnitudes of measurements over time are more correct than the absolute magnitudes presented. There are few exceptions to this statement which will be discussed below.

2. Some methods specifically detect the specie of interest, others infer its existence by the difference in measurement between a modified and unmodified air stream. The former methods are considered to be more accurate since less assumptions are needed to generate the information of interest.

3. The O_3 values reported are probably our most precise and accurate gas-phase information. The chemiluminescent method is direct, interference free, and precise. Gas phase titration (GPT) of diluted high concentration NO (from multiple certified tanks from different manufacturers) with ozone is the basic calibration method used for O_3, NO, and NO_2; this has been backed up by detailed comparison studies with other research groups including comparisons with UV-photometry transfer standards from EPA. UNC experience with this particular instrument extends over a five year period. It has a proven record of low span and zero drift and is generally trouble free. In addition, small zero errors are readily detectable in early morning run data when NO is usually quite high. The estimated total long term uncertainty band for our total data set is 10%.

4. The NO data (>0.05 ppm) reported are probably less accurate than the O_3 data because the instrument is not as stable as the O_3 meter, exhibiting greater span and zero drift between calibrations. The measurement of NO is direct and the reported magnitude depends almost entirely on calibration. Because $NO-O_3$ gas phase titration is used to calibrate the O_3 meter, a great deal of work has also been

performed on NO measurements. The two measurements are thus interlocked. Although direct comparisons with high concentration NO tanks from different manufacturers and used by different groups have been performed, in general, the accuracy of our NO measurements is somewhat inter-dependent upon the O_3 meter accuracy (balance of errors in NO-only and NOx-only modes). UNC experience with this particular instrument also extends over a five year period. It has had more failures and reported more bad data than the ozone meter. Earlier versions of the catalytic converter (gold-based) produced low concentration (<0.02 ppm) positive zero offsets for NO readings during runs but not on clean air streams. New converters produce a much better performance and do not exhibit the later afternoon zero problems. Estimated error bands are comparable to the O_3 accuracy, probably 10-12% above 0.1 ppm.

5. The NO_2 chemiluminescent data reported can be very inaccurate, especially after NO_2 maximum, depending upon the particular hydrocarbon and conditions of the run. Since NO_2 concentration is an inferred measurement (i.e., based on the difference between a modified and unmodified air stream) it is subject to a larger number of error sources than NO measurements. Early morning NO_2 measurements, when the extent of reaction is small, probably have accuracies similar to those of the NO measurements. Near NO_2 maximum and after, however, the reported chemiluminescent values represent not only NO_2 but other compounds which can be converted to NO by the catalytic system in the instrument. The Saltzman NO_2 data, even with its own problems (see below) is probably better at defining the post NO_2-maximum time profiles.

6. The Saltzman wet chemical method for NO_2 is probably as accurate as the chemiluminescent technique when the latter does not exhibit interference problems. The Saltzman procedure, however, has substantially less precision than any of our instrumental methods. The only reason it has been used is because it is probably the most specific (most interference-free) NO_2 method available to us. On the other hand, it is a manual (labor-intensive) method that requires a skilled, practiced technician to produce good data. Because the method is a multi-step process and each measurement is essentially independent of previous measurements, it is better to use a number of sequential measurements to define a trend than it is to trust a single measurement. Since comparison tests between chemiluminescent-NO_2 measurements before NO_2-maximum and

Saltzman manual measurements show very good agreement, the Saltzman absolute values are sometimes keyed or referenced to the early morning chemiluminescent NO_2 meter values (in addition to the use of individual wet-chemical calibration curves) to obtain more accurate values of NO_2 for later afternoon. Comparison of Saltzman NO_2, chemiluminescent NO_2, and PAN data supports the view that the chemiluminescent NO_2 afternoon readings are frequently high, but may not be equal to the sum of NO_2 and PAN readings. Saltzman NO_2 data are available for only a limited number of runs.

7. The routine measurement of PAN in the outdoor chamber started in 1977. Complete details on the analytical procedures used are given in Appendix B. Briefly, gas chromatographic procedures are used to separate the PAN which is detected by electron capture (ECD). Extensive testing has shown that the Bendix chemiluminscent NOx analyzer responds 100% to PAN. This response is used to calibrate the ECD by using pure samples of PAN diluted in air. The pure PAN samples are prepared by preparative gas chromatography and liquid N_2 freezeout, concentration system. Thus there is an interlock between the O_3 measurements, the NOx measurements, and the PAN measurements. In 1977 and 1978 other calibration procedures were used (see Appendix B). These procedures were not as accurate and the data have been reviewed and adjusted. These data are estimated to have an error band of +/- 20%. The 1979 PAN data are estimated to have an accuracy comparable to the NOx chemiluminscent measurents, about 10-12%. The 1980 PAN data are estimated to have 10-15% error bands.

8. The routine measurement of nitric acid (HNO_3) is a "state-of-the-art" process with many uncertainties and difficulties. The method uses a modified Mast Oxidant meter. The values reported are inferred values based upon the selective removal of HNO_3 by nylon fiber.

An improved HNO_3 measurement method was used in 1978. A new TECO NOx molybdenum converter was used in place of the standard converter in a Bendix-NOx chemiluminescence monitor. Utilizing a switching nylon filter arrangement for alternate measurement of total nitrogen and total nitrogen minus HNO_3, this instrument was tested on a nitric acid generator and found to have a 100% response for HNO_3, in agreement with Joseph and Spicer's findings (1978). This instrument replaced the Mast coulometric method used in

1977. The Mast method was subject to many uncertainties and required much maintenance and down time. To minimize possible sample line losses the TECO converter and nylon scrubbing system was placed directly under the chamber. The HNO_3 sample was exposed to less than 24 inches of sample line, and therefore the 30 ft sample line from the convertor to the Bendix NOx instrument contained only NO. The nitric acid generator was also placed underneath the chamber next to the convertor to insure that this arrangement worked properly.

9. The precision of the hydrocarbn data reported is probably very good. The accuracy depends upon several factors. The gas chromatographic system response is tested in detail about twice per year using area measures and comparisons with other research groups and NBS tanks. In the past individual calibrations were usually performed weekly using certified commercial tanks. For modeling type runs in 1978 calibrations were performed almost every day. The instrument's response remains quite stable. A microprocessor-based integrator system has been used to reduce data from four different chromatographs since 1978. The sensitivity of the system is illustrated in Figure 42. UNC has had almost four years experience with this GC system and we have found it to be a reliable and stable system. The only difficulties have been occasional failures of valve motors or controllers. For well resolved peaks the system probably has an accuracy of 10-15% and a precision of <5%.

10. Like the hydrocarbon measurements, the formaldehyde and acetaldehyde reported values have better precision than accuracy. The original method used was unique to UNC, utilizing a special GC. Formaldehyde was not fully resolved from a background peak and this limited the minimum detectable concentration and added some uncertainty to determining the baseline for peak height measurements. Acetaldehyde is fully resolved. Propylene and propane are also fully resolved on this system and they receive the same instrument processing as the aldehydes. Instrument response is checked by using certified commercial tanks for acetaldehyde and propane or propylene. Formaldehyde is more difficult. Calibration has been based on formaldehyde concentrations prepared in the dark in the chamber by evaporation of a weighted amount of solid paraformaldehyde, by comparison with the manual, wet chromatropic acid method, and by the preparation and dilution of bag samples using weighted amounts of solid paraformaldehyde. This GC system operated extremely well during the 1977 data season and

CONCENTRATIONS OF INDIVIDUAL SPECIES IN
0.39 PPMC NMHC UNC MIX

	COMPOUND	CONCENTRATION (PPMC)
1	2-METHYLPENTENE	0.035
2	2,4-DIMETHYLPENTENE	0.039
3	2,2,4-TRIMETHYLPENTANE	0.040
4	ETHYLENE	0.042
5	BUTENE-1	0.010
6	BUTENE-2	0.013
7	ISOPENTANE	0.053
8	N-PENTANE	0.092
9	2-METHYLBUTENE-1	0.008
10	2-METHYLBUTENE-2	0.007
11	PROPYLENE/ACETYLENE	0.047

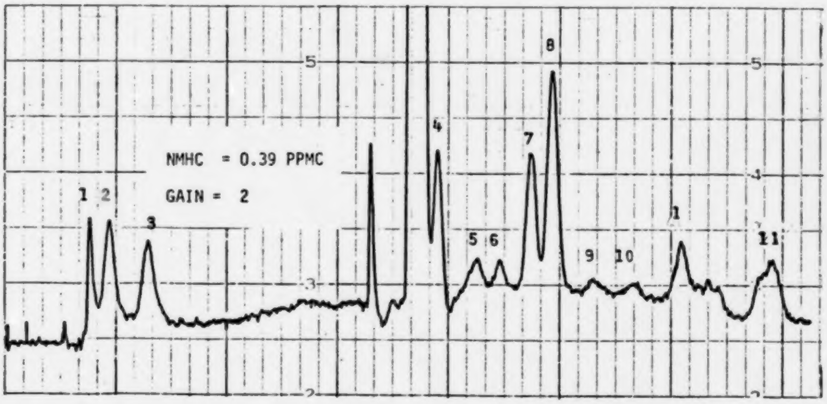

Figure 42. Maximum sensitivity of Carle Chromatograph.

probably had an accuracy of 10-20% and a precision of ~5% Deactivation of the porapak Q precolumn and its subsequent replacement lead to much lower sensitivity during 1978. We would estimate that the 1978 data have a 20-40% accuracy and a precision of ~10-15%.

In all of the 1979 runs formaldehyde data was taken with the above mentioned colorimetric method. The automated monitor is compact, well designed and easy to use. We have handled base line drift problems by an auto zero air supply which is switched in every hour. Modifications were made to eliminate this drift but we still recommend frequent "zeros". Calibration seems to hold within 10 percent over the period of a month. A 10 percent interference from acetaldehyde was observed over the range of 0.2-1 ppmC. New, more dilute solutions, only show a 5 percent interference. The major undesirable quality of this system is that it generates ~1 liter of dilute pararosanaline dye with dilute mercury salts for each 24 hours of operation.

11. Hydrogen Peroxide Detection. In the past hydrogen peroxide information has been gathered by UNC by colorimetric analysis using titanium tetrachloride solution and applying Lambert-Beers law to concentrations obtained from standards. The lowest concentration that can be measured accurately with this technique is 10 parts per billion (ppb) hydrogen peroxide. The chemiluminescent method of Kok et al., 1978, for the determination of hydrogen peroxide, was also utilized. This method is sensitive to concentrations as low as .5 ppb.

12. The Total solar radiation (TSR) data for 1979 are not valid for determining the magnitude of solar radiation, therefore, they are not valid for estimating the NO_2 photolytic rates. The TSR data are useful for determining clear or cloudy days and extent of cloud cover. The ultraviolet radiation (UV) data for 1979 are valid and relationships that can be derived from light data could be used with UV data to estimate NO_2 photolysis rates.

Table 26 summarizes the project's completeness, accuracy, and precision goals. The accuracy and precision values were estimated based on an examination of two years of calibration span and zero adjustments.

Table 26. Completeness, Accuracy, and Precision Goals

Parameter	Completeness	Accuracy	Precision (SD)
O_3	98	± 5	5
NO, NO_x, NO_x	98	±12	10
THC, CH_4, NMHC, CO	95	±15	10
C_2-C_{10}, HC alkenes alkanes aromatics	95	±10	10
Aromatics aromatic aldehydes phenols	95	±20	10
Acetaldehyde Propionaldehyde MEK acetone	95	±15	10
HCHO	95	±15	15
detailed aldehydes	95	±20	10
PAN	95	±20	10
Alkyl nitrates	95	±25	10
HNO_3	95	±20	20
H_2O_2	80	±30	20
Temp	100	± 5	0.5
TSR	100	± 5	0.5
UV	100	± 5	0.5
Dew Point	95	± 5	3.0

COMMENTS ABOUT CHAMBER REPRODUCIBILITY

During the course of a run season three or four matched runs are conducted in both chambers. This involves the slug injection of the same concentration of a given hydrocarbon or hydrocarbon mixture and the same NO and NO_2.

Figures 43 to 45 show some of these systems from the past seven years; almost no difference can be discerned in the response of the two chamber halves over this period.

In 1977 and 1978, a set of runs with similar initial conditions were repeated to observe differences in behavior that might occur from seasonal changes. Several 1.5 ppmC propylene/0.5 ppmC NOx and 1.5 ppmC ethylene/0.5 ppm NO_x runs are shown in Figures 46 and 47.

Figure 48 shows two high concentration propylene/NOx runs (3.6 ppmC + 0.5 ppm). These were conducted on October 21, 1977 and October 22, 1978 in the same chamber side, i.e. one year apart. Both runs experienced essentially the same dew point, temperature and solar radiation profiles; it is therefore not too surprising that these experiments might agree well. The agreement, however, is so close that when the pollutant profiles are overlapped they are almost indistinguishable.

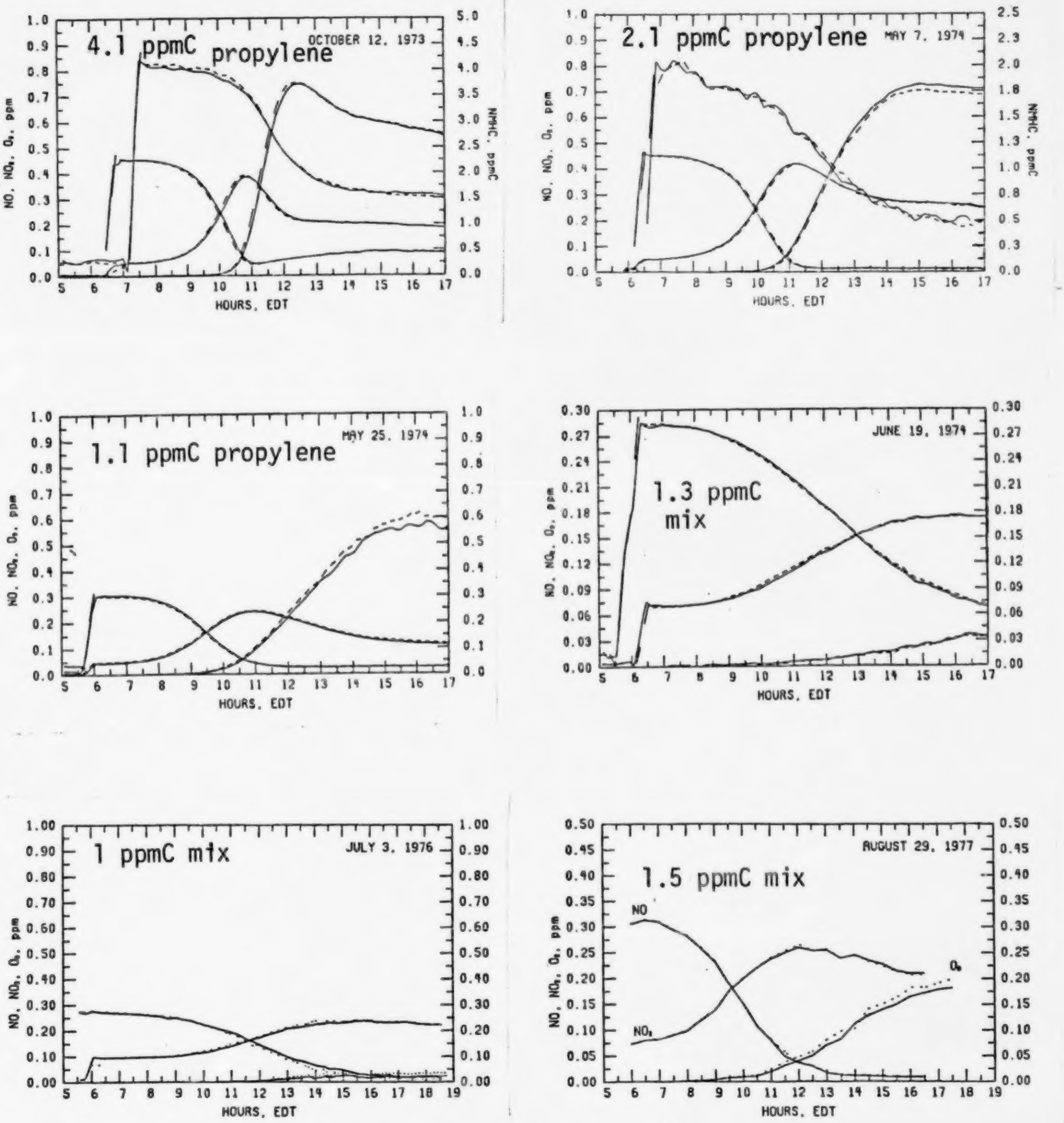

Figure 43. Similar chemical conditions in both halves of UNC chamber, 1973-77, RED side, BLUE side.

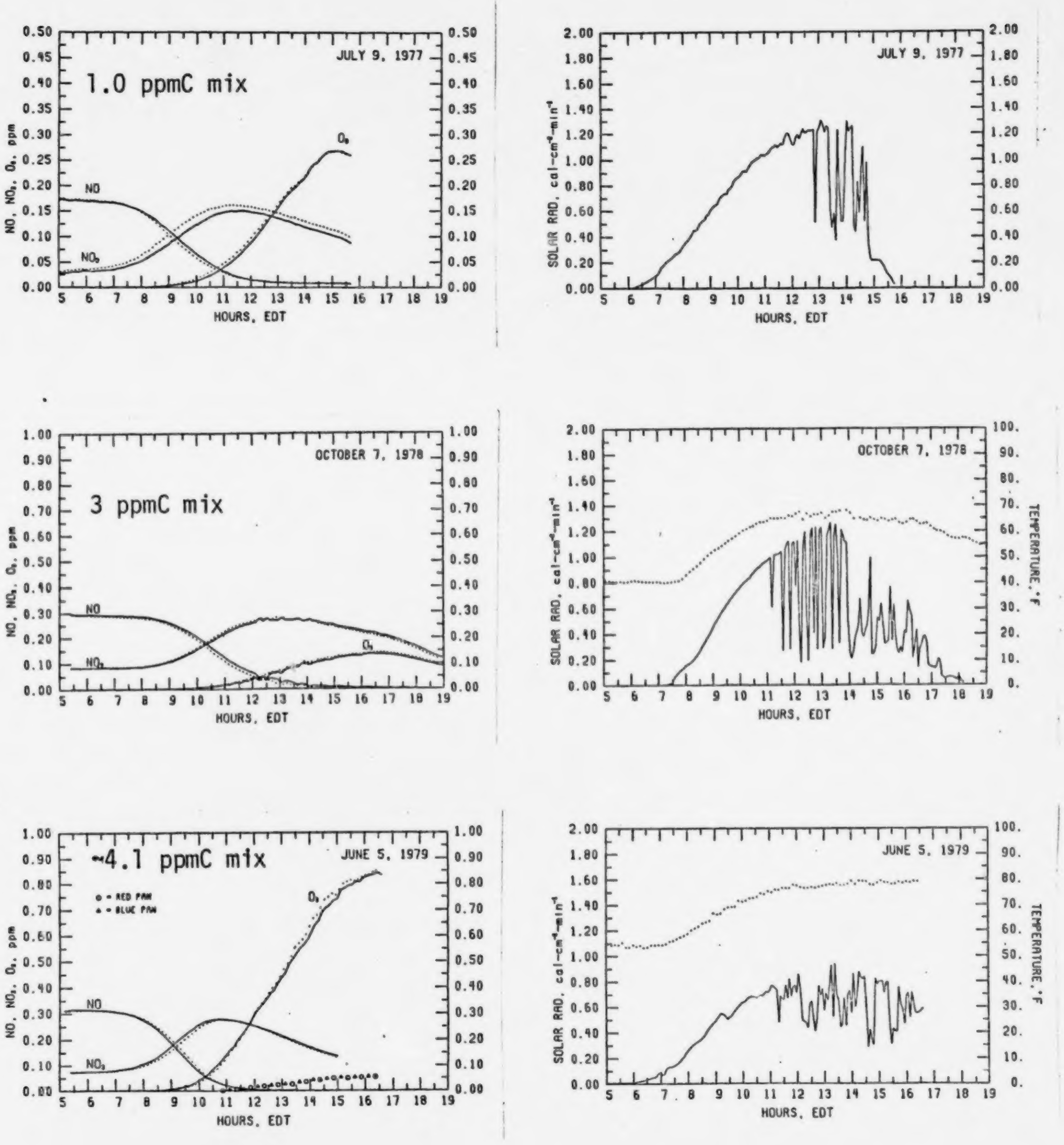

Figure 44. Similar chemical conditions in both halves of UNC chamber, 1977-79, RED side, BLUE side.

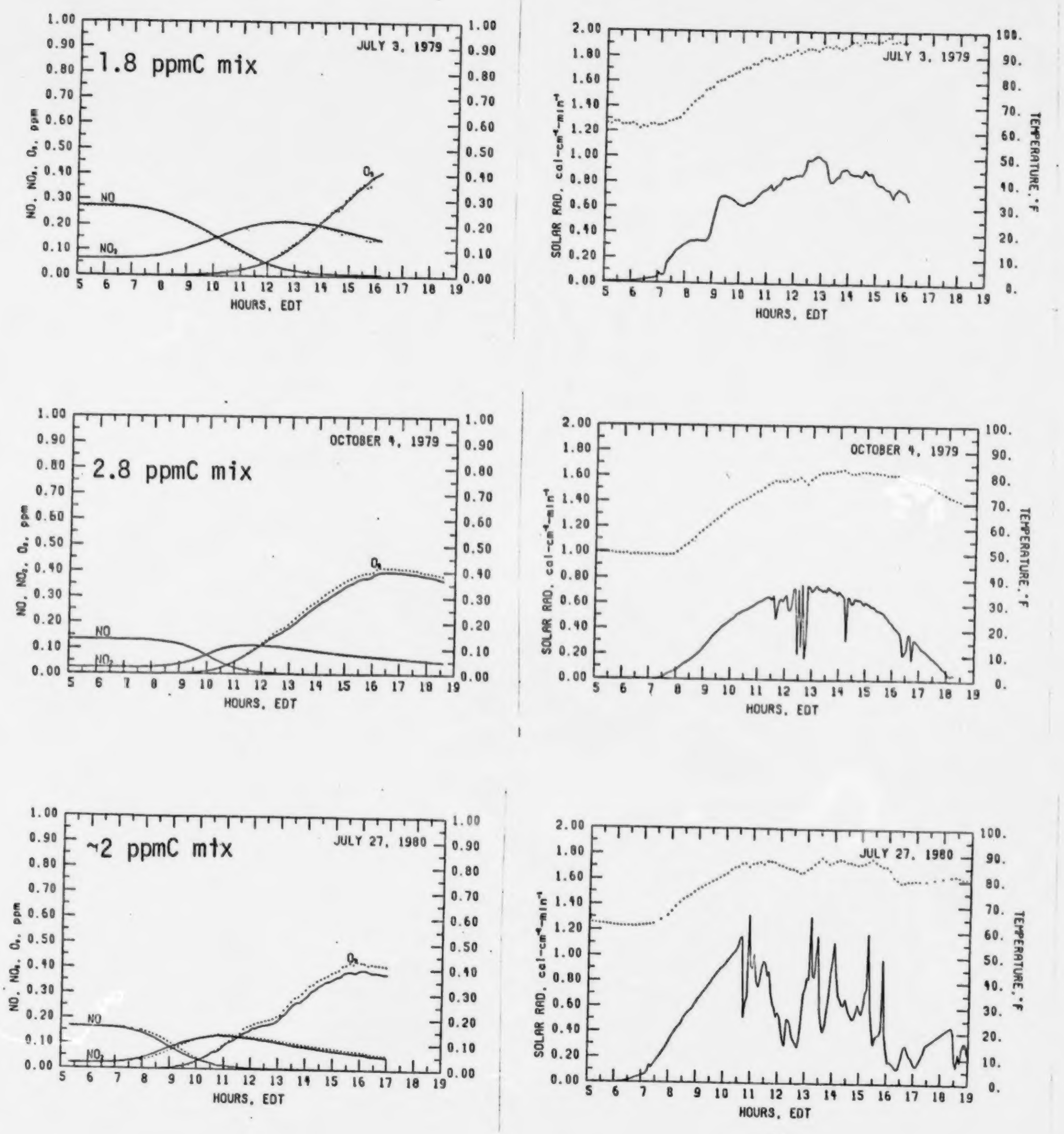

Figure 45. Similar chemical conditions in both halves of UNC chamber, 1979-80, RED side, BLUE side.

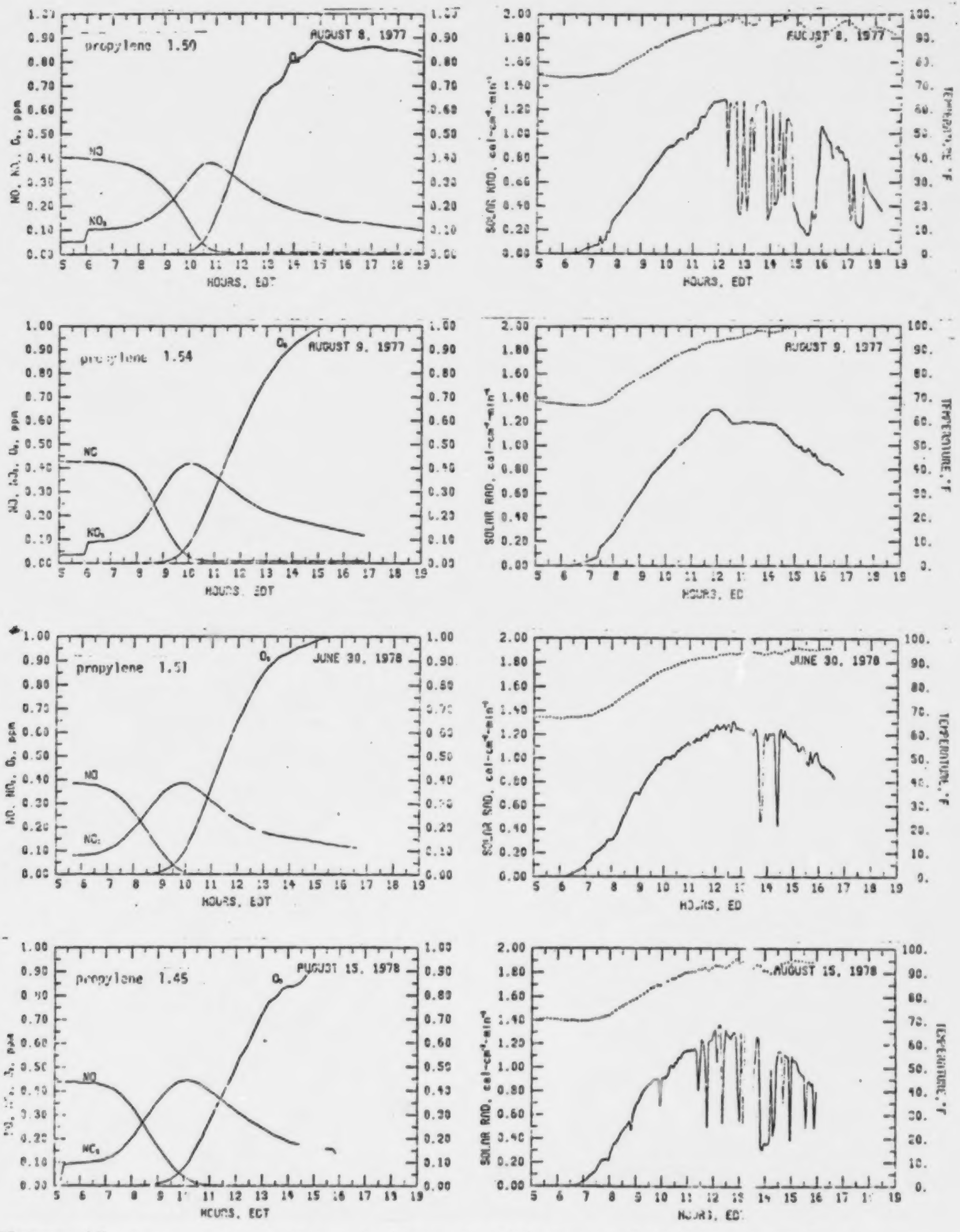

Figure 46. Approximately similar initial condition propylene experiments in UNC chamber over two year period.

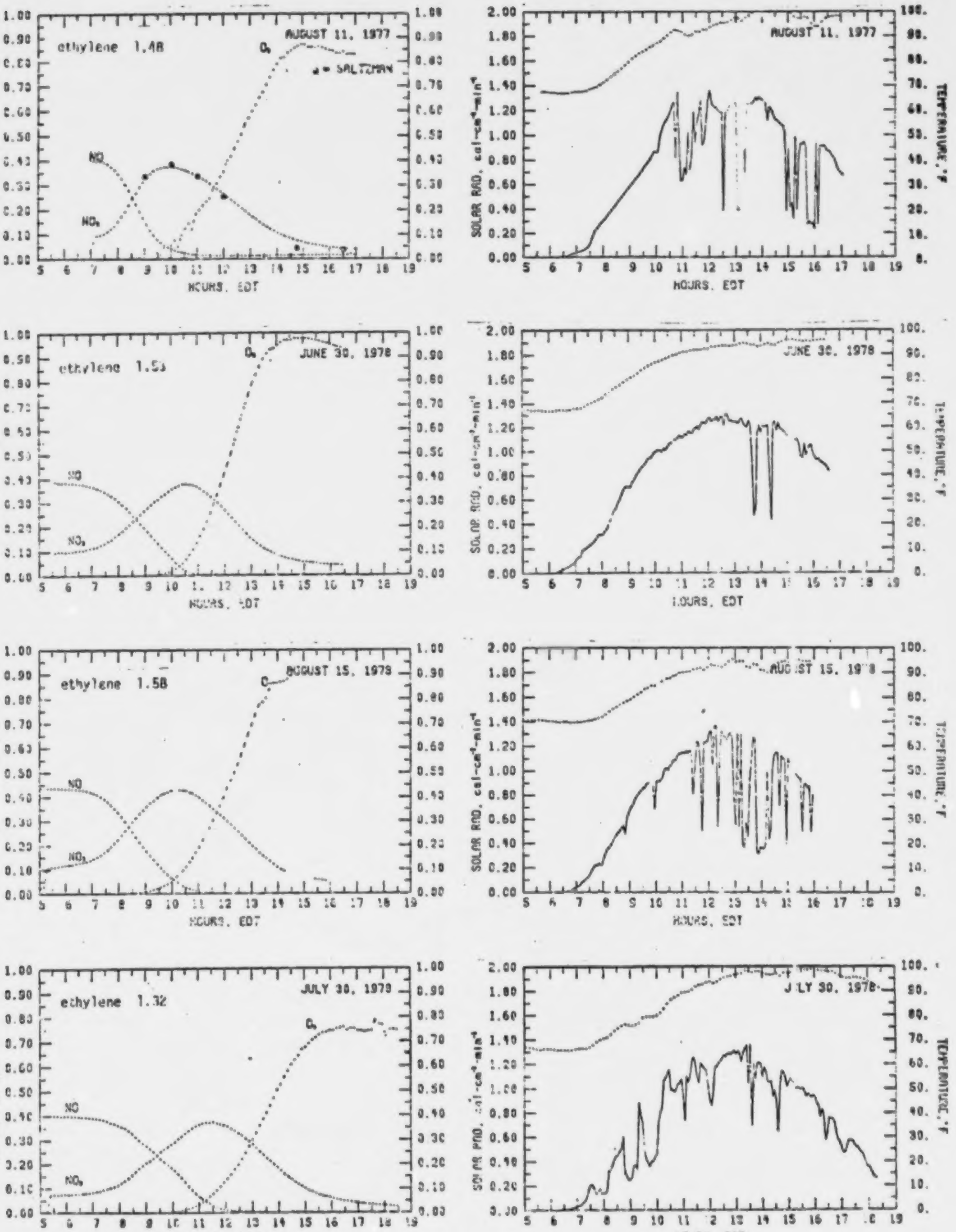

Figure 47. Approximately similar initial condition ethylene experiments in UNC chamber over two year period.

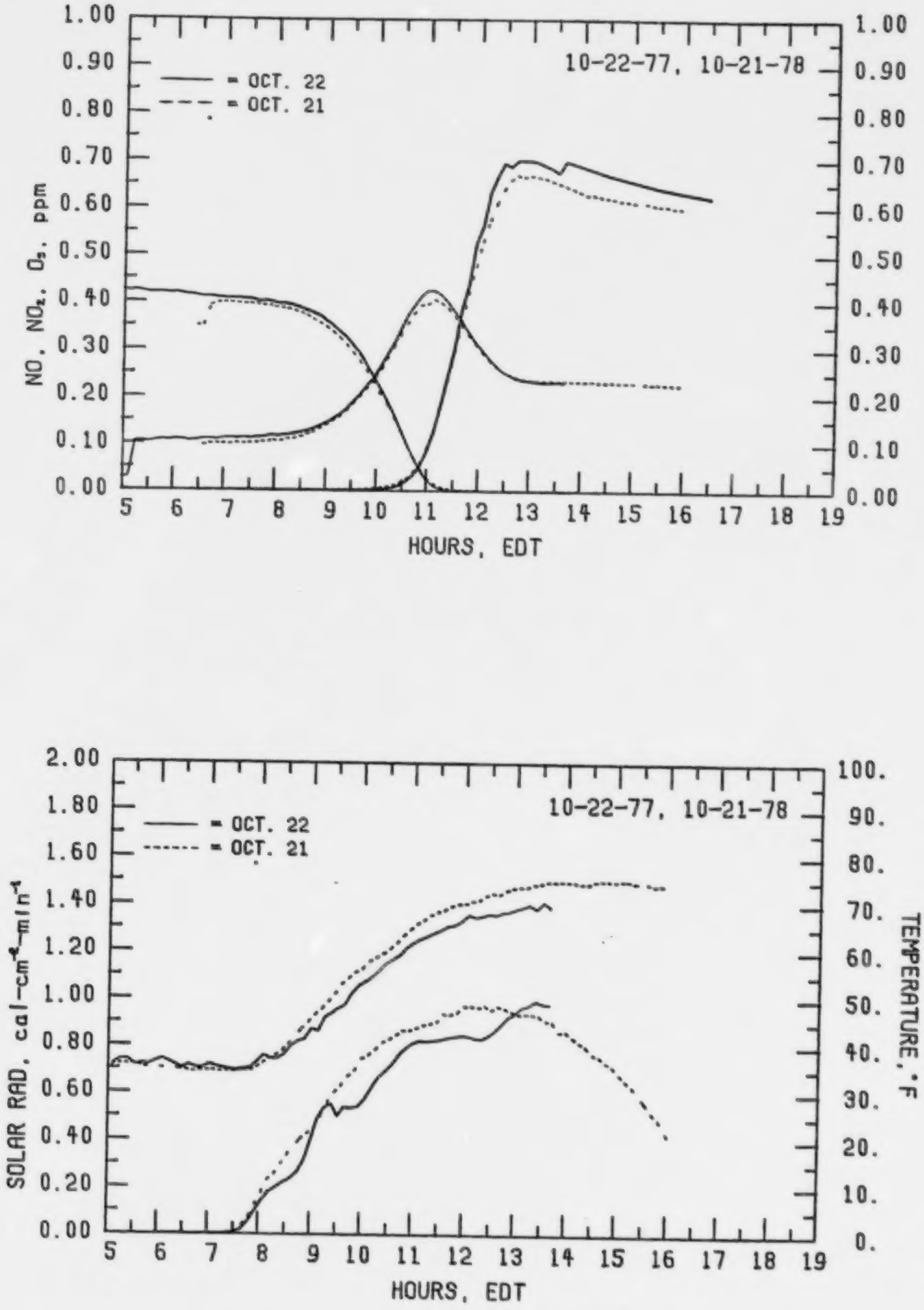

Figure 48. Duplicate propylene experiment one year apart.

SECTION 6

CONDENSED DATASET FOR TEN KEY RUNS

Hourly data and plots for ten runs are presented in this section. The hourly values included are NO, NO_2, O_3, temperature, DP, TSR and UV. Hydrocarbon and other product data which were not collected on the hour are also presented.

These runs were selected because they are representative of the entire data set, usually have reasonably complete product information, were conducted under favorable sky conditions, and offer the modeler a choice of different initial starting compounds. Initial conditions for these runs are given in Table 27.

Table 27. Initial Conditions for Selected Runs

			R	B
1.	August 8, 1977	NO	0.399	0.401
		NO_2	0.058	0.057
		Propylene	1.52	1.49
2.	October 22, 1977	NO	0.415	0.418
		NO_2	0.105	0.110
		Propylene		
		n-butane		8.09
3.	October 9, 1979	NO	0.171	0.171
		NO_2	0.036	0.036
		n-butane	14.35	
		n-pentane		14.23
4.	October 12, 1979	NO	0.364	0.364
		NO_2	0.115	0.115
		Propylene		1.33
		Ethylene	0.197	
		RCHO	1.26	
5.	August 5, 1979	NO	0.503	0.407
		NO_2	0.135	0.132
		Ethylene	4.11	
		HCHO		1.21
6.	August 1, 1979	NO	0.274	0.277
		NO_2	0.075	0.076
		HCHO		1.00
		RCHO	1.91	
7.	June 13, 1979	NO	0.367	0.36
		NO_2	0.08	0.083
		Propylene	2.81	2.73
		Toluene		3.16
8.	August 8, 1980	NO	0.322	0.330
		NO_2	0.097	0.089
		RCHO	1.90	
		Biacetyl		0.85
9.	July 30, 1980	NO	0.156	0.155
		NO_2	0.023	0.023
		Toluene	3.78	
		o-xylene		2.23
10.	June 23, 1980	NO	0.171	0.172
		NO_2	0.039	0.038
		α-pinene	1.90	
		isoprene		1.27

EPA Form 2350-4 (4-80)
(PREVIOUSLY CIN. EPA FORM 261)
U.S. GOVERNMENT PRINTING OFFICE: 1980-660-639
TYPING GUIDE SHEET

Date: August 8, 1977

TYPE: MATCHED PROPYLENE, MATCHED NOX

INITIAL CONDITIONS (ppmC)

	Red	Blue
NO	0.394	0.397
NO2	0.105	0.104
NOx	0.493	0.494
Propy	1.54	1.50

Time of Sunrise - 0636
Initial Temp (F)- 73.8
Max Temp (F) - 101.5

This is a matched propylene NOx run and illustrates the chamber reproducibility for both initial reactants and product time profiles. In this run the chamber was dry since the dew point trace indicates little humidity buildup with temperature. Propylene, O3, NO and NO2 measurements are 10%; acetaldehyde is 15%, formaldehyde and PAN 20%. TSR and UV data are good for this run. During this run there was a slight morning overcast from 0630-0800 and afternoon clouds after 1200. The less than perfect afternoon sun probably reduces the O3 potential of this run and introduces bumpyness to the afternoon O3 curve.

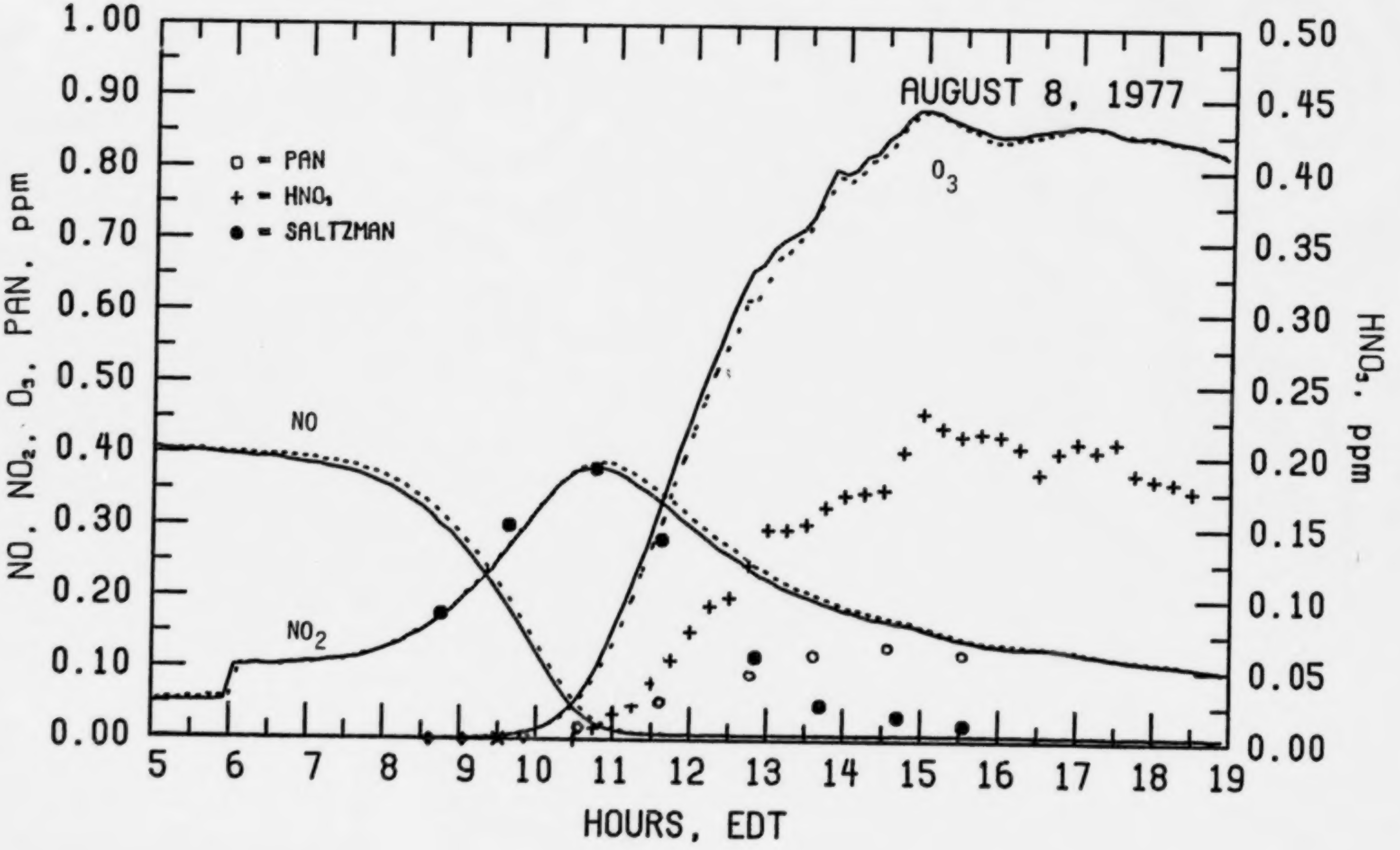

Figure 49. Nitrogen and Ozone Data.

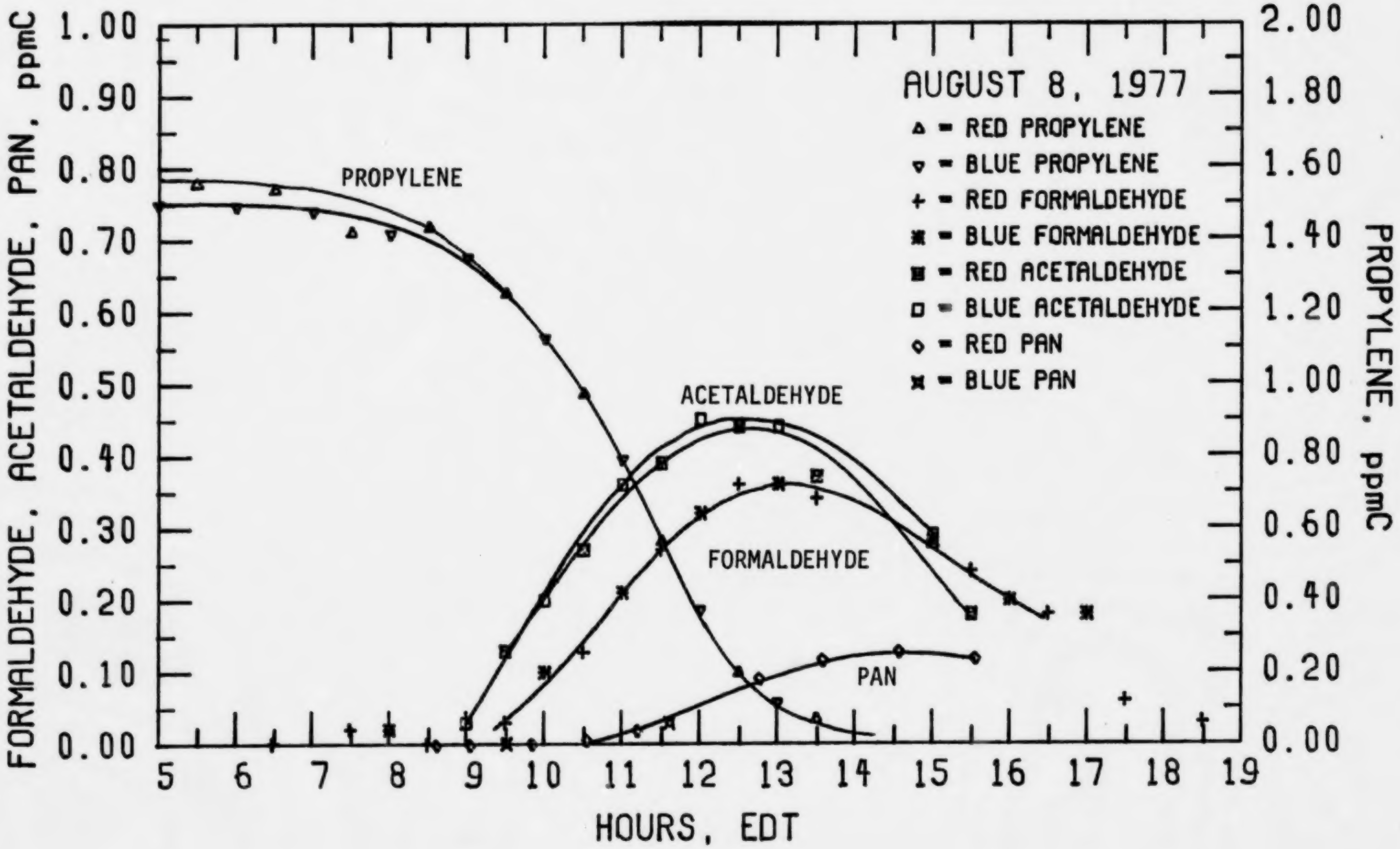

Figure 50. Carbon Reactant and Product Data.

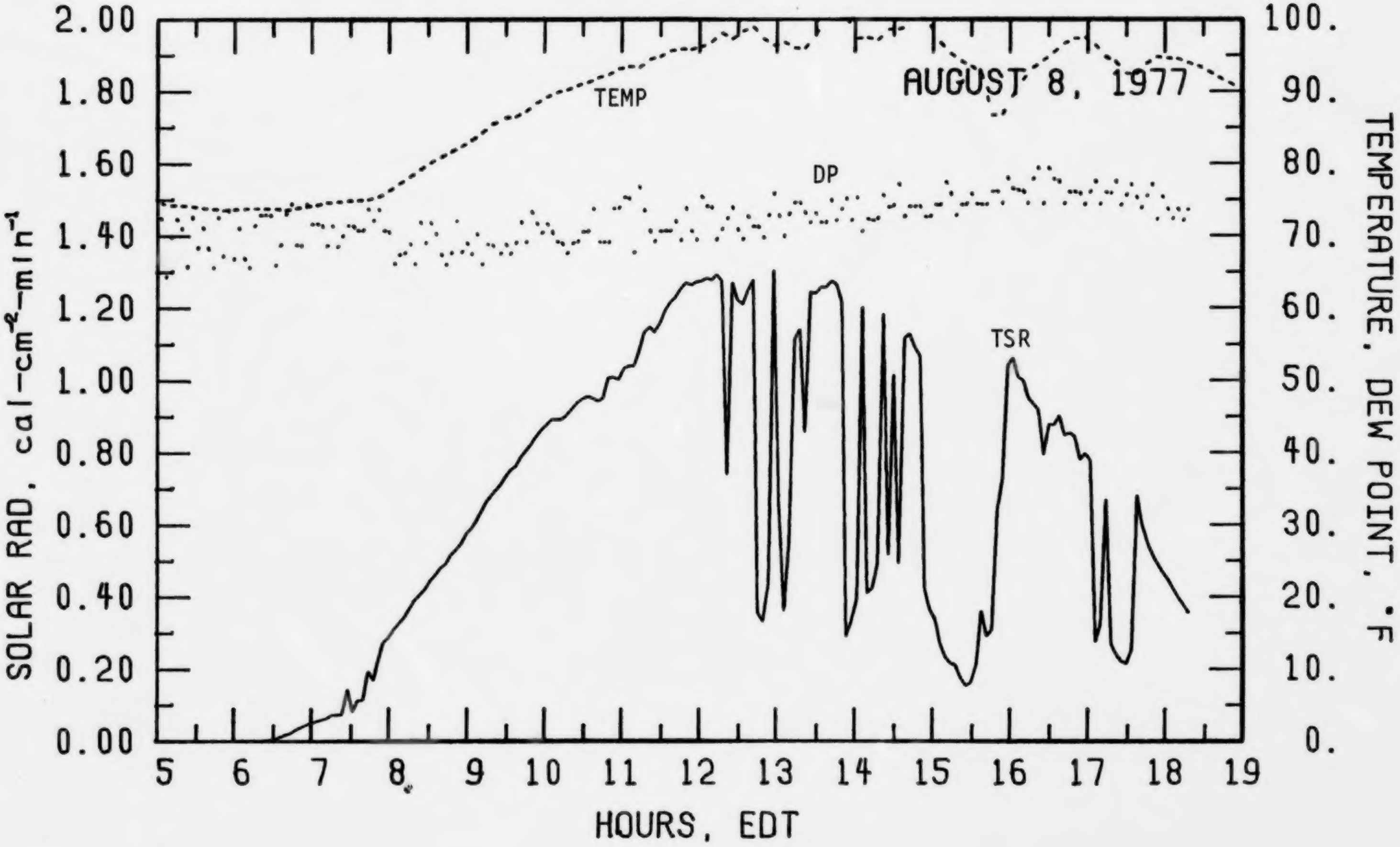

Figure 51. Total Solar Radiation, Dewpoint, and Temperature Data.

Table 28. Hourly Values Of Continuous Data For August 8, 1977

TIME		NO		NO2		O3		TEMP	DP	TSR	UV
R	B	R	B	R	B	R	B				
0500		0.4076		0.0496		0.0005		76.0		0.000	
	0504		0.4059		0.0534		0.0004	74.5		0.000	
0556		0.3977		0.0537		0.0005		75.1		0.000	
	0600		0.3991		0.0589		0.0005	73.7		0.000	
0700		0.3850		0.1078		0.0006		74.9		0.052	
	0704		0.3933		0.1061		0.0000	74.3		0.057	
0756		0.3590		0.1242		0.0007		75.9		0.278	
	0800		0.3686		0.1265		0.0008	76.3		0.292	
0900		0.2741		0.1959		0.002		79.5		0.579	
	0904		0.2794		0.2050		0.0022	83.3		0.593	
0958		0.1254		0.3187		0.0139		83.3		0.867	
	1002		0.1279		0.3284		0.0163	89.3		0.881	
1102		0.0119		0.3740		0.1664		85.4		1.036	
	1058		0.0167		0.3877		0.1306	93.1		1.004	
1158		0.0074		0.3020		0.4436		89.0		1.276	
	1202		0.0079		0.3096		0.4377	96.2		1.278	
1302		0.0075		0.2247		0.6892		90.8		0.662	
	1258		0.0072		0.2387		0.6454	96.3		1.305	
1358		0.0073		0.1830		0.7947		90.3		0.332	
	1402		0.0083		0.1963		0.7848	97.3		0.394	
1502		0.0080		0.1559		0.8836		90.5		0.338	
	1458		0.0087		0.1610		0.8819	99.0		0.364	
1558		0.0072		0.1336		0.8480		83.8		1.046	
	1602		0.0078		0.1366		0.8403	89.4		1.064	
1702		0.0067		0.1241		0.8630		89.5		0.779	
	1658		0.0068		0.1281		0.8605	97.5		0.797	
1758		0.0066		0.1111		0.8487		88.6		0.467	
	1802		0.0073		0.1120		0.8463	94.5		0.492	
1854		0.0066		0.1016		0.8218		85.4		0.191	
	1858		0.0072		0.0994		0.8197	90.3		0.181	

Table 29. Concentrations of Selected Species for

August 8, 1977

Nitric Acid

	RED	BLUE
10:30		0.000
10:45		0.006
11:15		0.024
11:00		0.018
11:30		0.040
11:45		0.056
12:00		0.076
12:15		0.094
12:30		0.100
12:45		0.123
13:00		0.148
13:15		0.148
13:30		0.152
13:45		0.164
14:00		0.172
14:15		0.174
14:30		0.176
14:45		0.203
15:00		0.230
15:15		0.220
15:30		0.214
15:45		0.216
16:00		0.214
16:15		0.206
16:30		0.188
16:45		0.203
17:00		0.210
17:15		0.204
17:30		0.210
17:45		0.188
18:00		0.184
18:15		0.162
18:30		0.176

Saltzman

	RED
08:45	0.176
09:37	0.300
10:38	0.379
11:37	0.281
12:51	0.117
13:42	0.050
14:43	0.034
15:33	0.023

PAN

	RED	BLUE
08:37	0.000	
09:03	0.000	
09:31		0.000
09:51	0.001	
10:33	0.006	
11:12	0.019	
11:36		0.029
12:46	0.092	
13:35	0.116	
14:34	0.128	
15:33	0.118	

Table 30. Concentrations of Selected Species for

August 8, 1977

	Propylene		Formaldehyde		Acetaldehyde	
	RED	BLUE	RED	BLUE	RED	BLUE
05:00		1.498		99999		99999
05:30		1.355		99999		99999
06:00		1.495		0.02		99999
06:30	1.538		0.00		99999	
07:00		1.481		99999		99999
07:30	1.418		0.02		99999	
08:00		1.418		0.02		99999
08:30	1.432		0.00		99999	
09:00		1.352		99999		0.03
09:30	1.248		0.03		0.130	
10:00		1.127		0.10		0.20
10:30	0.969		0.128		0.27	
11:00		0.791		0.21		0.36
11:30	0.560		0.27		0.39	
12:00		0.376		0.32		0.45
12:30	0.195		0.36		0.44	
13:00		0.117		0.36		0.44
13:30	0.066		0.34		0.37	
15:00		99999		0.28		0.29
15:30	99999		0.24		0.18	
16:00		99999		0.20		99999
16:30	99999		0.18		99999	
17:00		99999		0.18		99999
17:30	99999		0.06		99999	
18:30	99999		0.03		99999	

Date: October 22, 1977

TYPE: propylene vs. n-butane

INITIAL CONDITIONS (ppmC)

	RED	BLUE	
NO	0.408	0.406	
NO_2	0.050	0.053	Time of sunrise
NO_x	0.458	0.459	Initial Temp (oF) 33.1
propyl	3.69		Max Temp(oF) 75.4
butane		8.09	

This run is a relatively cool propylene run with good nitrogen product data (PAN, gaseous HNO_3) and carbon product data (formaldehyde, acetaldehyde, CO). The propylene side data have received extensive review and evaluation. Strip chart data were reviewed to support and validate computer collected data. There are no product data for the n-butane side.

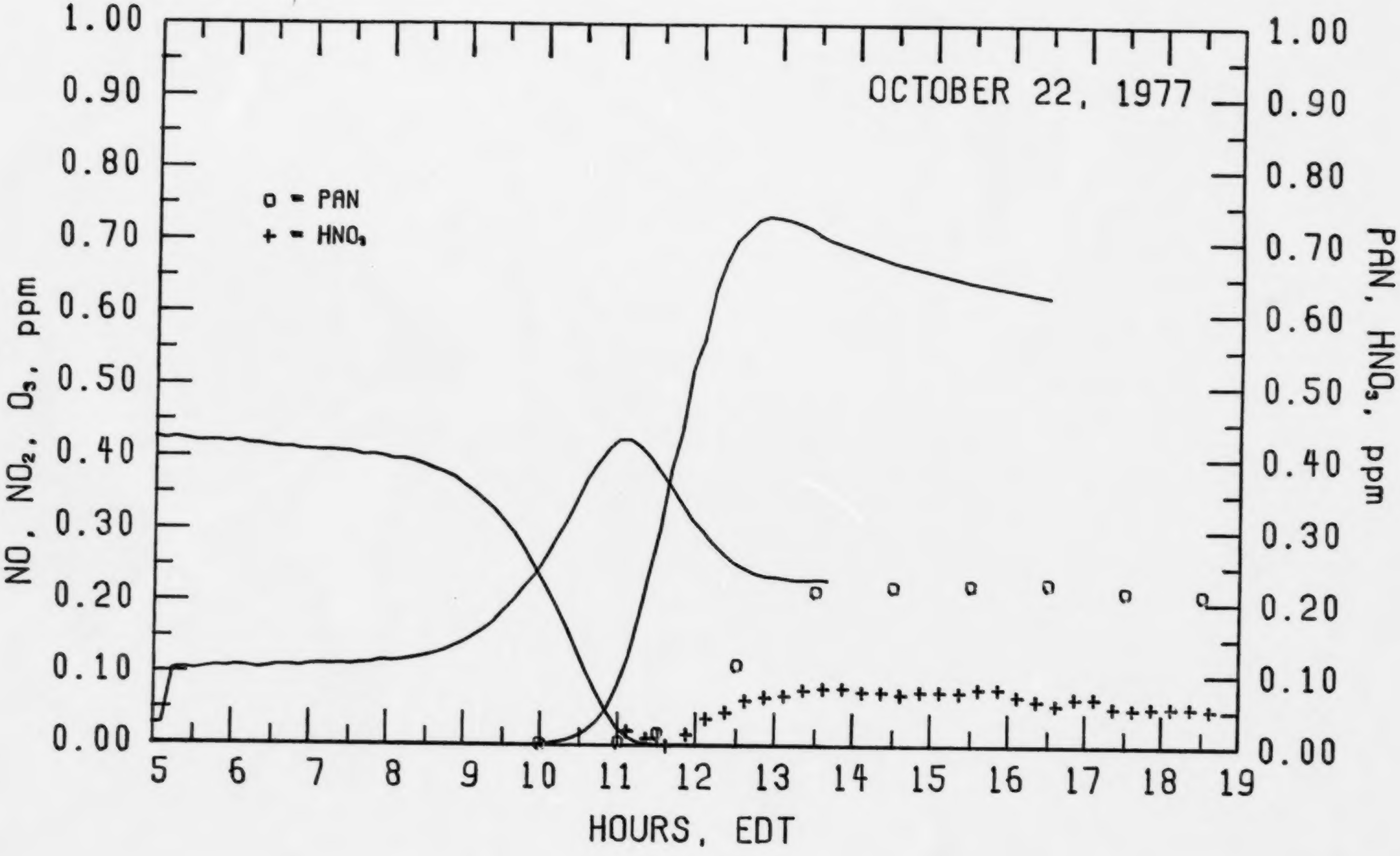

Figure 52. Nitrogen and Ozone Data.

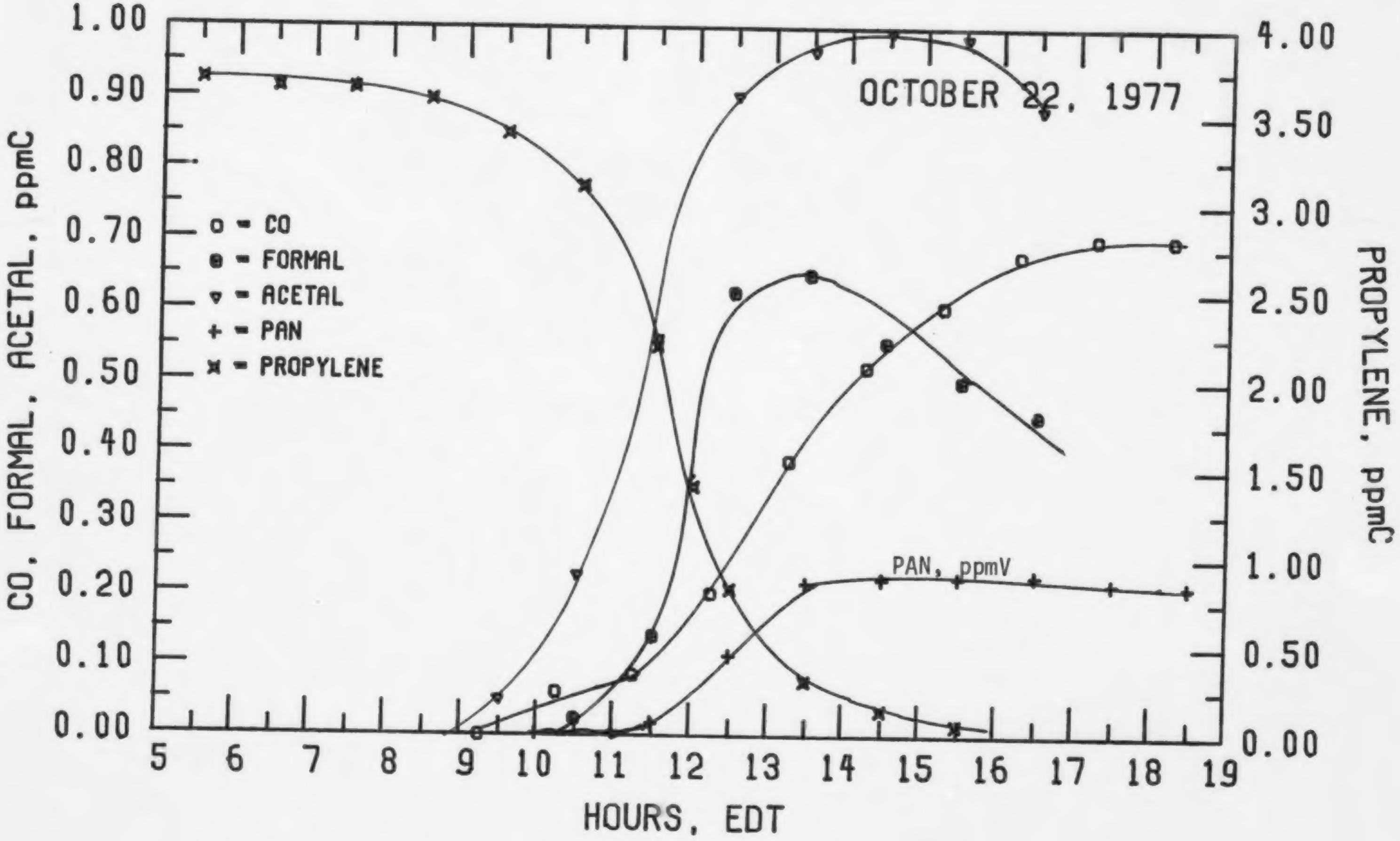

Figure 53. Carbon Reactant and Product Data.

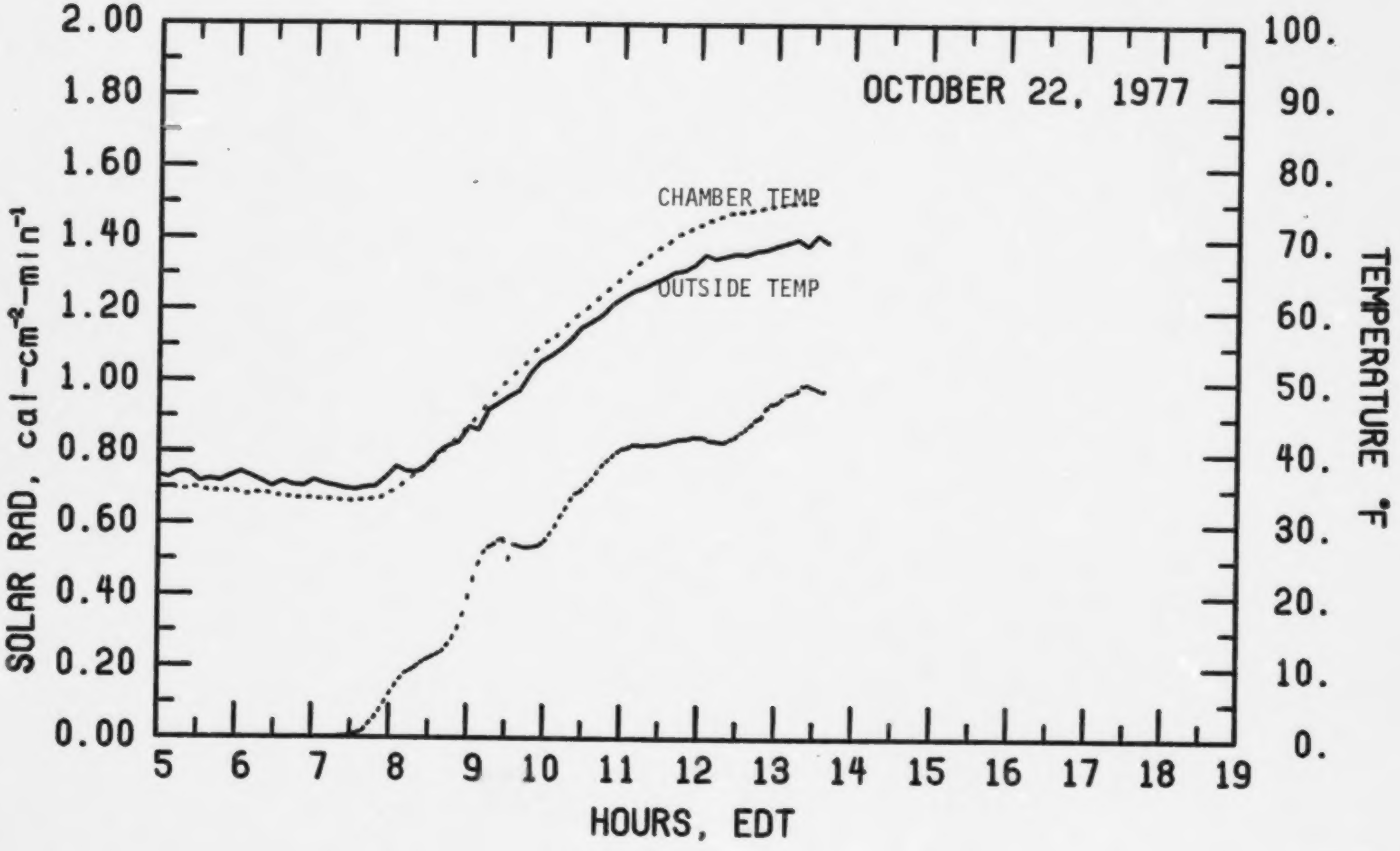

Figure 54. Total Solar Radiation and Temperature Data.

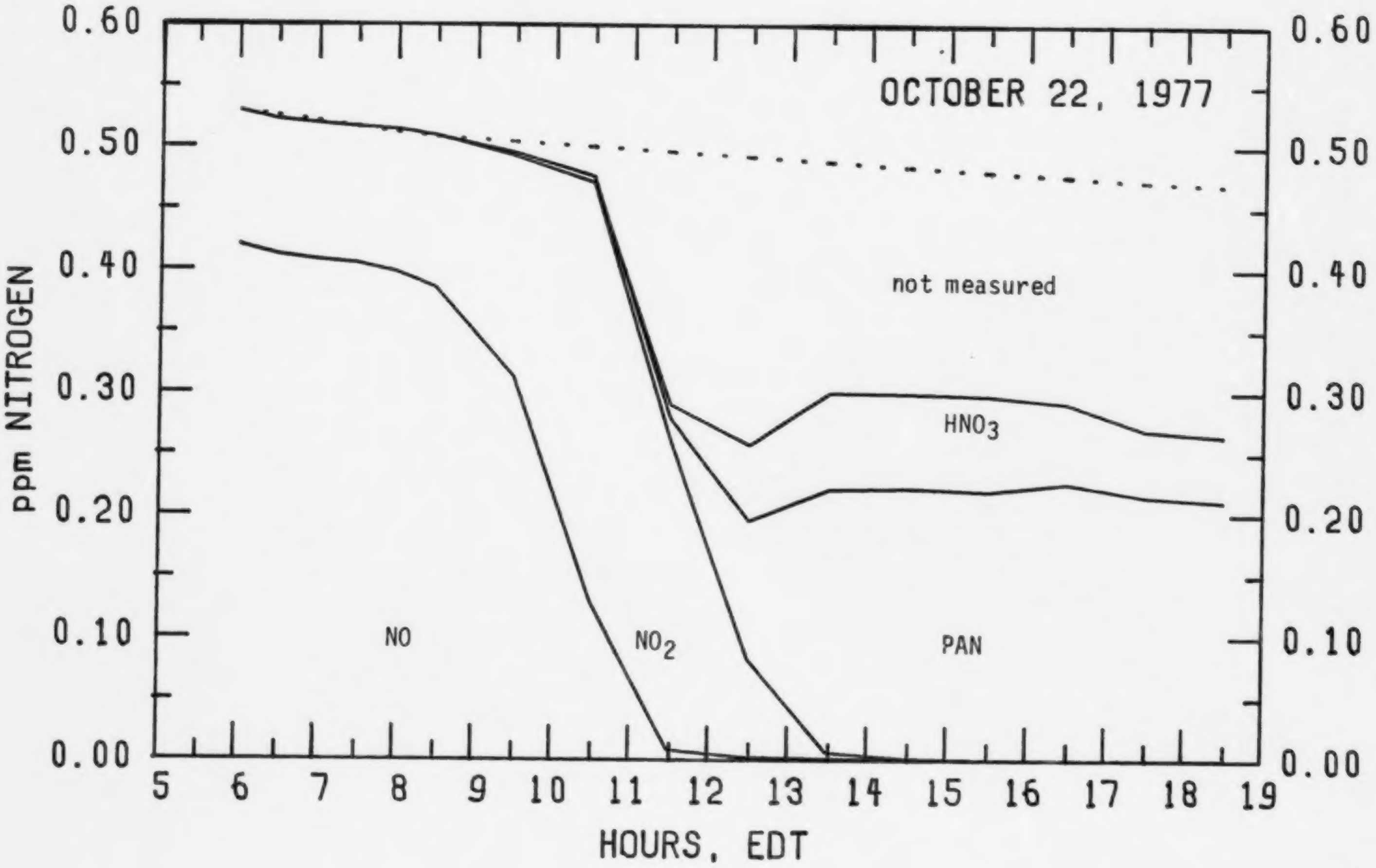

Figure 55. Nitrogen Balance. Dashed line accounts for dilution only. Each line represents the sum of all species below it.

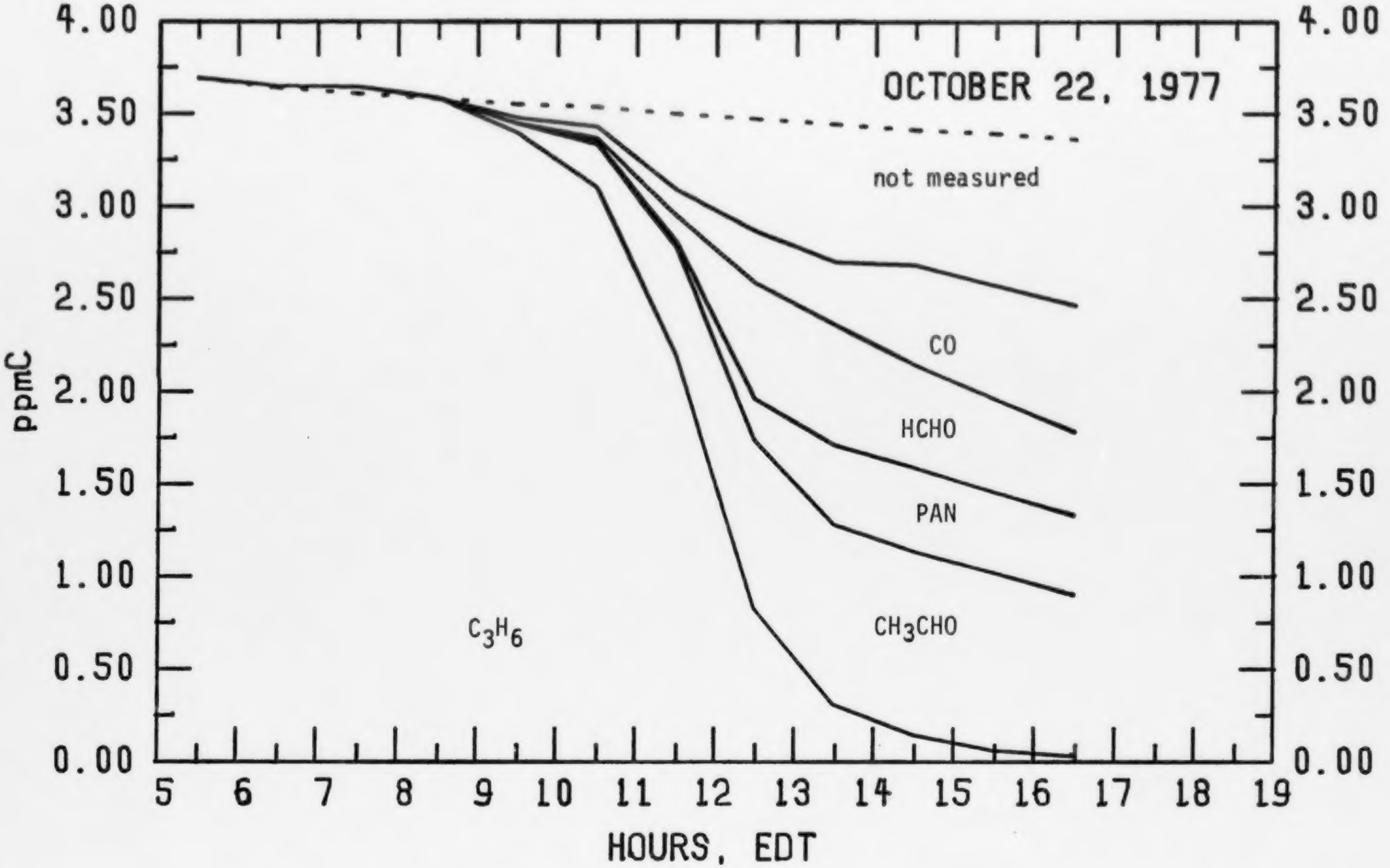

Figure 56. Carbon Balance. Dashed line accounts for dilution only. Each line represents the sum of all species below it.

Table 31. Hourly Values Of Continuous Data For October 22,1977

TIME		NO		NO2		O3		TEMP	DP	TSR	UV
R	B	R	B	R	B	R	B				
0700		0.408		0.111		0.000		36.0		0.002	
	0704		0.410		0.112		0.000	33.4		0.001	
0804		0.396		0.116		0.000		37.9		0.145	
	0800		0.405		0.112		0.000	34.4		0.123	
0900		0.360		0.143		0.000		43.6		0.392	
	0904		0.390		0.122		0.000	44.4		0.442	
1004		0.219		0.261		0.002		53.6		0.571	
	1000		0.363		0.132		0.000	55.6		0.552	
1100		0.023		0.425		0.083		61.8		0.812	
	1104		0.328		0.156		0.000	65.2		0.815	
1204		0.000		0.298		0.563		67.8		0.843	
	1200		0.288		0.164		0.000	71.9		0.844	
1300		0.000		0.234		0.700		69.1		0.941	
	1304		0.247		0.222		0.000	74.8		0.951	
1404		0.000		0.212		0.670					
	1400		0.216		0.238		0.001				
1500		0.000		0.154		0.646					
	1504		0.185		0.263		0.001				
1604		0.000		0.104		0.613					
	1600		0.158		0.289		0.001				
1700		0.000		0.077		0.589					
	1704		0.128		0.315		0.001				

Table 32. Concentrations of Selected Species for October 22, 1977

Nitric Acid

	RED
11:07	0.020
11:22	0.010
11:37	0.000
11:52	0.016
12:07	0.038
12:22	0.047
12:37	0.063
12:52	0.068
13:07	0.070
13:22	0.078
13:37	0.080
13:52	0.080
14:07	0.075
14:22	0.075
14:37	0.072
14:52	0.076
15:07	0.076
15:22	0.075
15:37	0.080
15:52	0.080
16:07	0.070
16:22	0.064
16:37	0.058
16:52	0.068
17:07	0.068
17:22	0.055
17:37	0.053
17:52	0.055
18:07	0.055
18:22	0.055
18:37	0.052

Formaldehyde

	RED
10:30	0.023
11:30	0.140
12:30	0.625
13:30	0.650
14:30	0.555
15:30	0.500
16:30	0.452

Acetaldehyde

	RED
09:30	0.04
10:30	0.179
11:30	0.443
12:30	0.714
13:30	0.764
14:30	0.786
15:30	0.779
16:30	0.700

Table 32. Continued

October 22, 1977

PAN

	RED
10:00	0.002
11:00	0.005
11:30	0.017
12:30	0.113
13:30	0.215
14:30	0.221
15:30	0.223
16:30	0.226
17:30	0.215
18:30	0.211

Carbon Monoxide

	RED
09:15	0.0
10:15	0.06
11:15	0.085
12:15	0.20
13:15	0.307
14:15	0.52
15:15	0.605
16:15	0.678
17:15	0.702
18:15	0.701

Butane

	RED	BLUE
05:00		4.73
06:00		8.09
07:00		8.10
08:00		8.10
09:00		7.98
10:00		7.95
11:00		7.95
12:00		7.93
13:00		7.93
14:00		7.81
15:00		7.66
16:00		7.39
17:30		7.23

Propylene

	RED
05:30	3.694
06:30	3.65
07:30	3.645
08:30	3.585
09:30	3.394
10:30	3.101
11:30	2.195
12:00	1.404
12:30	0.825
13:30	0.307
14:30	0.143
15:30	0.061

Date: October 9, 1979

Type: n-butane vs. n-pentane

INITIAL CONDITIONS (ppmC)

	RED	BLUE
NO	0.171	0.171
NO_2	0.036	0.036
NO_x	0.207	0.207
Butane	14.35	
Pentane		14.23

Time of sunrise: 7:08

Initial Temp (F): 54.5

Max. Temp (F): 84.7

This run compares the relative reactivity of n-pentane and n-butane. The TSR data are low and another clear october day from another year should be used. All nitrate concentrations are in ppbV. Nitrate calibrations for sec-butylnitrate, sec-pentylnitrate and n-pentyl-3-nitrate are based on n-butylnitrate calibrations. These values are given a high error band, perhaps as great as 40%. The two internal nitrates of n-pentane were not fully resolved. Based on the inflection in the peak, however, and estimating where they most probably elute it is estimated that there is a 45:55 split between n-pentyl-3-nitrate and sec-pentylnitrate. In the tables and on the tape these were treated as one compound and called C5INO3.

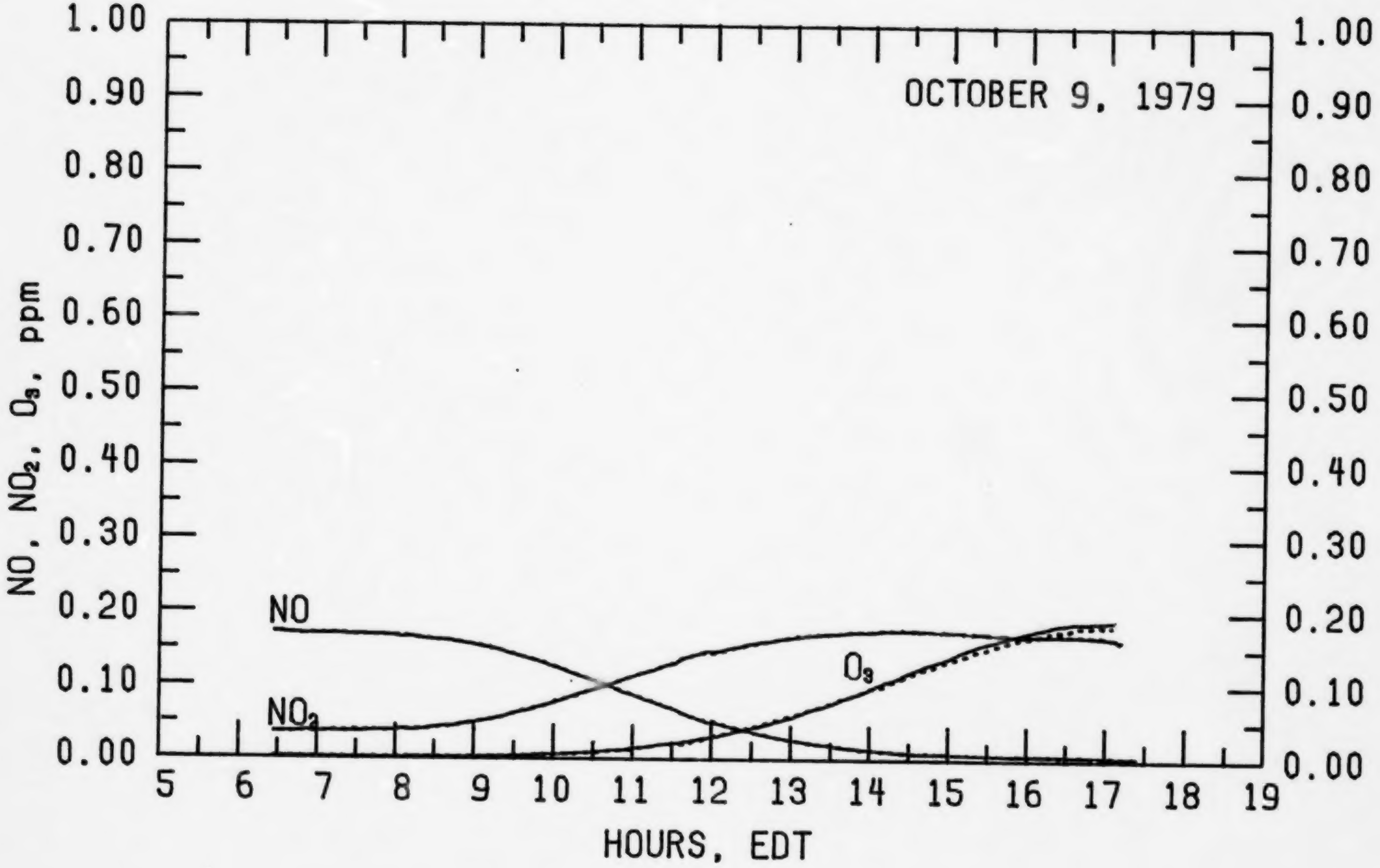

Figure 57. Nitrogen and Ozone Data, both chamber sides.

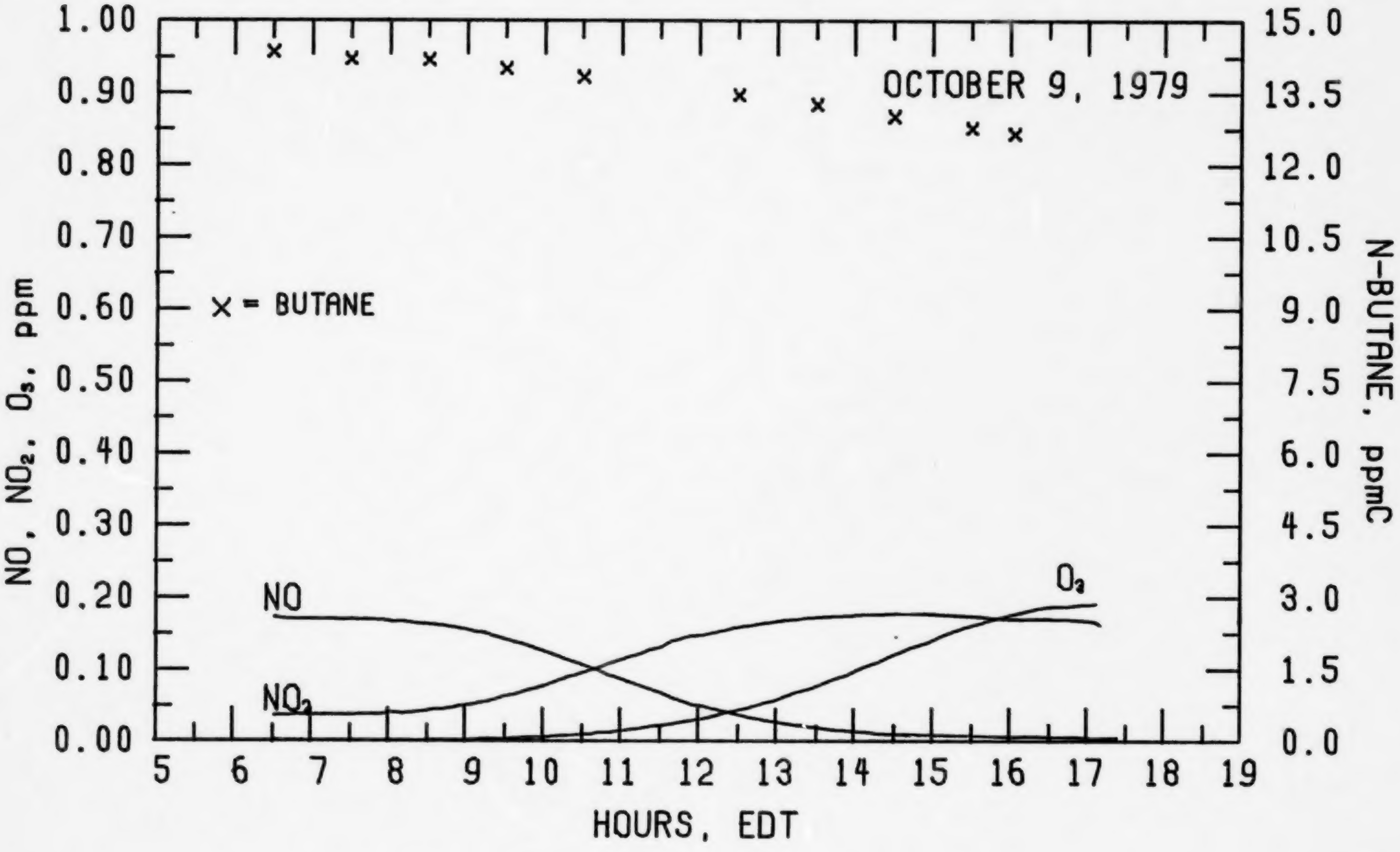

Figure 58. Nitrogen, Ozone, and Hydrocarbon, n-butane side only.

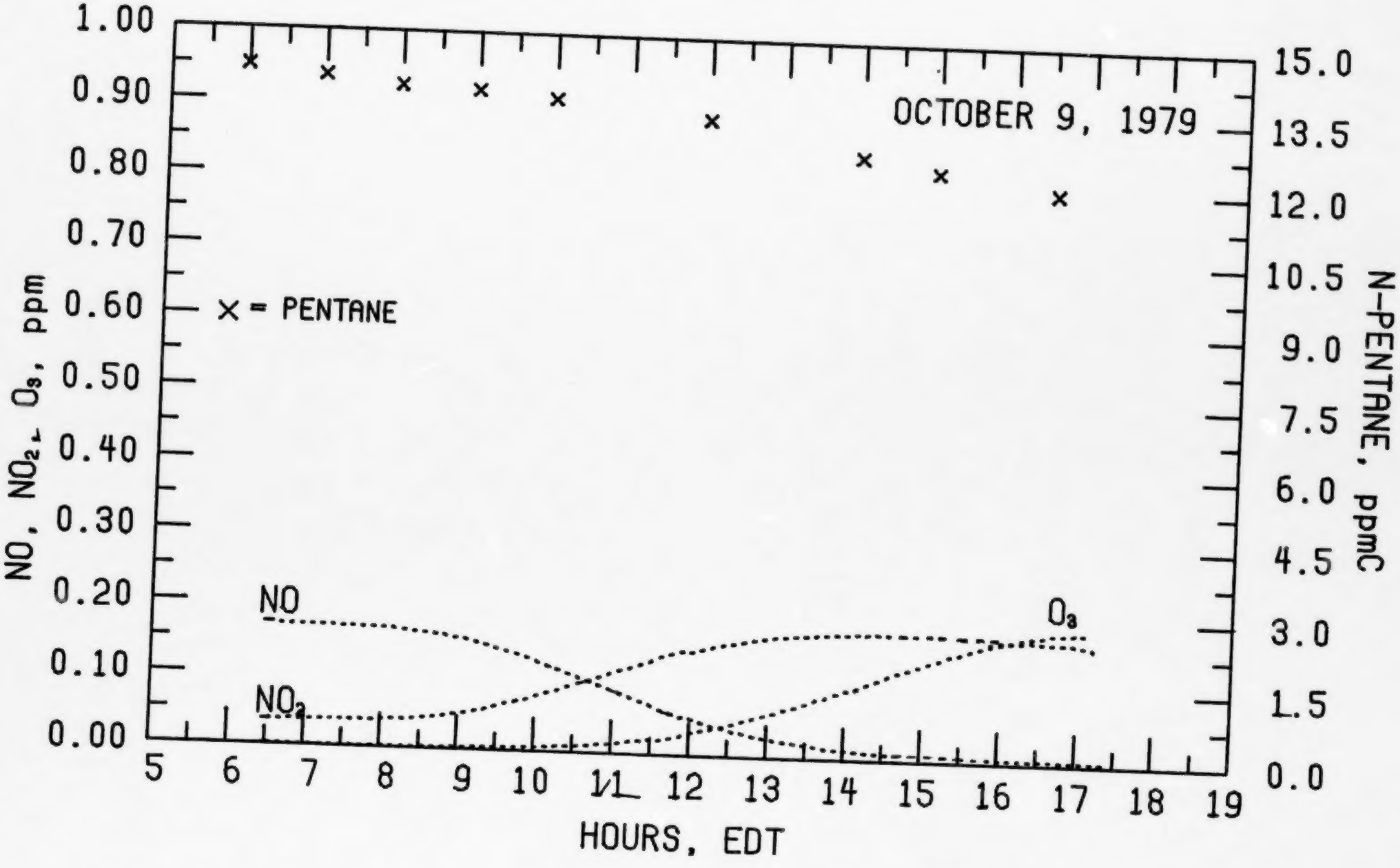

Figure 59. Nitrogen, Ozone, and Hydrocarbon n-pentane side only.

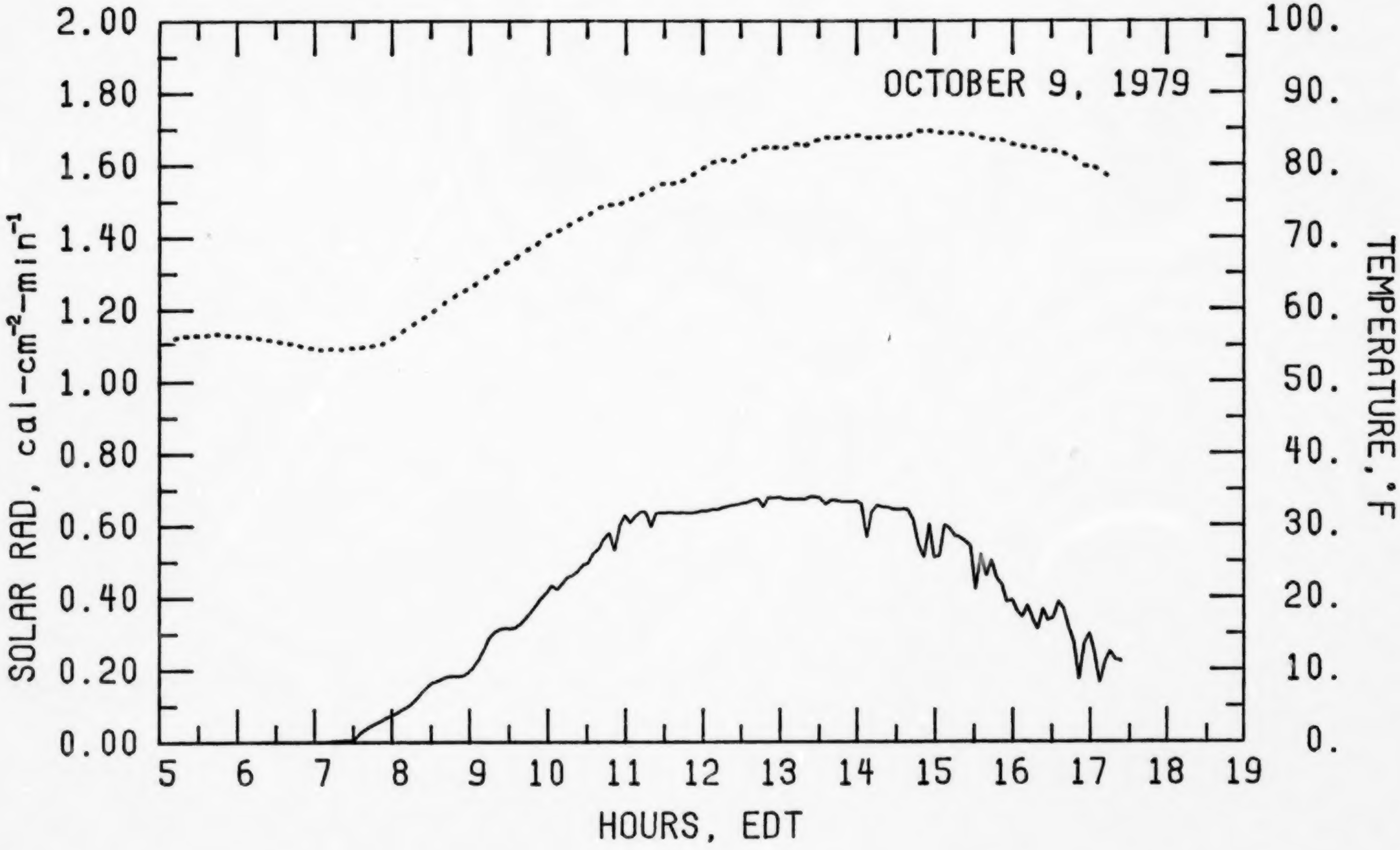

Figure 60. Total Solar Radiation and Temperature Data. TSR magnitude not valid.

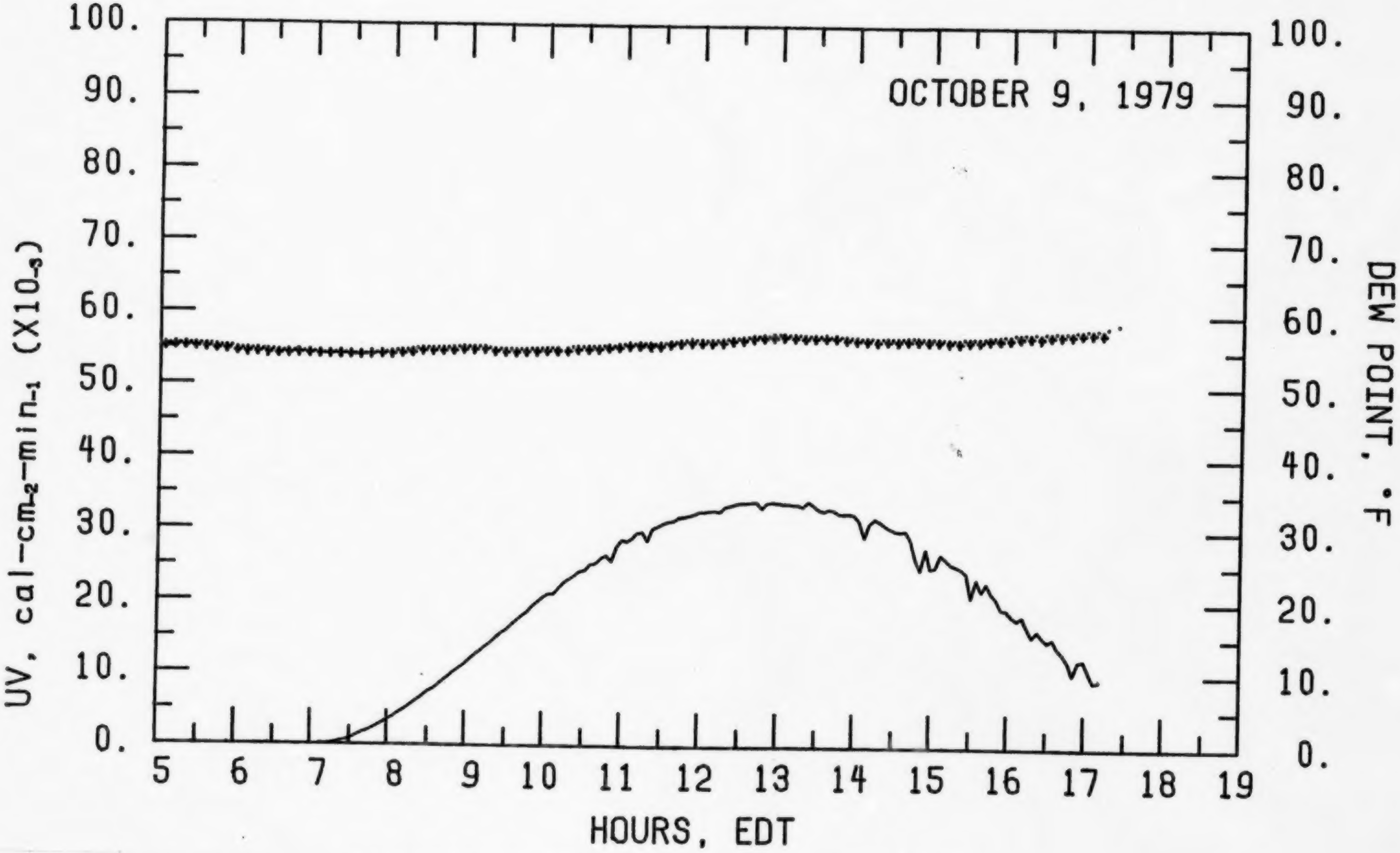

Figure 61. Ultraviolet Radiation and Dewpoint Data.

Table 33. Hourly Values Of Continuous Data For October 9, 1979

TIME		NO		NO2		O3		TEMP	DP	TSR	UV
R	B	R	B	R	B	R	B				
0700		0.1689		0.0359		0.005		54.5	54.44	0.000	0.00
	0704		0.1691		0.0364		0.0008	54.5	54.18	0.000	0.00
0804		0.1656		0.0400		0.0009		57.6	54.66	0.081	3.78
	0800		0.1670		0.0389		0.0023	56.0	54.18	0.075	3.42
0900		0.1552		0.0494		0.0022		61.5	55.26	0.194	11.34
	0904		0.1543		0.0507		0.0024	63.5	54.84	0.208	11.95
1004		0.1236		0.0784		0.0064		66.0	55.13	0.434	21.10
	1000		0.1254		0.0773		0.0059	70.4	4.721	0.416	20.61
1100		0.0870		0.1124		0.0152		69.7	55.80	0.631	28.66
	1104		0.0845		0.1154		0.0148	75.4	55.51	0.608	28.41
1204		0.0487		0.1474		0.0313		74.1	56.42	0.641	32.68
	1200		0.0516		0.1442		0.0319	79.5	56.00	0.641	32.68
1300		0.0263		0.1658		0.0570		76.4	57.27	0.679	33.90
	1304		0.0253		0.1677		0.0618	82.3	56.93	0.673	33.78
1404		0.0125		0.1753		0.0999		79.1	56.81	0.658	31.46
	1400		0.0134		0.1743		0.0968	84.1	56.47	0.667	32.32
1500		0.0091		0.1725		0.1388		79.2	56.86	0.511	24.88
	1504		0.0097		0.1721		0.1370	84.4	56.36	0.517	25.12
1604		0.0057		0.1701		0.1767		78.6	57.45	0.362	18.29
	1600		0.0061		0.1700		0.1673	82.8	56.73	0.395	19.15
1700		0.0047		0.1669		0.1895		76.3	58.11	.3001	12.32
	1704		0.0050		0.1662		0.1838	79.6	57.56	0.249	10.73

Table 34. Concentrations of Selected Species for

October 9, 1979

Pentane

	RED	BLUE
06:00		14.23
07:00		14.05
08:00		13.87
09:00		13.80
10:00		13.66
12:00		13.32
14:00		12.63
15:00		12.35
16:33		11.98

Butane

	RED
06:30	14.35
07:30	14.20
08:30	14.18
09:30	14.00
10:30	13.83
12:30	13.44
13:30	13.24
14:30	13.00
15:30	12.76
16:03	12.64

Formaldehyde

	RED	BLUE
09:30	0.006	
09:45	0.010	
10:00		0.010
10:15		0.010
10:30	0.010	
10:45	0.010	
11:00		0.010
11:15		0.010
11:30	0.012	
11:45	0.012	
12:00		0.016
12:15		0.018
12:30	0.016	
12:45	0.018	
13:00		0.018
13:15		0.020
13:30		0.020
14:30		0.024
14:45		0.024
15:00		0.022
15:15		0.024
15:30	0.026	
15:45		0.026
16:00	0.026	

C3-aldehyde

	RED	BLUE
13:54		0.03
14:53		0.07
15:51		0.07

Carbon Monoxide

	RED	BLUE
08:27	0.251	
08:57		0.257
09:12	0.251	
09:27	0.251	
09:57		0.251
11:12	0.251	
11:57	0.244	
12:12	0.251	
12:27		0.251
12:42		0.244
12:57	0.244	
13:12	0.251	
13:27		0.251
13:42		0.257
13:57	0.244	
14:12	0.257	
14:27		0.251
14:42		0.244
14:57	0.244	
15:12	0.244	
15:27		0.251
15:57	0.244	
16:12	0.251	
16:27		0.251

Methylethylketone

	RED
15:22	0.20
16:20	0.22

Table 35. Concentrations of Selected Species for

October 9, 1979

PAN

	RED	BLUE
10:55	0.09	
11:55	0.20	
12:25		0.50
12:55	0.40	
13:25		0.90
13:55	0.30	
14:25	0.70	
14:55	0.90	
15:25		2.70
15:55	1.10	
16:25		3.50

Acetaldehyde

	RED	BLUE
10:22	0.015	
11:22	0.035	
11:55		0.015
12:27	0.085	
12:57		0.030
13:25	0.100	
13:54		0.060
14:24		0.063
14:53		0.065
15:22	0.190	
15:51		0.075
16:20	0.200	

N-pentyl-3-nitrate

	RED	BLUE
10:25		0.30
11:25		0.30
12:25		0.40
13:25		0.70
15:25		1.20
16:25		1.00

Ethylnitrate

	RED	BLUE
12:55	0.05	
13:25		0.10
13:55	0.05	
14:25	0.10	
14:55	0.10	
15:25		0.20
15:55	0.15	
16:25		0.50

Sec-butylnitrate

	RED	BLUE
08:25		0.10
09:25		0.99
10:25		2.30
11:25		4.10
12:25		5.20
13:25		7.20
15:25		10.2
16:25		11.3

Sec-pentylnitrate and

N-pentyl-3-nitrate

	RED
08:55	0.90
09:55	2.70
10:55	5.90
11:55	9.70
12:55	12.8
13:55	16.0
14:25	17.2
14:55	18.7
15:55	21.7

Date: October 12, 1978

Type: Propylene vs. Ethylene/acetaldehyde

INITIAL CONDITIONS (ppmC)

	RED	BLUE
NO	0.364	0.364
NO_2	0.115	0.115
NO_x	0.479	0.479
Propylene		1.33
Ethylene	0.197	
Acetald	1.26	

Time of sunrise: 7:24

Initial Temp (F): 41.8

Max. Temp (F): 82.0

This run was conducted to compare the behavior of an ethylene/acetaldehyde/NO_x mixture with a propylene/NO_x system. Both TSR data and UV data can be used.

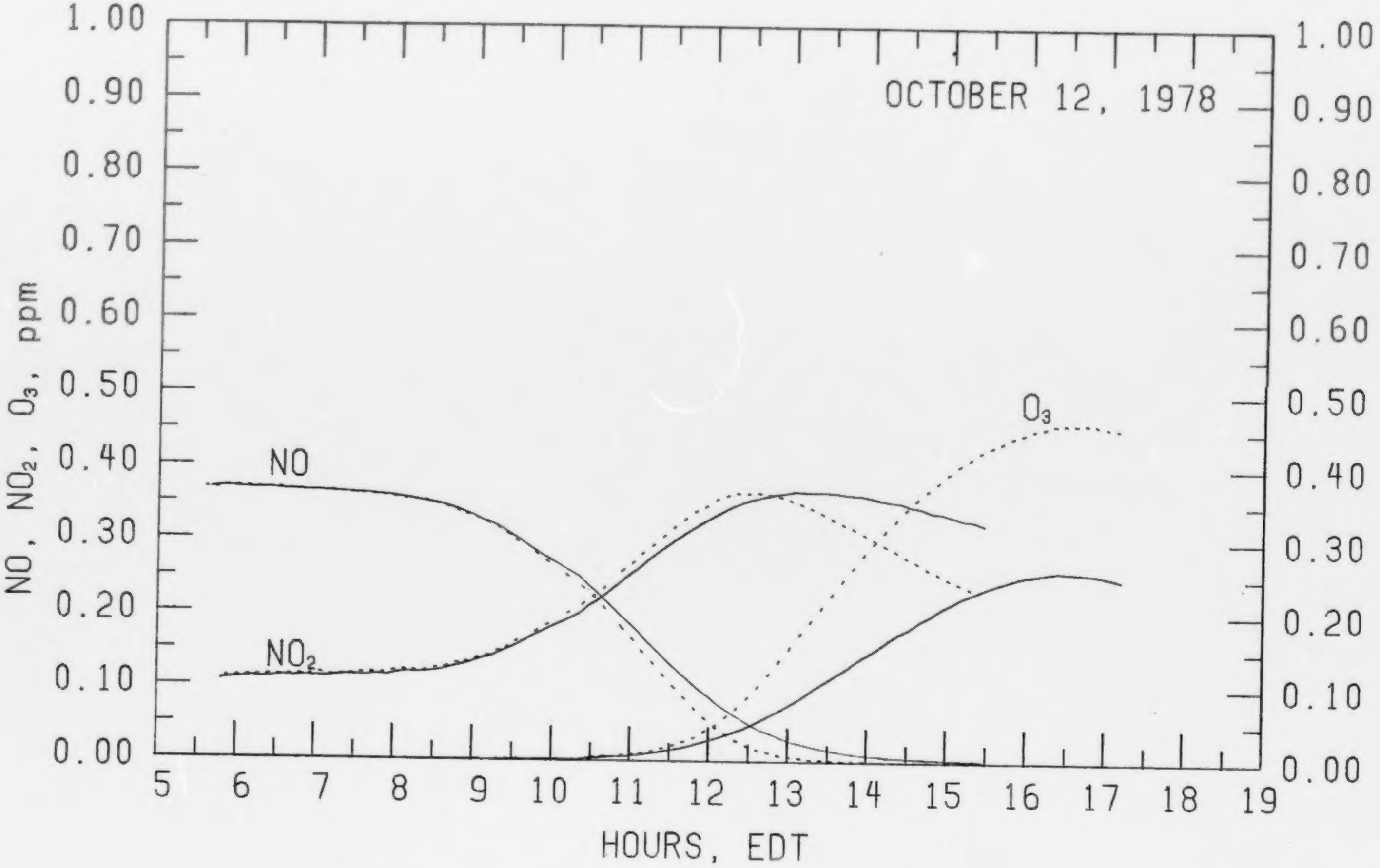

Figure 62. Nitrogen and Ozone Data.

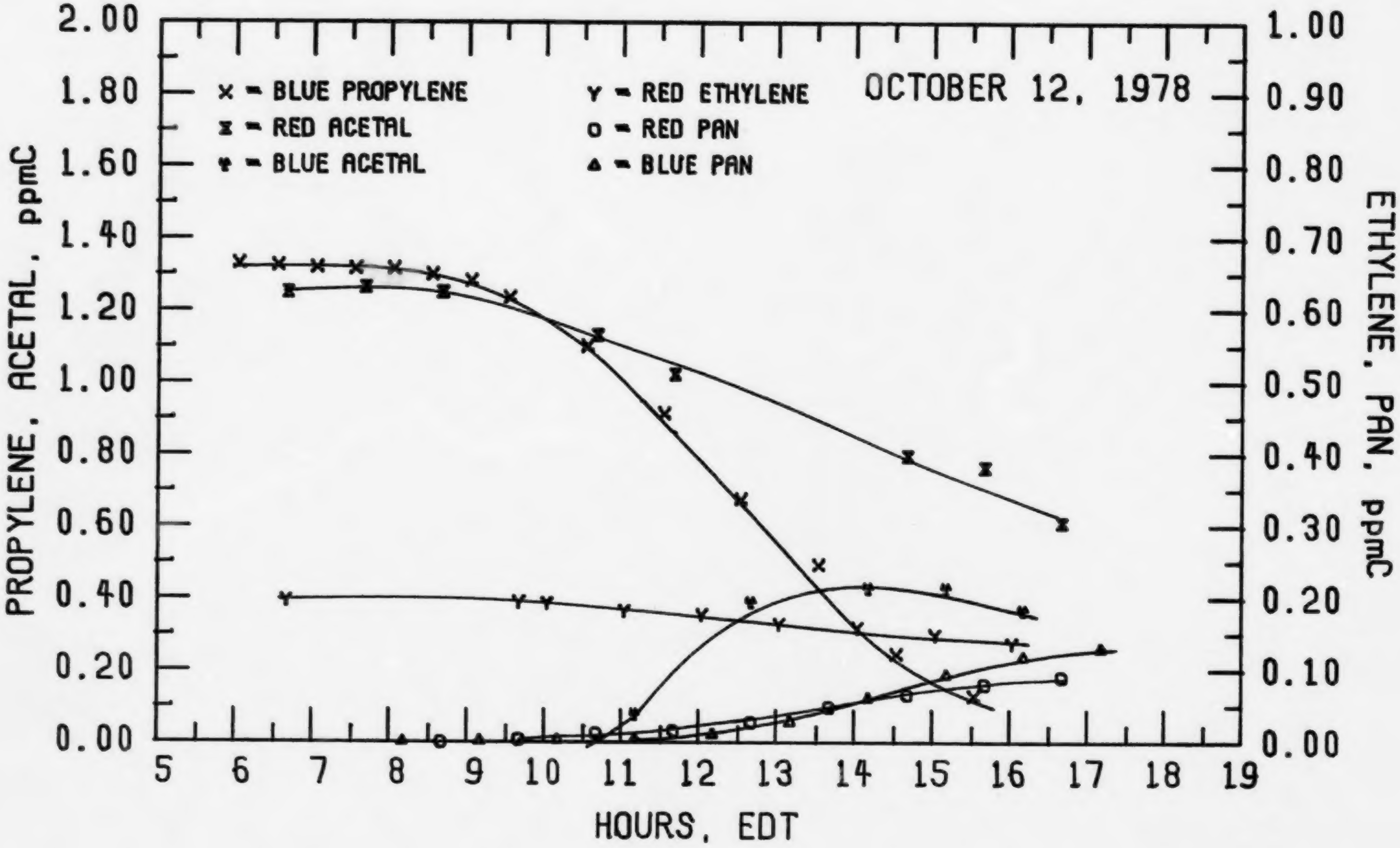

Figure 63. Carbon Reactant and Product Data.

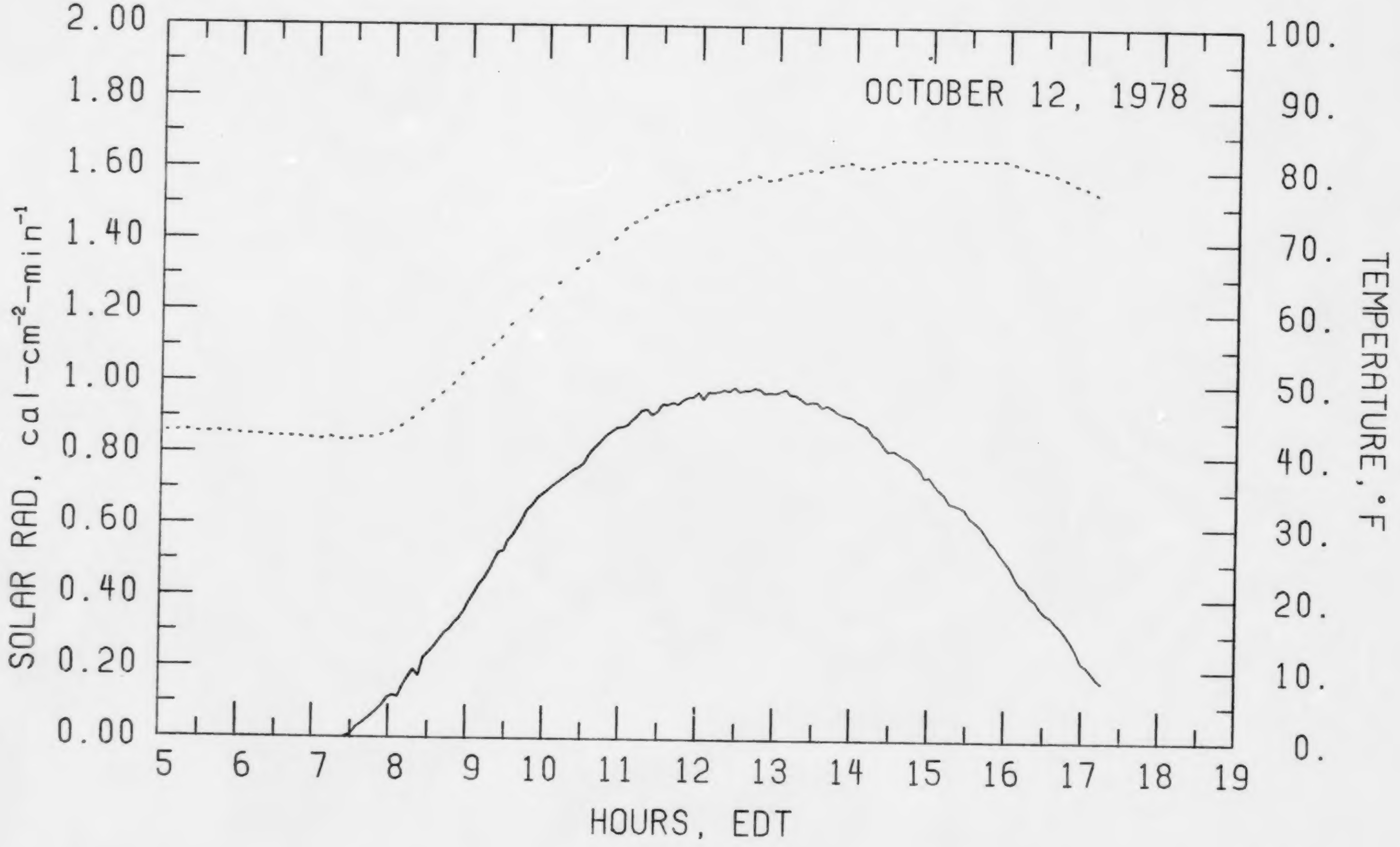

Figure 64. Total Solar Radiation and Temperature.

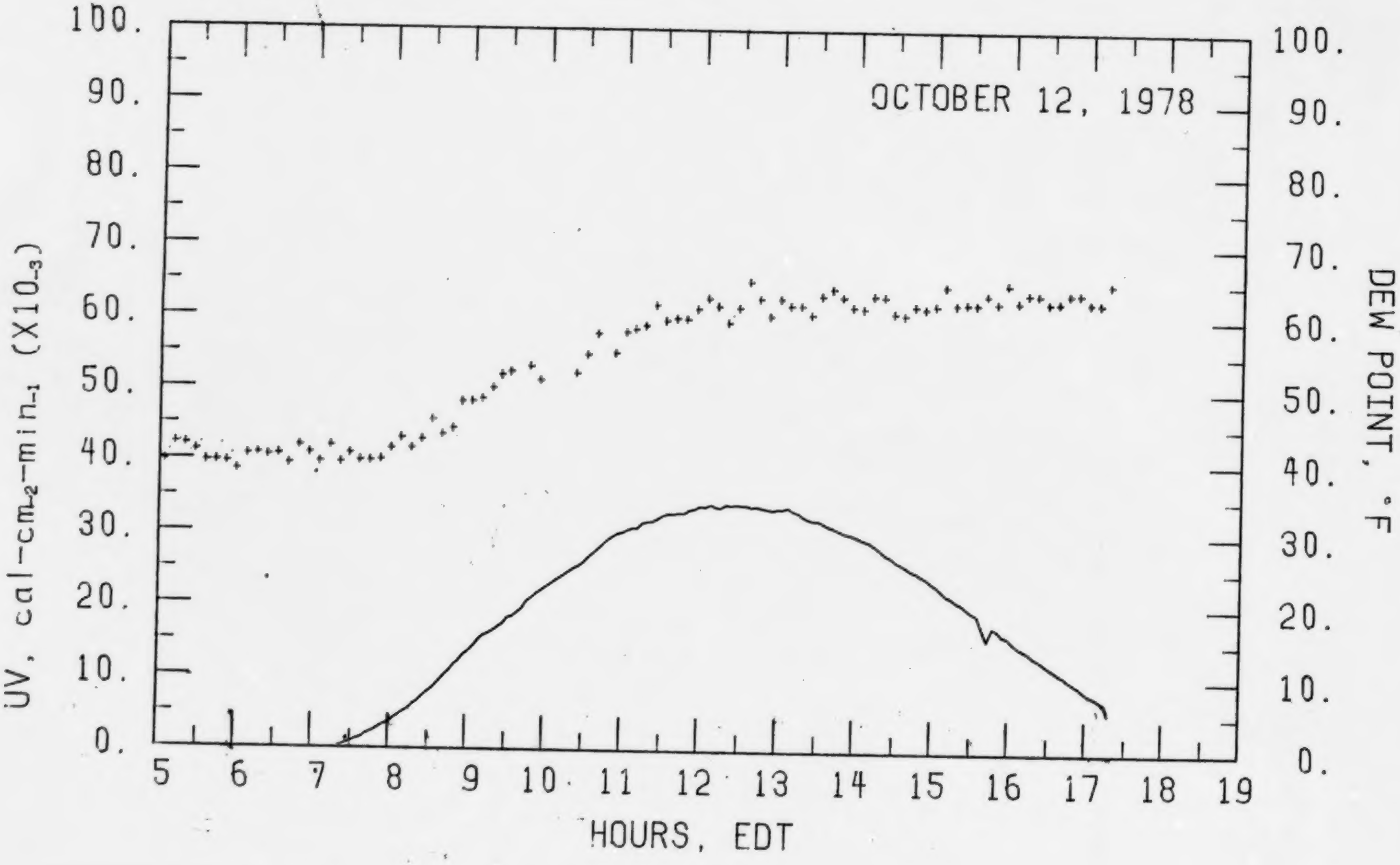

Figure 64a. Total Solar Radiation and Temperature.

Table 36. Hourly Values Of Continuous Data For October 12, 1978

TIME		NO		NO2		O3		TEMP	DP	TSR	UV
R	B	R	B	R	B	R	B				
0500		0.016		0.009		0.000		44.9	41.0	0.000	0.000
	0504		0.014		0.008		0.000	42.9	39.7	.0000	0.000
0604		0.369		0.111		0.000		44.8	40.5	0.000	0.000
	0600		0.370		0.112		0.000	42.6	38.5	0.000	0.000
0700		0.366		0.113		0.000		44.8	40.3	0.000	0.000
	0704		0.365		0.118		0.000	41.9	39.7	0.000	0.000
0804		0.358		0.119		0.000		45.6	43.2	0.121	4.024
	0800		0.358		0.121		0.000	42.9	41.6	0.133	13.50
0900		0.335		0.133		0.001		52.1	46.8	0.356	13.05
	0904		0.331		0.138		0.000	52.5	48.2	0.384	13.66
1004		0.251		0.201		0.002		64.7	55.7	0.748	24.88
	1000		0.273		0.185		0.000	61.7	51.3	0.678	21.83
1100		0.190		0.252		0.007		69.2	58.9	0.876	30.24
	1104		0.167		0.269		0.010	69.5	58.5	0.876	30.36
1204		0.087		0.331		0.029		72.8	62.8	0.974	34.02
	1200		0.060		0.346		0.040	76.1	61.3	0.961	33.66
1300		0.031		0.366		0.073		74.8	61.7	0.975	33.54
	1304		0.060		0.355		0.153	78.7	62.8	0.973	33.66
1404		0.009		0.361		0.147		77.4	62.3	0.908	30.00
	1400		0.001		0.310		0.281	81.1	61.7	0.910	30.24
1500		0.004		0.338		0.210		77.9	62.3	0.739	24.15
	1504		0.000		0.249		0.392	82.0	62.0	0.742	23.54
1604		0.000		0.305		0.255		77.6	65.1	0.508	6.098
	1600		0.000		0.177		0.447	81.5	64.9	0.526	16.34
1700		0.000		0.271		0.256		74.8	60.9	0.256	9.268
	1704		0.000		0.103		0.457	77.7	62.5	0.223	8.66

Table 37. Concentrations of Selected Species for October 12, 1978

PAN

	RED	BLUE
08:10		0.0000
08:40	0.0000	
09:10		0.0008
09:40	0.0021	
10:10		0.0013
10:40	0.0070	
11:10		0.0021
11:40	0.0095	
12:10		0.0062
12:40	0.0164	
13:10		0.0164
13:40	0.0287	
14:10		0.0357
14:40	0.0390	
15:10		0.0545
15:40	0.0472	
16:10		0.0688
16:40	0.0529	
17:10		0.0758

PROP

	RED	BLUE
06:02		1.331
06:32		1.325
07:02		1.319
07:32		1.316
08:02		1.316
08:32		1.300
09:02		1.282
09:32		1.236
10:32		1.101
11:32		0.913
12:32		0.676
13:32		0.493
14:32		0.246
15:32		0.130

ETHY

06:40	0.197
09:40	0.194
10:02	0.192
11:02	0.182
12:02	0.177
13:02	0.164
14:02	0.159
15:02	0.149
16:02	0.137

ACET

	RED	BLUE
06:40	1.250	
07:40	1.264	
08:40	1.250	
10:40	1.131	
11:10		0.078
11:40	1.022	
12:40		0.390
14:10		0.429
14:40	0.796	
15:10		0.429
15:40	0.764	
16:10		0.367
16:40	0.609	

DATE: August 5, 1979

TYPE: ETHYLENE VS FORMALDEHYDE (DRY DOWN IN
FORMALDEHYDE SIDE)

INITIAL CONDITIONS (ppmC)

	Red	Blue
NO	0.503	0.407
NO2	0.135	0.132
NOx	0.638	0.539
HCHO		1.209
Ethy	4.114	

Time of Sunrise - 0612
Initial Temp (F) - 74.0
Max Temp (F) - 102.7

This is a high concentration formaldehyde-NOx and ethylene-NOx run. Prior to injection of formaldehyde, the blue chamber was dried by recirculation of chamber air past the refrigeration cooling coils. This was done to eliminate the possibility of any formaldehyde wall losses after injection. The initial temperature was 74°F, the initial dew point in the formaldehyde side 50°F, and the initial dew point in the ethylene side was 65°. Little increase in water vapor can be observed in the formaldehyde side while in the undried side a small increase following the diurnal temperature profile occurred. Initial formaldehyde concentrations in the chamber are very stable until sunrise. The accuracy of the formaldehyde and ethylene data are probably better than 7%. NOx and O3 values are 10%. Inspection of the data shows almost complete conversion of formaldehyde to carbon monoxide and ethylene to formaldehyde and CO. Failure of the data acquisition system prevented the collection of TSR and UV data from 9:30 - 13:00. Climatological data suggests, however, that clear sky conditions prevailed. In addition 1979 TSR data are low because moisture had infiltrated the sensor. If TSR data are to be used in modeling it is suggested that a clear day from another year such as August 8, 1977 be used. UV data, however, are good.

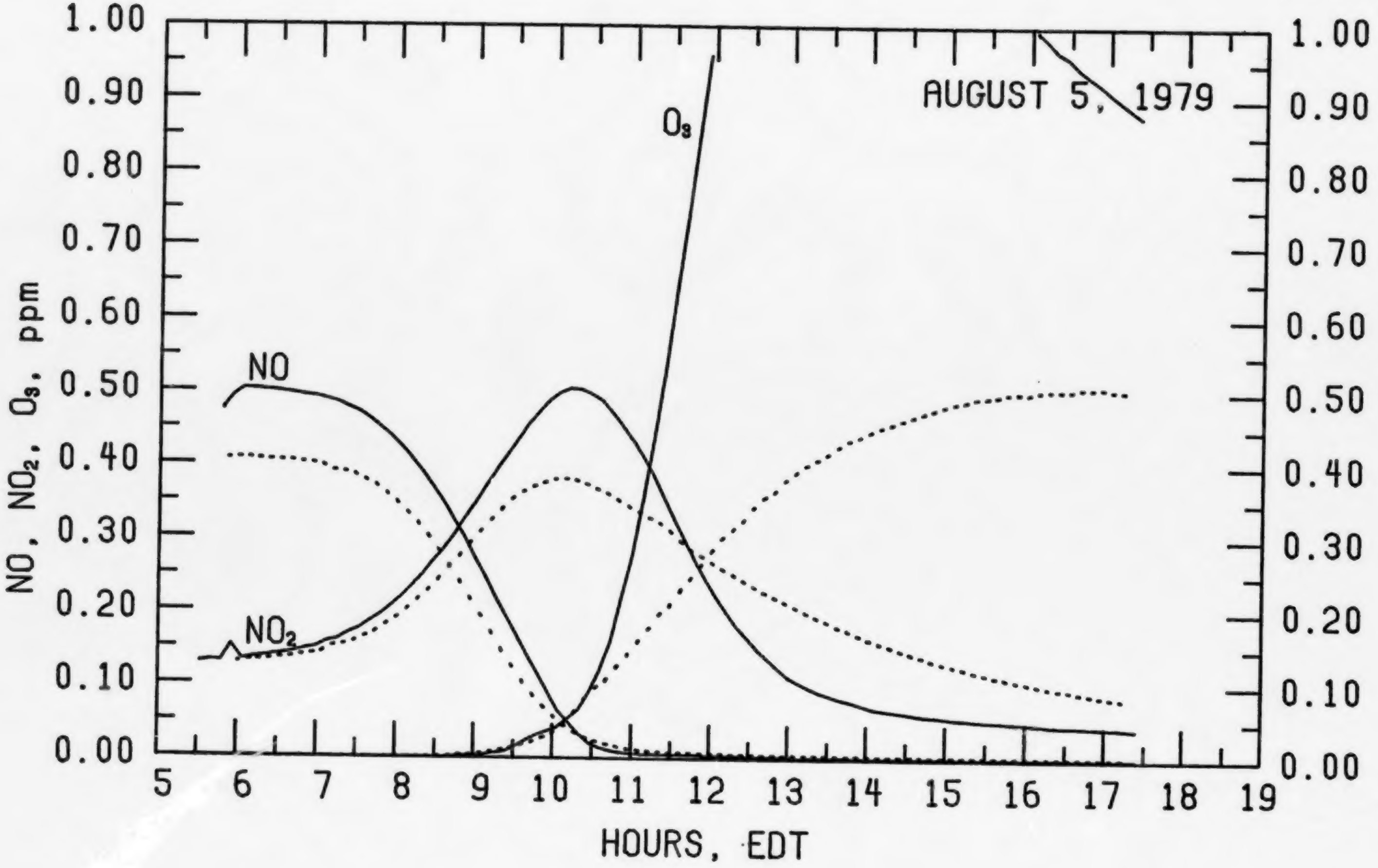

Figure 65. Nitrogen and Ozone Data.

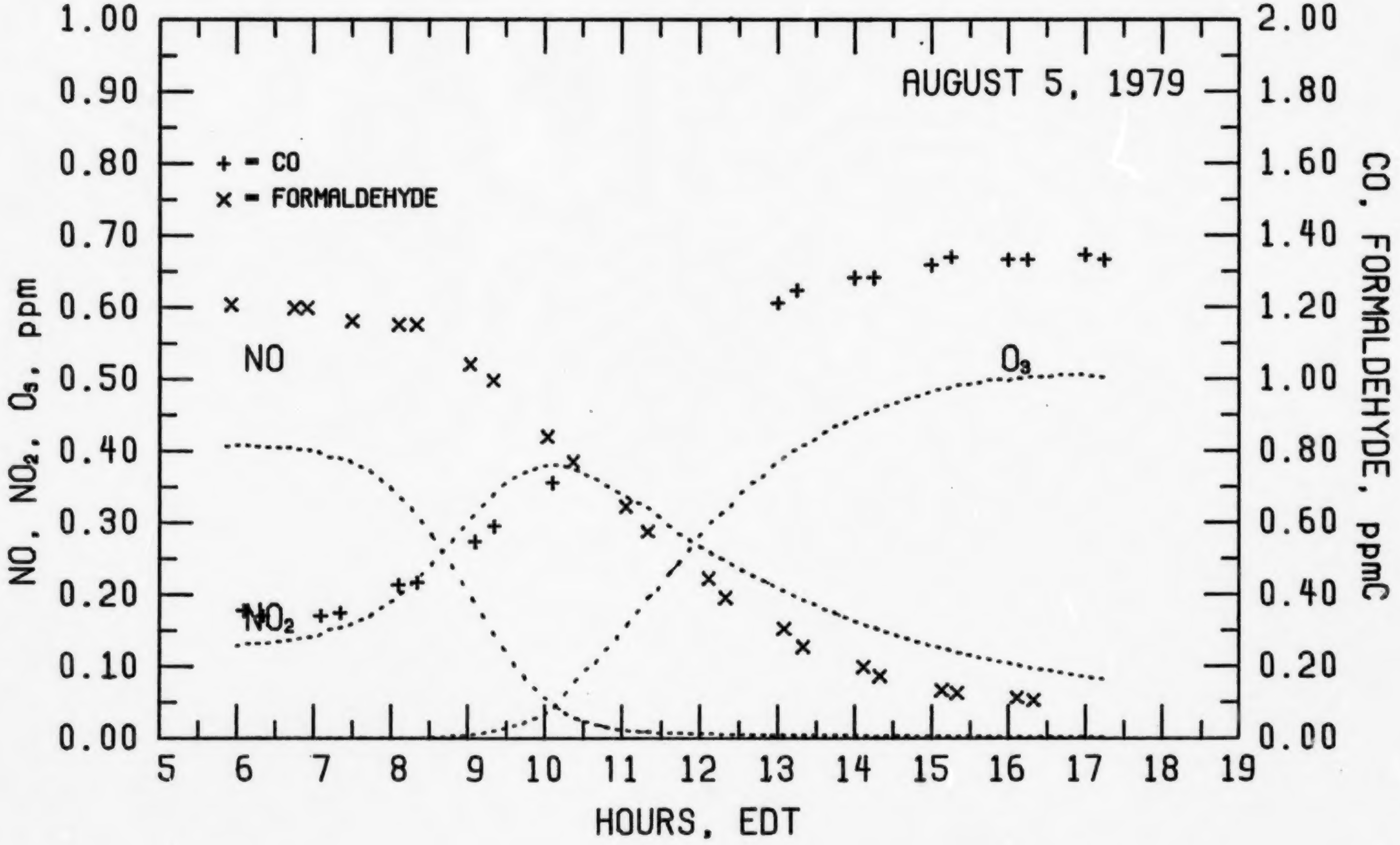

Figure 66. Nitrogen, Ozone, and Carbon Data, formaldehyde only. (Blue side)

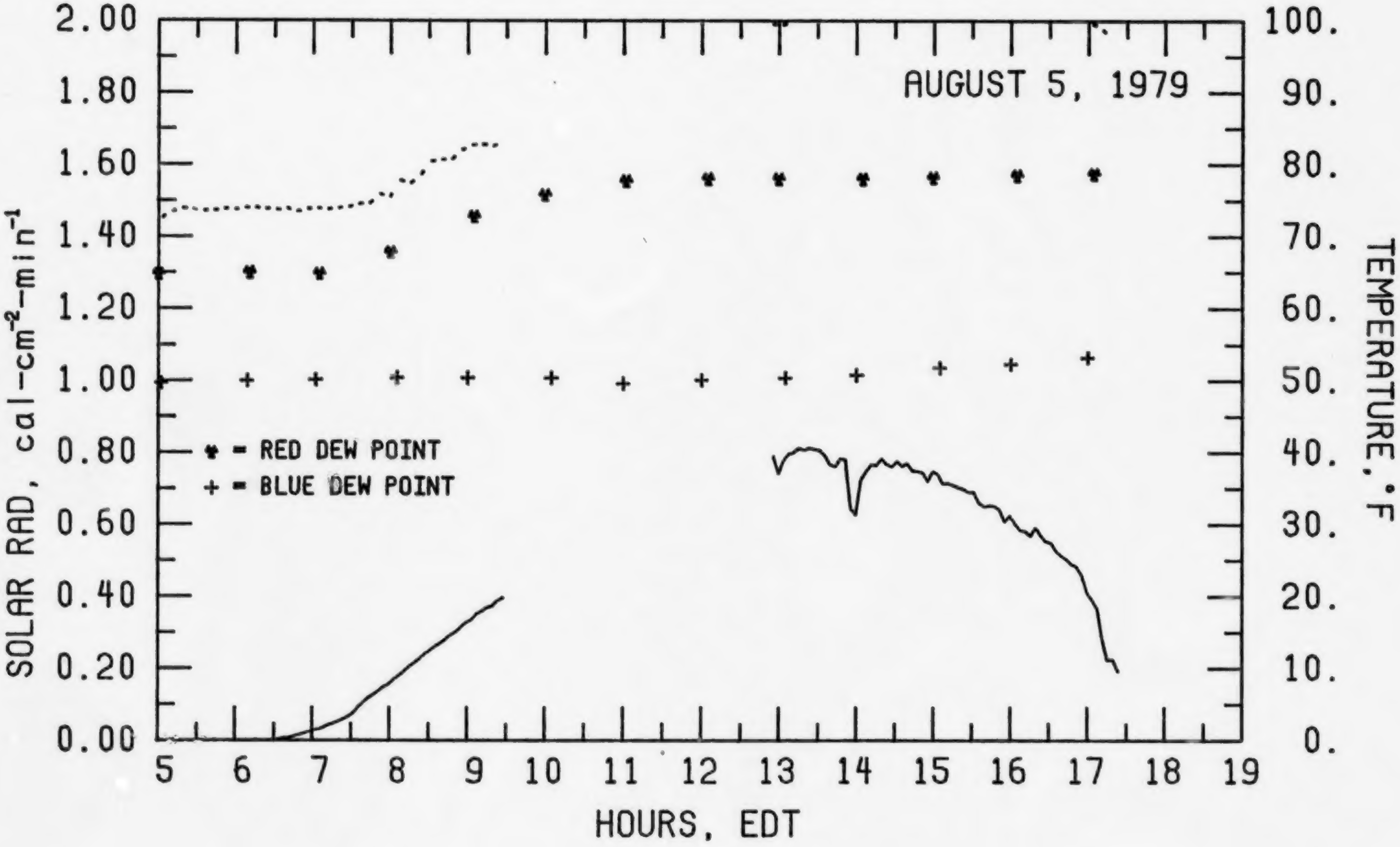

Figure 67. Total Solar Radiation, Temperature and Dewpoint Data. TSR magnitude not valid.

Table 38. Hourly Values Of Continuous Data For August 5, 1979

TIME		NO		NO2		O3		TEMP	DP	TSR	UV
R	B	R	B	R	B	R	B				
0700		0.4923		0.1499		0.000		67.1	64.8	0.027	
	0704		0.3986		0.1431		0.001	73.9	50.1	0.031	
0804		0.4233		0.2185		0.001		70.8	67.8	0.171	
	0800		0.3492		0.1901		0.001	75.6	50.4	0.157	
0900		0.2729		0.3469		0.003		74.9	72.8	0.330	
	0904		0.1957		0.3077		0.006	82.7	50.4	0.337	
1004		0.0649		0.4938		0.042			75.8		
	1000		0.0577		0.3802		0.034		50.4		
1100		0.0072		0.4332		0.276			77.7		
	1104		0.0113		0.3361		0.158		49.6		
1204		0.0041		0.2205		1.048			78.0		
	1200		0.0072		0.2675		0.282		50.1		
1300		0.0028		0.1117		1.294		86.5	78.0	0.742	39.39
	1304		0.0057		0.2075		0.390	99.3	50.4	0.777	40.61
1404		0.0022		0.0696		1.207		86.8	78.0	0.724	38.54
	1400		0.0045		0.1634		0.447	101.4	50.8	0.627	34.63
1500		0.0018		0.0568		1.103		88.9	78.2	0.79	37.80
	1504		0.0041		0.1277		0.486	101.4	51.8	0.739	37.07
1604		0.0016		0.0489		0.994		89.7	78.5	.602	28.90
	1600		0.0033		0.1050		0.499	100.7	52.3	0.624	30.00
1700		0.0012		0.0446		0.910		88.9	53.2	0.411	19.27
	1704		0.0032		0.0851		0.504	99.6	78.7	0.390	18.05

Table 39. Concentrations of Selected Species for August 5, 1979

Carbon Monoxide

	RED	BLUE
05:36	0.335	
05:51	0.350	
06:06		0.357
06:21		0.342
06:36	0.371	
06:51	0.378	
07:06		0.342
07:21		0.350
07:36	0.357	
07:51	0.357	
08:06		0.428
08:21		0.435
08:36	0.550	
08:51	0.550	
09:06		0.549
09:21		0.592
09:36	0.564	
09:51	0.571	
10:06		0.713
13:00		1.213
13:15		1.243
13:30	1.819	
13:45	1.954	
14:00		1.284
14:15		1.284
14:30	2.226	
14:45	2.347	
15:00		1.320
15:15		1.341
15:30	2.497	
15:45	2.554	
16:00		1.334
16:15		1.334
16:30	2.639	
16:45	2.696	
17:00		1.348
17:15		1.334

Formaldehyde

	RED	BLUE
05:56		1.209
06:45		1.200
06:55		1.200
07:30		1.163
07:40	0.019	
07:50	0.019	
08:06		1.153
08:20		1.153
08:35	0.091	
08:50	0.113	
09:02		1.042
09:20		0.997
09:35	0.259	
09:50	0.324	
10:02		0.841
10:22		0.772
10:35	0.618	
10:50	0.757	
11:03		0.647
11:20		0.577
11:35	1.198	
11:50	1.330	
12:07		0.447
12:20		0.394
12:35	1.479	
12:50	1.488	
13:05		0.307
13:20		0.257
13:35	1.392	
13:50	1.380	
14:07		0.201
14:20		0.175
14:35	1.241	
14:50	1.230	
15:08		0.136
15:20		0.128
15:35	1.088	
15:50	1.075	
16:07		0.115
16:20		0.108
16:35	0.977	
16:45	0.973	

Ethylene

	RED
06:10	4.057
06:36	4.114
07:06	4.084
07:36	4.056
08:36	3.923
09:36	3.708
10:36	3.336
11:36	2.438
12:36	1.531
13:36	0.988
16:36	0.360

DATE: August 1, 1979

TYPE: ACETALDEHYDE VS FORMALDEHYDE (DRY DOWN IN FORMALDEHYDE SIDE)

INITIAL CONDITIONS (ppmC)

	Red	Blue
NO	0.274	0.277
NO2	0.075	0.076
NOx	0.349	0.333
Form		1.00
ACET	1.90	

Time of Sunrise - 0632
Initial Temp (F) - 79.0
Max Temp (F) - 104.6

The BLUE chamber was dried prior to injecting formaldehyde by recirculation of the chamber air past air conditioning dryer coils. The starting dew point was 64.5 in BLUE and 70.5'F in RED. There was no increase in dew point in the dried side while the dew point in the RED side initially increased slightly following the diurnal temperature pattern. Formaldehyde was injected by subliming 0.19 ug of solid paraformaldehyde into the BLUE chamber. Acetaldehyde was injected from a high concentration tank. Formaldehyde measurements taken in the acetaldehyde side were corrected for a 10% positive carbon interference of acetaldehyde to the reverse West-Gaeke automated formaldehyde instrument. Formaldehyde data in the BLUE side are better than 7% and in the RED side 10%. CO, NO, and O3 data are 10%; acetaldehyde 15% and PAN 20%. TSR and UV data are missing beyond 12:52. It should be assumed that the remainder of the day is clear. In addition 1979 TSR data are low and clear August TSR values from another year such as August 8, 1977 should be used. UV data are good.

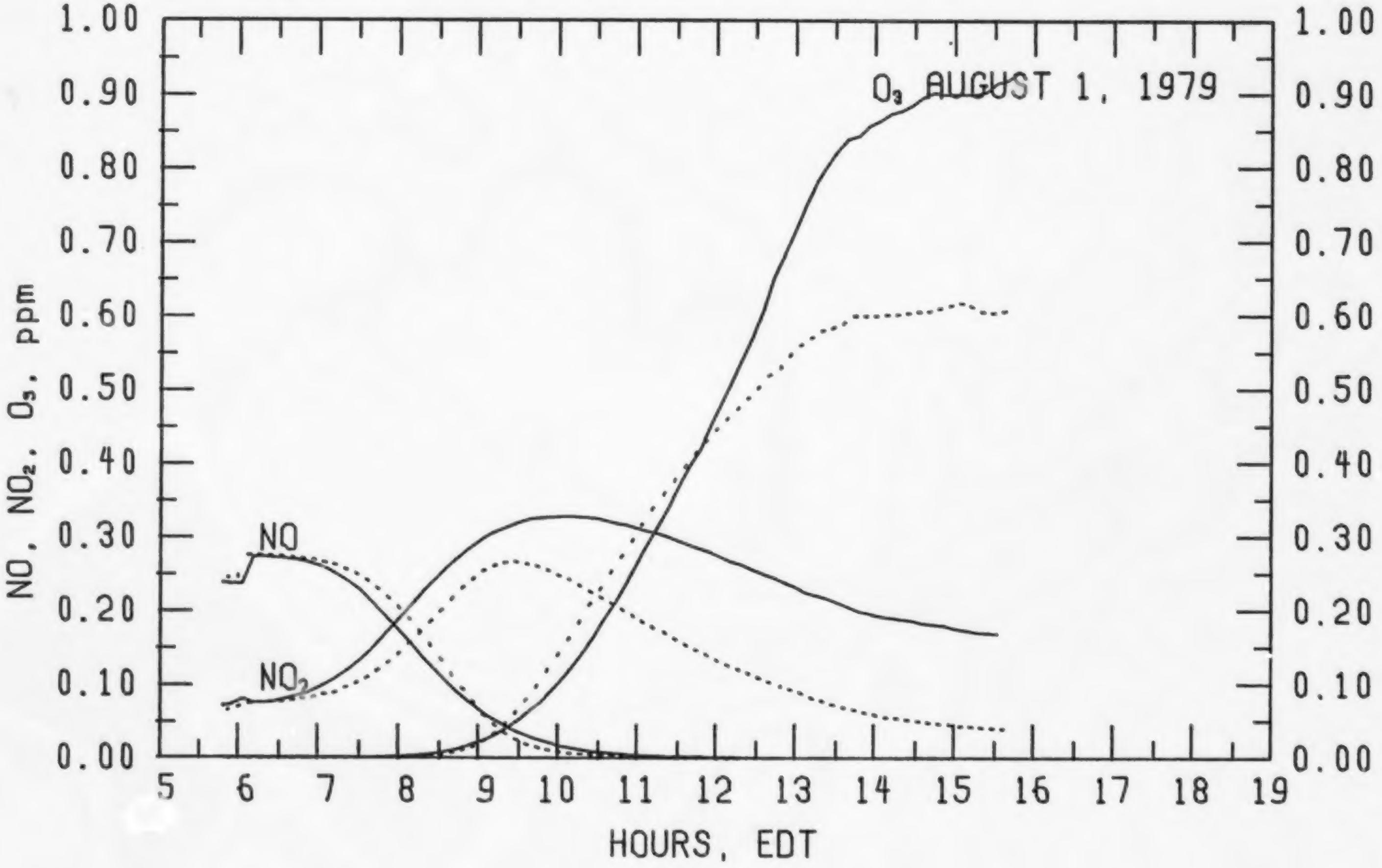

Figure 68. Nitrogen and Ozone Data.

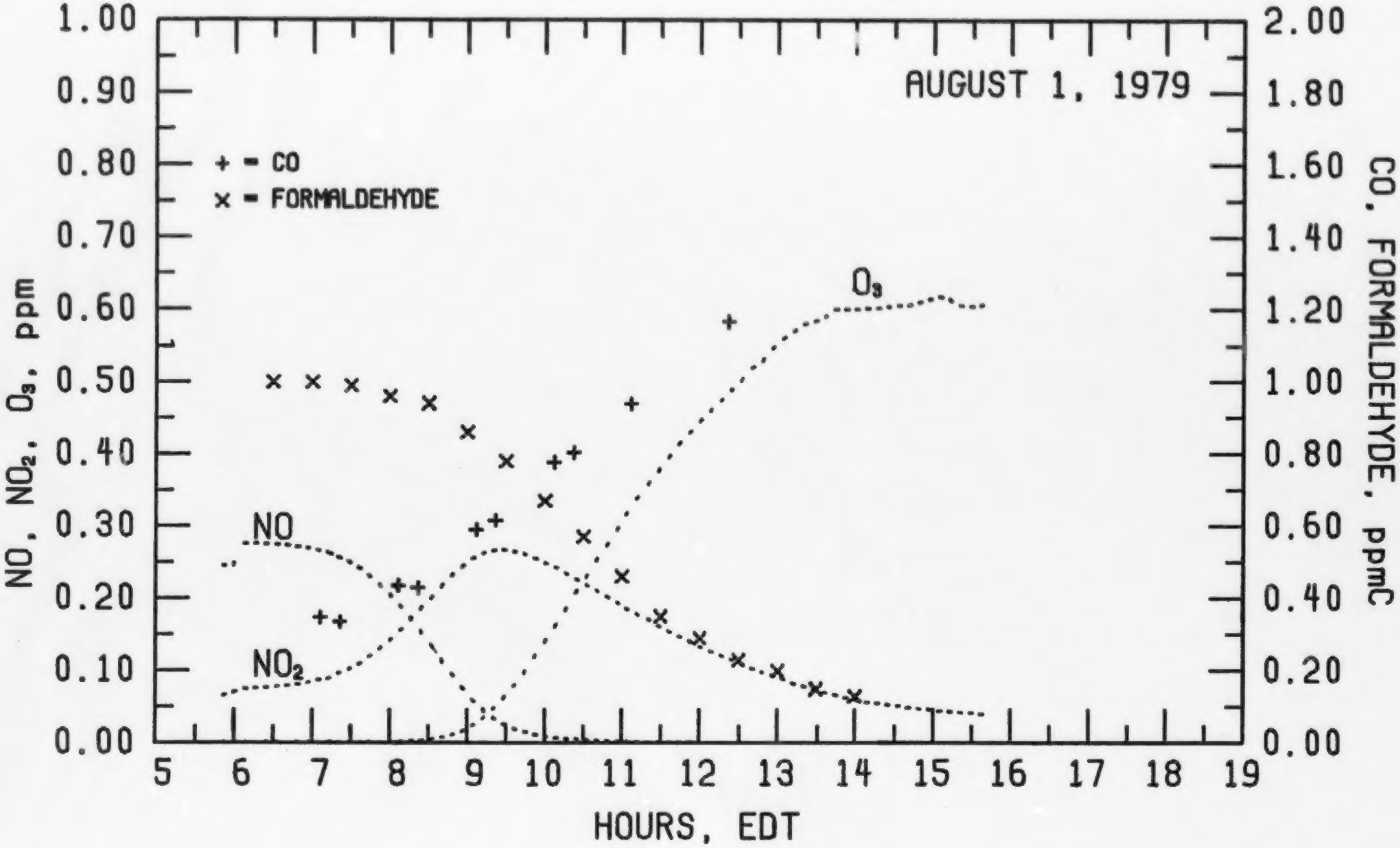

Figure 69. Nitrogen, Ozone, and Carbon Data, formaldehyde only. (Blue side).

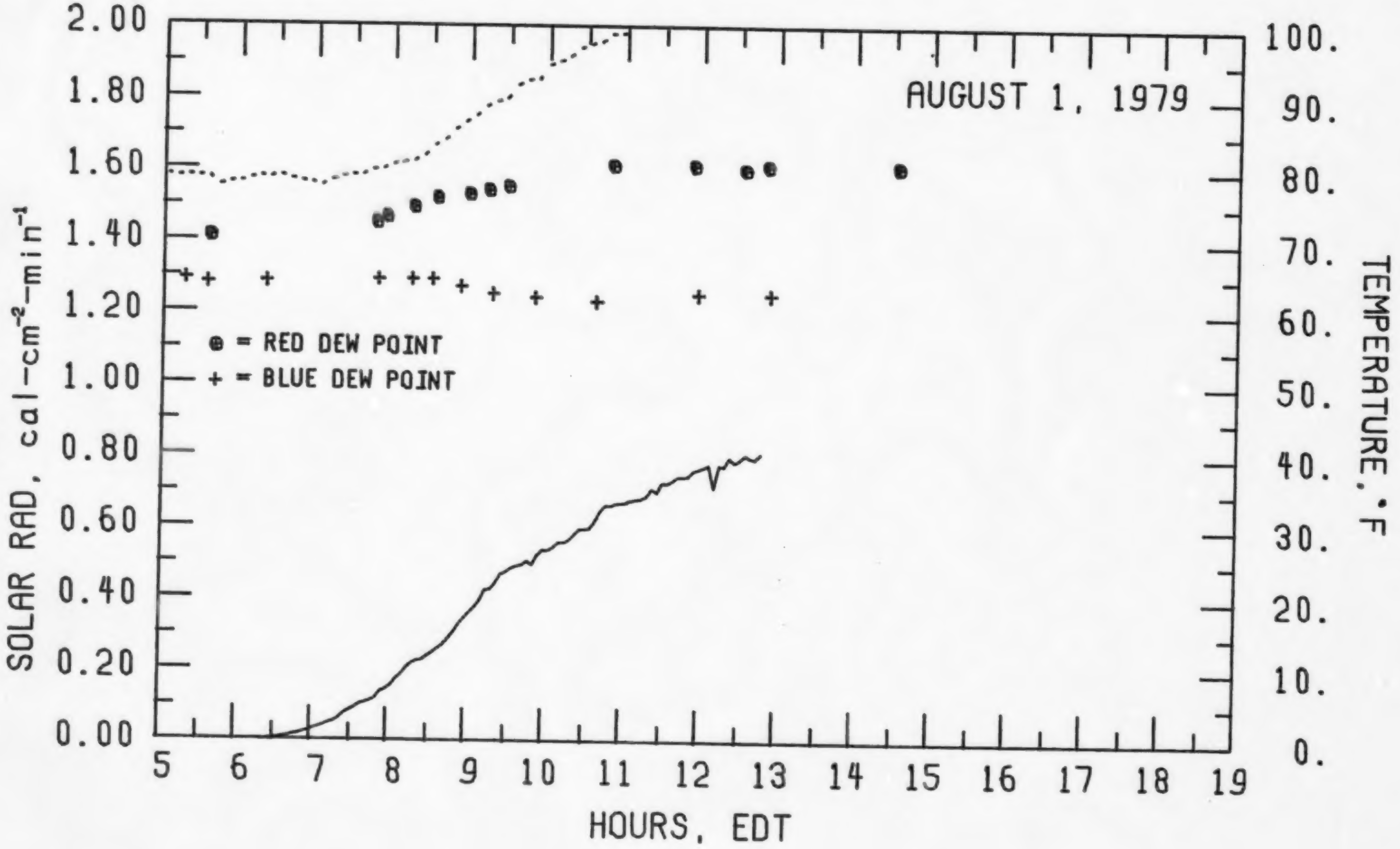

Figure 70. Total Solar Radiation, Temperature and Dewpoint Data. TSR magnitude not valid.

Table 40. Hourly Values Of Continuous Data For August 1, 1979

TIME		NO		NO2		O3		TEMP	DP	TSR	UV
R	B	R	B	R	B	R	B				
0700		0.2631		0.0952		0.0006		69.9		0.026	2.32
	0704		0.2675		0.0874		0.0007	77.6		0.033	2.68
0804		0.1687		0.1953		0.0024		74.1		0.155	8.78
	0800		0.2068		0.1417		0.0014	80.7		0.144	8.54
0900		0.0687		0.2931		0.0218		78.3		0.344	17.07
	0904		0.0610		0.2549		0.0235	87.5		0.359	17.44
1004		0.0167		0.3283		0.1077		83.4		0.534	25.49
	1000		0.0105		0.2485		0.1400	94.7		0.536	25.49
1107		0.0046		0.3061		0.2869		87.3		0.675	33.90
	1103		0.0029		0.1859		0.3156	99.5		0.869	33.05
1204		0.0024		0.2720		0.4804		89.5		0.770	38.17
	1200		0.0015		0.1331		0.4446	103.3		0.765	37.80
1300		0.0000		0.2323		0.7160					
	1304		0.0000		0.0892		0.5600				
1404		0.0000		0.1921		0.8640					
	1400		0.0000		0.0598		0.6000				
1500		0.0000		0.1745		0.9000					
	1504		0.0000		0.0441		0.6180				

Table 41. Concentrations of Selected Species for August 1, 1979

Formaldehyde

	RED	BLUE
05:43	0.00	
06:00		0.00
06:30		1.00
06:42	0.00	
07:00		1.00
07:30		0.99
07:41	0.001	
08:00		0.96
08:30		0.94
08:40	0.05	
09:00		0.86
09:30		0.78
09:39	0.091	
10:00		0.67
10:30		0.57
10:38	0.095	
11:00		0.46
11:30		0.35
11:57	0.193	
12:00		0.29
12:30		0.23
12:57	0.297	
13:00		0.20
13:30		0.15
13:56	0.360	
14:00		0.13
14:56	0.390	
15:56	0.410	

Carbon Monoxide

	RED	BLUE
06:37	0.342	
06:52	0.342	
07:07		0.348
07:22		0.335
07:37	0.375	
07:52	0.368	
08:07		0.435
08:22		0.429
09:07		0.590
09:22		0.616
09:37	0.362	
09:52	0.368	
10:07		0.777
10:22		0.804
10:37	0.435	
10:52	0.469	
11:07		0.938
11:37	0.435	
11:52	0.469	
12:22		1.166
12:07	0.509	
12:37	0.529	
13:25	0.670	

Acetaldehyde

	RED
05:43	1.90
06:42	1.91
07:41	1.80
08:40	1.65
09:39	1.51
10:38	1.38
11:57	1.11
12:57	0.87
13:56	0.69
14:56	0.56
15:56	0.44

PAN

	RED	BLUE
10:15	.062	
10:45		.003
11:15	.091	
11:55		.005
12:25	.147	
12:55		.007
13:20	.191	
13:50		.008
14:20	.210	
14:50	.200	
15:20		.008
15:50	.191	

Date: June 13, 1979

Type: Matched Propylene/NO_x with toluene on one side

INITIAL CONDITIONS (ppmC)

	RED	BLUE
NO	0.367	0.360
NO_2	0.080	0.083
NO_x	0.457	0.443
Propylene	2.81	2.73
Toluene		3.16

Time of sunrise:	5:44
Initial Temp (F):	53.0
Max. Temp (F):	88.0

This run was performed to assess the impact of additional toluene on a propylene/NO_x system. The toluene side formed O_3 earlier and sightly faster. It does appear however that the toluene side does eventually consume more NO_x and hence this side makes less O_3.

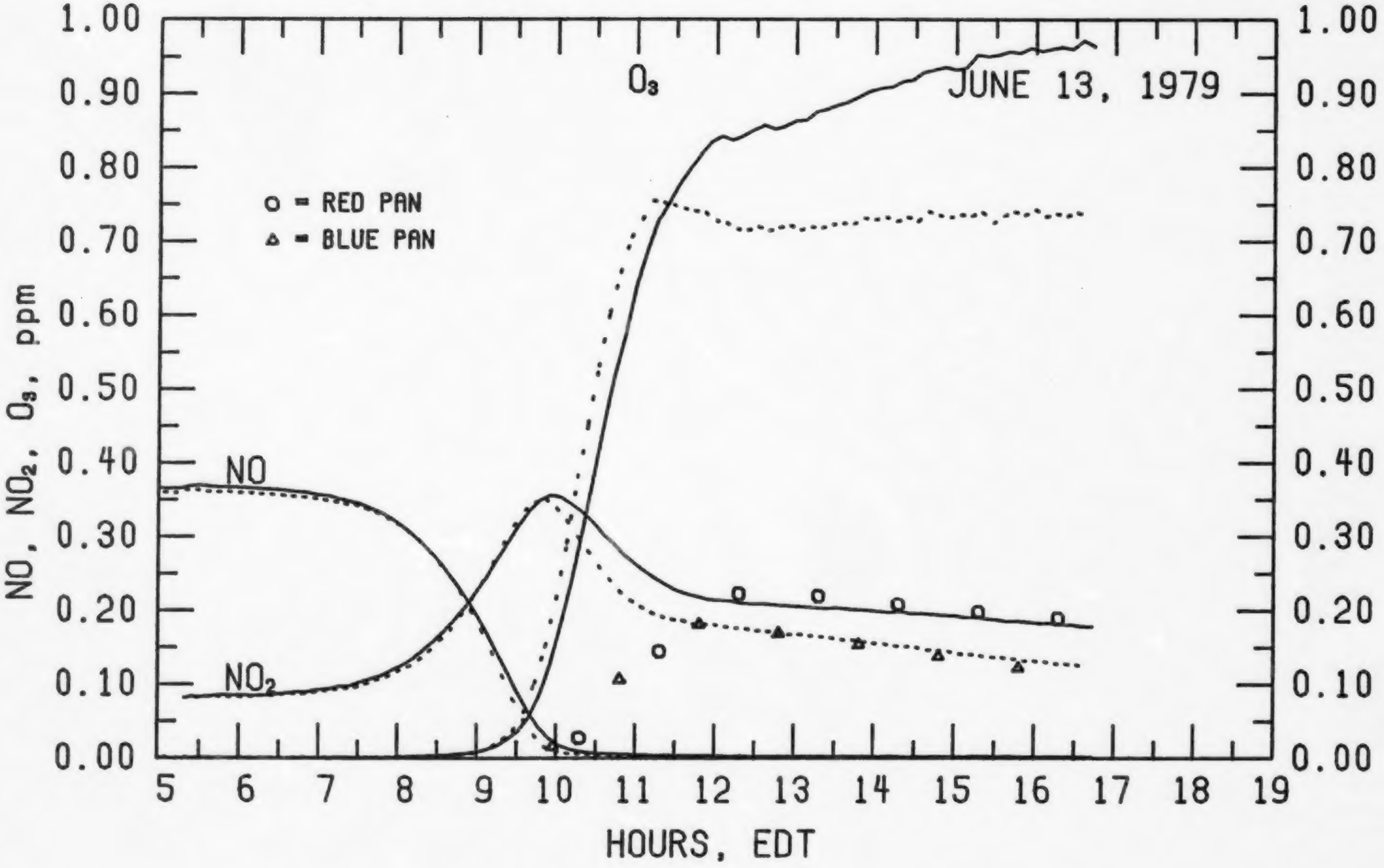

Figure 71. Nitrogen and Ozone Data.

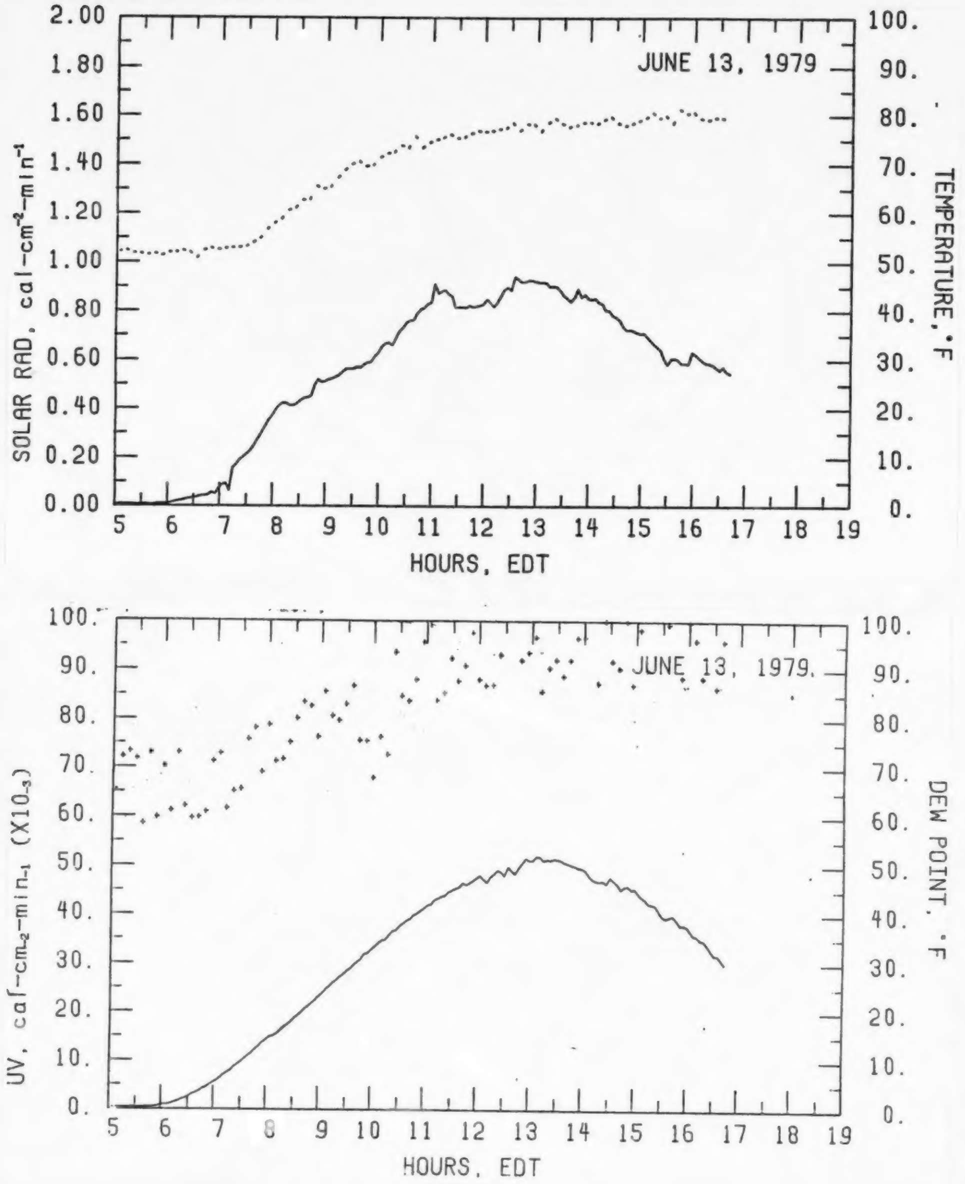

Figure 72. Total Solar Radiation and Temperature Data (TSR magnitude not valid).

Table 42. Hourly Values Of Continuous Data For June 13, 1979

TIME		NO		NO2		O3		TEMP	DP	TSR	UV
R	B	R	B	R	B	R	B				
0500		0.366		0.000		0.000			64.9	0.007	0.243
	0504		0.360		0.000		0.002	52.2	65.5	0.007	0.244
0604		0.366		0.086		0.000			59.4	0.014	0.854
	0600		0.359		0.083		0.002	51.9	70.1	0.012	0.732
0700		0.356		0.093		0.001			61.5	0.074	5.554
	0704		0.349		0.092		0.003	52.7	72.8	0.089	8.85
0804		0.314		0.126		0.002			62.4	0.396	14.88
	0800		0.318		0.118		0.005	57.9	78.7	0.373	14.23
0900		0.196		0.226		0.010			63.7	0.513	23.17
	0904		0.175		0.237		0.010	65.4	85.6	0.520	23.78
1004		0.017		0.353		0.180			63.8	0.653	33.54
	1000		0.101		0.339		0.216	71.5	87.9	0.629	32.93
1100		0.005		0.264		0.640			72.4	0.838	41.34
	1104		0.003		0.206		0.731	75.1	91.3	0.913	41.95
1204		0.003		0.215		0.844			74.5	0.815	48.05
	1200		0.002		0.181		0.844	76.7	93.5	0.930	47.56
1300		0.003		0.207		0.865			88.9	0.923	51.10
	1304		0.002		0.168		0.916	76.9	96.6	0.919	51.10
1404		0.002		0.199		0.909			87.2	0.851	49.15
	1400		0.001		0.156		0.930	78.8	96.5	0.855	49.51
1500		0.002		0.193		0.933			88.0	0.709	45.37
	1504		0.001		0.141		0.937	79.6	98.2	0.711	44.51
1604		0.001		0.183		0.959			84.9	0.622	36.71
	1600		0.001		0.132		0.944	80.7	99.8	0.632	37.68

Table 43. Concentrations of Selected Species for June 13, 1979

CO

	RED	BLUE
08:30	0.350	
08:45	0.357	
09:00		0.357
09:15		0.350
09:30	0.320	
09:45	0.350	
10:00		0.375
10:15		0.375
10:30	0.430	
10:45	0.436	
11:00		0.492
11:15		0.615
11:30	0.639	
11:45	0.645	
12:00		0.695
12:15		0.750
12:30	0.830	
12:45	0.799	
13:00		0.861
13:15		0.965
13:30	0.977	
13:45	0.934	
14:00		0.984
14:15		1.088
14:30	1.119	
14:45	1.088	
15:00		1.143
15:15		1.187
15:30	1.199	
15:45	1.217	
16:00		1.229
16:15		1.266
16:30	1.260	

PAN

	RED	BLUE
09:58		0.016
10:18	0.028	
10:48		0.107
11:18	0.145	
11:48		0.161
12:18	0.223	
12:48		0.169
13:18	0.220	
13:48		0.154
14:18	0.209	
14:48		0.136
15:18	0.199	
15:48		0.122
16:18	0.190	

PROP

	RED	BLUE
05:15		2.725
05:45	2.736	
06:15		2.711
06:45	2.807	
07:15		2.679
07:45	2.700	
08:15		2.612
08:45	2.529	
09:15		2.344
09:45	2.085	
10:15		1.469
10:45	1.029	
11:15		0.470
11:45	0.311	
12:15		0.178
12:45	0.096	
13:15		0.070
13:45	0.030	
14:15		0.028

FORM

	RED	BLUE
08:42	0.058	
08:53		0.057
09:37	0.081	
09:48		0.125
10:33		0.245
10:44	0.261	
11:31	0.280	
11:43		0.340
13:11	0.410	
13:25		0.320
13:35	0.220	

SALT

	RED	BLUE
08:32	0.19	
08:45		0.26
09:21	0.34	
09:33		0.32
10:07	0.36	
10:25		0.30
10:49	0.237	
11:00		0.066
11:45	0.065	
12:05		0.029

TOLU

	RED	BLUE
06:15		3.103
07:15		3.157
08:15		3.128
09:15		3.050
10:15		2.791
11:15		2.467
12:15		2.270
13:15		2.164
14:15		1.957
15:15		1.798
16:15		1.713

ACET

	RED	BLUE
08:44	0.084	
09:16		0.168
09:49	0.320	
10:21		0.610
10:54	0.800	
11:26		0.831
11:59	0.838	
12:31	0.777	
13:04		0.754
13:36	0.671	
14:09		0.617
14:41	0.533	
15:14		0.533
15:46	0.442	
16:19		0.457

Date: August 8, 1980

Type: Acetaldehyde vs. Biacetyl

INITIAL CONDITIONS (ppmC)

	RED	BLUE
NO	0.322	0.330
NO_2	0.097	0.089
NO_x	0.419	0.419
Acetald	1.90	
Biacetyl		0.85

Time of sunrise: 6:18
Initial Temp (F): 70.4
Max. Temp (F): 99.4

The purpose of this run was to help describe the chemistry of biacetyl. It was run vs. acetaldehyde because peroxyacyl is thought to be a major decomposition product of biacetyl. The Blue side was dried down prior to injection. 3.7 ppbV of trichloroethylene was initially added to both sides. At 9:10, approximately 1 ppbV of trichloroethylene was added to Blue and 4.7 ppbV to Red. Biacetyl measurement made on a PAN column and ECD are +/-20%, formaldehyde +/-20%, PAN +/-15% at high concentrations due to nonlinearity of ECD above 0.2-0.4 ppmV. CO meter not operational on this day. Red temperature data from inside chamber; blue outside. This was reversed in prior years. UV data may be > 15% low. TSR data are good.

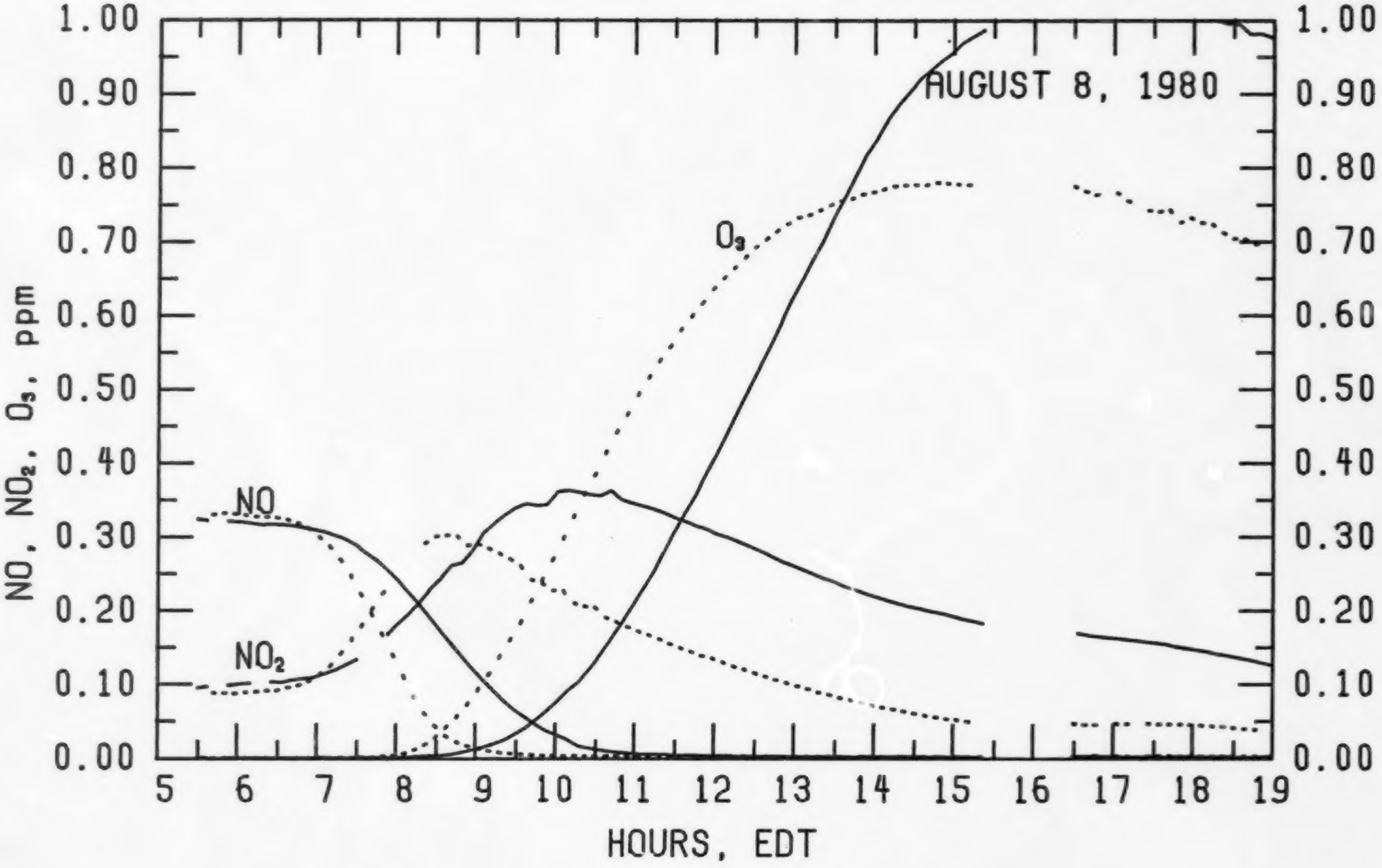

Figure 73. Nitrogen and Ozone Data.

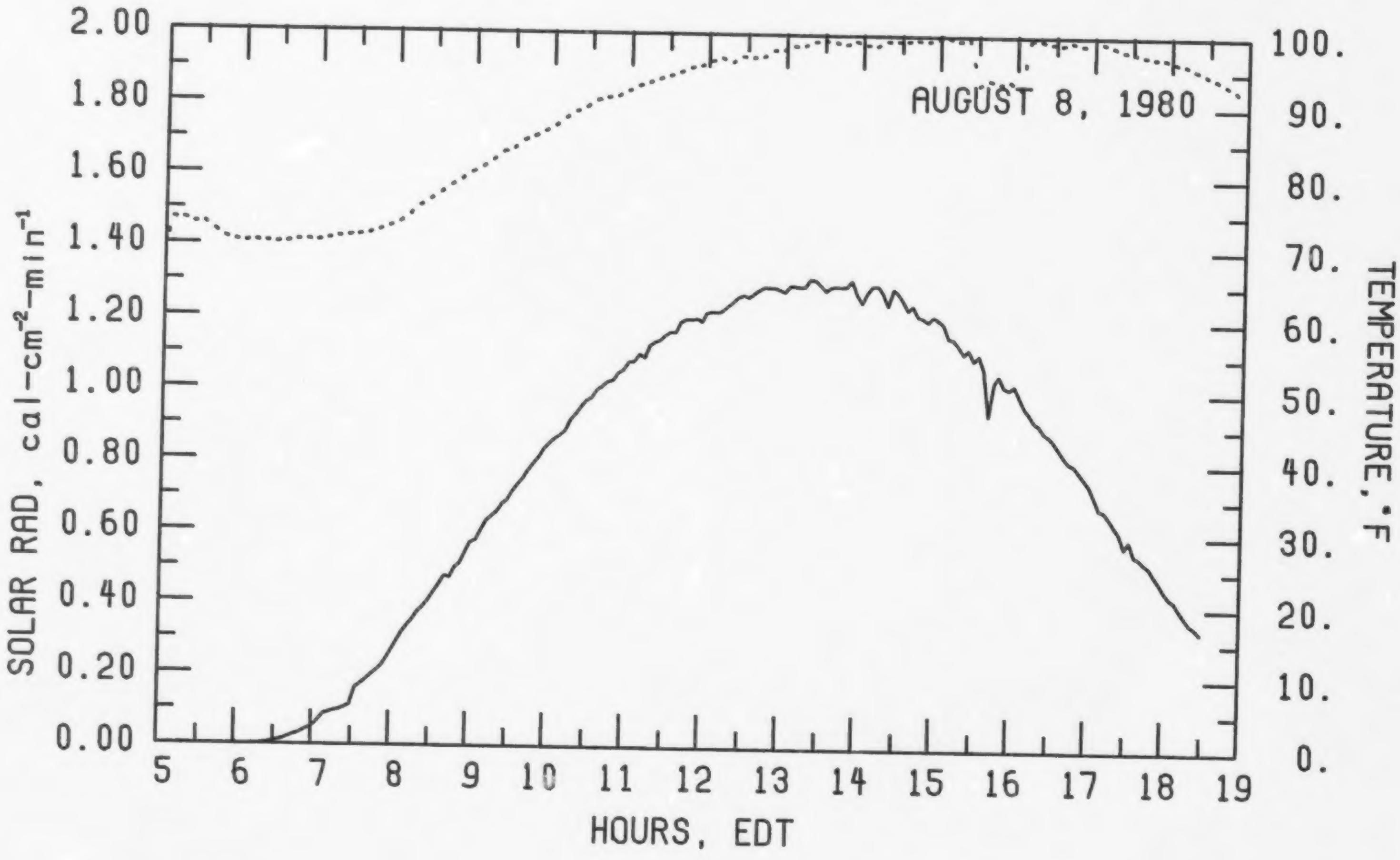

Figure 74. Total Solar Radiation and Temperature Data.

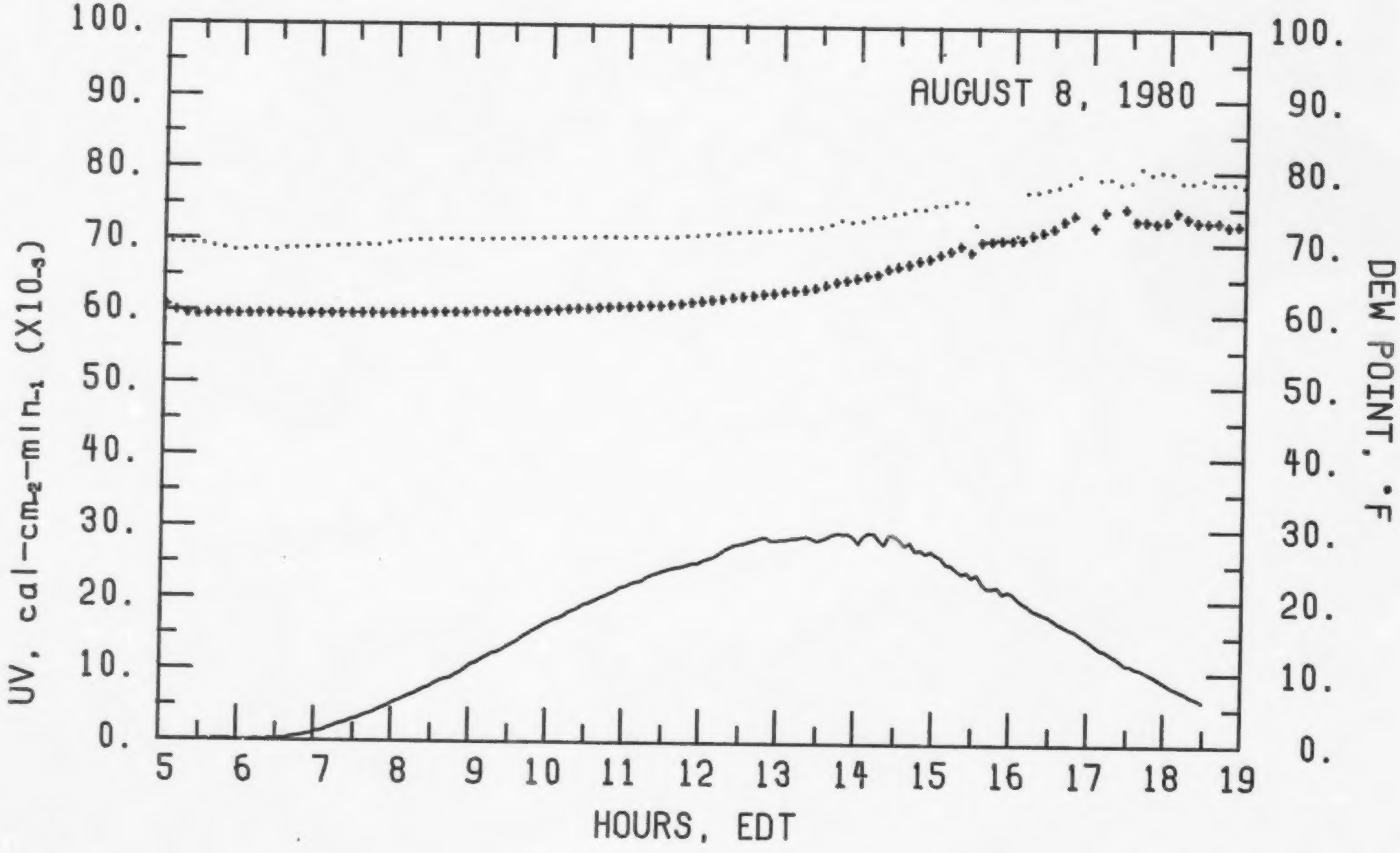

Figure 75. Ultraviolet Radiation and Dewpoint Data (+, Blue).

Table 44. Hourly Values Of Continuous Data For August 8, 1980

TIME		NO		NO2		O3		TEMP	DP	TSR	UV
R	B	R	B	R	B	R	B				
0458		0.002		0.007		0.022		73.5	69.5	0.000	0.000
	0502		0.003		0.006		0.015	71.4	60.6	0.000	0.000
0602		0.320		0.101		0.000		70.4	68.4	0.000	0.000
	0558		0.331		0.088		0.001	70.6	59.5	0.000	0.000
0658		0.309		0.110		0.001		70.6	68.8	0.046	0.976
	0702		0.300		0.114		0.001	71.3	59.6	0.054	1.342
0802		0.241		0.183		0.002		73.3	69.7	0.271	5.486
	0758		0.140		0.243		0.004	74.1	59.7	0.245	5.000
0858		0.122		0.282		0.011		80.3	70.0	0.541	10.24
	0902		0.013		0.290		0.091	78.4	59.9	0.570	10.85
1002		0.031		0.362		0.078		86.9	70.4	0.851	16.83
	0958		0.004		0.227		0.268	81.7	60.2	0.836	16.46
1058		0.016		0.345		0.206		91.9	70.4	1.059	21.71
	1102		0.003		0.172		0.492	86.8	60.7	1.082	21.83
1202		0.004		0.304		0.414		96.2	70.9	1.221	25.49
	1158		0.003		0.135		0.636	88.6	61.6	1.193	25.12
1258		0.003		0.261		0.623		97.9	71.6	1.286	28.29
	1302		0.003		0.098		0.733	91.4	63.0	1.279	28.42
1402		0.003		0.218		0.842		98.6	72.9	1.250	27.93
	1358		0.003		0.072		0.767	91.7	64.9	1.274	28.90
1458		0.003		0.192		0.956		99.5	75.3	1.215	26.95
	1502		0.002		0.052		0.778	92.2	68.4	1.203	26.34
1602		0.003		0.175		0.986		99.3	77.0	0.882	17.33
	1558		0.002		0.051		0.781	91.9	70.1	1.054	24.87
1658		0.002		0.162		1.043		98.2	79.6	0.776	14.98
	1702		0.002		0.047		0.767	91.5	72.4	0.744	14.51
1802		0.002		0.148		1.007		96.4	79.9	0.449	8.66
	1758		0.001		0.045		0.733	92.0	73.3	0.473	9.024

Table 45. Concentrations of Selected Species for August 8, 1980

PAN

	RED	BLUE
06:30		0.00
06:59	0.00	
07:30		7.20
07:59	8.64	
08:30		77.76
08:56	28.08	
09:18		153.36
09:43		189.36
10:13	59.76	
10:43		203.76
11:13	93.60	
11:43		158.40
12:13	137.52	
12:43		109.44
13:13	192.96	
13:44		69.84
14:13	259.76	
14:44		45.36
15:13	236.00	
15:44		32.40
16:13	206.64	
16:44		23.04
17:13	195.84	
17:44		20.16
18:13	162.72	

FORM

	RED	BLUE
06:45		0.043
07:10		0.051
07:30	0.014	
08:20		0.081
08:40	0.113	
08:50		0.130
09:00	0.138	
09:20		0.167
09:30		0.192
10:00	0.170	
10:30		0.192
11:00	0.192	
11:30		0.189
12:00	0.286	
12:30		0.127
13:00	0.340	
13:30		0.105
14:00	0.362	
14:30		0.054
15:00	0.383	
15:30		0.022

ACET

06:04	1.90
07:04	1.90
08:04	1.90
09:04	1.80
10:04	1.68
11:04	1.56
12:04	1.35
13:02	1.06
13:59	0.91
14:58	0.65
15:58	0.55

BIACET

	RED	BLUE
06:30		0.850
07:30		0.750
08:30		0.540
09:18		0.320
09:43		0.270
10:43		0.065
11:43		0.042
12:43		0.020
13:44		0.017
14:44		0.011
15:44		0.011

CL3ETH

	RED	BLUE
06:00	3.74	
06:30		3.74
07:00	3.47	
07:30		4.01
08:00	4.27	
08:30		3.74
09:12	8.52	
09:18		7.47
09:43		4.68
10:13	8.21	
10:43		3.43
11:13	7.79	
11:43		2.60
12:13	7.58	
12:43		2.39
13:13	7.27	
13:43		2.08
14:13	7.07	
14:43		1.66
15:13	6.75	

Date: July 30, 1980

Type: Toluene vs. o-Xylene

INITIAL CONDITIONS (ppmC)

	RED	BLUE
NO	0.156	0.155
NO_2	0.023	0.023
NO_x	0.179	0.178
Toluene	3.78	
o-Xylene		2.23

Time of sunrise: 6:02

Initial Temp (F): 66.9

Max. Temp (F): 98.6

This dual aromatic run compared the reactivity of toluene and O-xylene. It has reasonably complete product data and fairly good carbon balances were obtained. Two peaks eluted with the retention time of propionaldehyde and acetone. These have been lumped together and called C3 carbonyls. Another peak had a retention time similiar to that of MEK. These compounds have not been verified by GCMS. Compounds with (*) were derived by DNPH HPLC analysis at EPA-RTP. A high uncertainty must presently be attached to these numbers(+/- a factor of 2) due to the newness of the method and the lack of routine calibrations for these compounds. Hydrocarbons +/- 7%,formaldehyde +/- 15%, PAN +/-15%, biacetyl +/- 20%. CO meter not operational this day. UV data for 1980 may be about 15% low. Comparison of 1980 UV with that of other years will be made available.

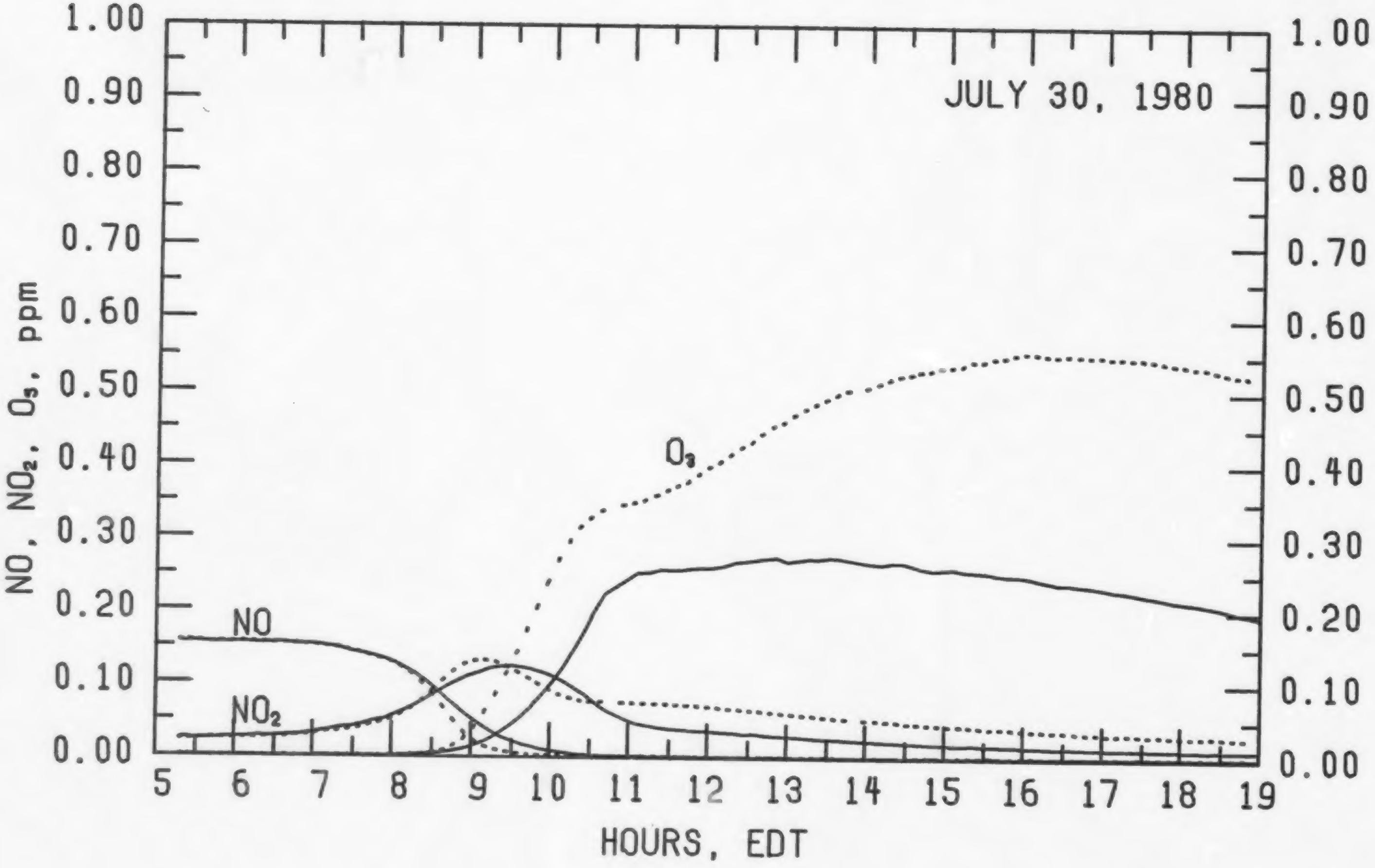

Figure 76. Nitrogen and Ozone Data.

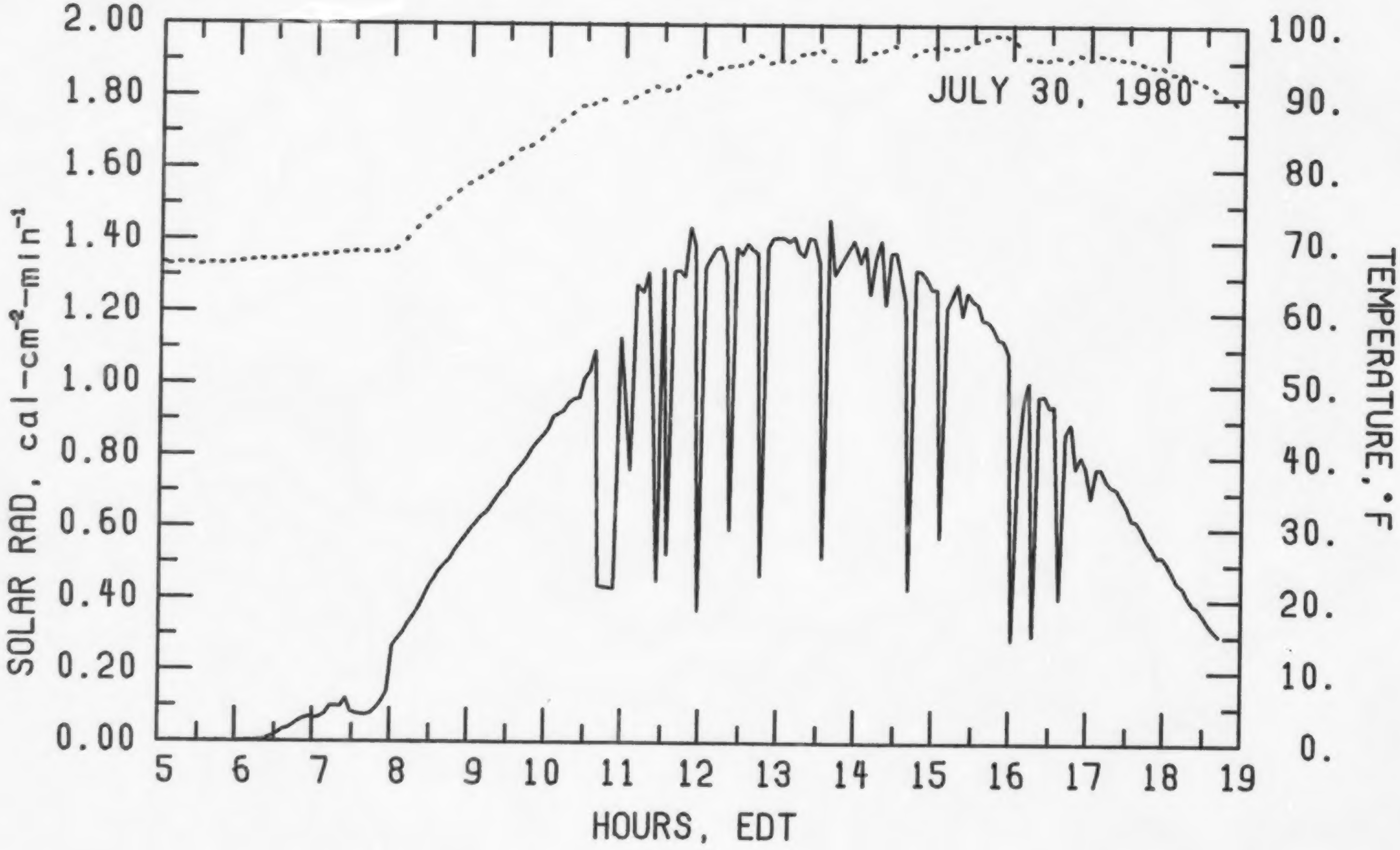

Figure 77. Total Solar Radiation and Temperature Data.

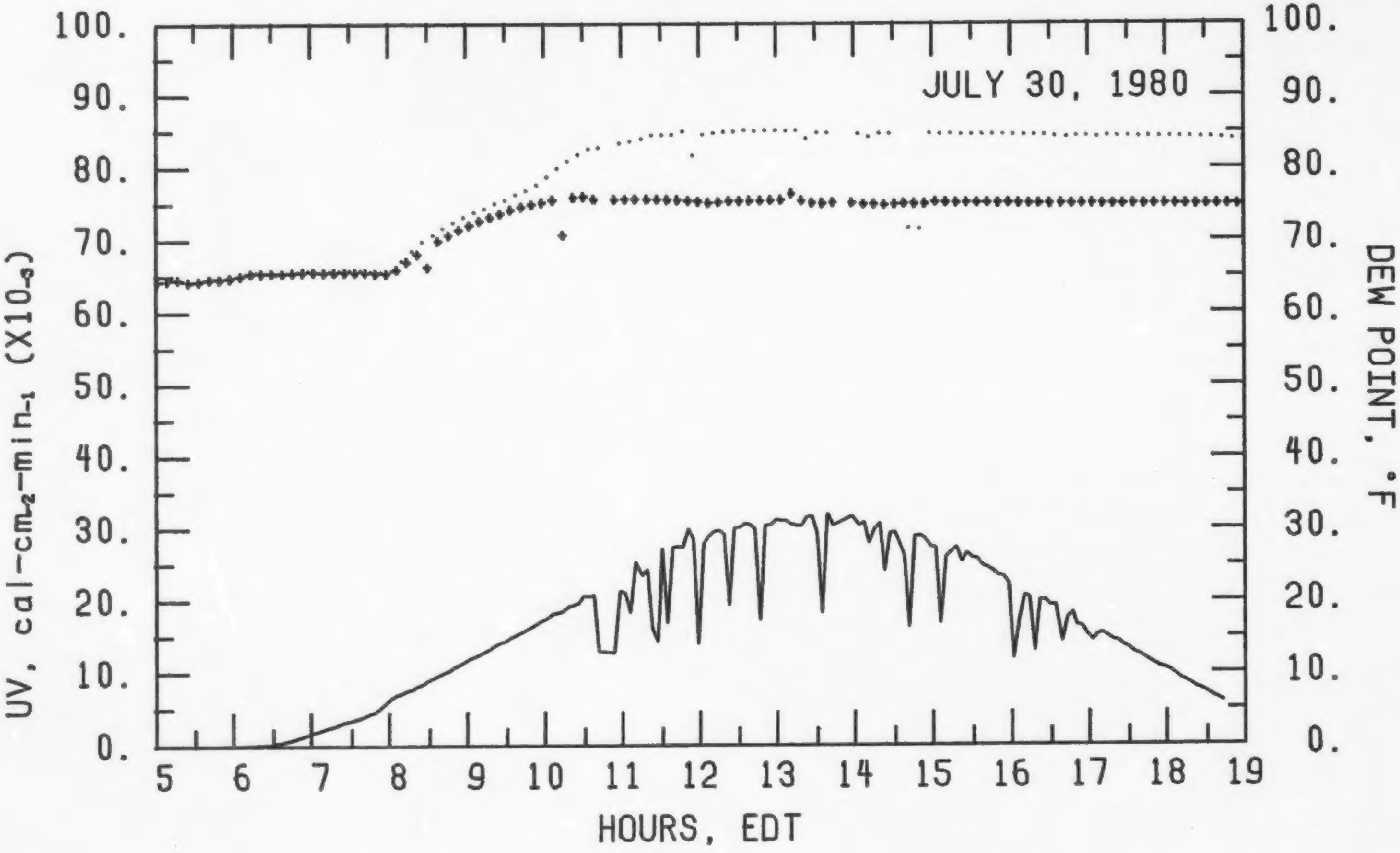

Figure 78. Ultraviolet Radiation and Dewpoint Data (+, Blue).

Table 46. Hourly Values Of Continuous Data For July 30, 1980

TIME		NO		NO2		O3		TEMP	DP	TSR	UV
R	B	R	B	R	B	R	B				
0458		0.006		0.006		0.000		66.5	64.4	0.000	0.000
	0502		0.005		0.203		0.001	66.8	64.3	0.000	0.000
0602		0.155		0.025		0.001		66.9	64.8	0.000	0.000
	0558		0.154		0.033		0.000	67.9	65.8	0.000	0.000
0658		0.152		0.031		0.000		67.6	65.8	0.069	1.585
	0702		0.151		0.030		0.002	68.7	65.6	0.065	1.829
0802		0.127		0.056		0.009		68.6	65.8	0.267	6.585
	0758		0.130		0.049		0.009	69.1	65.4	0.140	5.976
0858		0.054		0.111		0.012		77.7	73.2	0.574	11.59
	0902		0.022		0.130		0.039	75.8	72.1	0.595	12.07
1002		0.073		0.110		0.102		85.1	78.8	0.876	17.68
	0958		0.002		0.092		0.238	80.8	75.2	0.856	17.32
1058		0.011		0.050		0.242		89.0	83.5	1.128	21.34
	1102		0.001		0.074		0.347	85.0	75.7	0.948	21.10
1202		0.000		0.035		0.259		92.9	84.6	1.325	27.93
	1158		0.000		0.069		0.396	86.4	75.3	1.367	24.02
1258		0.000		0.025		0.268		95.1	85.1	1.408	31.22
	1302		0.000		0.059		0.468	88.5	75.5	1.409	31.10
1402		0.000		0.022		0.265		95.1	84.6	1.341	30.37
	1358		0.000		0.051		0.505	89.4	75.1	1.401	31.71
1458		0.000		0.019		0.258		96.9	84.7	1.266	27.44
	1502		0.000		0.044		0.535	90.2	75.2	1.265	27.20
1602		0.000		0.015		0.247		97.6	84.5	0.987	21.95
	1558		0.000		0.039		0.555	91.4	75.1	1.086	22.32
1658		0.000		0.013		0.232		95.3	84.3	0.769	15.24
	1702		0.000		0.033		0.549	90.1	75.0	0.785	14.39
1802		0.000		0.012		0.214		93.4	84.2	0.502	10.12
	1758		0.000		0.031		0.539	88.0	74.9	0.523	10.49
1858		0.000		0.011		0.194		88.7	83.6	0.227	4.634
	1902		0.000		0.026		0.499	82.9	74.8	0.214	4.268

Table 47. Concentrations of Selected Species for July 30, 1980

	FORM RED	FORM BLUE
07:30		0.000
08:00	0.000	
08:13	0.003	
08:16		0.009
08:32		0.017
08:45	0.015	
09:00	0.020	
09:10	0.023	
09:15		0.035
09:30		0.073
09:40		0.087
09:46	0.035	
10:05	0.044	
10:15		0.128
10:30		0.160
11:30		0.180
11:35		0.189
11:45	0.093	
12:10	0.090	
12:20		0.189
12:30		0.203
12:50	0.087	
13:00	0.078	
13:20		0.145
13:40		0.139
13:45	0.081	
14:10	0.081	
14:25		0.131
14:45	0.081	
15:00	0.078	
15:15		0.087
15:35	0.078	
16:05	0.073	
16:15		0.087

	PAN RED	PAN BLUE
05:30		0.00
06:00	0.00	
06:30		0.68
07:00	0.34	
07:30		0.68
08:00	0.34	
08:30		1.70
09:00	2.72	
09:30		32.30
10:00	11.22	
10:30		91.12
11:00	34.00	
11:30		89.76
12:00	36.72	
12:30		81.26
13:00	26.52	
13:30		56.10
14:00	18.02	
14:30		46.92
15:00	13.60	
15:30		39.10
16:00	10.88	
16:30		32.30
17:00	10.20	
17:30		28.22
18:00	8.84	

	BIACET RED	BIACET BLUE
05:30		0.000
06:30		0.000
07:30		0.006
08:30		0.027
09:30		0.064
10:30		0.065
11:30		0.043
12:30		0.033
13:30		0.026
14:30		0.022
15:30		0.015
16:30		0.013
17:30		0.011

	C3CARB RED	C3CARB BLUE
09:56	0.01	
10:36		0.13
10:54	0.11	
11:25		0.14
11:53	0.08	
12:23		0.08
12:52	0.08	
13:21		0.15
13:50	0.13	
14:19		0.20
14:49	0.14	
15:19		0.24
15:48	0.18	

	ACET RED	ACET BLUE
08:30		0.05
08:58	0.08	
09:37		0.16
09:56	0.19	
10:36		0.21
10:54	0.19	
11:25		0.21
11:53	0.27	
12:23		0.27
12:52	0.29	
13:21		0.37
13:50	0.35	
14:19		0.32
14:49	0.37	
15:19		0.40
15:48	0.35	

	OXYL RED	OXYL BLUE
06:29		2.23
07:29		2.14
08:29		1.92
09:29		1.35
10:29		0.84
11:29		0.61
12:29		0.45
13:29		0.20
14:29		0.10
15:29		0.07

	GLY* RED	GLY* BLUE
06:30		0.005
07:00	0.009	
07:30		0.014
08:00	0.008	
08:30		0.014
09:30	0.005	
10:00		0.017
10:30	0.007	
11:00		0.012
11:30	0.014	
12:30	0.048	
13:00		0.051
13:30	0.082	

	TOLU
05:59	3.74
06:59	3.78
07:59	3.68
08:59	3.31
09:59	2.88
10:59	2.32
11:59	2.07
12:59	1.70
13:59	1.57
14:59	1.60

	MEK RED	MEK BLUE
08:30		0.04
08:58	0.07	
09:37		0.07
09:56	0.05	
10:36		0.11
10:54	0.13	
11:25		0.13
11:53	0.13	
12:23		0.14
12:52	0.13	
13:21		0.16
13:50	0.20	
14:19		0.20
14:49	0.20	
15:19		0.25
15:48	0.23	

	MEGLY* RED	MEGLY* BLUE
10:00		0.072
10:30	0.029	
11:00		0.043
11:30	0.043	
12:30	0.047	
13:00		0.115
13:30	0.097	

	BIAC* RED	BIAC* BLUE
12:00		0.048
13:00		0.048

	OTUL* RED	OTUL* BLUE
13:00		0.20

	BENZ*
10:30	0.11
11:30	0.12
12:30	0.12
13:30	0.30

Date: June 23, 1980

Type: a-Pinene vs. Isoprene

INITIAL CONDITIONS (ppmC)

	RED	BLUE
NO	0.171	0.172
NO_2	0.039	0.039
NO_x	0.210	0.210
a-Pinene	1.90	
Isoprene		1.27

Time of sunrise: 5:40

Initial Temp (F): 56.1

Max. Temp (F): 91.9

This run compares the relative reactivity of isoprene and a-pinene/NO_x systems. The automated C_2-C_{10} hydrocarbon instrument was slightly out of timing resulting in a large uncertainty with HC measurements (+/- 20%). Uncertainties associated with other measurements are MACR and MVK, +/-20%, HCHO, +/-15%, PAN, +/-15%, and CO, +/-20%. 1980 UV data are at least 15% low compared to other years. 1980 TSR data are good.

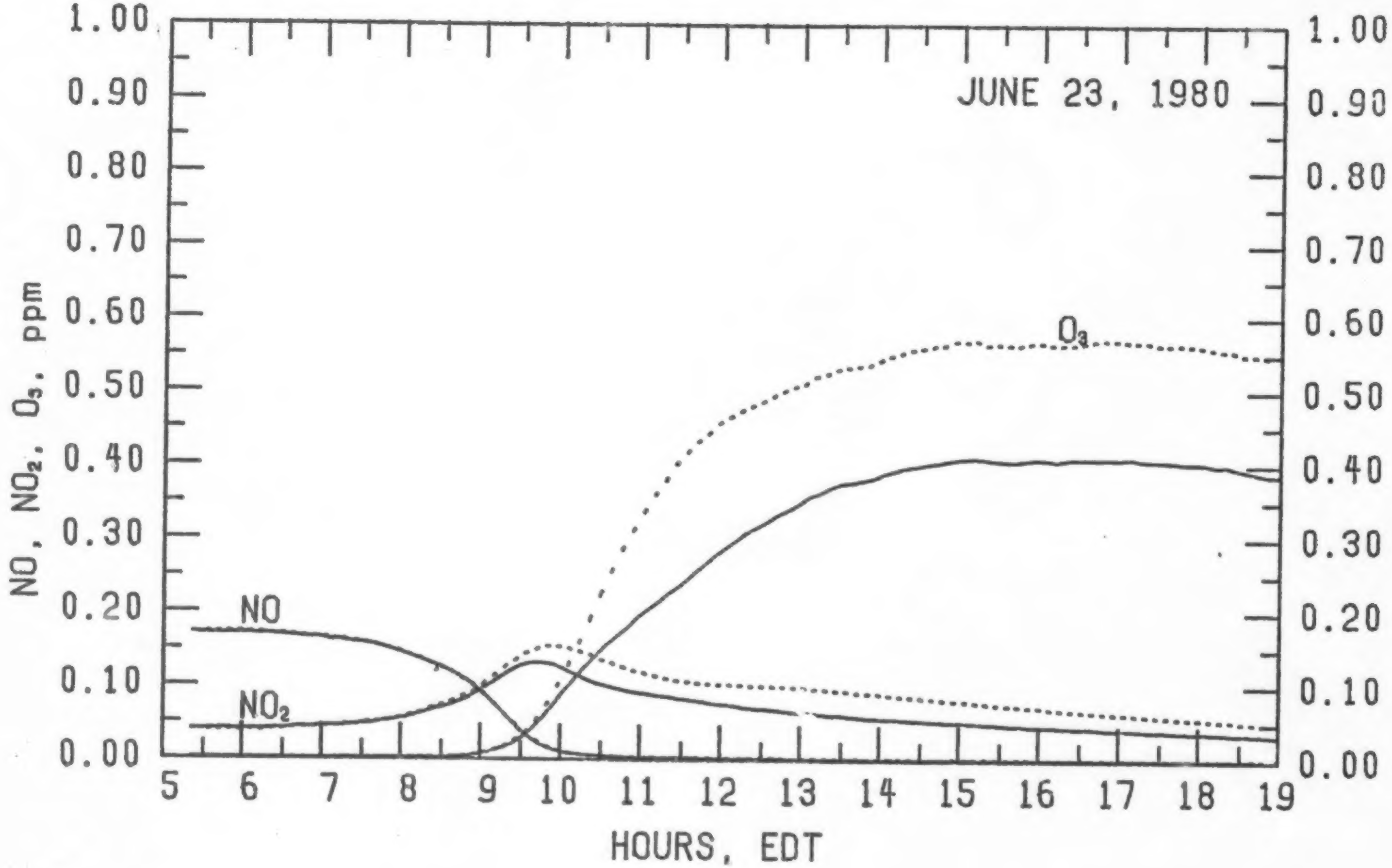

Figure 79. Nitrogen and Ozone Data.

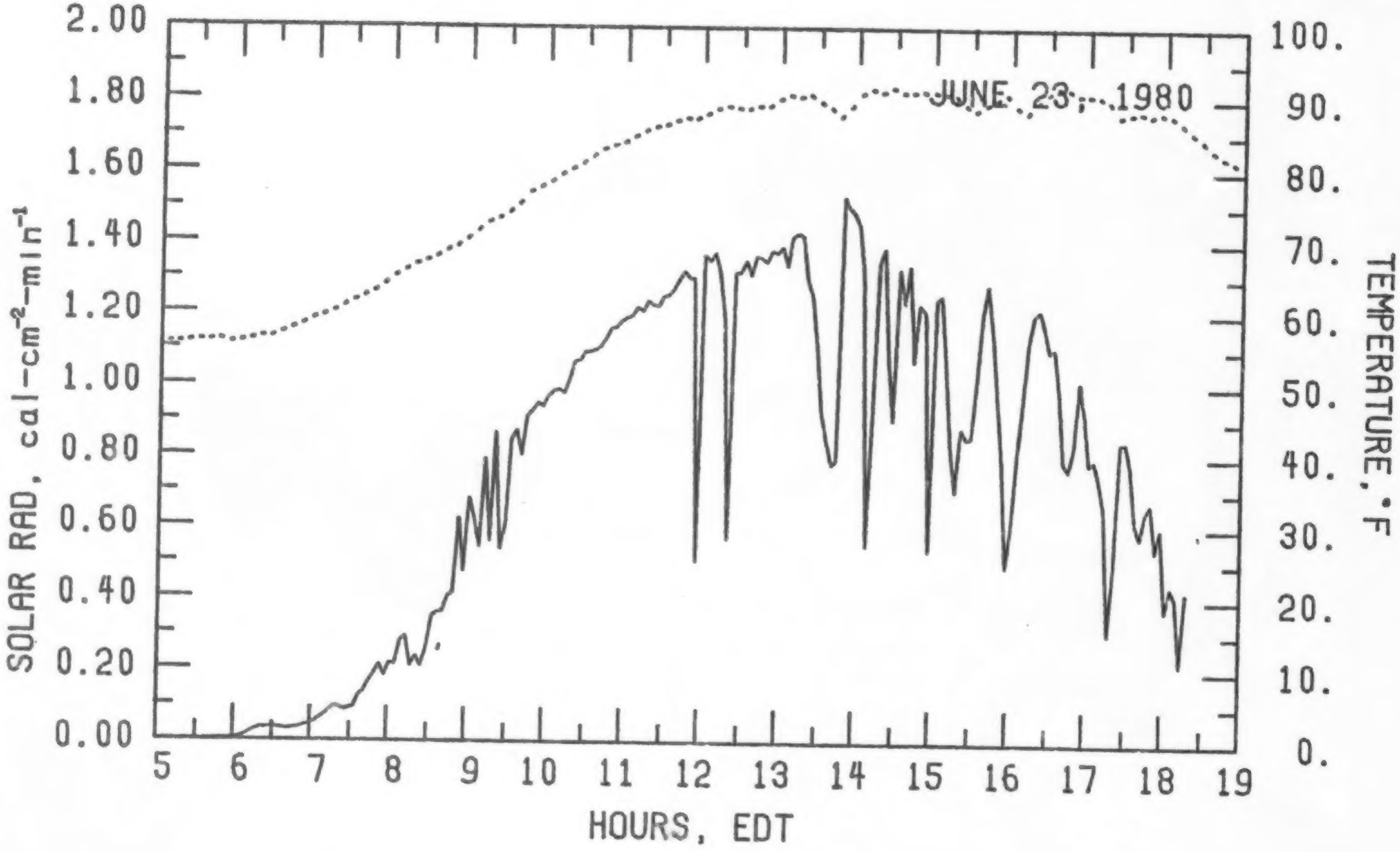

Figure 80. Total Solar Radiation and Temperature Data.

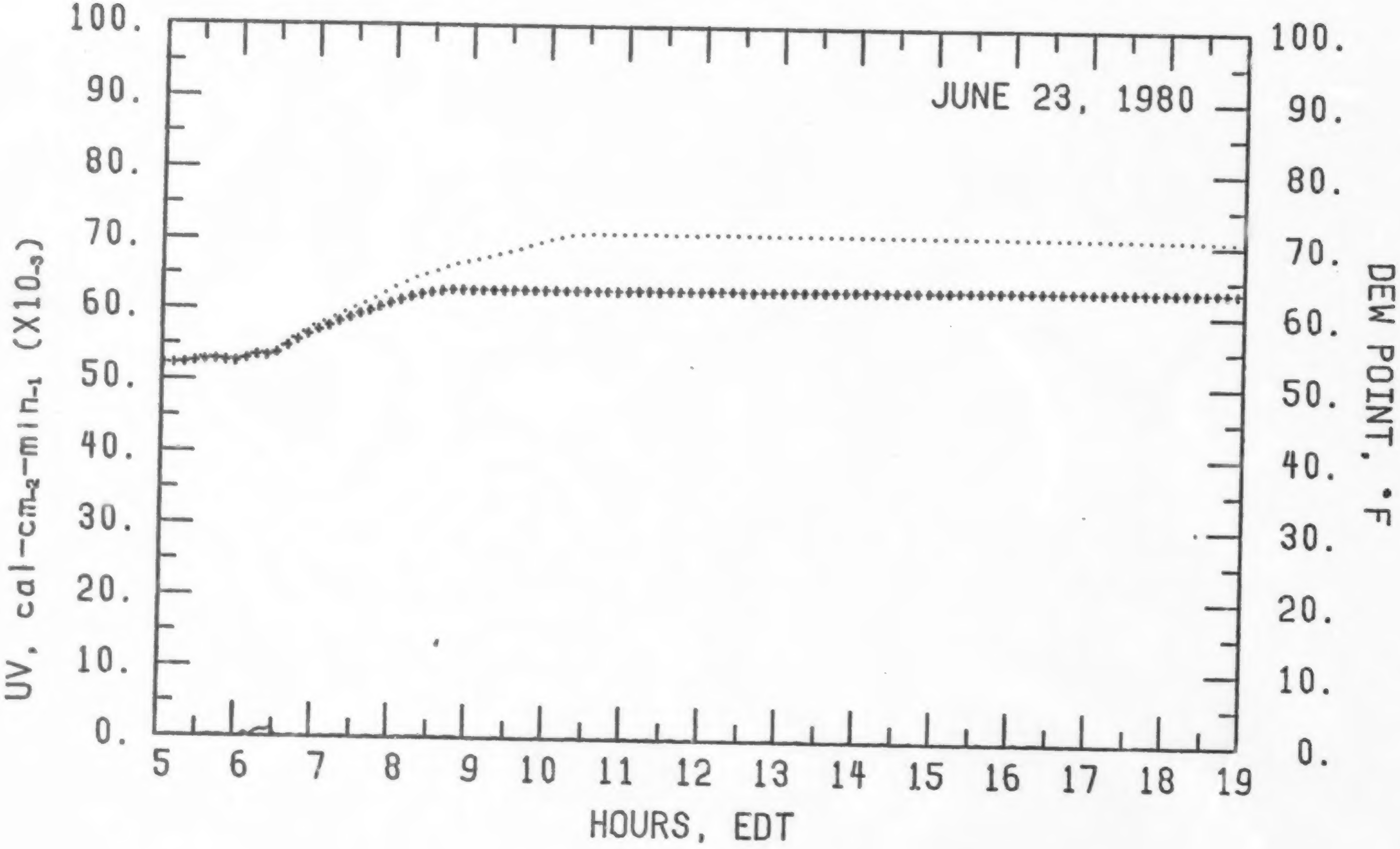

Figure 81. Dewpoint Data (+, Blue).

Table 48. Hourly Values Of Continuous Data For June 23, 1980

TIME		NO		NO2		O3		TEMP	DP	TSR	UV
R	B	R	B	R	B	R	B				
0458		0.004		0.005		0.011		55.7		0.000	
	0502		0.004		0.004		0.010	56.8		0.000	
0602		0.171		0.040		0.000		55.9		0.005	
	0558		0.173		0.038		0.001	56.6		0.004	
0658		0.166		0.044		0.000		59.2		0.044	
	0702		0.166		0.044		0.000	59.6		0.048	
0802		0.145		0.056		0.001		65.3		0.216	
	0758		0.148		0.055		0.001	64.6		0.184	
0858		0.096		0.092		0.006		70.4		0.476	
	0902		0.091		0.101		0.008	69.3		0.679	
1002		0.009		0.123		0.091		78.4		0.969	
	0958		0.013		0.153		0.099	74.8		0.939	
1058		0.004		0.091		0.194		83.9		1.180	
	1102		0.003		0.118		0.336	78.5		1.191	
1202		0.003		0.075		0.286		87.9		1.364	
	1158		0.003		0.102		0.456	81.4		1.371	
1258		0.002		0.065		0.347		90.1		1.372	
	1302		0.002		0.097		0.510	82.8		1.388	
1402		0.002		0.056		0.389		90.8		1.447	
	1358		0.002		0.090		0.549	84.1		1.483	
1459		0.001		0.051		0.408		91.1		0.637	
	1503		0.002		0.080		0.568	85.0		1.241	
1603		0.001		0.045		0.407		89.1		0.598	
	1559		0.002		0.072		0.567	83.3		0.893	
1659		0.001		0.041		0.410		90.7		0.625	
	1703		0.002		0.063		0.568	84.3		0.783	
1803		0.001		0.038		0.402		87.9		0.376	
	1759		0.001		0.056		0.561	82.7		0.603	
1859		0.001		0.033		0.386		80.8		0.173	

Table 49. Concentrations of Selected Species for June 23, 1980

CO

	RED	BLUE
06:05		0.338
06:20		0.338
06:35	0.250	
06:50	0.313	
07:05		0.288
07:20		0.288
07:35	0.338	
07:50	0.288	
08:05		0.288
08:20		0.338
08:35	0.263	
08:50	0.338	
09:05		0.325
09:20		0.300
09:35	0.300	
09:50	0.325	
10:05		0.275
10:20		0.288
10:35	0.238	
10:50	0.275	
11:05		0.275
11:20		0.288
11:35		0.300
11:50	0.313	
12:05		0.663
12:20		0.600
12:35	0.413	
12:50	0.475	
13:20		0.838
13:35		1.013
13:50		0.950
14:05		0.888
14:35	0.588	
14:50	0.625	
15:05		0.800
15:20		1.163
15:35		1.000
15:50		0.838
16:05		0.725
16:35	0.463	
16:50	0.488	
17:05		0.400
17:20		0.400
17:35	0.363	
17:50	0.388	
18:05		0.313
18:20		0.325
18:35	0.250	
18:50	0.325	

MVK

	RED	BLUE
08:30		0.017
09:30		0.070
10:30		0.198
11:30		0.140
12:30		0.050

FORM

	RED	BLUE
09:00	0.010	
09:05	0.010	
09:10	0.012	
09:35		0.042
09:40		0.054
09:45		0.062
10:00	0.036	
10:05	0.042	
10:10	0.044	
10:15	0.048	
10:40		0.136
10:45		0.152
11:00	0.070	
11:05	0.070	
11:10	0.080	
11:15	0.080	
11:30		0.196
11:42		0.196
11:45		0.194
12:05	0.080	
12:10	0.070	
12:15	0.060	
12:45		0.160
13:05	0.030	
13:10	0.030	
13:15	0.026	
13:30		0.104
13:35		0.104
13:40		0.102
13:45		0.100
15:35		0.056
15:40		0.056
15:45		0.056

MACR

	RED	BLUE
08:30		0.016
09:30		0.066
10:30		0.165
11:30		0.130
12:30		0.100

PAN

	RED	BLUE
08:30		1.8
09:00	6.0	
09:30		12.9
10:00	20.1	
10:30		52.2
11:00	28.8	
11:30		81.0
12:00	33.5	
12:30		81.3
13:00	35.7	
13:30		74.1
14:00	30.3	
14:30		61.5
15:00	30.9	
15:30		58.5
16:05	28.2	
16:35		49.8
17:05	26.1	
17:35		46.8
18:05	24.6	

APINE

06:00	1.9
07:00	1.8
08:00	1.5
09:00	1.1
10:00	0.5

ISOPRENE

	RED	BLUE
06:30		1.27
07:30		1.22
08:30		1.146
09:30		0.874
10:30		0.24
11:30		0.02

SECTION 7

ILLUSTRATIONS OF SIGNIFICANT FEATURES IN THE DATA SET

The purpose of this section is to show, mainly by plots, some of the significant features of the dataset. Included in this chapter are illustrations of:

- paraffin experiments with: n-butane, n-pentane, n-octane, 2,3-dimethyl-butane.
- formaldehyde and acetaldehyde experiments
- aromatic experiments
- urban-like HC mixture experiment (dynamic/static)
- high concentration CO and propylene experiments]
- high concentration formaldehyde and propylene experiment]
- wet/dry cool propylene experiments

BUTANE-NO_x EXPERIMENTS

Eleven runs containing butane are included in the dataset. The 1979 experiments had fuller analytical data (Figure 82). Two of the 1979 runs were conducted during the summer months and two were during the fall. Formaldehyde, acetaldehyde and MEK were the major oxygenated hydrocarbon products from the butane-NO_x irradiations. Generally these products accounted for more than 65 percent of the reacted carbon. Sec-butyl nitrate was the largest nitrate product; ethyl nitrate, PAN and n-butyl nitrate were also observed. Nitrates accounted for ~8 percent of the reacted carbon. Table 27 shows that approximately 75-80 percent of the reacted carbon appeared as measured products in three of the four runs. The October 18, 1979 run only gave a 58 percent accountability. As mentioned before, slight errors (e.g. a possible leak or an error of 2.5 percent in the initial or final butane measurements) could cause this discrepancy.

N-PENTANE/NO_x EXPERIMENT

An experiment with 14.2 ppmC of n-pentane and 0.204 ppm of NO_x was run on October 9, 1979. On the other side of the chamber there was a similar carbon concentration of n-butane and 0.2 ppm NO_x. The species profiles for these experiments are given in Figure 83. Note that the NO, NO_2 and O_3 traces for both sides of this run are almost indistinguishable, yet further examination of the n-pentane side indicates that approximately 30 percent more carbon as n-pentane had reacted to give similar NO_x and O_3 behavior. Also, a much lower carbon accountability was

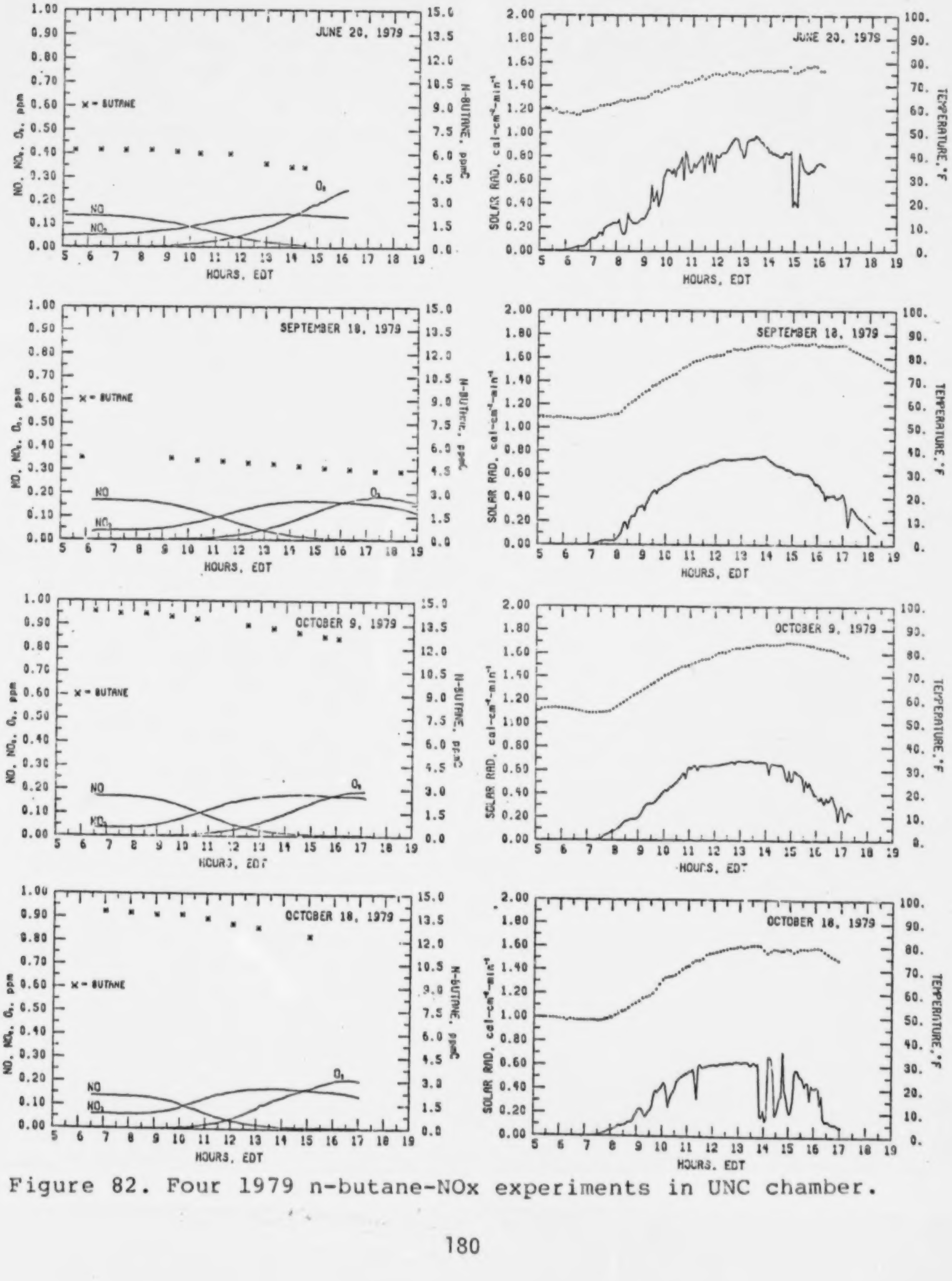

Figure 82. Four 1979 n-butane-NOx experiments in UNC chamber.

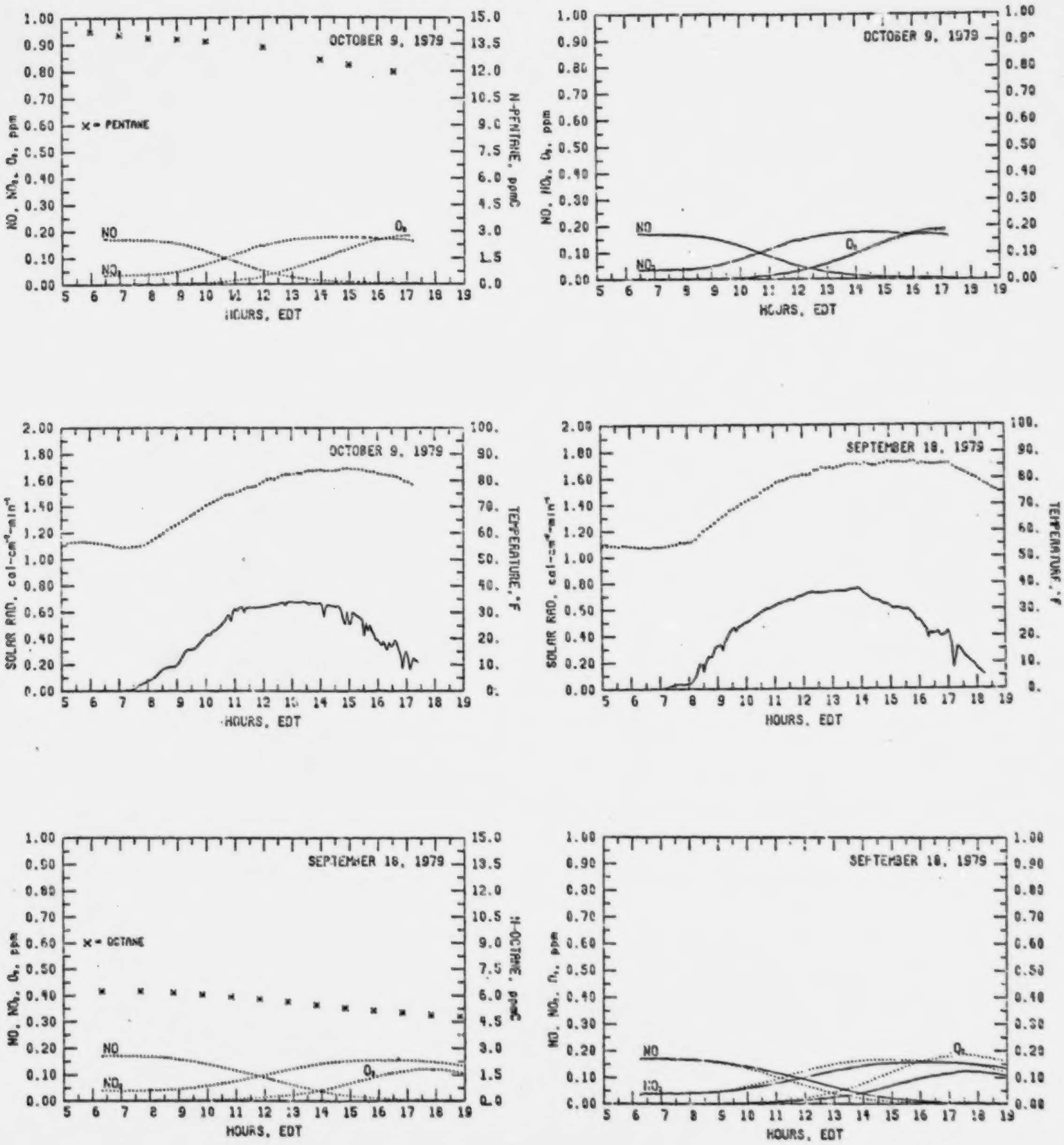

Figure 83. N-pentane and n-octane experiments in UNC chamber.

obtained for the n-pentane side (Table 50). The most probable explanation is that products like diethyl ketone and methyl propyl ketone were not analyzed and therefore not included in the carbon balance.

The alkyl nitrate chromatogram from this run shows a major broad peak with a slight "discontinuity" eluting just after PAN (Figure 84). The retention time for this peak coincides with that of n-butyl nitrate. On the GC column that we are using (10 percent Carbowax 400 on Gas CromG 60-80 mesh), it has been demonstrated that internally substituted nitrates elute at almost the same time as normally substituted nitrates with one less carbon (e.g. ethyl and isopropyl nitrate as well as n-propyl and sec-butyl nitrate. Thus this broad peak could be the two internally substituted nitrates of n-pentane. If one assumes that n-pentyl-3-nitrate elutes before n-pentyl-2-nitrate and also considers the "inflection" point in the chromatogram, a 45:55 split between the 3 and the 2-substituted n-pentyl nitrates could be inferred. Of course, this is speculation and awaits GCMS confirmation. As a final point it is worth noting that in the n-pentane run a greater percentage of the reacted carbon appeared in the form of alkyl nitrates than in the butane runs. The significance of this will be discussed in the next section.

2,3-DIMETHYL BUTANE-NO_x EXPERIMENTS

Three experiments of this type were made and their characteristic profiles for NO, NO_2, O_3 and HC appear in Figure 85. Table 27 shows two cases in which acetone, the major oxygenated product, more than accounted for all of the reacted 2,3-dimethyl butane carbon. This suggests that chamber dilution was very low on these days, that there was a slight positive drift in the GC measuring 2,3-dimethyl butane or that calibration for acetone was high on these days.

Inspection of the alkyl nitrate analysis from these experiments shows a small peak with the same retention time as isopropyl nitrate and a major GC response just before the water peak. Hydroxyl radical abstraction of either tertiary hydrogen on the number 2 or 3 carbon of 2,3-dimethyl butylnitrate should ultimately lead to 2,3-dimethyl butyl-2-nitrate, as shown below. Hence the larger peak has been assigned to 2,3-dimethyl butyl-2-nitrate. A pure sample of this compound could not be obtained, so calibration is based on the area response of n-butyl nitrate. This probably attaches an uncertainty of ~40 percent to reported concentrations.

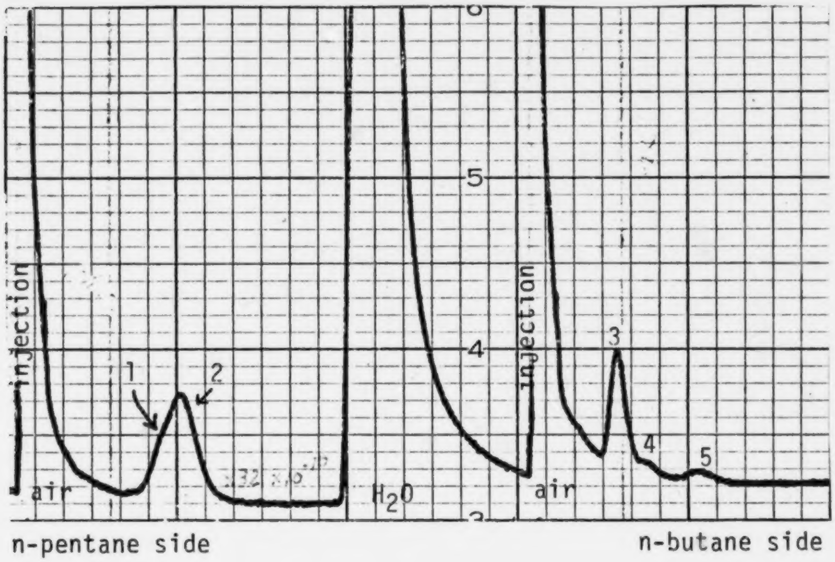

	Concentration, ppbC
1. n-pentyl-3-nitrate 2. n-pentyl-2-nitrate	9.7 ±40%
3. sec-butyl nitrate	5.1 ±40%
4. PAN	0.5 ±20%
5. n-butyl nitrate	0.4 ±20%

Figure 84. Alkyl nitrate chromatogram from October 9, 1979; 40" x 1/8" Teflon carbowax 400 on Gaschrom G; 60-80 mesh; 2cc auto gas sample loop; oven at 24.5°C; N_2 flow 5cc per minute; Varian 940 ECD 1 mv chart at 10" per minute.

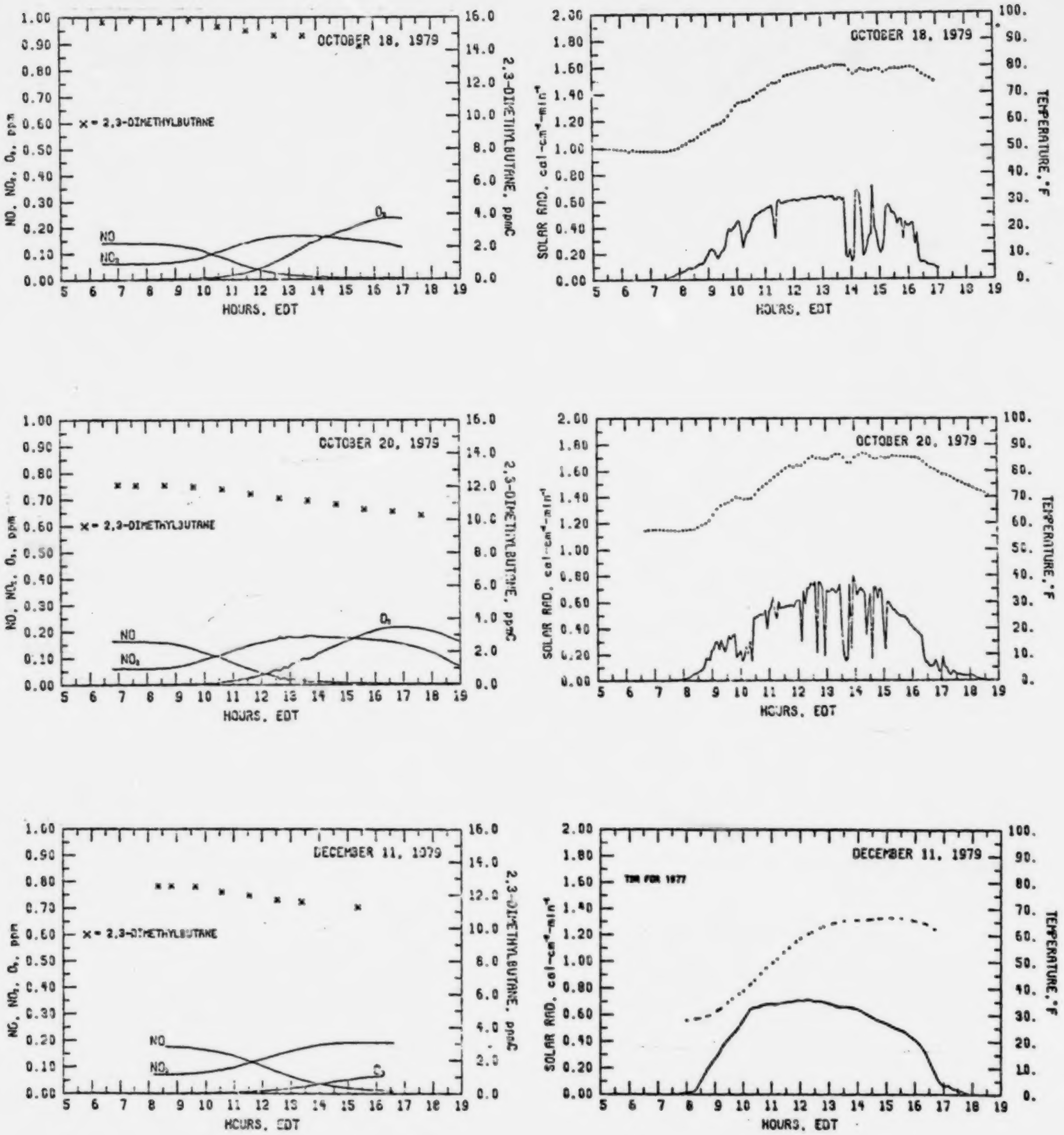

Figure 85. Three 2,3-dimethylbutane-NOx experiments in UNC chamber.

Table 50 shows that for each ppmC of 2,3-dimethyl butane reacted, approximately 16 percent of the carbon shows up as alkyl nitrate products. For n-pentane the figure is 10 percent and for n-butane, about 8 percent. These numbers are very similar to those found in the University of California at Riverside (UCR) chamber. Per molecule reacted, n-pentane loses 60 percent more carbon and 2,3-dimethyl butane ~300 percent more carbon to alkyl nitrate products than does n-butane. This is consistent with the UCR observation that longer chain (or higher molecular weight) paraffins have a stronger tendency to form more alkyl nitrates than do shorter chain paraffinic hydrocarbons.

With regard to alkyl nitrate formation, one can gain some preliminary insight into possible thermal stability of the tertiary alkoxyl radical formed in the above OH abstraction sequence by contrasting product yields under different seasonal conditions. In the cool December 11 run, 0.06 ppm O_3 was made compared to the June and October runs which made ~0.2 ppm O_3. The acetone and isopropyl nitrate produced from the December run were 30-40 percent lower than the October runs but the C_6 nitrate production was higher. This is consistent with the expectation that under cooler temperatures the tertiary alkoxyl radical would be more vibrationally stable and have less tendency to decompose to form acetone and isopropyl nitrate, as shown below. There is another alternative, the RO2 + NO adduct could be more stable, leading to more $RONO_2$ and less NO_2 + RO.

N-OCTANE-NO_2 EXPERIMENT

The one run with n-octane vs. NO_x occurred on September 18, 1979. Time behavior for the n-octane side appears to be a bit "slower" than that of the n-butane experiment on the chamber's other side. The carbon and alkyl nitrate accountability was very low for this run because most of the oxygenate and nitrate products could not be measured on the columns we were using. A broad unquantifiable peak did appear in the chromatogram on the alkyl nitrate column after the water response. Note that in terms of NO oxidation and O_3 production, n-octane, 2,3-dimethyl butane, n-pentane and n-butane do show great similarity. 2,3-dimethyl butane is perhaps slightly more reactive and n-octane slightly less reactive at the high HC/NO_x rates used, but in general the only major difference is the form and the amount of nitrogen which is lost from

Table 50

Afternoon Carbon Balances for 1979 Paraffin - NO_x Experiments in UNC Chamber

Date	Compound	I HC ppmc	I NO_x ppm	O_3 ppm	ΔCO ppm	HCHO ppm	C_2HCO ppmC	C_3HCO/ Acetone MEK ppmC	ΣC_2-C_6 Nitrate products ppmC	ΣAll Products ppmC	Reacted** HC ppmC	Percentage of Reacted Carbon: Oxygenates	Percentage of Reacted Carbon: PAN + Nitrates	Percentage of Reacted Carbon: All Products
6/20/79	n-butane	6.20	0.181	0.259	0.02	0.03*	0.14	0.25	0.05	0.49	0.62	70.4	8.1	79.0
9/18/79	n-butane	5.30	0.206	0.120	0.02	0.03*	0.144	0.15*	0.04	0.374	0.47	71.1	8.5	74.6
10/9/79	n-butane	14.35	0.204	0.191	0.02*	0.026	0.20	0.21	0.056	0.512	0.68	67.1	8.1	75.2
10/18/79	n-butane	13.84	0.200	0.181	0.02	0.03*	0.19	0.17	0.061	0.471	0.81	50.6	7.5	58.3
10/9/79	n-pentane	14.20	0.204	0.184	0.0	0.026	0.075	0.07	0.97	0.268	0.89	19.2	10.9	30.1
9/18/79	n-octane	6.22	0.207	0.120	0.00	0.02	0.03	0.00	0.15	0.065	0.74	6.7	2.0	8.7
10/18/79	2,3 dime-butane	15.96	0.201	0.230	0.00	0.03	0.00	0.86	0.124	1.014	0.78	114.1	15.9	130.0
10/20/79	2,3 dime-butane	12.09	0.229	0.216	0.00	0.03*	0.00	1.00	0.11*	1.14	0.90	114.5	12.2	126.7
12/11/79	2,3 dime-butane	12.56	0.247	0.064	0.00*	0.025	0.00	0.5	0.145	0.681	0.73	72.9	20.0	92.9
6/20/79	MEK	6.00	0.179	0.595	0.11	0.15*	0.14	0.0	0.178	0.578	1.95	20.5	9.1	29.6
10/20/79	MEK	13.54	0.228	0.560	0.13	0.15*	0.29	0.0	0.18*	0.750	1.09	52.3	16.5	68.8
12/11/79	acetone	14.05	0.241	0.018	0.05*	0.06	0.00	0.0	0.0085	0.119	0.55	20.0	1.6	21.6

---

* Estimated concentration from other experiments.

**Dilution adjusted initial hydrocarbon concentration minus afternoon hydrocarbon concentration; dilution of the chambers from leaks and sampling is approximately 8% ±2 [illegible] over 12 hours.

the system. This can be extremely important in a mechanism which tends to over predict O_3 from a hydrocarbon mix because it may be that not enough afternoon NO_2 is being shunted into alkyl nitrate products.

MEK-NO_x EXPERIMENTS

Smog chamber experiments starting with methyl ethyl ketone (MEK) and NO_2 were specifically selected to be run along with the alkane runs because MEK is an important product from OH attack on n-butane. The reactivity of MEK compared to n-butane can be seen by contrasting the two sides of the June 20, 1979 run (Figure 86). With approximately 6 ppm of carbon and 0.2 ppm of NO_x in both sides, the side with MEK produced ~0.6 ppm O_3 while the n-butane side made only 0.25 ppm O_3. It follows that once n-butane decomposes to MEK, MEK can contribute substantial reactivity.

The principal measured products of the MEK run were CO, acetaldehyde and PAN. Propionaldehyde was not seen in the oxygenate chromatograms. The sume of the measured products accounted for only 34 percent of the reacted carbon in the June 20 run and 70 percent in the October 18 run. Additional MEK runs are planned to resolve these differences.

FORMALDEHYDE EXPERIMENTS

Five high quality formaldehyde experiments were run in 1979; the initial conditions for these runs have been given in Table 5. The sky conditions for these runs were generally good and the side with formaldehyde had been dried. NO, NO_2, O_3 and HCHO traces for these experiments are shown in Figures 87 and 88.

AROMATIC-NO_x SYSTEMS

The purpose of these preliminary aromatic runs was to determine as many reaction products as possible without sacrificing effort and attention to the paraffinic, formaldehyde or SAI run series. Within these bounds, analytical methods were set up to determine:

1. The relative yields of benzaldehyde and cresol from toluene systems, and
2. Possible ring cleavage products like methyl glyoxal and biacetyl from toluene and o-xylene systems.

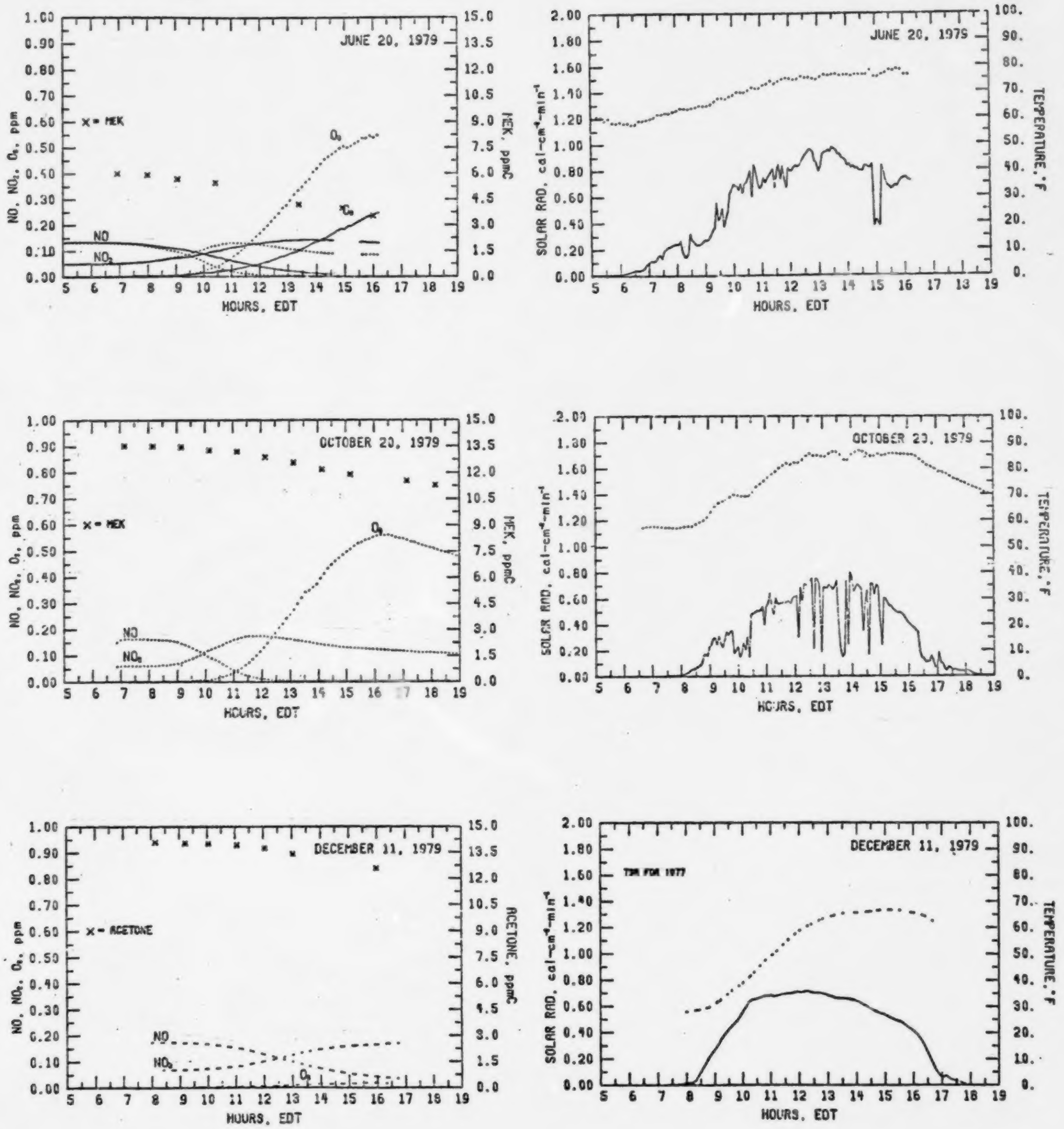

Figure 86. MEK and acetone experiments in UNC chamber.

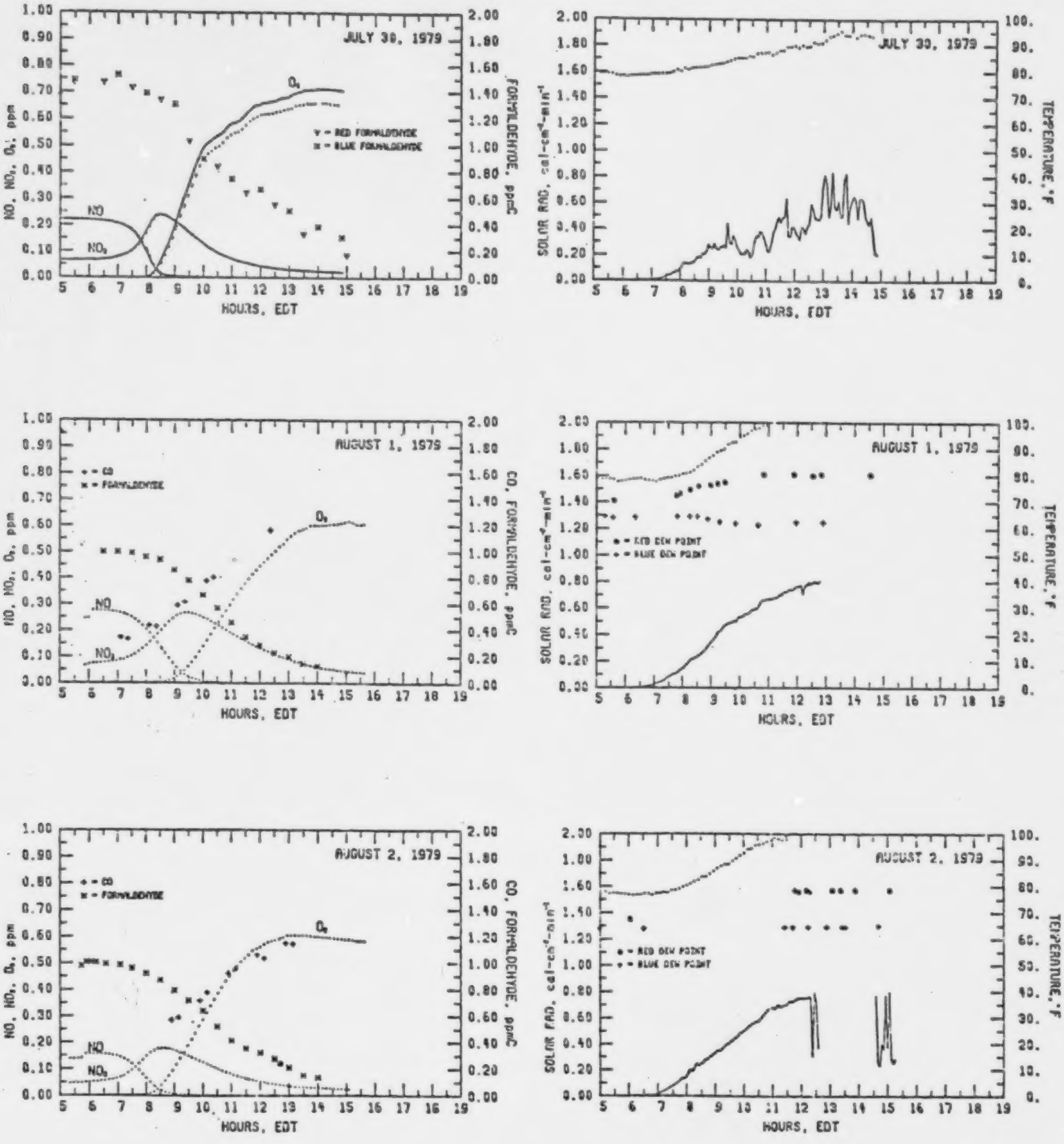

Figure 87. Five formaldehyde-NOx experiments in UNC chamber.

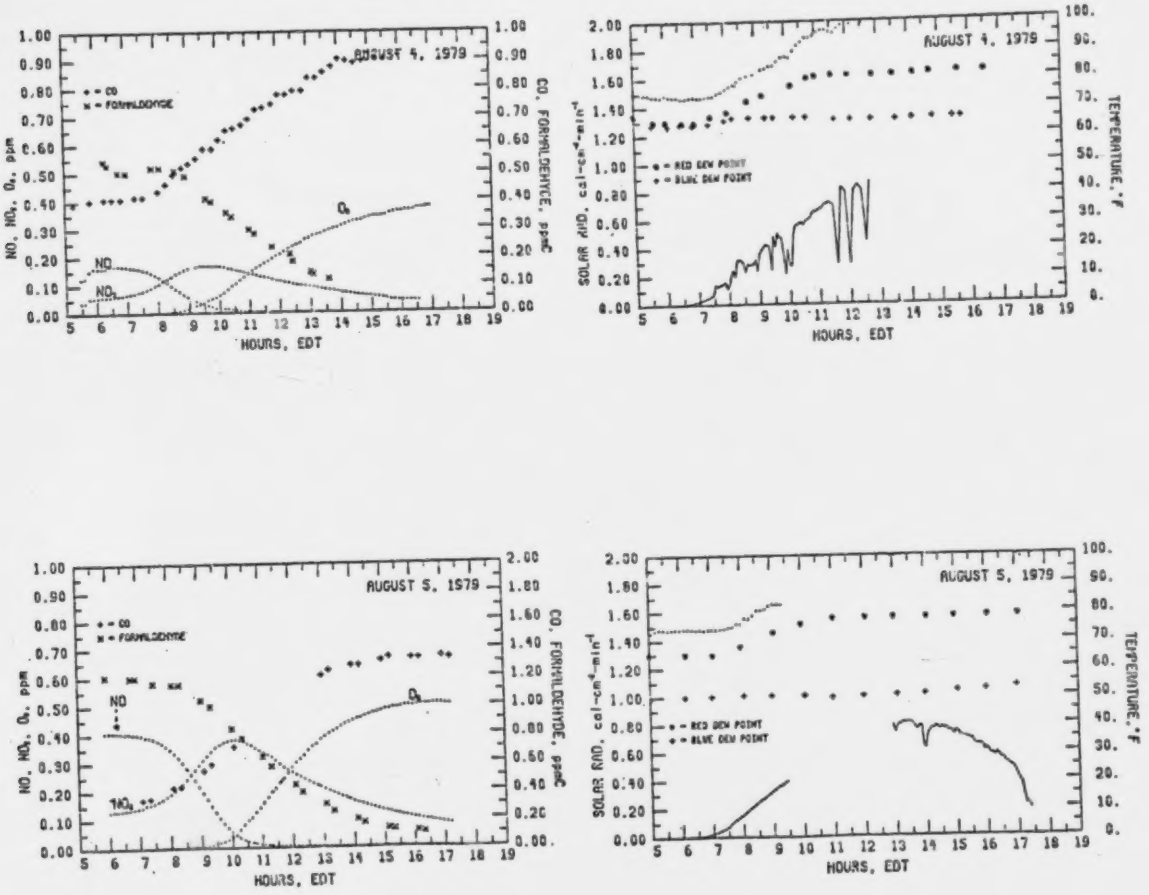

Figure 87. (cont) Five formaldehyde-NOx experiments in UNC chamber.

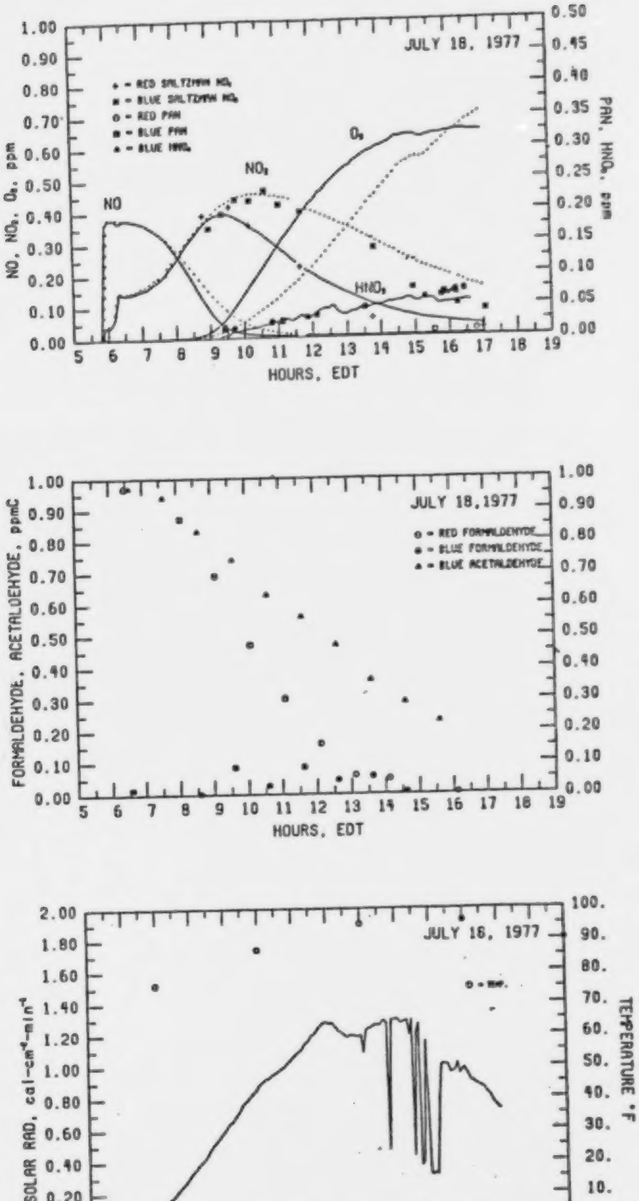

Figure 88. Data for July 18, 1977 formaldehyde/acetaldehyde experiment in UNC chamber.

Four aromatic experiments were conducted in 1979 (Figure 89). Preliminary reduction of chromatographic data obtained from the June 27 run indicates that less than 6 percent of the reacted carbon from the toluene side appeared as benzaldehyde and a slightly lower percentage as cresols.

Other compounds present in the product analysis for these runs were at the level of "ghost" interferences which can result from the presence of ozone in air samples taken on Tenex.

The August 15 run compares a toluene-NO_x system and an o-xylene-NO_x system. PAN was the major measured nitrogen product other than NO_2. A small concentration of biacetyl was detected in the o-xylene side, although calibration of this response requires more work. The afternoon product analysis for both sides is given in Table 51. Tentative identification of the o-xylene products is based on literature chromatograms of a SP2100 column similar to ours.

In the dual run of August 15, 1979 approximately half of the reacted carbon did not show up in measured products. Benzaldehyde and cresols accounted for 8 and 16 percent of the carbon on the toluene side. The product peaks from the o-xylene side which were identified as 2,3-dimethyl phenol and o-tolualdehyde only accounted for 9 percent and 11 percent. Presumably most of the rest of the unmeasured reacted carbon was in the form of ring cleavage glyoxal type products. It is clear that these glyoxal-type compounds must be measured.

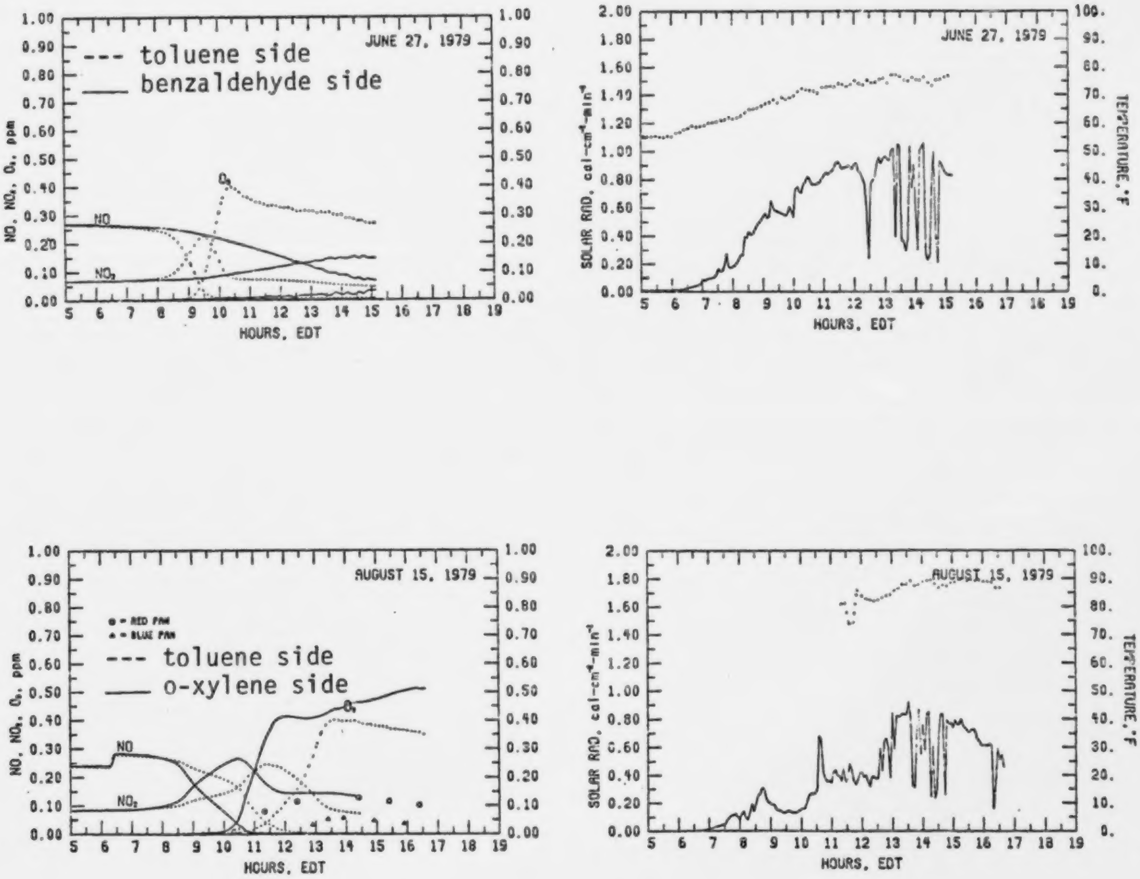

Figure 89. 1979 aromatic experiments in UNC chamber.

Table 51

Product Concentrations from Toluene and O-xylene NO_x Systems
August 15, 1979

Compound*	O-xylene side ppmC	Toluene side ppmC
CO	0.34	0.16
HCHO	0.28	0.13
Acetaldehyde	0.025	0.01
PAN	0.124	0.055
Chemi NO_2	0.135	0.081
H_2O_2	0.0038	0.0035
Benzaldehyde		0.17
Cresols		0.14
Nitro toluenes		0.044
2,3 dimethylphenol	0.25	
O-tolualdehyde	0.30	
C_3 and C_4 ketone	0.15	0.07
Biacetyl ?	0.02	
m & p nitro xylenes	0.03	
o-xylene	2.02	
Toluene		2.85
Carbon	3.54	3.77
IHC	4.74	4.94
Reacted carbon	2.72	2.09
Products	1.52	0.0
% Unmeasured Carbon	44	63

*all products at ~1330

EFFECT OF DYNAMIC OPERATING CONDITIONS ON OZONE FORMATION

In a typical urban environment, reactant material is usually emitted throughout the day. The volume into which the reactants are mixed determines the concentration of precursors available for O_3 formation. Static smog chamber experiments on the other hand, start with all the mass present initially.

The UNC dual chamber has been used to compare static experiments with those in which the same mass was added to the same volume, but ramp-injected slowly over a 12 hour period (0600-1800 EDT).

The experiment simulated a highly simplified urban condition. It was assumed that an air parcel moved along a trajectory over a uniform emissions surface from 0600 to 1200 EDT. At 1200 EDT the parcel left the emissions surface. During its movement over the surface from 0900 to 1200 EDT, the mixing height doubled in a linear manner. Therefore, in the absence of reaction, the concentration of precursors in the air parcel would increase linearly from 0600 to 0900, and then, the concentration (mass/volume) would remain constant while an additional 3 hours of emissions was added to a volume that was doubled in 3 hours.

This run was compared to a static run which started with the same mass as would be present, in the absence of reaction, at the end of the dynamic run (and also at 0900 EDT). The run was accomplished by ramp injecting NO and HC into a static chamber from 0600 to 0900 EDT, and then diluting the chamber by 50 percent while continuing to inject NO and HC at a rate equal to the mass lost by dilution, assuming no reaction. The results are shown in Figure 90. Except for O_3 at the very end of the run and the ramp NO and HC injection, there is almost no difference in the profiles.

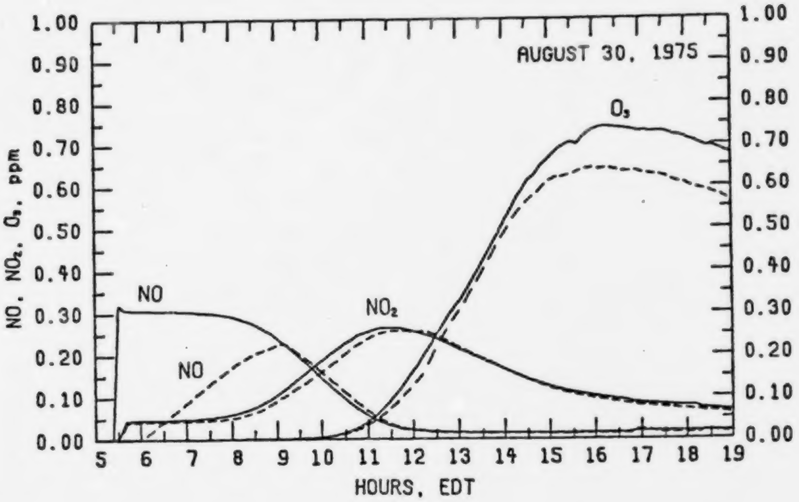

Static (—) and Ramp injection (0600-0900) with 50% dilution (0900-1200) and continued ramp injection (0900-1200) at rate equal to mass removal by dilution if no reaction (--). Initial conditions in static side: NO, 0.31 ppm; NO_2, 0.05 ppm; urban hydrocarbon mix, 4.56 ppmC. An initial condition of 0.05 ppm NO was established in ramp side (--). NO and six injected in (--) so as to achieve same condition at 0900.

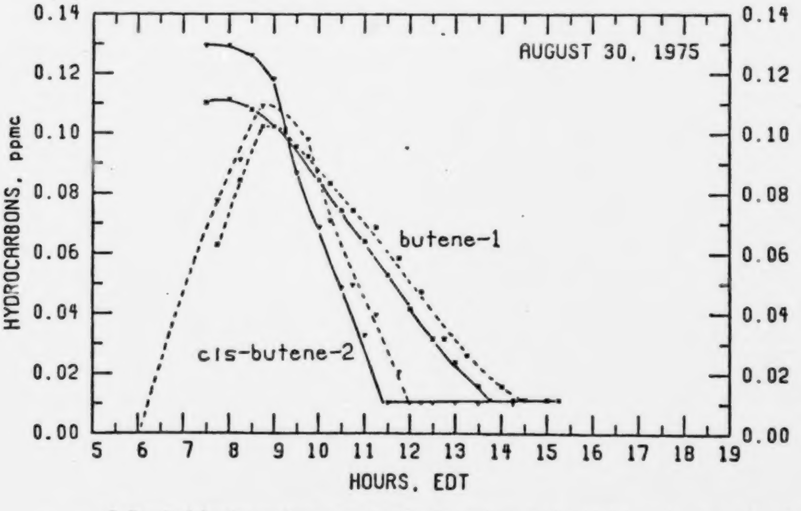

Selected hydrocarbon compounds in urban hydrocarbon mix for static (—) and ramp injection (--) dual run in UNC outdoor smog chamber.

Figure 90. Example of static and dynamic HC mix experiment in UNC chamber continued.

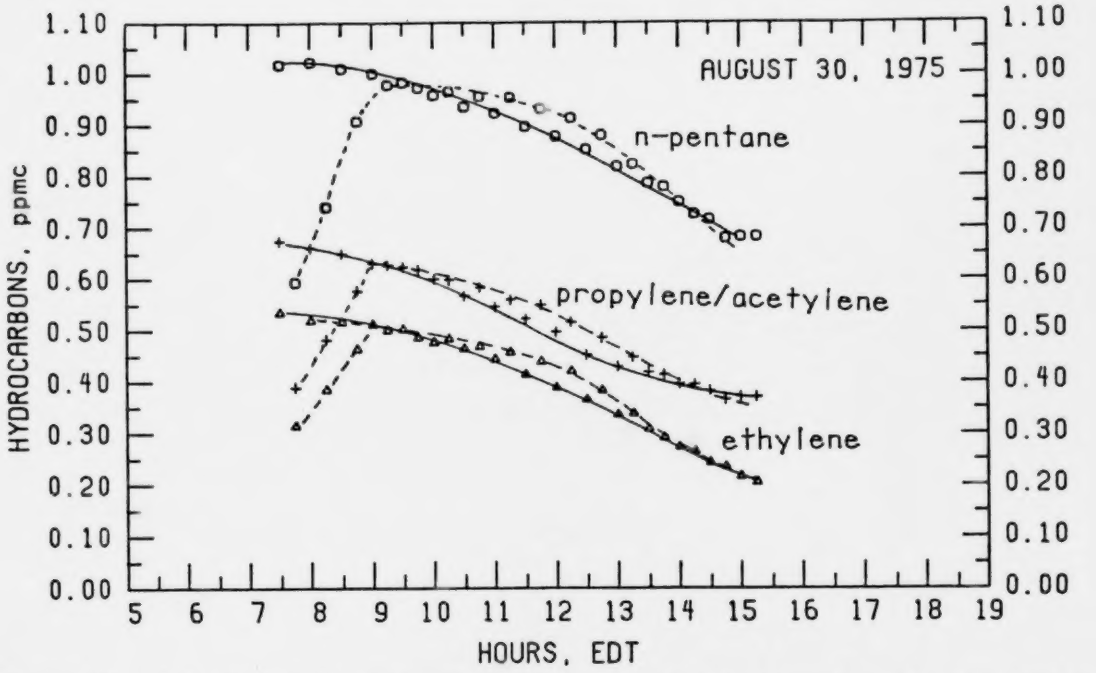

Figure 47. Selected hydrocarbon compounds in urban hydrocarbon mix for static (—) and ramp injection (--) dual run in UNC outdoor smog chamber.

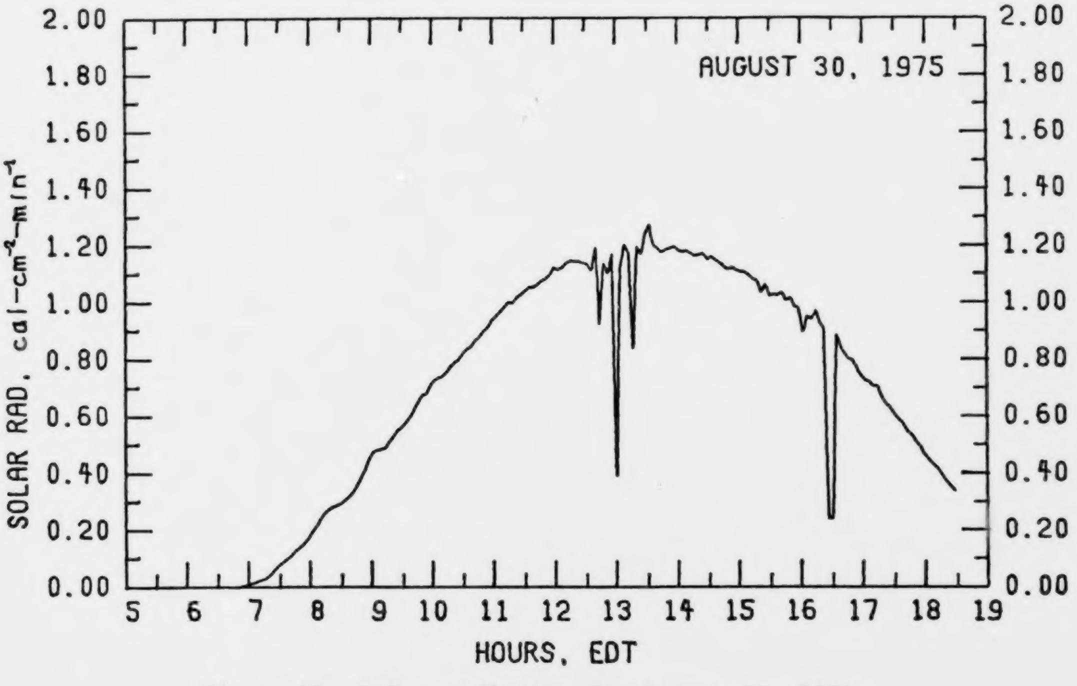

Figure 48. Solar radiation for August 30, 1975.

Figure 90. (cont)Example of static and dynamic HC mix experiment in UNC chamber continued.

JUNE 3, 1977 PROPYLENE + FORMALDEHYDE/PROPYLENE RUN

The two runs on this day (Figure 91) were designed to investigate the effects of adding excess formaldehyde to a propylene-NOx system. It was hypothesized from models of the formaldehyde mechanism that if enough formaldehyde was added, the formaldehyde would substantially increase the OH concentration. Some of this extra OH would react with NO_2 and cause more HNO_3 to be produced. This in turn would show up as a net loss of NOx which would reduce the O_3 potential of the smog system. Approximately 1.7 ppmC of propylene was added to both sides. The RED chamber then received an additional 0.6 ppm of formaldehyde.

The morning was overcast but cleared quickly with only a few clouds for a short time near noon. At sunrise the temperature was about 16 C (60 F); the maximum was about 32 C (90 F) at 1500 EDT. A nitrogen balance is not presented here because neither PAN nor HNO_3 data are available. Saltzman NO_2 data were obtained. The NO_2 data after 1200 EDT are probably 100% PAN.

It can be seen that extra radicals from the formaldehyde caused the NO_2 maximum to be reached, and O_3 production to be initiated one hour sooner than in the propylene-only side. Also, Saltzman data show that the NO_2 was removed very much faster than in the propylene-only side. Further, even though the formaldehyde side is faster (reaching O_3 maximum sooner than the propylene-only side), the O_3 maximum concentration is actually less than the side with propylene only, because the formaldehyde-propylene side ran out of NO_2. There is a difference in PAN concentration between the two sides suggesting that indeed more HNO_3 was formed in the RED (formaldehyde) side.

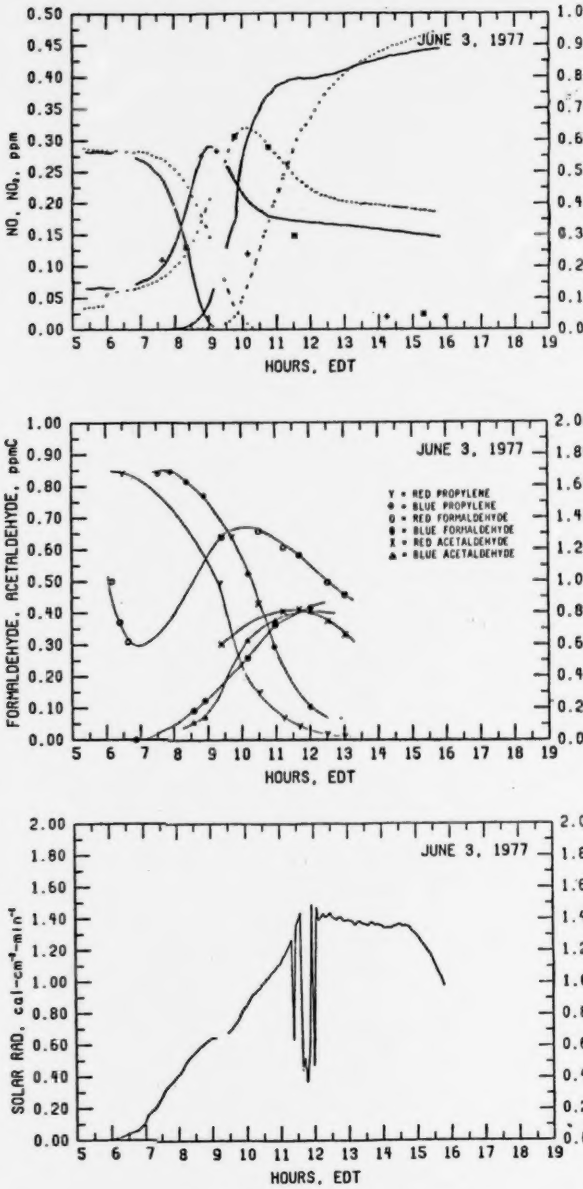

Figure 91. Illustration of effect of addition of initial formaldehyde (0.6 ppm) to a propylene/NOx experiment in UNC chamber.

JULY 15, 1977 PROPYLENE + ACETALDEHYDE/PROPYLENE RUN

This run consisted of equal concentrations of propylene and NOx in each side with acetaldehyde added to one side. The experiment was designed to observe the effects of the extra acyl radicals from acetaldehyde on the ratio of PAN to HNO_3 formed. It was generally a clear, hot day with no clouds appearing until approximately 1330 EDT, after O_3 concentrations were already high.

The HNO_3 analyzer was used on the side with acetaldehyde. PAN and Saltzman NO_2 were measured on both sides. It can be seen in Figure 92 that the addition of acetaldehyde to this propylene/NOx system increases the effective conversion rate of NO to NO_2 and remarkably increases the amount of O_3 produced (more than the instrument range).

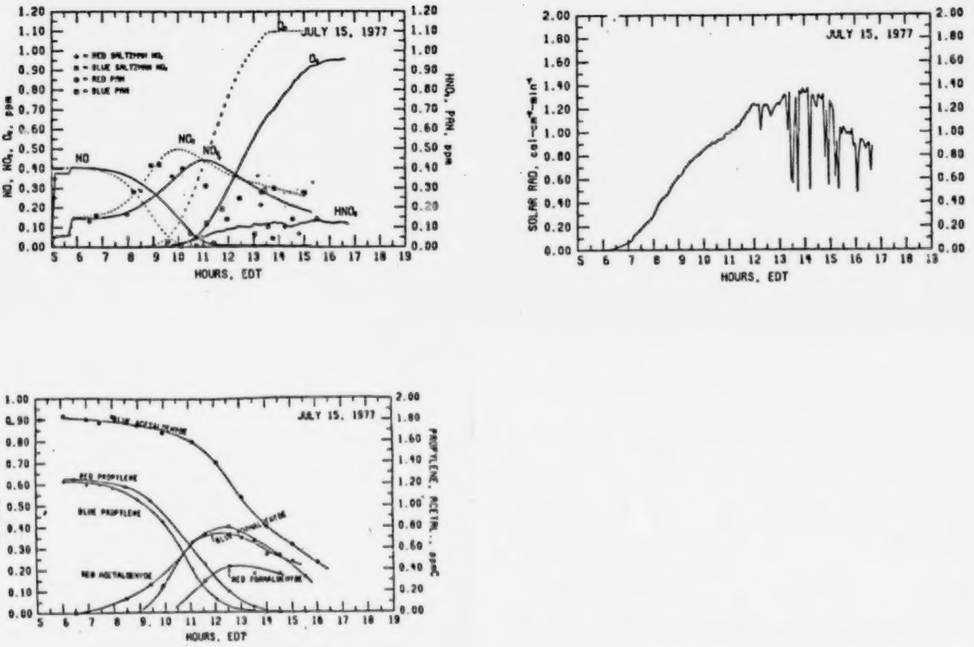

Figure 92. Illustration of effect of addition of initial acetaldehyde (1.8 ppmC) to propylene/NOx experiment in UNC chamber.

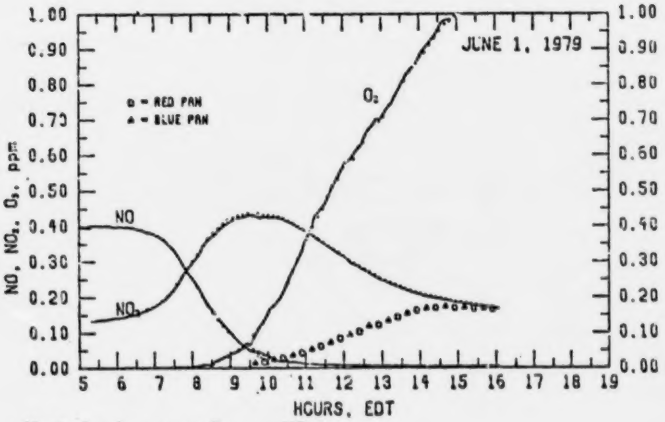

Matched propylene-NO_X

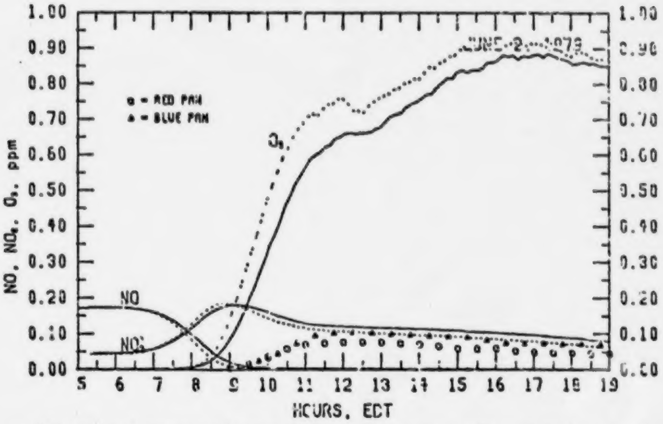

Matched propylene-NO_X; 41 ppm CO added to (---)

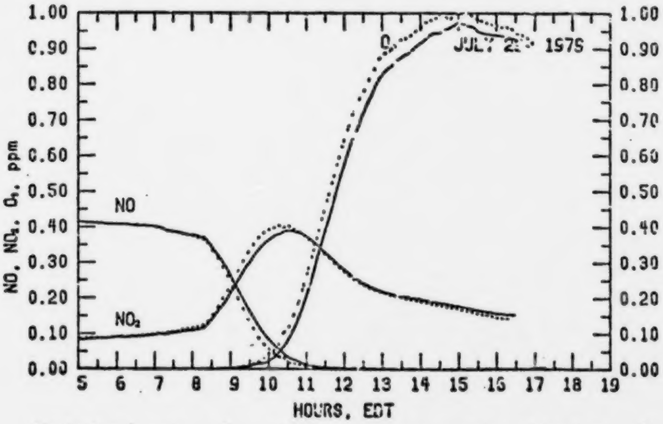

Matched propylene-NO_X; 12 ppm CO added to (---)

Figure 93. Illustration of effect of addition of initial carbon monoxide (41 and 12 ppm) to propylene/NOx experiment in UNC chamber.

WET-DRY EXPERIMENTS

Modeling work by UNC has concentrated mainly on the results of the propylene smog chamber runs of August 8, 1977, October 22, 1977, January 28, 29, 1978, and October 21, 1978. In all of these experiments, the initial NO_x was about 0.5 ppm (20 percent NO_2) and they were all NO_x limited. The initial propylene concentration was about 1.5 ppmC in the August run and about 3.5 ppmC in all of the cooler experiments. The experiment of October 21, 1978 had matched initial coditions in each side of the chamber. However, the BLUE side had been dried with molecular sieve.

The first version of the UNC propylene mechanism which included a temperature dependent PNA reaction could model sucessfully the August and October, 1977 experiments. The same model, however, given the temperature and light profiles and initial conditions of the cold January experiments, resulted in very low ozone prediction. Kinetic rate parameters (activation energies, frequency factors, and rate constants) were adjusted within acceptable uncertainty limits for many reactions capable of accounting for seasonal effects. The formation of PNA (peroxynitric acid) had been incorporated into the earlier version of the mechanism with a rate constant of 9,000 $ppm^{-1}min^{-1}$. A good simulation for the January runs could be obtained if the rate constant was lowered to about 2000 $ppm^{-1}min^{-1}$. Not only were the ozone concentrations predicted, but the trends and magnitudes of the other important timing events were also simulated. It was also discovered that a better fit for the October 22, 1977 experiment was obtained when the formation rate of PNA was set at 7,000, that the August simulation was insensitive to the formation rate, and that a value as high as 9,000 (as the earlier model version used) could be accommodated. These results seemed to indicate that the formation rate should increase with temperature; or, that the decomposition rate at higher temperatures should be decreased, and at lower temperatures increased.

Several estimates for a new activation energy (and frequency factor) were tried. The resulting simulations had about the right ozone maximum but had grossly misshapen profiles. But more important was the fact that the timing of the events of the October 21, 1978 simulations (BLUE side air dried) were different even though the initial conditions were carefully matched; each side was subject to the same

Table 52

Critical Data for Humid VS. Dry Runs

Date	Run Type	$[NO_2]_o$		$[NO_x]_o$		$[HC]_o$ ppmC		$[D.P.]_F$		$[T°]_i$	$[T°]_f$	Time Cross		$[NO_2]$ Max		Time NO_2 Max		$[O_3]$ max		Time O_3 max		Sun
		Blue	Red	Blue	Red	Blue	Red	Blue	Red			Blue	Red	Blue	Red	Blue	Red	Blue	Red	Blue	Red	
10/21/78	Match propylene Blue dried	0.110	0.111	0.503	0.505	3.45	3.48	43	58	34.7	72.4	9:41	9:50	0.484	0.461	10:48	11:05	+11% 0.745	0.670	12:30	12:42	90%
6/29/79	Match propylene Blue dried	0.085	0.094	0.458	0.464	3.504	3.553	57	69	58	79.2	8:32	8:31	0.396	0.387	9:26	9:24	0.891	0.893	13:35	12:32	23%
10/16/79	Match propylene Blue dried	0.085	0.083	0.371	0.371	3.126	3.172	32	48	40.8	74.5	9:55	9:46	0.341	0.342	10:58	10:52	+1.9% 0.822	0.807	13:01	12:47	80%
10/26/79	Match propylene Blue dried Red misted	0.091	0.092	0.494	0.496	4.765	4.839	28	56	35	61	9:54	10:00	0.472	0.452	10:43	10:59	+41% 0.822	0.582	12:14	12:24	100%
10/29/79	Match ethylene Blue dried	0.087	0.086	0.476	0.474	3.189	3.212	58.5	68.4	44	75	10:47	10:58	0.411	0.403	12:06	12:27	+24% 0.760	0.613	14:25	14:59	55%
10/31/79	Match ethylene Blue dried	0.097	0.098	0.497	0.498	3.706	3.743	28	62.5	50	72	11:08	10:49	0.43	0.416	12:26	12:19	+7.3% 0.887	0.827	3:30	3:02	Clear
11/8/79	Match ethylene Blue dried Red misted	0.096	0.097	0.492	0.494	3.818	3.79	27.4	47.6	31.2	60.3	12:03	11:42	0.387	0.356	14:34	14:34	+>100% 0.31	0.15	16:23		Cloudy

a. All dewpoints and temperatures are in °F.

b. $[D.P.]_F$ is dew point at O_3 maximum.

c. $[T°]_i$ and $[T°]_f$ are temperatures at time of sunrise and O_3 maximum

d. "Misted" means ~400 ml of distilled water added to inside of vertical walls of undried side.

e. 11/8/79 run - O_3 data missing until end of run on Red side. O_3 max concentration is estimated.

temperature. The difference in events and timing could not be simulated by having an inordinately high rate for formaldehyde wall loss reactions in the wet side.

It was concluded that the formation rate must vary proportionally with some other parameter that could be associated with temperature. In 1977 Hamilton presented experimental results showing a positive water vapor effect on the formation of H_2O_2 from the reaction of two hydroperoxy radicals. He suggested that one radical hydrates and reacts with another unhydrated HO_2 radical. Water vapor is proportional to dew point which is limited by temperature.

This approach was tested in the model. By analogy the formation of PNA was made water vapor dependent. Remarkably, the concentration of water vapor (obtained from dew point measurement), multiplied by a new constant, provided the desired rates and enabled the model to simulate the full range of these experiments without any rate constant changes. This mechanism also modeled the "wet and dry" sides of October 21, 1978.

The role of PNA in the UNC model for propylene and ethylene is similar to the role of PAN in the propylene mechanism. PNA forms from the reaction of HO_2 and NO_2 (proportional to water concentration) and thermally decomposes back to the same reactants. At 298 °K PNA decomposes about a hundred times faster than PAN. Therefore, PAN and PNA provide a mechanism to temporarily store NO_2 and a radical. Like PAN, the amount of PNA that accumulates is dependent on the ratio of the formation rate to the decomposition rate. This ratio therefore is dependent on the concentrations of HO_2, NO_2, H_2O and temperature. The accumulation of PNA therefore seems to delay the photochemical system, by taking NO_2 and an important radical out of the system and then releasing it later. This causes lower NO_2 and O_3 maximum concentrations.

On the basis of the proposed PNA chemistry we would predict the summer, dry vs. more humid, matched propylene experiments would not show strong "PNA effects"; high temperatures would prevent significant PNA accumulation at any period during a run. In runs with low propylene/NO_x ratios reactant concentrations would be less sensitive to this mechanism and finally, cooler and more humid conditions would tend to show the most dramatic "PNA effects".

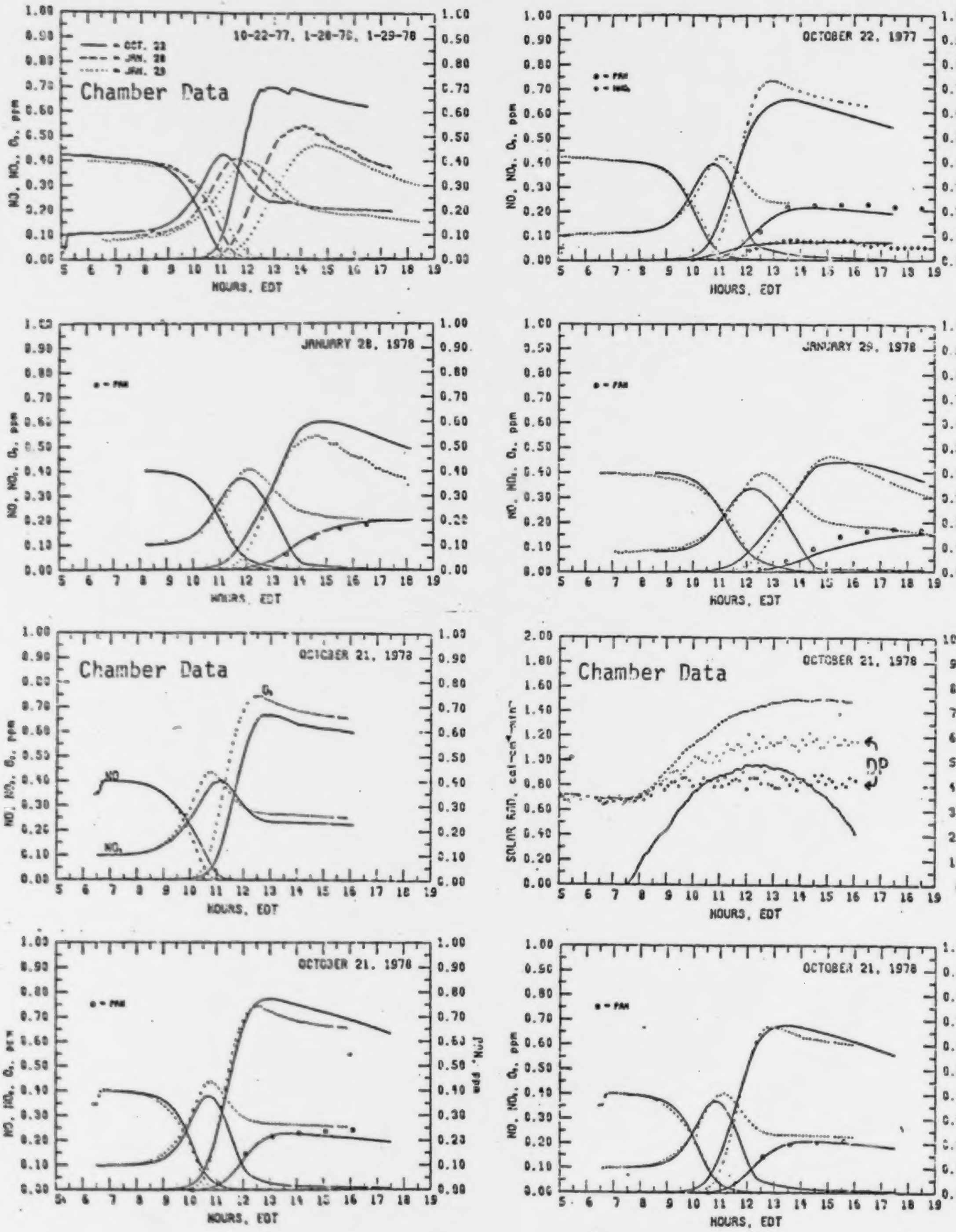

Figure 94. Water effect experiments. Unless otherwise indicated, (---) represents UNC smog chamber data, (——) represents model.

It was decided that more experiments should be conducted, with matched initial conditions on each side but with drier air on one side, to test the mechanism's success. Table 52 lists these experiments and some of the more important results.

June 29, 1979 was a high [propylene][NO$_2$] experiment with initial conditions similar to October 21, 1978. The major difference is the warmer weather and "summer light". The dew points for each side were relatively higher than in the October run, but still significant drying was achieved. The temperatures on this day were also higher and therefore the PNA decomposition rate on each side was very high. As stated before, these circumstances tended to minimize the effect of PNA formation in this experiment. Consequently, this experiment resulted in being an almost perfect match.

October 16, 1979 was a regular "dry-down" experiment with propylene. The weather conditions were fair and dry, so that although drying had taken place on one side, the other side was not very humid. The dry side had a slightly higher O_3 maximum. The minimum difference observed is thought to be caused by the low moisture concentration of the undried side. Although the differences in the water concentrations on each side were great (high k_{wet}/k_{dry}), the absolute value of k_{wet} was low because the air was very dry and therefore relatively little PNA was formed.

The results of October 21, 1978 (Figure 95) have already been presented. This experiment was used to develop the water dependent PNA mechanism. Note from Table 29 that the dried side (always BLUE in these experiments) produced an O_3 maximum 11 percent higher than the wet side. NO$_2$ maximum also was higher on the BLUE side. The dried side was also 9 minutes faster to O_3 maximum. Dewpoint and temperature at time of O_3 maximum are also listed in Table 29.

October 26, 1979 was a modification of the regular type of "dry-down" experiment. Using a fine misting device, about 400 ml of distilled water was sprayed on the walls inside the chamber in the RED side before injections were made. The water did not run down the sides of the chamber. The addition of water was made to increase the difference of dew point and to further test the PNA theory. The temperature of this day was also somewhater cooler than observed on the October 21, 1978 experiment. Initial propylene was also higher: ~4.8 ppmC. The dried side produced a 41 percent higher O_3 maximum concentration than the misted side. The BLUE O_3 maximum was also 10.3 percent higher than the BLUE O_3 maximum of October 21, 1978. The dried side was faster in converting NO to NO_2 and as expected had a higher NO_2 maximum. This experiment seems to agree with the general theory. Looking at the RED side however, one sees that the O_3 maximum was lower than expected.

October 29, 1979 was a regular dry down experiment with ethylene. The dry side produced a 24 percent higher O_3 maximum, a slightly higher NO_2 maximum; and was faster to reach crossover (11 minutes), NO_2 maximum (21 minutes) and O_3 maximum (24 minutes).

October 31, 1979 was generally a repeat of October 29, 1979 although the drying was much better. The dry side of this run produced a 7.3 percent higher O_3 maximum and a higher O2 maximum. The BLUE side however was slower. We have no clear explanation for these results.

November 8, 1979, a matched ethylene experiment, had one side misted while the other side received extensive drying. Unfortunately the wet side lacks O_3 data until late in the afternoon. The dry side produced twice the ozone but since it was such a cloudy day the misted side became severely light limited. A higher NO_2 maximum was also observed on the dry side of this run. Time to NO_2 maximum was the same on the two sides, but time to crossover was later on the dry side by 21 minutes.

Although there are some exceptions, our general conclusions are that water vapor does have an effect on these hydrocarbon and NO_x systems and on ozone production. These experiments indicate that humidity is unimportant on warm days as the model suggests, even for high propylene/NO_x conditions. The greatest effects will be seen in cool systems between air with high water content and air with low water content. But more important is the fact that this mechanism seems necessary to model experimental HC/NO_x systems in colder environments where the air is naturally drier (Figure 94). We have found that temperature dependent reaction alone cannot account for the observed results. Finally, seasonal effects of water vapor and temperature changes may be important considerations for cities and states in cooler and drier climates, where modeling will be utilized in determining control strategies for photochemical oxidants.

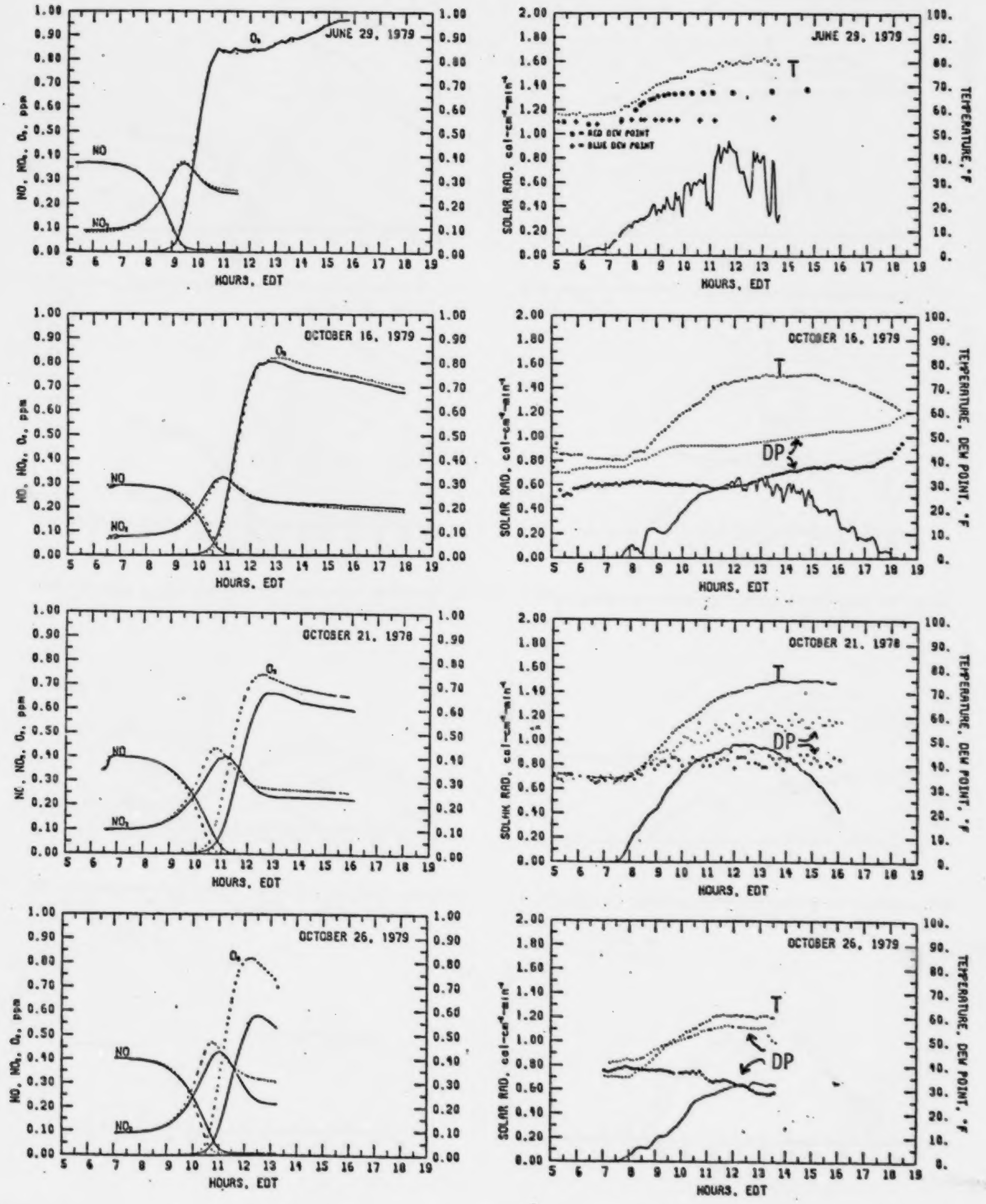

Figure 95. Chamber data for series of wet/dry experiments.

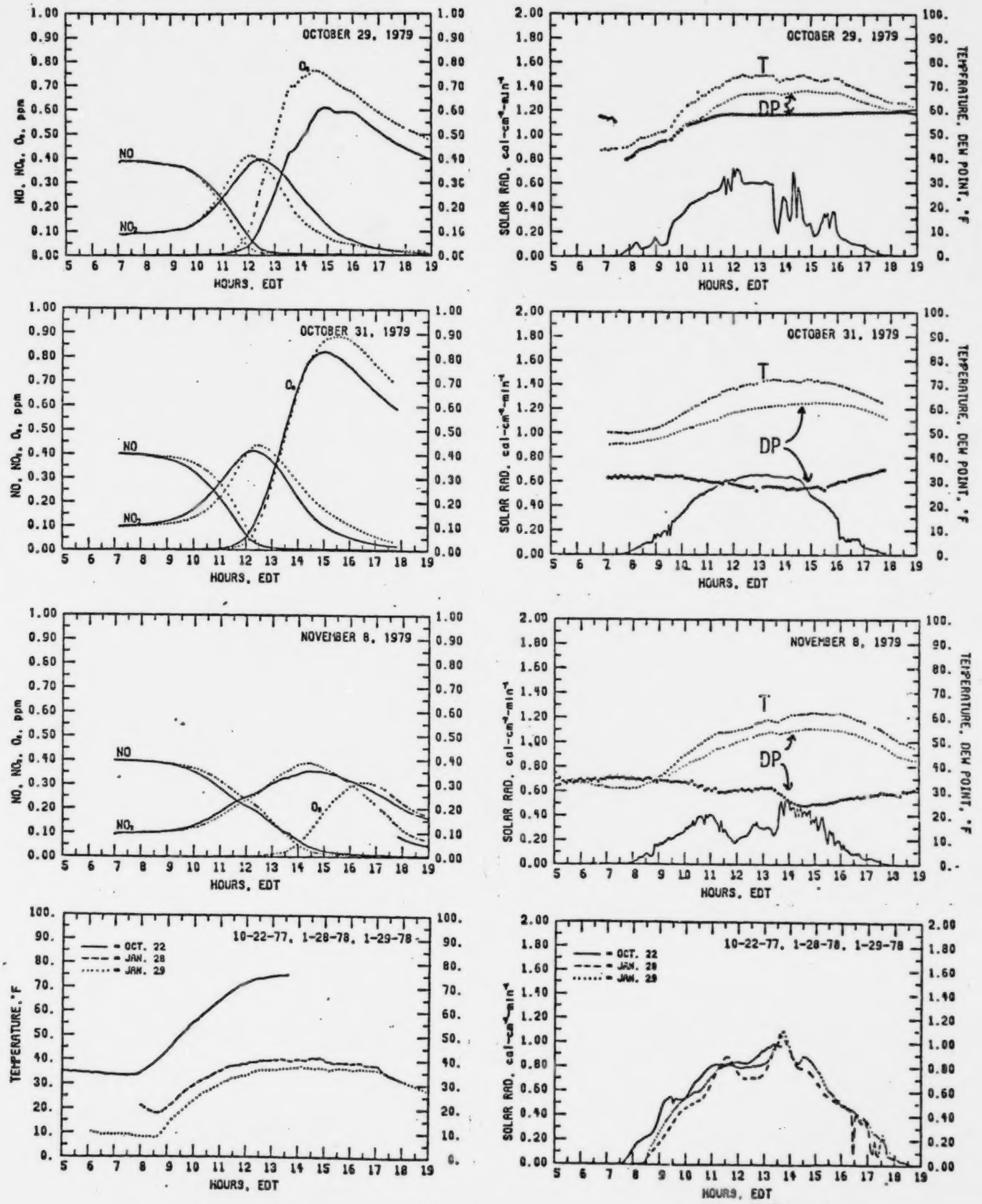

Figure 95. (cont) Chamber data for series of wet/dry experiments.

REFERENCES

Braslau, N., J. V. Dave (1973), "Effect of Aerosols on the Transfer of Solar Energy Through Realistic Model Atmosphere. Part I: Non-Absorbing Aerosols," J. Appl. Meteorol., Vol. 12, pp. 601-615.

Braslau, N., J. V. Dave (1973a), "Effect of Aerosols on the Transfer of Solar Energy Through Realistic Model Atmosphere. Part II: Partly-Absorbing Aerosols," J. Appl. Meteorol., Vol. 12, pp. 616-619.

Cox, R. A., R. G. Derwent (1976), "The Ultraviolet Absorption Spectrum of Gaseous Nitrous Acid," J. Photochemistry, Vol. 6, pp. 23-34.

Dave, J. V. (1972), "Development of Programs for Computing Characteristics of Ultraviolet Radiation," Final Rept. under Contract NAS5-21680, NASA Rept. CR-139134, Nat. Aeronautics and Space Admin., Goddard Space Flight Ctr., Greenbelt, Maryland (NTIS No. N75-10746/6SL).

Demerjian, K. L., K. L. Schere, J. T. Peterson (1980), "Theoretical Estimates of Actinic (Spherically Integrated) Flux and Photolytic Rate Constants of Atmospheric Species in the Lower Troposphere," in Advances in Environmental Science Technology, J. N. Pitts and R. L. Metcalf, eds. (John Wiley & Sons, New York, New York).

Hamilton, E. J., Ruey-Rong Lii (1977), "The Dependence on H_2O and on NH_3 of the Kinetics of the Self-Reaction of HO_2 in the Gas-Phase Formation of HO_2. H_2O and $HO_2.NH_3$ Complexes," Int. J. Chem. Kin., Vol. IX, pp. 875-885.

Howard, C. J. (1977), "Kinetics of the Reaction of HO_2 With NO_2," J. Chem. Phys., Vol. 67, pp. 5258-5263.

Joseph, D. W., C. W.Spicer (1978), "Chemiluminescence Method for Atmospheric Monitoring of Nitric Acid and Nitrogen Oxides," Anal. Chem., Vol. 50, pp. 1400-1403.

Saeger, M. (1977), "An Experimental Determination of the Specific Photolysis Rate of Nitrogen Dioxide," Masters Report, Chapel Hill, University of North Carolina.

Sickles, J. E., H. E. Jeffries (1975), "Development and Operation of a Device for the Continuous Measurement of K_1 for Nitrogen Dioxide", Dept. of Environmental Sciences and Engineering,University of North Carolina, Chapel Hill, North Carolina, Publ. No. 396.

Stedman, D. H., R. B. Harvey, R. R. Dickerson (1977), "Measurement of Photons Involved in Photochemical Oxidant Formation," International Conference on Photochemical Oxidant Pollution and Its Control, Proceedings: Vol II, EPA-600/3-77-001b.

Stockwell, W. R., J. G. Calvert (1978), "The Near Ultraviolet Absorption Spectrum of Gaseous HONO and N_2O_5," J. Photochemistry, Vol. 8, pp. 193-203.

Whitten, G. X., H. Hogo, M. J. Meldgin, J. P. Killus, P. J. Bekowies (1979), "Modeling of Simulated Photochemical Smog wtih Kinetic Mechanisms," EPA-600/3-79-001a, Systems Applications, Inc., San Rafael, California.

Whitten, G. Z., R. Johnson, H. Hogo (1980), "Photochemical Modeling of Smog Chamber Data," Monthly Progress Report, Systems Applications, Inc. San Rafael, California.

Appendix A

CHAMBER AND FACILITY DESCRIPTION

Description

Location. The site is approximately 32 kilometers from the University of North Carolina at Chapel Hill. It is in Chatham County, North Carolina and is approximately 10 kilometers from the small town of Pittsboro. Chatham County is one of the most rural, least industrialized counties in North Carolina and is heavily wooded. The background concentrations of NO_x and nonmethane hydrocarbons are usually less than 5 ppb and less than 80 ppbC. More importantly, the air exhibits very low reactivity in the chamber.

Materials. The chamber surfaces are FEP Teflon^R. The film's transmission in the UV and visible regions of the solar spectrum is excellent, and it has only a few absorption bands in the IR, a property necessary to reduce the "greenhouse effect". It has a very low permeability for most chemical species and can be heat sealed to form large durable panels. For this application its worst property is its ability to hold a static charge for long periods of time. Type A film, 0.13 mm thick is used.

Physical Design. Inlet and outlet doors, stirring fans, manifolds and other fittings are inserted through a solid floor. The sides are free for light entry. The floor of the chamber is elevated approximately 1.2 m to allow for easy access under the chamber.

The design is an A-frame 9.14 m wide, 12.10 m long and 6.10 m high at the peak on a plywood floor 1.22 m above the ground. Wooden beams, 5.08 cm by 20.32 cm, located on edge at 99.1 cm centers form an exterior framework on top of the plywood floor. Continuous 16.46 m lengths of film are attached to the inside by aluminum u-channels, screwed firmly to the wooden beams thus compressing the film against the external support. See Figures 1 and 2.

One piece, heat sealed Teflon film panels are used in such places as the triangular end panels and floors. The floor-to-side seals are achieved by a 0.61 m overlap of side panel film over floor panel film. A rubber strip under the film and an aluminum strip over top of the film complete the seal. All other seals are Teflon-to-Teflon under pressure of the aluminum u

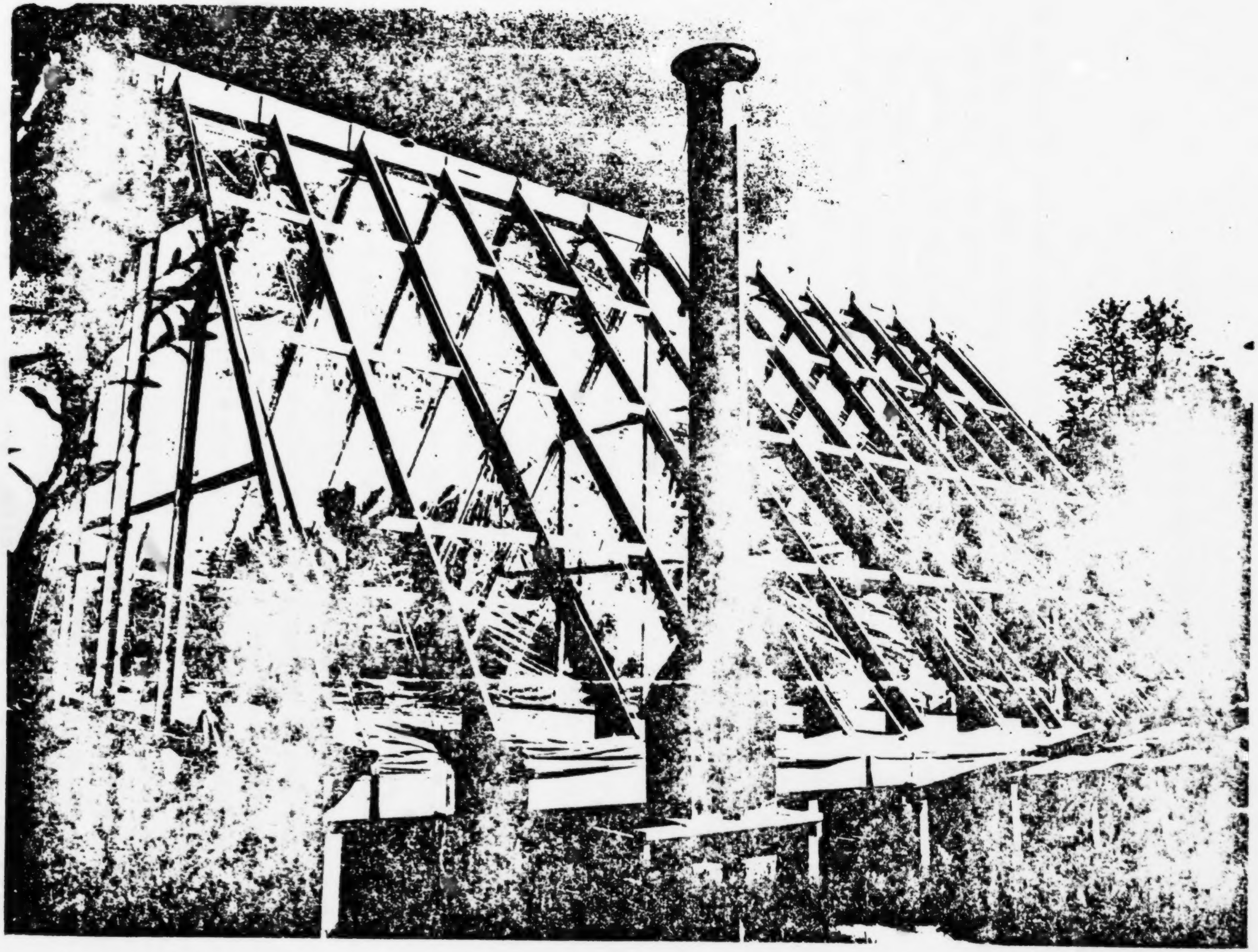

Figure 1. The University of North Carolina Outdoor Smog Chamber. (Courtesy of the Greensboro Daily News)

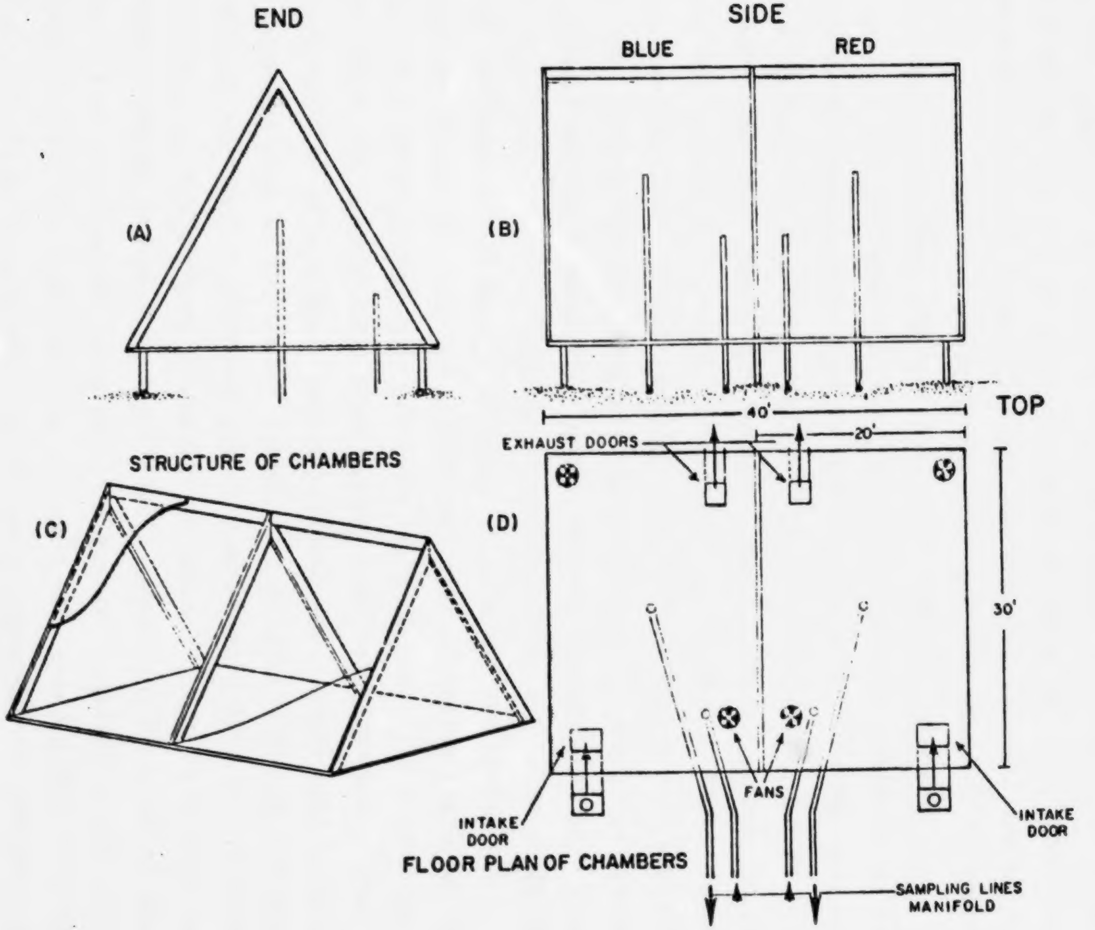
END
(A)
SIDE
BLUE
RED
(B)
STRUCTURE OF CHAMBERS
(C)
TOP
40'
20'
EXHAUST DOORS
(D)
30'
FANS
INTAKE DOOR
INTAKE DOOR
FLOOR PLAN OF CHAMBERS
SAMPLING LINES MANIFOLD

Figure 2. Schematic of UNC Outdoor Smog Chamber

channel. A single unsupported heat sealed Teflon panel similar to the end panels is used to separate the chamber into two halves of equal volume. It is sealed to the floor and side panels in the same manner as described above. Aluminum foil is placed under the film on the floor to reflect the light and heat backup through the chamber. This is necessary to reduce solar heating of the air to a value that is within normal urban environments and to compensate for transmission losses through the Teflon film.

Orientation. The chamber is oriented with its long axis approximately north to south. The actual long axis orientation is along a $27^0 - 207^0$ true heading. The orientation with respect to the sunrise and sunset at different times of the year and the altitude of the sun at noon for different times of the year are illustrated in Figures 3 and 4.

Air Handling Systems. There are four air handling systems in each half of the chamber, one for exhausting, one for sampling, one for recirculating through dehumidifiers, and one for mixing. The exhaust system consists of two intake stacks, 0.61 m x 0.91 m intake doors, 0.61 m x 0.61 m exhaust doors, and an exhaust blower. The exhaust blower is a dual blower on a single shaft driven by a 1.5 horsepower motor. Air enters the system through the two 5.49 m high by 30.5 cm diameter stacks. This system is designed to permit rapid exhausting of chamber contents and replacement with ambient air. The filling rate is 7190 l/min. The chamber can be flushed with a 99.6% decay of initial contents in 2 hours.

The second air handling or manifold system is for sampling and injection of pollutant materails into the chamber halves. To insure representative sampling, a 3.17 cm I.D. glass manifold runs from a point 1.83 m above the floor in the center of each chamber half down through the floor and over to a sampling laboratory. The sampling volume required by all the instruments does not exceed 5 l/min but to reduce losses due to long resident times it is necessary to have higher flows in the manifold. The flow rate in the manifold is 60 lpm. The manfold system is wrapped with a controlled heating tape to maintain the sample slightly warmer than the chamber temperature. To avoid the necessity of makeup air, the sampling manifold is a closed loop. Squirrel cage blowers with housings and fans that are Teflon coated are used to circulate air through the manifolds. The unused sample air is then returned through a 3.17 cm I.D. glass manifold to the chamber. These return manifolds provide a convenient method for injecting the initial reactants. There is also a special heated Teflon manifold for formaldehyde sampling.

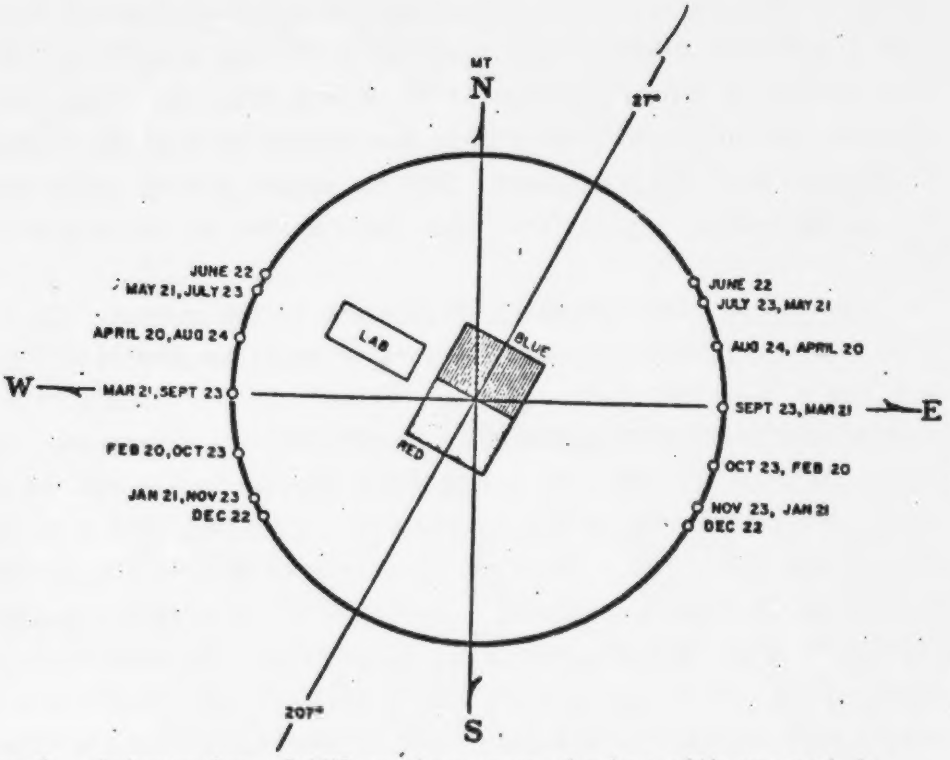
MT
N
27°
JUNE 22
MAY 21, JULY 23
APRIL 20, AUG 24
W
MAR 21, SEPT 23
FEB 20, OCT 23
JAN 21, NOV 23
DEC 22
LAB
BLUE
RED
JUNE 22
JULY 23, MAY 21
AUG 24, APRIL 20
SEPT 23, MAR 21
E
OCT 23, FEB 20
NOV 23, JAN 21
DEC 22
207°
S

Figure 3. Orientation of UNC outdoor smog chamber with respect to seasonal sunrise and sunset positions.

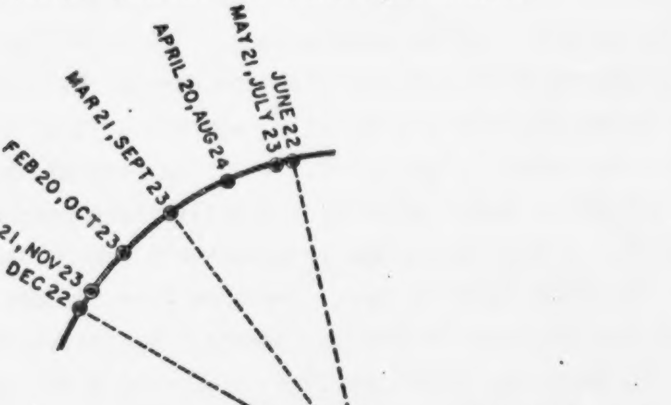
JUNE 22
MAY 21, JULY 23
APRIL 20, AUG 24
MAR 21, SEPT 23
FEB 20, OCT 23
JAN 21, NOV 23
DEC 22
Outdoor Dual Smog Chamber
S

Figure 4. Solar altitude and zenith angle at noon at the UNC outdoor smog chamber for each month.

Inside each chamber half are two mixing fans located in opposite corners. These provide circulation and mixing of the chamber contents. The fans are 50.8 cm diameter cast aluminum units that are FEP Teflon coated. They operate in a horizontal position, 0.76 m above the floor on 2.54 cm diameter Teflon coated steel shafts that extend through the chamber floor. Under the floor, 1/4 horsepower, 1750 rpm motors provide power through a belt and pulley system to each fan. Each fan operates at approximately 31.15 m^3/min.

Laboratory. The laboratory is adjacent to the chamber. It is a 3.66 m W x 15.24 m L x 3.05 m H wooden structure oriented perpendicular to the chamber and 3.66 m away from it to avoid any shadowing. The first 5.49 m nearest the chamber contain the instrumentation, manifolds, and calibration systems. The next 5.49 m contain the data acquisition computer system and the operations area. The last 4.27 m of the laboratory is a utility area with running water and storage facilities. Gas tanks necessary to operate the instruments and perform calibration are located in a 1.22 m x 1.83 m room completely closed-off from, but attached to the laboratory. The injection system gas tanks and valves are housed in a second 1.52 m x 1.52 m well-insulated, heated room adjacent to the end of the laboratory nearest the chamber.

Injection System. Pollutants are injected into the chamber sides via the return side of the sampling manifolds. The return manifolds enter the chamber sides under one of the mixing fans. The injection process uses gas cylinders containing pollutants at high concentrations (1000-10,000 ppm range), two stage, stainless steel diaphragm regulators, on-off solenoid valves, and a precision needle valve. The flow rate of injected material into the manifolds is established by a 5 millisecond response time mass flow meter. The total injection volume is accurately controlled as a function of the time the solenoid valve is open. The open time of each solenoid valve is controlled by the computer system on command. Conditions can be varied sufficiently to have the injection time range from a few seconds for each component to 1-2 hours for a programmed injection used to simulate the buildup of pollutants in urban areas.

Data Acquisition System. A computer based data acquisition and control system (DAS) is used to acquire, process, and record data for the chamber instrument system. The complete system is shown schematically in Figure 5.

Output signals from each instrument are wired to a crossbar scanner (or analog signal multiplexer). Under control of programs in the computer, the scanner connects the selected signal leads to the input of the digital voltmeter. The digital voltmeter, which has excellent noise and spurious signal suppression and can measure a 1 volt signal with a resolution of 10 microvolts, is triggered to acquire a reading and to supply the binary coded decimal, 5-1/2 digit number to the computer. The computer proccesses the information and then commands the scanner to move to the next channel and repeat the process. The data processing will be described in a later chapter. The timing of the computer processes is under the control of a digital date and time-of-day clock which signals event times to the computer. Another digital timer operates Teflon solenoid valves on the inlet of each instrument to connect the instruments to one chamber half during a given cycle of data acquisition.

This system provides fully automatic acquisitions and processing of data during a run and provides the operator with immediate, full data in physical units. Given this information about what is happening, the operator can then concentrate on what he wants to do. It also allows the massive amount of information generated during a run to be processed in a more effectual manner after the run is over.

Experimental Method and Procedures

Instrumentation. The instruments are located in a temperature-controlled laboratory adjacent to the chamber. Gas instruments include equipment for measuring alkanes, alkenes, aromatics, aldehydes, phenols, nitric oxide, nitrogen dioxide, ozone, PAN, HNO_3, alkyl nitrates, H_2O_2, total hydrocarbons (THC), methane, and CO. Standard meteorological instruments are used to measure solar radiation, ultra-violet radiation, air temperature, and dew point. A Perkin Elmer Sigma 10 processor-based charomatograph integration system is used to acquire data and control the gas chromatographic (GC) methods. Table 1 lists the instrument models and their characteristics.

At the sample inlet of each gas instrument is a three way Teflon ac solenoid valve. Since there are two intake manifolds (one for each chamber half), air from either manifold can be drawn through the three-way valve and into the instrument. In this manner timesharing of one instrument between the two chamber halves is possible.

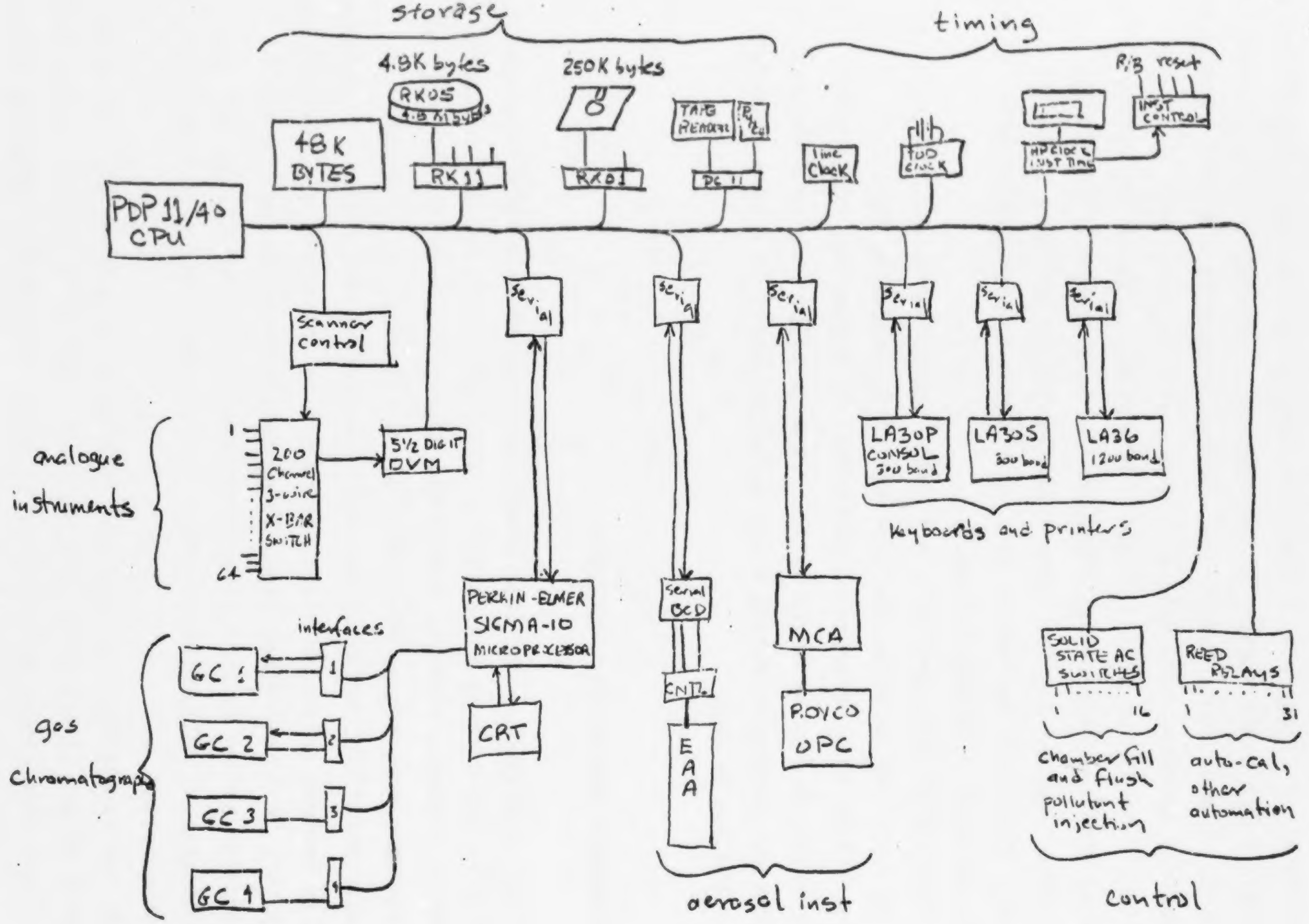
storase
4.8K bytes
RK05
4.8 M bytes
250K bytes
TAPE Reader
PDP 11/40 CPU
48K BYTES
RK11
RX01
PC 11
timing
line Clock
TOD Clock
HP Clock Inst Time
INST CONTROL
R,B reset
Scanner control
Serial
5 1/2 DIGIT DVM
analogue instruments
1
200 Channel 3-wire X-BAR SWITCH
64
LA30P CONSOL 300 baud
LA30S 300 baud
LA36 1200 baud
keyboards and printers
PERKIN-ELMER SIGMA-10 MICROPROCESSOR
CRT
interfaces
1
2
3
4
GC 1
GC 2
GC 3
GC 4
gas chromatographs
Serial BCD
CNTL
E A A
MCA
ROYCO OPC
aerosol inst
SOLID STATE AC SWITCHES
1
16
chamber fill and flush pollutant injection
REED RELAYS
1
31
auto-cal, other automation
control

Figure 5. Data Acquisition and Control System

Standard Operating Procedure. Most experiments are initiated early in the morning by the site computer which has been programmed the night before to carry out a detailed set of commands. Prior to an experimental run, the chamber is automatically purged overnight with background ambient air. Several hours before dawn the DAS begins recording measurements of the background concentration. Single instruments are timeshared on an alternating four minute cycle between the two sides. The chamber intake and exhaust doors are sealed and the initial concentrations of reactants of interest are injected before sunrise. The computer selects the proper tank and calculates the correct time to achieve the desired initial concentrations. Injections are normally short "slug" injections; most experiments have initial hydrocarbon, NO, and NO_2. Monitoring of the chemical and physical species mentioned earlier continues usually until 1800 EDT when the experiment is terminated. The computer then performs several close-down procedures: turning off certain instruments, opening chamber vent doors, and turning on the exhaust fan to purge the chamber. Instructions for another experiment can then be programmed.

Variations of the standard operating procedures include: 1) changing humidity before the experiment, 2) injecting pollutants slowly during the experiment, 3) diluting the chamber(s) during the experiment to simulate mixing height profiles, 4) transfer of contents of one chamber side to the other, and injecting initial conditions into the chamber containing part or all of the product of a day-old experiment. Most pollutants are injected from high concentration gas cylinders (10,000 ppm) which can be controlled by the computer. Some pollutants are liquids with vapor pressure too low to have high vapor concentration (cylinder) prepared. These are injected manually. Carefully measured samples are heated in a U-tube in which warm zero air is passed through to the return manifold. Automated liquid injectors will be installed soon.

DATA TREATMENT PROCEDURES

General. Figure 8 is the flowchart of the processes used to treat the data collected. The processes are divided into those that occur during a run, those performed immediately after a run, and those that are done later. The operations are carried out on three different computers, and the Broomall plotter. The PDP 11/40 is at the computer site and is responsible for

Table 1. Instrument Characteristics

Substance	Method	Manufac. & Model	MDC	Range	Mode	Time Shared
O_3	Chemiluminescence	Bendix 8002	0.001	0-2	Continuous	Yes
NO, NO_x, NO_2	Chemiluminescence	Bendix 8101-B	0.005	0-1	Cyclic-30 sec each	Yes
HC's alkenes alkanes aromatics	GC-FI Automated, programmable, Multiple column	Carle 211	0.005-0.010	0-100	Cyclic 15 or 30 min	Yes
THC CO CH_4	GC-FI Automated Multiple column	Beckman 6800	0.010	0-30	Cyclic 5 min or 15 min	Yes
HCHO	Automated Colorimetric (reverse West-Gaeke)	CEA 555	0.01	0-2	Continuous	Yes
Acetaldehyde Propionaldehyde MEK	GC-FI	Carle 211M	0.02-0.05 0.1 0.07	0-100	Cyclic 30 min	Yes
Aromatics HC aromatic aldehydes phenols	GC-FI	Perkin Elmer 900	~0.010	0-100	Manual	Yes
PAN	GC-EC	Analog Tech. Corp. 140 A EC Var. Freq. pulsed bias detector	0.0004	0-1	Cyclic	Yes
Alkyl nitrates	GC-EC	Varian Aerograph DC biased EC Model 940	0.0003-0.0008	0-1	Cyclic	Yes
HNO_3	Chemiluminescence Molybdenum converter Nylon scrubber	Bendix 8101-B TECO Molybdenum Converter	0.003	0-1	Cyclic 15 min	No
H_2O_2	Bubbler-Man Automated Chemilum. analysis		0.0001	0-1	Manual	Yes
Temp	Thermistor	YSI	0.2 F	20-110°F	Continuous	No
TSR	Pyranometer	Eppley Black & White	7.5 mv/cal/cm^2-min	0-2 cal/cm^2-min	Continuous	NO
UV	Pyranometer	Eppley UV	0.2 mv/cal/cm^2-min	0-0.1 cal/cm^2-min	Continuous	No
Dew Point	Cooled mirror & conductivity	EG&G 880 Gen. Eastern 600	0.1°F	-40°F-120°F	Continuous	Yes

```
 RUN DX1:DATRAN
SPECIFY OPTIONS DESIRED (AS option,option,option <CR>):   GAS
INJECTION TANK VALUES AS OF: 27-SEP-79
GAS     CONC(PPMC)   FLOW(L/MIN)
NO        10700.          6.
NO2       20500.         10.
PROPYL    21396.         10.
UNCMIX    10471.         10.
ETHYL1     2028.         10.
N2      1000000.         10.
AUTOMX    10487.         10.
ACETAL     4110.         10.
BUTAN1    92400.         10.
BUTPPL    11456.         10.
CO       100000.         10.
PROPAN    22068.         10.
ETHYL2    20663.         10.
BUTAN2    20760.         10.
SOURCE FILE NAME?   FEB1
DATE OF RUN (AS dd-MMM-yy):   1-FEB-80
ERRORS ARE FLAGGED BY [NN]

 [THIS IS AN ACTUAL EXAMPLE RUN]
 IMMED VENT; CLR CHARTS;
 AT 3:30 SET CHARTS; OSC 35 ON 45 SEC EVERY 15 MIN; [CO]
 AT 3:50 CLOSE;
 AT 3:59 SET 6; [CARLE 1 AND 2]
 AT 4:00 UNTIL 19:20 START DVM;
 AT 5:00 INJECT NO 13 TO 400 PPBC IN BOTH PURGE;
 AT 5:10 INJECT UNCMIX 10 TO 4 PPMC IN BOTH PURGE;
                                                ^
    [ 1]         WARNING- INJECTION TOO LONG, BEING SPLIT
    [ 2]         WARNING- INJECTION TOO LONG, BEING SPLIT

 AT 5:30 INJECT NO2 12 TO 100 PPBC IN BOTH PURGE;
 AT 19:20 VENT; HALT;
 RSTART 0:00 VENT; CLR CHARTS;
 RSTART 3:30 SET CHARTS; CLOSE;
 RSTART 3:30 MOD 1 OSC 35 ON 45 SEC EVERY 15 MIN;
 RSTART 4:00 START DVM;
 !
```

Figure 6. Sample Command File

acquiring the data. Shown in Figure 5 is the configuration of the control and data acquisition system, which was described earlier. The PDP 11/03, the IBM 370/360 and the Broomall plotter are on campus grounds, and complete the data treatment procedure.

During Run. DATCOL and DATRAN are written in assembly language and PASCAL. DATCOL performs several functions, such as accepting instructions from the keyboard and interpreting a command file (optional) which prepares the chamber, makes injections, turns on the necessary instruments, and finally purges the chamber and turns off the instrumentation at the end of the experiment. Command files can be written in an English text (easily readable) style. An example is shown in Figure 6. A program DATRAN translates this file into a file which DATCOL can interpret (Figure 7). DATCOL also controls the data acquisition process, and records:

1) the instrument analog outputs;
2) the GC files produced by the Perkin Elmer Sigma 10 GC integrator and processor;
3) the adjustment file (computer readable instructions for data adjustment); and
4) the comments files, all on the RK05 hard disk.

It also maintains status information to restart and continue an experiment after a power failure.

The operator has a choice with DATCOL, of either 1) having the data printed during the whole experiment; 2) printing data for only select times during the experiment; 3) having earlier data printed; or 4) not printing data at all.

The operator can also, at any time during the experiment, enter through the keyboard information such as calibration corrections for any instrument or that an instrument is not functional and for what time interval this information applies. This type of information is entered by DATCOL into an Adjustment file. This file can be read and interpreted by other computers and can be directly applied to correcting and processing data later. The operator can at any time also enter general comments through the keyboard which DATCOL stores in a comment file. Such information when transferred along with the digital data greatly aids in processing.

Strip charts are operated for almost every instrument as a back-up to the computer.

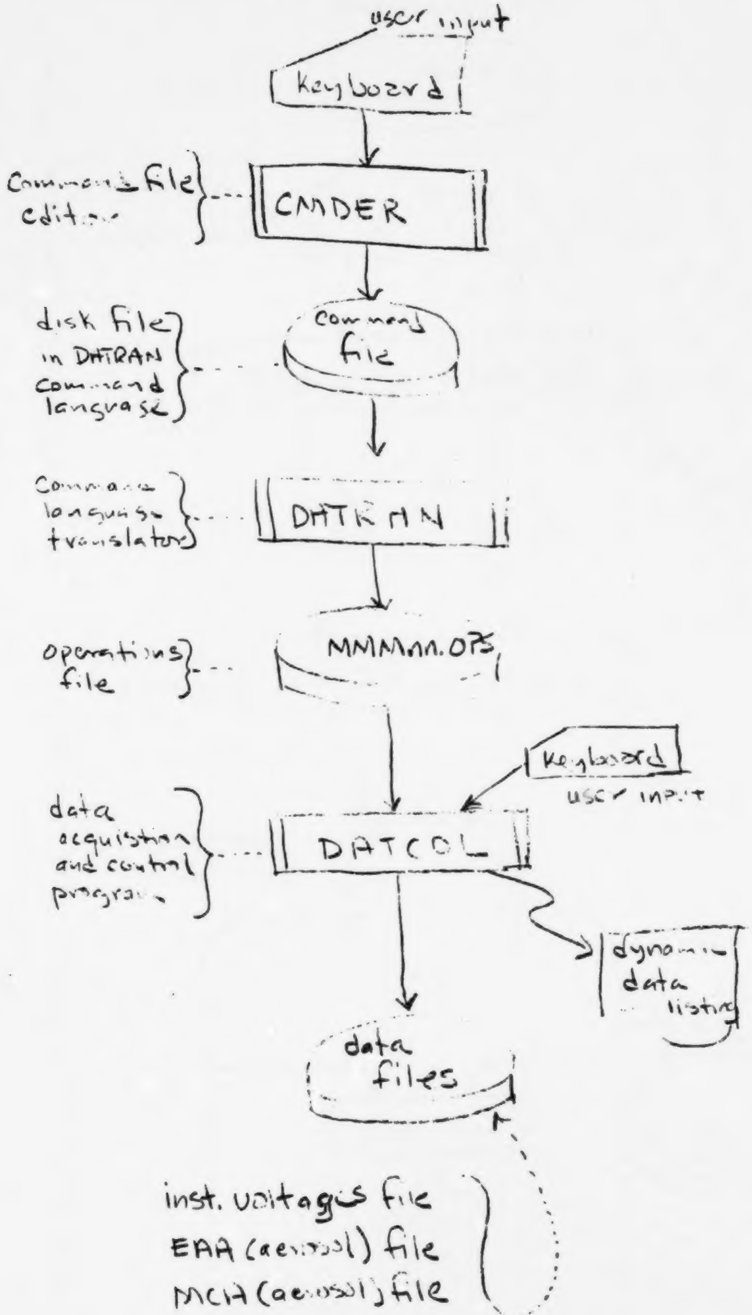
user input
keyboard
Command file editing
CMDER
command file
disk file in DATRAN command language
Command language translator
DATRAN
MMMnn.OPS
operations file
keyboard
user input
data acquistion and control program
DATCOL
dynamic data listing
data files
inst. voltages file
EAA (aerosol) file
MCA (aerosol) file
GC processed file
Remarks file
Adjustments file
command file

Figure 7. Data Acquisition Process

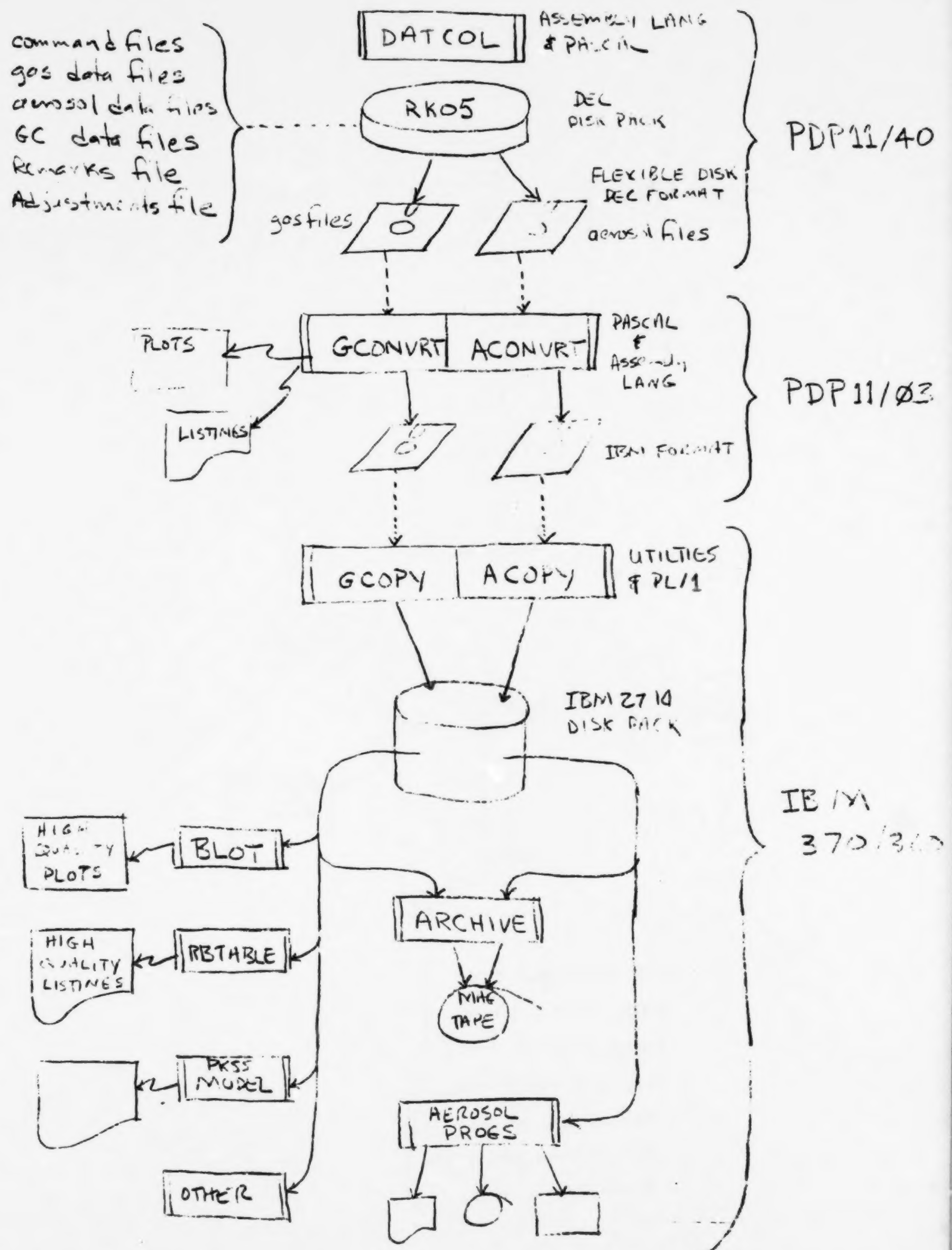
command files
gos data files
aerosol data files
GC data files
Remarks file
Adjustments file
DATCOL
ASSEMBLY LANG
& PASCAL
RK05
DEC
DISK PACK
PDP11/40
FLEXIBLE DISK
DEC FORMAT
gos files
aerosol files
PLOTS
GCONVRT
ACONVRT
PASCAL
&
Assembly
LANG
PDP11/03
LISTINGS
IBM FORMAT
GCOPY
ACOPY
UTILTIES
& PL/1
IBM 2714
DISK PACK
IBM
370/3
HIGH
QUALITY
PLOTS
BLOT
ARCHIVE
HIGH
QUALITY
LISTINGS
RBTABLE
MAG
TAPE
PKSS
MODEL
AEROSOL
PROGS
OTHER

Figure 8. Data Treatment Process

APPENDIX B

DESCRIPTION OF MEASUREMENT TECHNIQUES IMPLEMENTED DURING THIS PROJECT

AUTOMATIC C_1-C_{10} CHROMATOGRAPH

It has been previously documented that the reference method for the measurement of ambient nonmethane hydrocarbons does have certain operating difficulties and is limited in its use as a research tool. For these reasons an automatic gas chromatograph was developed to perform routine analysis of selected C_1-C_8 hydrocarbons. The design criteria were the following:

1. perform automatic injection, separation, and analysis of C_1-C_8 compounds in less than 30 minutes
2. require no preconcentration of the air sample and operate isothermally
3. have a sensitivity of 10 ppbC for each species on the chromatograph

The instrument was built using a Carle Model 211 Chromatograph and flame ionization detector (FID). An automatic six-port sample valve and two six-port automatic switching valves shunt the sample to the appropriate column. These valves are activated by a 30 minute programmable valve controller. Three chromatographic columns perform the analytical separation. An additional 2' x 1/8" column of carbowax 400 was installed just before the flame detector to give column bleed balance and prevent excess baseline displacement after valve switches.

The columns are:

Column No. 1	6' x 1/8" Carbowax 1540 + 5 % Apeizon L on Supelcoport 80/100 mesh support	separates C_6-C_8 paraffins, olefins and aromatics

Column No. 2	6' x 1/8" N-octane/Poracil C 100/120 mesh (baked at 240^{o}C for 2 hrs.) + 2' x 1/8" 20% Apeizon L on Supelcoport 80/100 mesh	separates C_4 & C_5 olefins and some C_6 paraffins
Column No. 3	2' x 1/8" FL alumina treated with 5% NaCl	separates C_1-C_3

The column configurations for each valve position are shown in Figure 1. The indicated restrictors are adjustable S.S. 1/16" Nupro needle valves and are used to match the pressure drop across various columns as these columns are switched in and out of the flow circuit. Automatic injection is made with all three columns in series. One and one half minutes are required for the individual compounds to become distributed into the proper columns. Since column 1 is the first to be encountered, C_6-C_8 are retained, while C_1-C_5 pass on to column 2. Methane is the only compound which actually moves to column 3 during this time. After this first 1.5 minutes with the columns in series, a valve switch removes column 2 and 3 from the flow path and permits the compounds in column 1 to elute into the FID. The system remains in this configuration for 5.5 minutes so that C_6-C_{10} paraffins and toluene can be measured. We can also extend this time to 14 minutes to pick up α-pinene or xylenes. A second valve switch then briefly (1 minute) places columns 1, 2, and 3 back in series so that methane and ethylene can be detected. During this period, propane and propylene move from column 2 to column 3 but do not elute before the third valve switch. This switch removes column 3 and leaves columns 1 and 2 in series with the detector. Butenes, pentanes and pentenes then elute from column 2. Finally with only 2.5 minutes remaining in the 15 minute cycle, the columns are placed back in series so that propane, propylene and acetylene can be measured. Chromatograms of the UNC mix are shown in Figure 2.

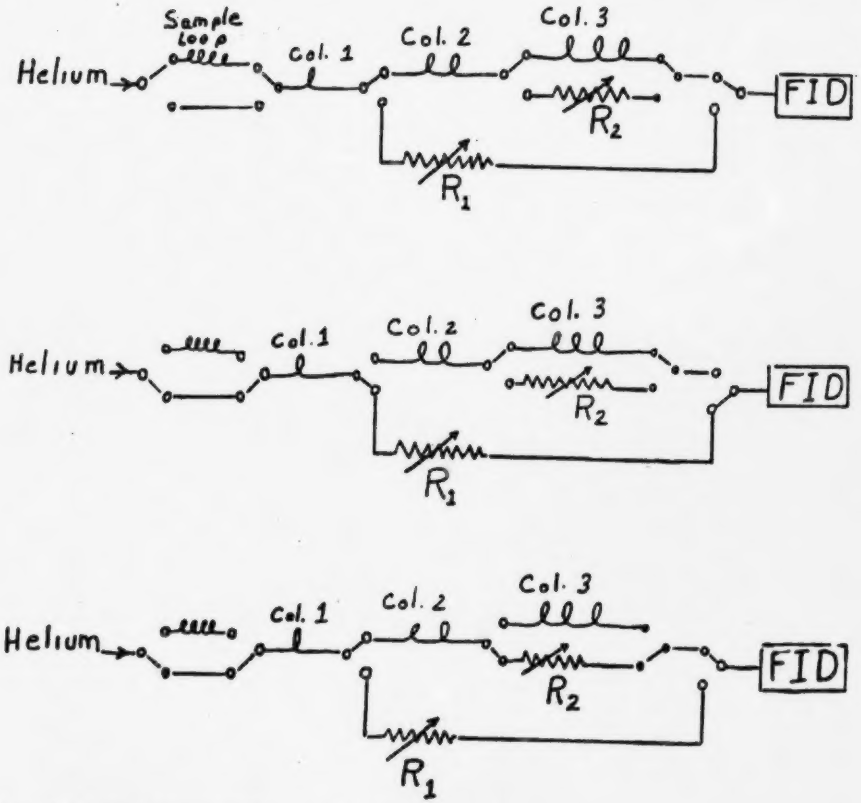
INJECT

Col 1,2,3,
in Series

First Valve Switch
Col. 1 in Series
with FID

Third Valve Switch
Col. 1 & 2 in Series

Helium
Sample loop
Col. 1
Col. 2
Col. 3
R₂
R₁
FID
Helium
Col. 1
Col. 2
Col. 3
R₂
R₁
FID
Helium
Col. 1
Col. 2
Col. 3
R₂
R₁
FID

Figure 1. Column and Valve Configurations for C_1-C_{10} Automatic Carle Chromatograph.

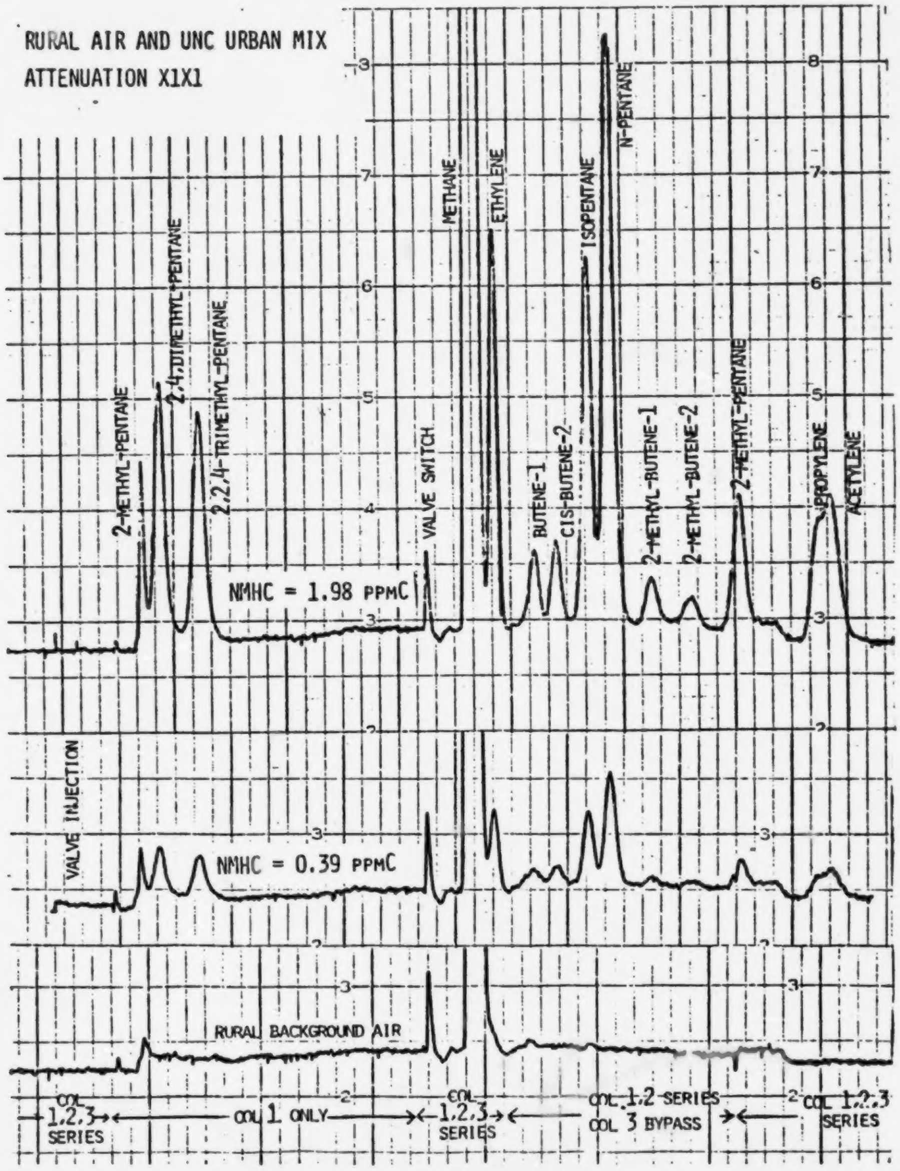

Figure 2. Chromatogram of UNC urban type hydrocarbon mixture on Carle 211 chromatograph.

The system described has been in continuous operation at the University of North Carolina Smog Chamber Facility for more than 5 years. The operating sensitivity can be as low as 7 to 15 ppbC (at a signal to noise ratio of 2) on the most sensitive scale. This is based on the known distribution of hydrocarbon species in the UNC atmospheric urban mix and individual calibrations of typical compounds (Figure 3). To obtain this sensitivity, a 5 cc gas sample loop was substituted for the original 2 cc loop. In doing this, however, the separation of acetylene from propylene and ethylene from ethane was reduced. Routine calibration of the instrument is usually performed the day before and during the day of the smog chamber run. We have estimated that the accuracy of this method for most hydrocarbons is between 5 and 10%.

The versatility of the system permits us to automatically run systems with, for example, propylene and butane on one day, mix vs. ethylene and toluene on the second and isoprene and α-pinene on the third without any changes in the instrument operating conditions. Critical operating conditions are given below:

Carle Model 211 Analytical GC
Detector - FID sensitivity 0.016 coulombs/gram carbon
detectability minimum 2.5 x 10^{-12} g/sec
Electrometer sensitivity - 1 x 10^{-12} amps
Sample valve - 6 port, 5 groove, mini volume Carle valve
Series-bypass valves - 6 port, 2 groove, mini volume Carle valve
Carle Model 100 valve minder
Valve actuators - automatic bidirectional Carle valve actuator motors
He flow = 33 cc/min
H_2 flow = 40 cc/min
Air flow = 350 cc/min
Oven = 64°C thermal

CONCENTRATIONS OF INDIVIDUAL SPECIES IN
0.39 PPMC NMHC UNC MIX

	COMPOUND	CONCENTRATION (PPMC)
1	2-METHYLPENTENE	0.035
2	2,4-DIMETHYLPENTENE	0.039
3	2,2,4-TRIMETHYLPENTANE	0.040
4	ETHYLENE	0.042
5	BUTENE-1	0.010
6	BUTENE-2	0.013
7	ISOPENTANE	0.053
8	N-PENTANE	0.092
9	2-METHYLBUTENE-1	0.008
10	2-METHYLBUTENE-2	0.007
11	PROPYLENE/ACETYLENE	0.047

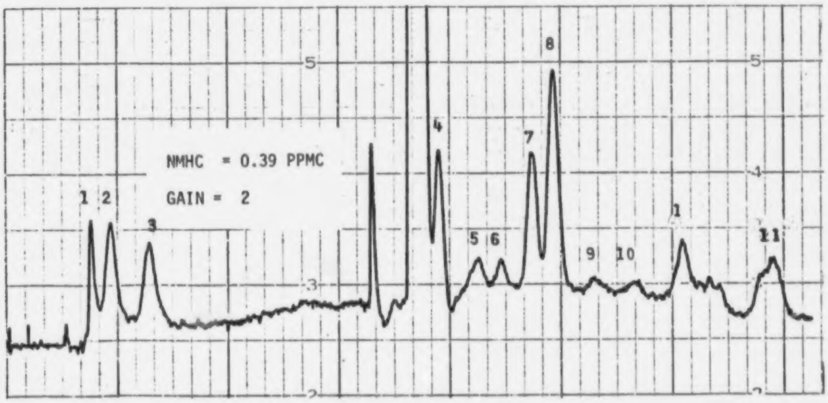

Figure 3. Maximum Sensitivity of Carle Chromatograph on Attenuation of x1 and gain of 2.

AUTOMATED FORMALDEHYDE-ACETALDEHYDE CHROMATOGRAPH

In 1976 an automated gas chromatographic system to measure formaldehyde and acetaldehyde was built by Carle Instruments for UNC. This instrument automatically injected a 2 cc air sample onto an 11', 1/8" S.S. Porapak Q precolumn (isothermal oven at 73°F). Light hydrocarbons pass directly through to the flame detector, while formaldehyde, propylene, methanol and acetaldehyde are retained. As soon as the light hydrocarbons are passed, the precolumn is placed in series with a 2', 1/8" S.S. Porapak Q analytical column. The contents of the second Porapak column flow directly into a 400°F Ni catalyst methanizer before they reach the detector. In the methanizer, formaldehyde is converted to methane and measured as methane in the flame detector. Thirty minutes are required for an analysis. We have encountered some background interference in the region of the chromatogram where formaldehyde is eluted and currently this defines the lower limit of detectability for the formaldehyde.

Column Modifications

Various means were used to reduce the water ghost peak interference on Porapak Q. This peak most probably results from a displacement of impurities in the Porapak Q by water in the air sample. We observed a strong reduction in the interference when dry formaldehyde air samples were used. As vapor phase water was added back in, the interference would grow. After long periods of purging at high temperatures we were able to maintain a column which did exhibit reasonable separation between the ghost and formaldehyde peaks (Figure 4). The instrument was operated in this fashion from May-December 1977 with almost no maintenance. Impurities in a helium carrier tank installed in January 1978 resulted in deterioration of the analytical 11' x 1/8" S.S. Porapak Q precolumn. Attempts to use glass or Ni alloy columns with Porapak QS have met with marginal success; the instrument was used during 1978 with a significant loss in sensitivity.

In 1979 an inert solid support (Teflon 6) with a partition liquid phase (5% Carbowax 20 M plus 5% Triton 305) was used in a 12' x 1/8" glass column. This column would separate formaldehyde but we found significant memory problems with this system and have used it primarily to measure C_2-C_5 carbonyls.

FORMALDEHYDE DETECTION BY AUTOMATED COLORIMETRY

In June of 1979 UNC purchased an automated colorimetric formaldehyde system from CEA Corporation (Westwood, NJ). This sytem employs the reverse West and Gaeke technique and hence requires a constant supply of wet chemicals. Highly purified pararosanaline is essential (we have purchased it directly from CEA). The other compounds, mercuric chloride, sodium chloride, and sodium sulfite, need to be reagent grade. A flow diagram of the system is shown in Figure 5.

Liquid standards can be prepared from 37% formalin solution and diluted in the same sodium tetra mecurate (TMC) used in the instrument. These are then added directly through the TMC feed tube. A dynamically generated HCHO airstream using a formaldehyde permeation tube (Metronics

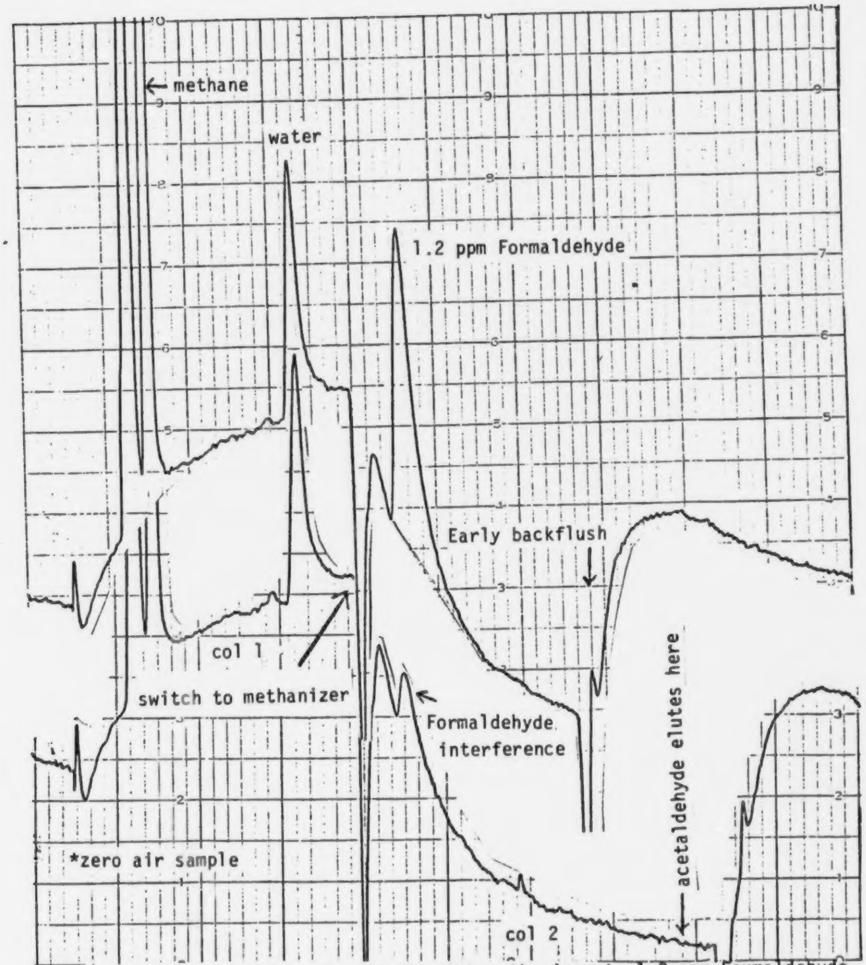

Figure 4. Response of Carle 211 GC with methanizer to 1.2 ppm Formaldehyde and zero air with 1.5 ppm methane. oven=73°C,He=67 cc/min, H_2= 80 cc/min, recorder 1 mV fs, atten.=x1, range=x1 col 1=11 ft, 1/8" ss porpack Q, 40:60 mesh, col 2=2 ft, 1/8" porpack Q, 40:60 mesh.

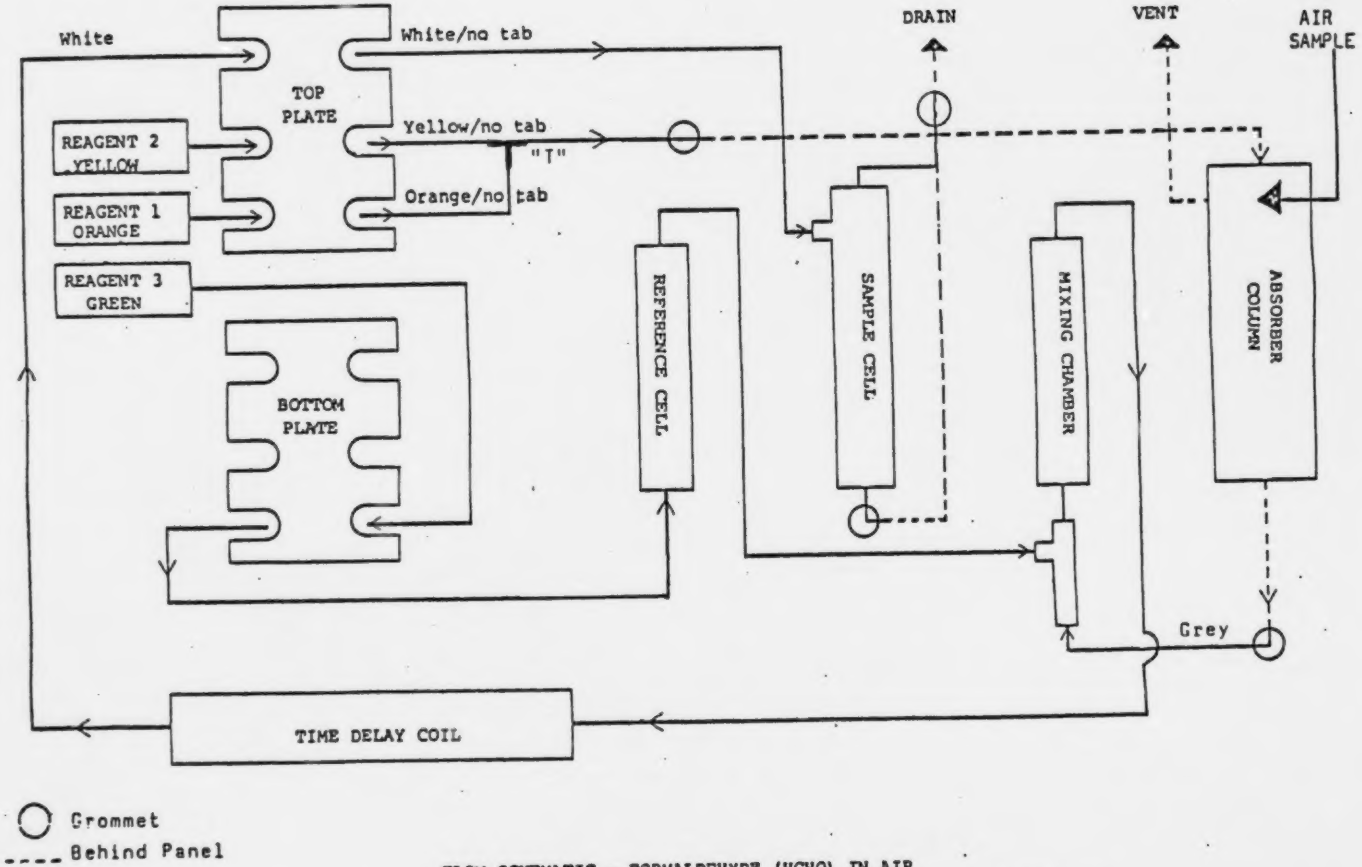
White
White/no tab
TOP PLATE
REAGENT 2 YELLOW
Yellow/no tab
"T"
REAGENT 1 ORANGE
Orange/no tab
REAGENT 3 GREEN
BOTTOM PLATE
REFERENCE CELL
SAMPLE CELL
MIXING CHAMBER
ABSORBER COLUMN
DRAIN
VENT
AIR SAMPLE
Grey
TIME DELAY COIL
Grommet
Behind Panel

FLOW SCHEMATIC - FORMALDEHYDE (HCHO) IN AIR

Figure 5. Solution flow diagram for CEA automated formaldehyde instrument.

Corporation, Santa Clara, California) was used to supply known levels of gas phase formaldehyde. In addition, calibration samples of formaldehyde were prepared in the chamber. The chamber is usually dried to a dew point of 60% and known quantities of solid paraformaldehyde are then injected.

During the 3 month 1979 data season we found this system to show less than a 10% change in response to known formaldehyde samples. Using the original solutions recommended by CEA we observed a 5% positive interference from acetaldehyde in the concentration range of 0.1-1 ppmV. In 1979 experiments where acetaldehyde was generated, the HCHO data were adjusted to subtract out the positive acetaldehyde interference. In 1980 CEA recommended a 6-fold reduction in the concentration of TMC and sulfite. In addition, sulfite and TMC were to be introduced separately instead of premixing these two solutions. This increased the lifetime of the TMC from 1 day to 2 weeks. Newly mixed sulfite solution and dilute pararosanaline are still required every 24 hours. The less concentrated reagents did not cause a loss in sensitivity of this sytem and minimized the acetaldehyde interference to 1%. We did however notice a deterioration in precision from calibration to calibration. This was especially true after new tubes were added to the peristaltic pump. Finally, the system that we have been using can exhibit a 30-50% zero drift over a 3-4 hour period. This drift does not affect the span response but requires frequent zero samples. Later, an auto zero valve was installed at the intake of our heated sample manifold. Examples of the system's response to 1.2 and 0.5 ppmC formaldehyde air samples are shown in Figure 6.

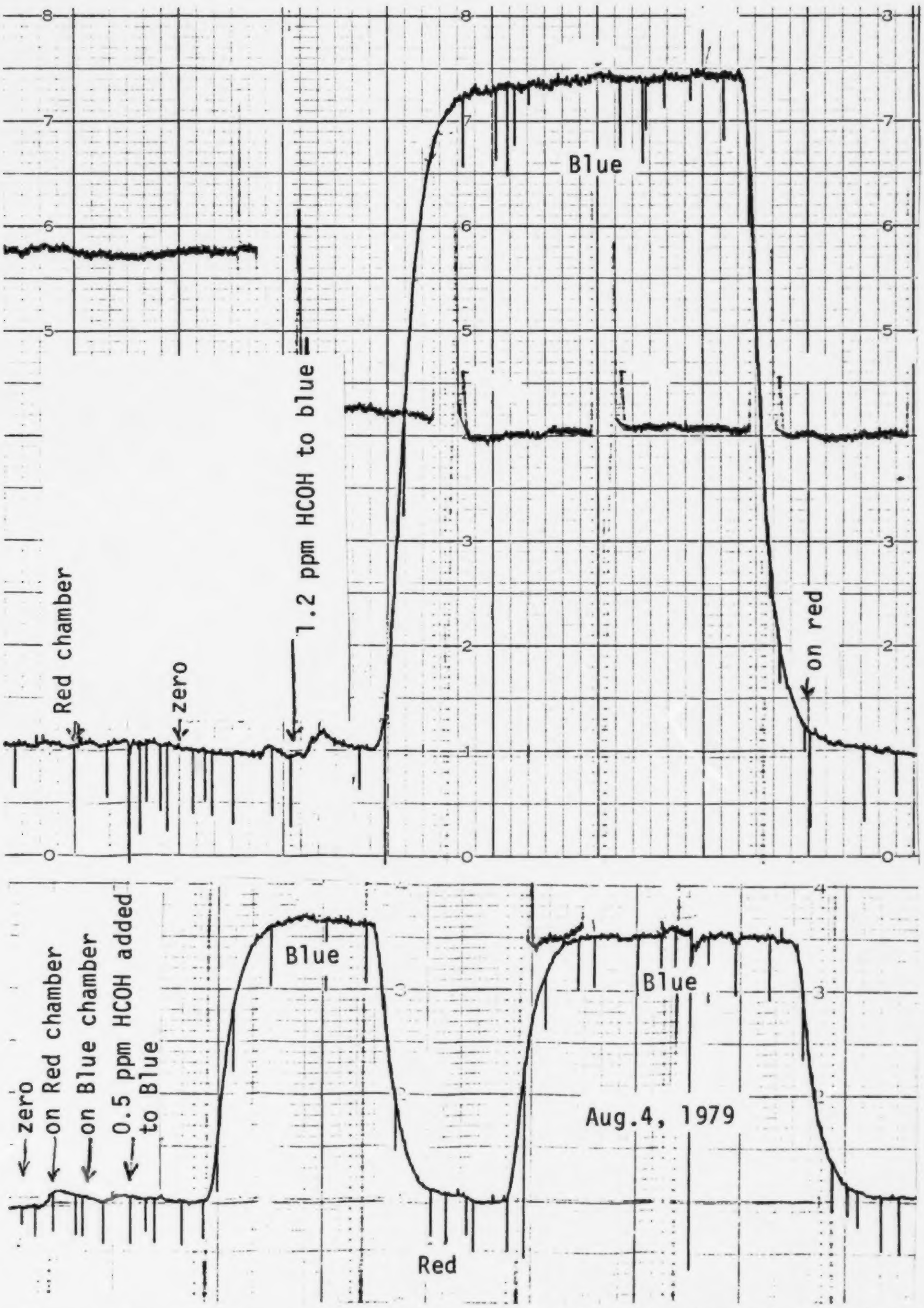

Figure 6. Response of CEA auto formaldehyde instrument to 0.5 and 1.2 ppm of HCOH injected in dry UNC chambers on August 4, 1979 and August 5, 1979.

DINITROPHENYLHYDRAZONE PROCEDURE FOR CARBONYL ANALYSIS

The analysis of C_1-C_8 carbonyl species in ambient air by reaction with 2,4 dinitrophenylhydrazone (DNPH) and subsequent reverse phase high pressure liquid chromatography of the hydrazone derivatives has been reported by Kuwata et al.[3] This procedure is fairly specific and can also be used to measure dicarbonyls. The reaction of DNPH with acetaldehyde is shown below.

$$>C=O \;+\; H_2N\text{-}NHDNP \;\xrightleftharpoons{H+}\; >C=NNHDNP \;+\; H_2O$$

Ambient aldehydes are usually sampled with an impinger arrangement into an absorbing reagent which contains acidified DNPH. Two extractions of the absorbing sample with chloroform, a wash with 2N HCl, and then distilled water, and finally sample concentration to a solid is required. Hull recently proposed a modified bubbler absorbing reagent so that direct HPLC analysis on the absorbing liquid is possible. The absorbing reagent is prepared by dissolving 0.25 g of purified DNPH in one liter of HPLC grade acetonitrile (ACN). This is followed by the addition of 0.2 ml

H_2SO_4. Two ml of absorbing reagent in a Mae West type bubbler and a sample flow rate of 0.5 l/min are recommended. In addition the impinger base is placed in ice to reduce ACN evaporation. Hull has indicated that excessive water in the air sample can reverse the equilibrium for ketones in the above noted hydrazine reaction and that condensed water in the asorbing reagent from ambient moisture should be limited to 50 µl/ml. Aldehydes are not affected by water. Outdoor chamber humidities can easily range between 20,000 and 30,000 ppm. This has limited us to a 2-4 liter air sample.

Analysis was performed on a Varian 5010 HPLC with a Varian micropak MCH-10 reverse phase, 30 cm, 9mm column and a fixed 254 nm detector. Initially the system was isocratically run at a 60:40 ACN:H_2O mixture and a solution flow of 1.6 ml/min. High concentration liquid standards in the gas phase equivalent range of 2-6 ppmV were prepared by direct dilution of 5 µl of authentic knowns into 100 ml of acetonitrile. Five to twenty µl of this solution were then added to 2 ml of DNPH absorbing reagent. The final DNPH samples were heated in 2 ml Supelco reaction vials at 80°C for 45 minutes. Comparisons with gas phase calibration samples are currently being made.

A sample chromatogram of a mixture of aldehydes, ketones and dicarbonyls is shown in Figure 7 . It has been observed that retention times on our system can vary significantly from day to day. It is therefore essential to run frequent calibration mixtures. Preliminary tests in our laboratory show that 45 minutes of heating is required to complete the derivation process for compounds that elute as late as biacetyl. Heating beyond this time did not increase chromatographic responses. C_1-C_3 carbonyls seem to require only 15 minutes. Liquid

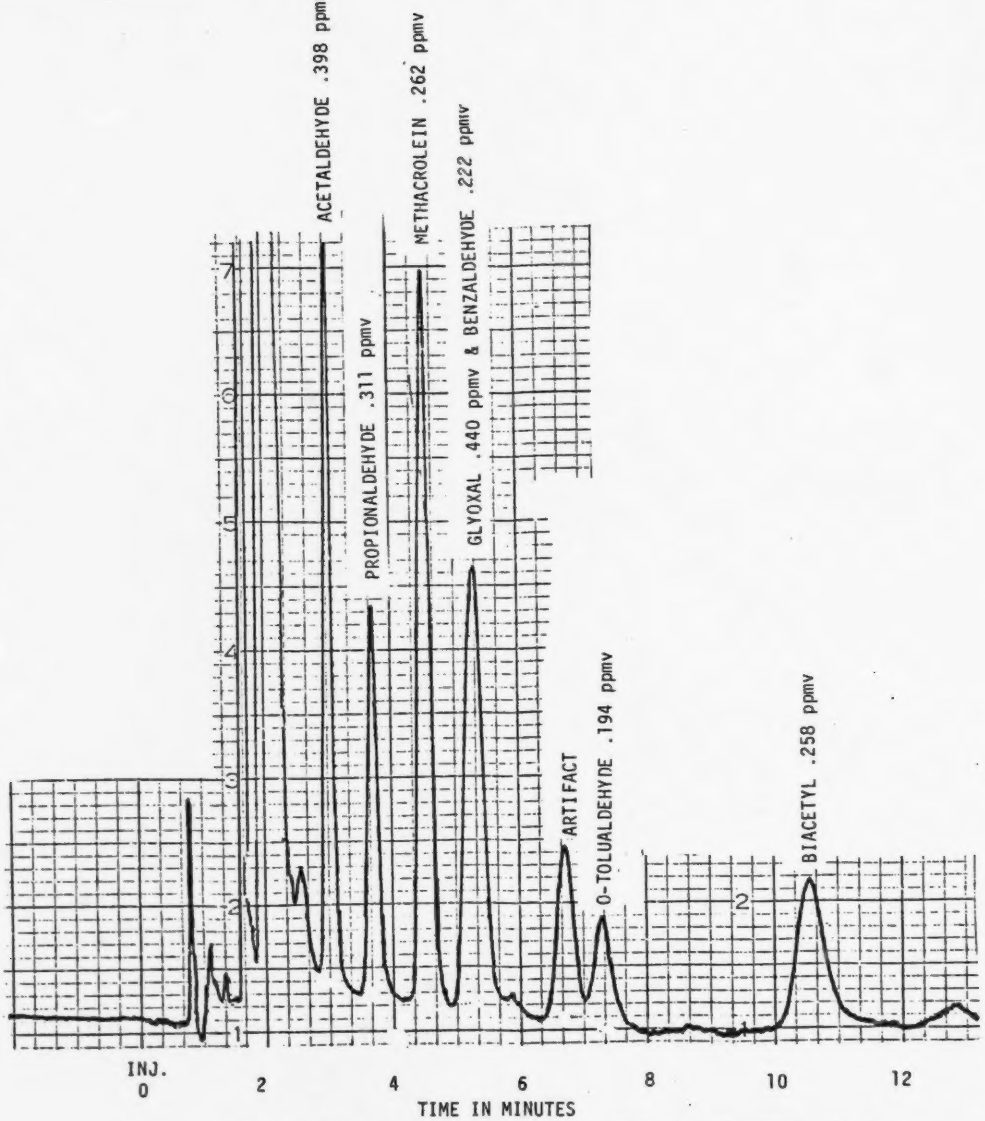

Figure 71. An example of the response of the HPLC with the DNPH method.

calibration samples which have been heated initially for 3 hours and then stored at room temperature appear to be stable with little deterioration for periods up to 1 month. Similar samples which are heated every three days were not as stable over the same time period.

Ambient bubbler samples should be stored at 50^0F or less until they are analyzed. The chromatograms from chamber samples which were stored at room temperature for 2 months exhibited many spurious peaks; quantification of compounds of interest was not possible. It is important that bubbler samples be analyzed as soon as possible.

Hull has suggested that a 360 nm detector be used to eliminate possible interferences of benzene and toluene in the C_1-C_3 aldehyde region. Although the absorption of benzene and toluene is 1/25 of the hydrazones at 254 nm, it is felt that further quantification of this potential interference is necessary.

In our system we have noticed an increased interference from the 2,4 dinitrophenylhydrazone peak into the formaldehyde-hydrazone elution region. We are not sure if this is due to a deterioration in the DNPH solution or the HPLC analytical column. When formaldehyde is of specific interest we have shifted to an isocratic 55:45 mixture of ACN:H_2O to provide better separation of the formaldehyde and DNPH isomers.

PAN ANALYSIS

PAN measurements reported during 1977-78 were made on a 1/8" x 36" glass column packed with 10% Carbowax 600 on Gas Chrom G (60-80 mesh) and detected with a Varian 940 electron capture detector. Both the column and the detector were held at room temperature, and 5% methane-argon was used as the carrier gas. The system was originally set up for UNC by EPA project officer Mr. Bruce Gay, Jr. Shortly after location at the UNC research facility a 6-port auto sample valve was installed so that unattended sample injection could be performed. With a standing current of 20x 10^{-9} amps we found good response linearly between 0.01 ppmV and 0.5 ppmV of PAN. Above 0.5 ppmV the signal became slightly nonlinear with concentration. In 1978 a pulse frequency electron capture detector was purchased from Analog Technology Corporation. This detector seemed to give a linear response over the range of 0.01 to 12 ppmV of PAN. The response of both of these systems to 0.12 ppmV of PAN is shown in Figure 8.

PAN CALIBRATION

From June 1977 to August 1978, high concentration PAN samples (2-17) ppm) in Teflon bags were generated and standardized at ETP-RTP in a 15 m pathlength IR spectrometer and then transported 25 miles in unairconditioned vehicles to the UNC smog chamber facility. These bags were then immediately diluted (0.1-0.5 ppm) and PAN response factors were established based on the original calibration and associated dilution. Generally there was a difference between the calibration values developed from the 1977 and 1978 PAN calibration bags. Decomposition during transportation, dilution problems, initial calibration by IR, and ambient column temperature fluctuations were among the possible causes for these differences.

From late November 1977 to July 1978, electron capture PAN data were usually 40-50% higher than the afternoon chemiluminescence NO_2 concentrations in propylene-NO_x smog systems that completely consumed

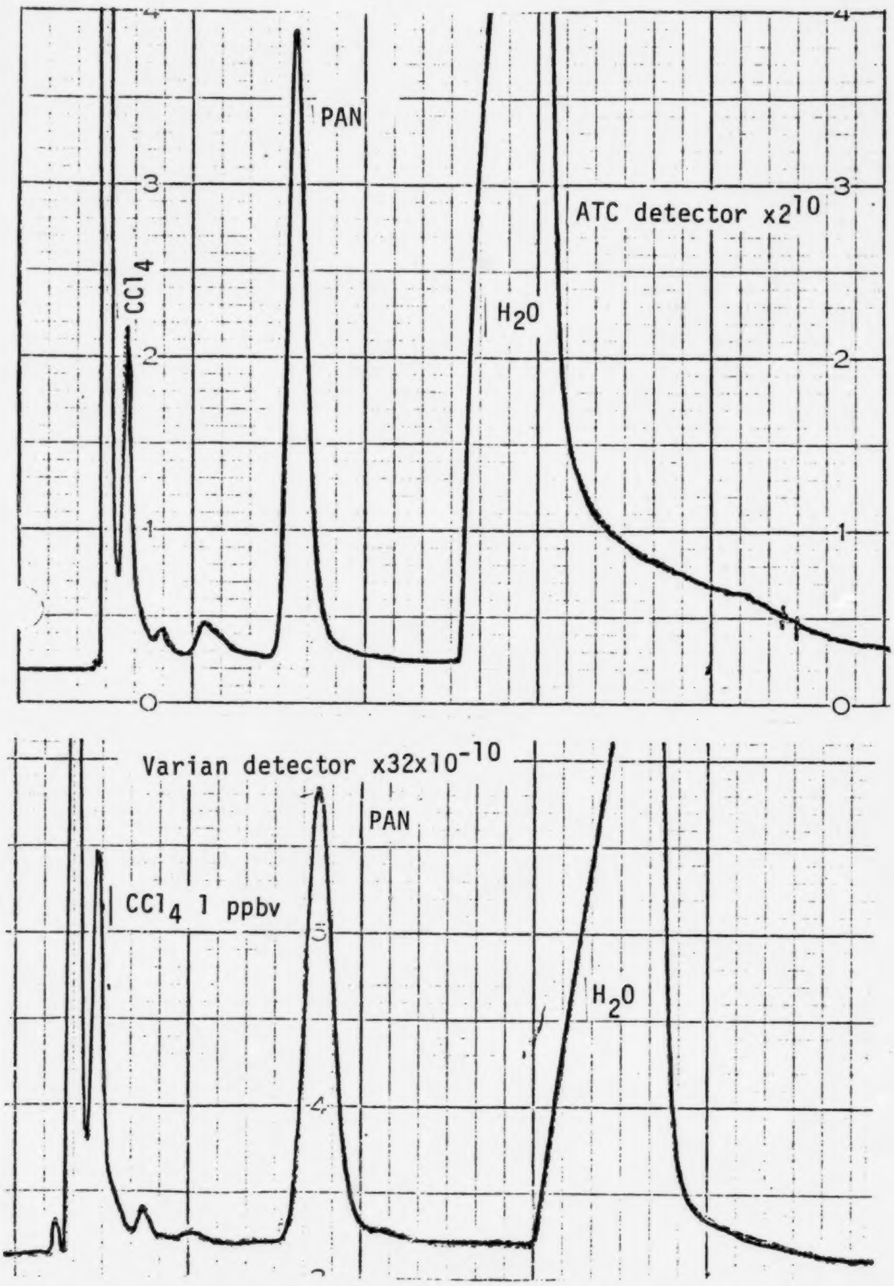

Figure 8. Response of two UNC electron capture dectectors to 0.12 ppmv PAN May 1978.

NO_2. August to mid-October 1978 electron capture PAN concentrations from similar type propylene-NO_2 systems were only 65-70% of the afternoon chemiluminescence NO_2. In these types of smog systems it has been clearly demonstrated that very low concentrations of NO and NO_2 are present in the afternoon; also the UNC NO_x meter has been tested for response to nitric acid and has exhibited none. Hence the rather large afternoon chemiluminescence NO_2 readings from these smog systems are considered to be almost entirely a "chemiluminescent PAN response".

By mid-October 1978, UNC implemented a wet chemical modified Saltzman procedure developed by Stephens and Price. The calibration values derived from this method gave PAN concentrations which were 0-30% lower than the "chemiluminescent PAN response". In 1979 high concentration pure PAN samples were prepared from an irradiated biacetyl-NO_2 bag system using a large preparation column and a liquid nitrogen freeze-out concentrator system. The diluted purified PAN was then measured with a calibrated EPA chemiluminescence NO_x analyzer and a calibrated PAN analyzer similar to the one used at UNC. Both EPA units gave the same concentration response. This PAN bag was then immediately transported to UNC in an air conditioned car and measured on the calibrated UNC chemiluminescence NO_x meter and UNC PAN monitor. The UNC NO_x meter gave the same reading as the EPA NO_x and PAN monitors. This strongly suggests that both the EPA and UNC NO_x monitors have a 100% response to PAN. Since that time UNC has generated high concentrations of PAN and purified the PAN by the EPA method described above. The pure PAN samples were standardized with the UNC chemiluminescence NO_x meter and this was used to calibrate the UNC PAN meter. Thus the 1979 UNC PAN concentrations have been directly linked or keyed to "chemiluminescence PAN readings. To make the 1977 and 1978 PAN data set consistent with the 1979 data set, 1977 and 1978 PAN values were compared with the many propylene-NO_x smog systems which had gone to completion and had given a stable afternoon "chemiluminescent PAN" concentration.

Ideally, we have found the best way to generate calibration samples of PAN is by the above cryogenic procedure. If this is not possible we would recommend that 4 ppmC + 0.5 ppm of propylene and NO_x (40% NO_2) be irradiated outdoors for 3-4 hours during the mid-morning and the early afternoon. With a calibrated chemiluminescent NO_x meter, follow the NO and NO_2 concentration beyond the NO_2 peak until NO_2 stabilizes. This system should generate from 0.15 to 0.25 ppmV of PAN.

ALKYLNITRATES

C_1-C_5 alkylnitrates can be detected on the same system that is used to measure PAN. Calibration samples (Figure 9) ethyl, isopropyl, propyl, and butylnitrates were performed by carefully injecting microliter volumes of the authentic samples into the outdoor chambers and applying the appropriate dilution and temperature factors. Calibration factors for compounds for which we did not have authentic samples (like sec-butylnitrate and isopentylnitrate) were estimated from the ECD response of n-butylnitrate. An uncertainty of $\pm$40% was then assigned to these compounds.

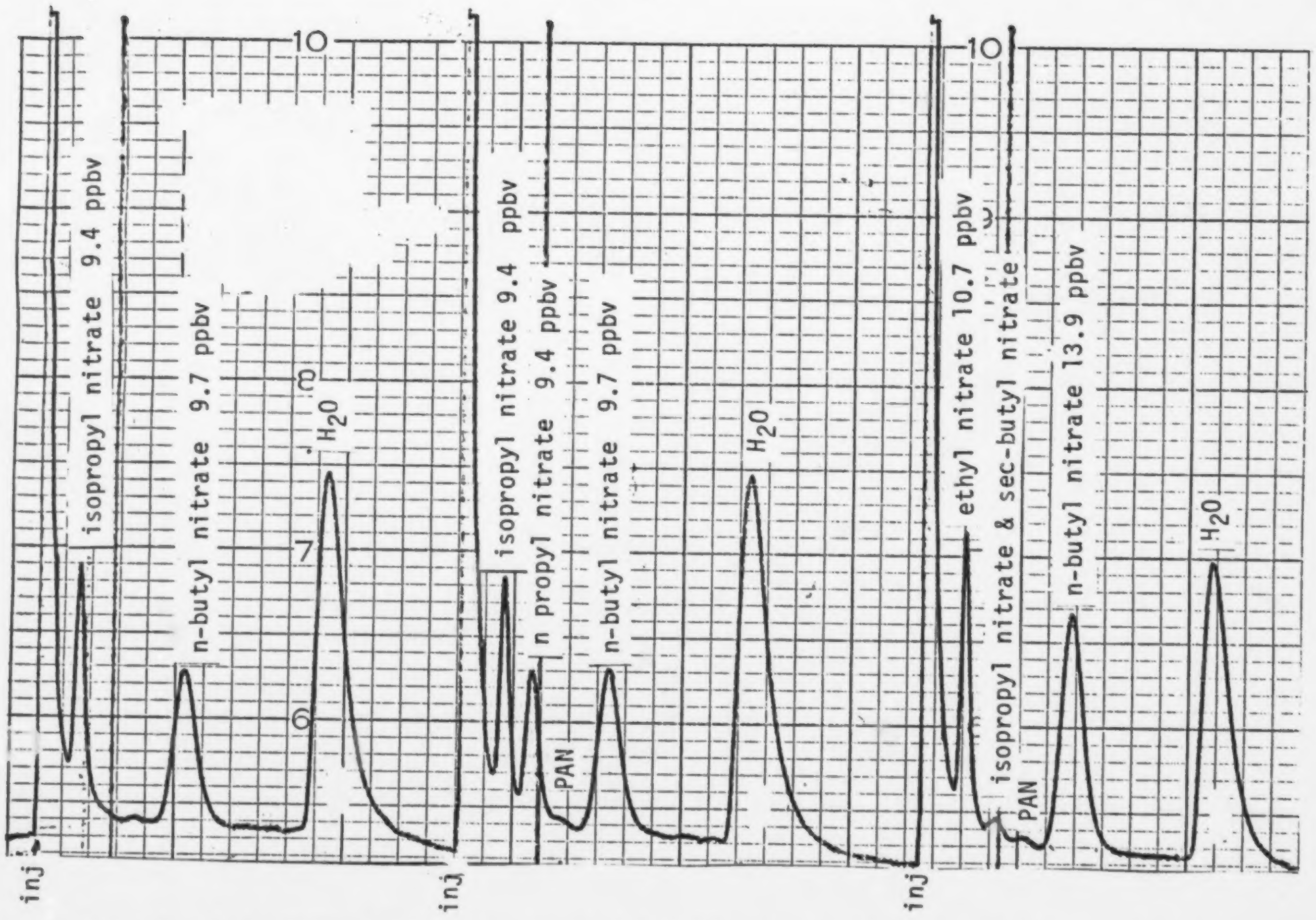

Figure 9. Detection of alkylnitrates with automated PAN GC, Varian 940 ECD. N_2 flow = 5 cc/min, oven and dector at 24.5^{o}C, standing current on 32x10^{-9} amps = 91% of full scale, chart = .1"/min, atten.= x32x10^{-10} amps.

MODIFIED MAST OZONE METER FOR MONITORING HNO_3

A modified Mast model 724-2 ozone meter as described by Miller and Spicer (1975) was used to continuously monitor gaseous nitric acid. The analyzer consists of a sample conditioning procedure and a microcoulomb cell utilizing a reagent adapted for sensing acids rather than oxidants.

The reagent contains KI and KIO_3 which reacts with acids:

$$HX + H_2O \rightarrow H_3O^+ + X^-$$

$$6\ H_3O^+ + IO_3^- + 5\ I^- \rightarrow 3\ I_2 + 9\ H_2O$$

At the cathode of the cell, a thin layer of H_2 (g) is produced by a polarization current: $2\ e^- + 2\ H^+ \rightarrow H_2$. When the voltage is first applied across the cell, the hydrogen layer builds to a maximum and the polarization current ceases. When I_2 is produced from the acid sampled, it reacts with the H_2: $H_2 + I_2 \rightarrow 2\ HI$. The removal of H_2 causes a repolarization current to reestablish equilibrium. Therefore, the current is directly proportional to the mass of acid sampled per unit time.

Figure 10 shows the general design of the sensor (microcoulomb) cell. The chemical solution for detecting acids is pumped at a constant rate into the cell. It then flows in a fine film down the electrode support E, (which contains many turns of a cathode wire C, and a single turn of a wire anode A) and is allowed to flow into a waste reservoir W. An air sample is pulled into the cell and comes into contact with the solution film on the electrode suport. A small potential is applied across the

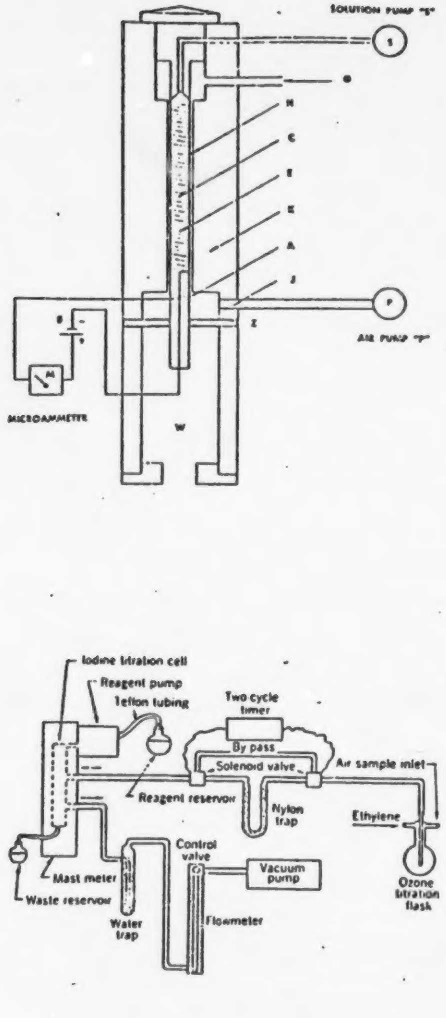
SOLUTION PUMP "S"
S
G
H
C
E
K
A
J
P
Z
AIR PUMP "P"
B
-
+
M
MICROAMMETER
W
Iodine titration cell
Reagent pump
Teflon tubing
Two cycle timer
By pass
Solenoid valve
Air sample inlet
Reagent reservoir
Nylon trap
Ethylene
Control valve
Vacuum pump
Mast meter
Waste reservoir
Water trap
Flowmeter
Ozone titration flask

Figure 10. Schematics of Mast electrochemical cell and configuration of entire microcoulombmetric instrument for measurement of gaseous HNO_3.

cell and the resultant current flow is converted to voltage by a current-to-voltage operational amplifier circuit. The method has a sensitivity to HNO_3 of about 5-10 ppb.

Note that this system will respond to O_3 and NO_2. Therefore, a sample pretreatment titration with ethylene is necessary to remove O_3. The sample is then alternately switched either through a nylon wool filter or around the nylon filter. The nylon wool filter selectively removes nitric acid without removing NO_2. The difference in the resultant voltage from the analyzer is proportional to the amount of gaseous nitric acid. A sample trace is shown in Figure 11.

Miller and Spicer (1975) discussed several discouraging observations while calibrating the modified Mast nitric acid analyzer: 1) the acid will significantly absorb then desorb from new Teflon sampling tubing, 2) at low to moderate humidities nitric acid persists in the gas phase, but at somewhat higher humidities the acid seems to initially cluster as aerosols as indicated by a condensation nuclei counter, and 3) because of a "memory effect", at least five minutes are required for alternate cycles.

CHEMILUMINESCENCE METHOD FOR NITRIC ACID MONITORING

Several research groups had reported various responses of commercial chemiluminescent NO_x analyzers to HNO_3, ranging from 0% to 100% response. The reason for this wide range was due to the different types of catalyst used to reduce NO_2 to NO. Joseph and Spicer (1978) reported on a method to measure nitric acid utilizing chemiluminescence and a molybdenum catalyst system. They used the same nylon wool filtering arrangement that was used on the modified Mast analyzer. It was found that the method responded 100% to HNO_3 and compared well with the Mast system

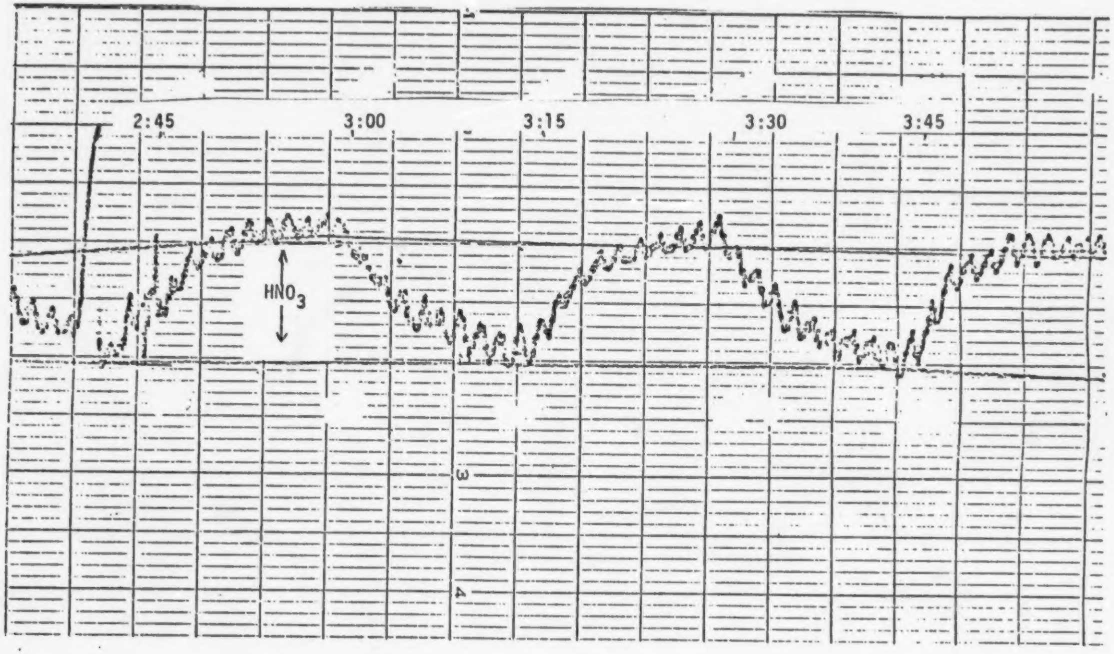

FIGURE 11. Example of signal trace from modified Mast microcoulombmetric method for gaseous HNO_3 monitoring.

which had previously been successfully compared with a Fourier transform spectroscopy-infrared system.

A molybdenum catalyst converter was purchased in 1978 by UNC and connected in series with the sample line leading directly to the photomultiplier tube of a Bendix chemiluminescent NO_x monitor. A switching nylon wool filter arrangement was used similar to that used in the Mast nitric analyzer. To minimize possible sample line losses, the molybdenum catalyst was placed directly under the chamber with the nylon filter system on the inlet. Less than 24 inches of sample line was exposed to HNO_3. The sample air in the line from the catalyst to the NO converter (~30 feet) contained only NO. This system produced a trace similar to the Mast system: the output alternating between total nitrogen and total nitrogen minus HNO_3. A sample trace is shown in Figure 12.

CALIBRATION OF NITRIC ACID ANALYZERS

Calibration was at first attempted (1977) by carefully measuring the response of the analyzer to NO_2 and O_3 (no ethylene used). Response factors of 2, 20 and 10 microamperes per ppm for NO_2, O_3 and HNO_3 were reported by Miller and Spicer. HNO_3 was therefore "calibrated" by observing the response of the analyzer to NO_2 and O_3, and then scaling with the relative HNO_3 response factor reported by Miller and Spicer. This, of course, was not a direct calibration technique, and it was necessary to assume that the reported response factors were accurate. Spicer and Miller (1976) suggested that the analyzer be calibrated with static test concentrations in Teflon bags. These were generated from purified nitric acid which was prepared under a high vacuum. During the initial check-out of the UNC Mast system, the

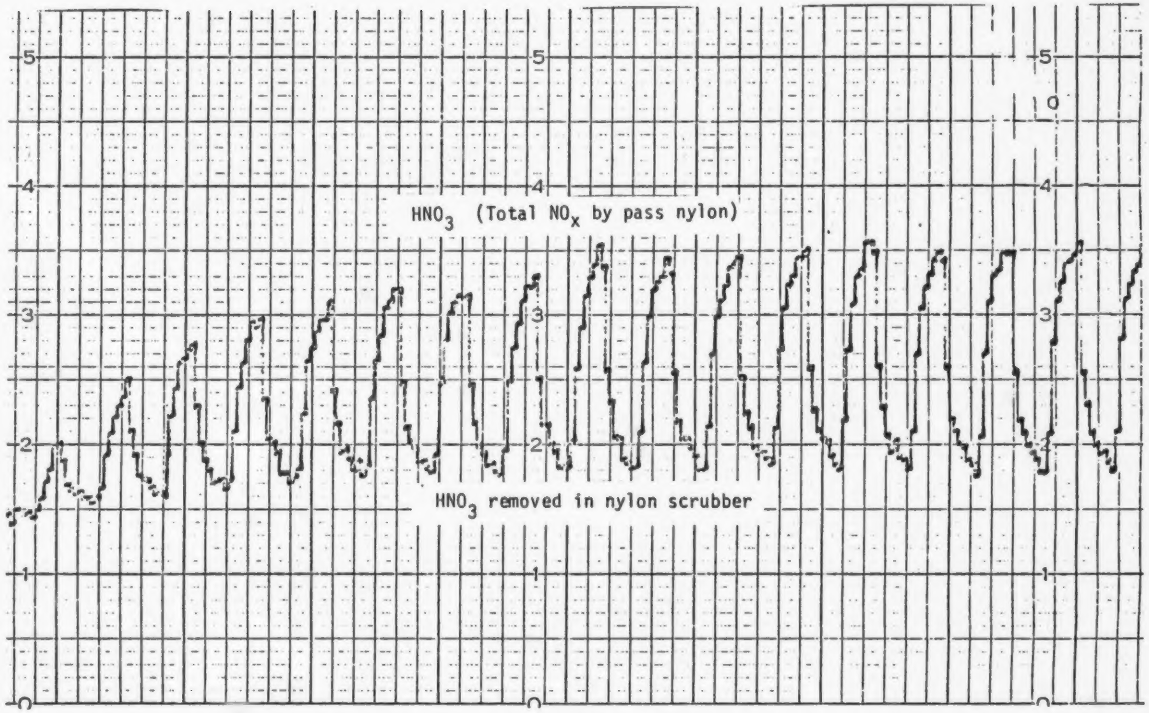

FIGURE 12. Example of signal trace from molybdenum catalyst chemiluminescence method for gaseous HNO_3 monitoring.

instrument was allowed to sample from a Teflon bag in which enough concentrated HNO_3 was injected to obtain a 0.2 ppm concentration. No nitric acid was measured. The bag was heated and still no nitric acid was observed. Finally enough nitric acid was injected to produce a 20 ppm concentration. The analyzer did respond, taking almost 60 minutes to reach a maximum response of 0.8 ppm. When taken off the bag and allowed to sample room air, about fifteen minutes were needed for the response to drop to zero. It was concluded that a static bag calibration source was unsatisfactory because nitric acid has a tendency to absorb and desorb from "clean" Teflon. Previously, Gantner had used HCl gas to calibrate the Mast HNO_3 system. Known concentrations of HCl were also difficult to maintain in a bag system, presumably because of similar wall problems.

It was concluded that a continuous source of HNO_3 would be necessary to minimize these effects by allowing equilibrium of the surfaces involved thereby insuring an accurate response and calibration to HNO_3. A generator was assembled using a diffusion method, described by Nelson (1977). The design is relatively simple (Figure 13). It employs a Teflon sealed flask containing concentrated HNO_3 and a capillary tube. The exposed end of the capillary tube conducts vapor phase nitric acid between the generator flask and a mixing chamber. Experimentation led to a capillary size, temperature and flow produced an acceptable range of HNO_3 concentrations. A 6 cm x 0.5 mm capillary diffused at a rate ($30-40^{o}C$) such that a one to four liter per minute flow rate would yield 0.35 to 0.45 ppm of nitric acid. The generator was insulated and temperature controlled.

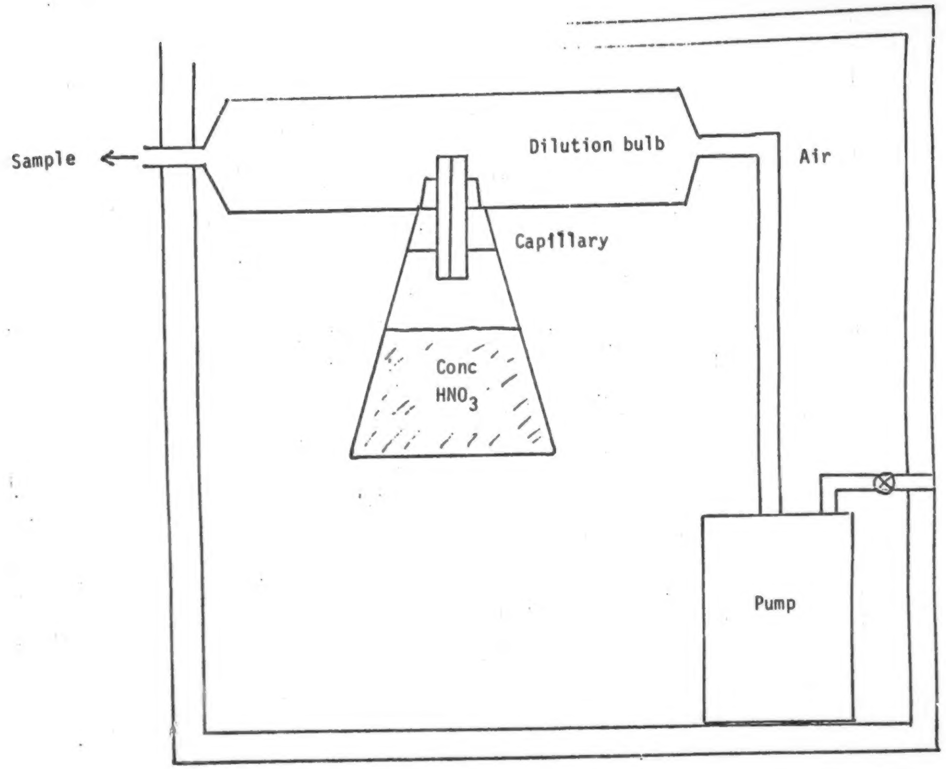
Sample
Dilution bulb
Air
Capillary
Conc
HNO_3
Pump

FIGURE 13. Schematic of gaseous HNO_3 generator.

The generator was calibrated by utilizing the Spicer bubbler technique (1977) for nitric acid. This method utilizes the chromotropic acid reagent for analysis of nitrates developed by West (1966). A fritted bubbler was filled with 10 ml of 0.03 N NaOH and used to collect a portion of the output of the generator, while the Mast or chemiluminescence system monitored the generator simultaneously. The Mast system would agree well as long as it was "acting" properly. The calibration curve used for the bubbler analysis is shown in Figure 14. To insure that either nitric acid analyzer was working properly, the generator was kept near the analyzer, even when the instrument was under the chamber.

ANALYSIS AND CALIBRATION OF H_2O_2

In 1977 gas phase hydrogen peroxide data were taken at UNC by colorimetric analysis using titanium tetrachloride solution and applying Lambert-Beers law to concentrations obtained from standards. The lowest concentration that can be measured accurately with this technique is 10 ppb hydrogen peroxide. More recently Kok et al. (1978) have developed a chemiluminescent method for the determination of hydrogen peroxide with a reported sensitivity to concentrations as low as 0.5 ppb. Since ambient hydrogen peroxide concentrations and the concentrations developed from photochemical smog in ambient atmospheres are found to be less than 25 ppb, this technique provides an extremely useful method for quantifying hydrogen peroxide production in our experiments.

Implementation of this technique was done in close collaboration with Messrs. Bruce Gay, Jr. and George Namie at the EPA Environmental Research Lab at EPA. Samples were collected by bubbling air through a midget impinger (in an ice bath) for approximately 10 minutes at about 2 liters per

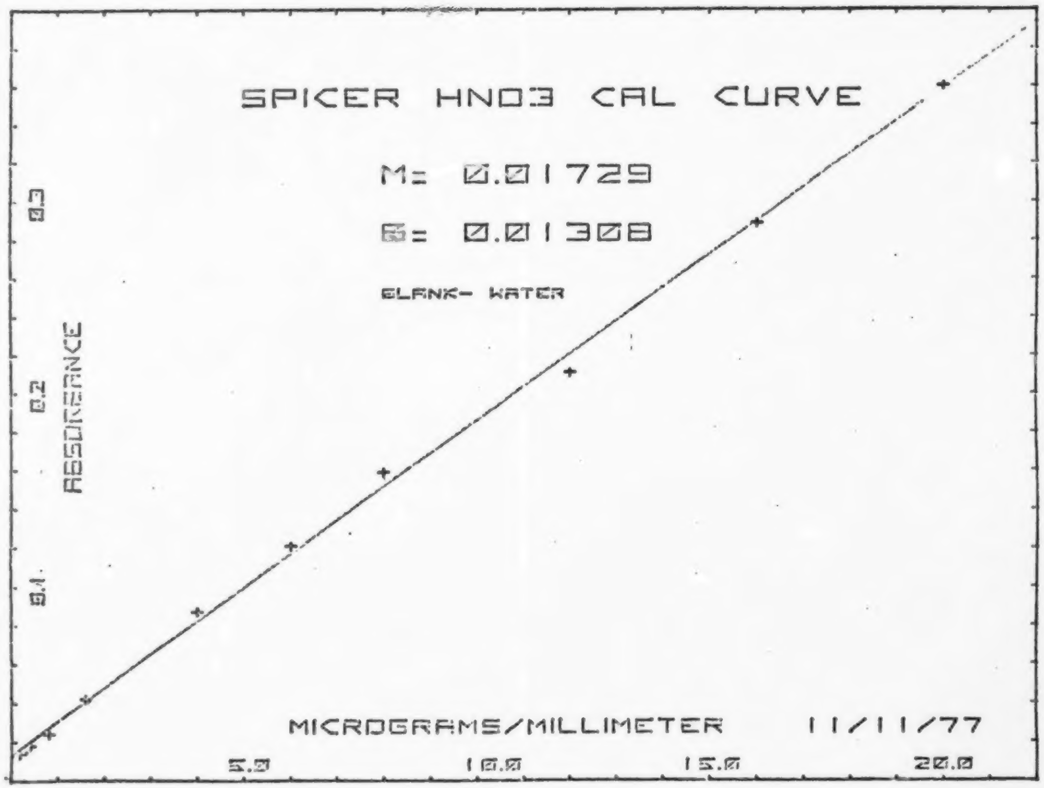

FIGURE 14. Calibration curve for Spicer method of HNO_3 analysis.

minute. This sample solution is mixed with alkaline (12.8 pH) luminol solution and copper (II) nitrate-sodium hydroxide solution in a small glass spiral reaction vessel at a constant flow rate provided by a technicon peristaltic pump. The luminol is oxidized, light is emitted and the light is detected by a photomultiplier tube.

We have standardized fresh 0.1% hydrogen peroxide solution by two titration methods: 1) $KMnO_4$ reduction titration, 2) standard iodometric titration with KI. Note that the second titration is extremely slow and it is necessary to wait about one hour between mixing the H_2O_2 and KI solutions and titrating. These two methods are in good relative agreement. Serial dilutions with hydrogen peroxide-free water indicate that low concentrations of hydrogen peroxide can be prepared with reasonable certainty from higher concentration hydrogen peroxide samples. We have observed an extremely linear response from less than 1 ppb to 100 ppb.

Our present ability to detect ppb levels of dry calibration samples of H_2O_2 (dew pt $0^{o}F$) is indicated in Figure 15. We have noted a significant positive O_3 interference to this method when O_3 values exceeded 0.1 ppm in the sample air. This interference was reproduced at EPA when a comparison between the EPA and UNC systems was made at EPA. Dr. Kok indicated that perhaps this interference was due to impure luminol.

Attempts to inject high concentrations (0.1-1 ppm) of H_2O_2 and measure these levels in the chambers was not successful. Extreme chamber drying appears to be necessary to maintain H_2O_2 in the gas phase. During smog chamber runs in which H_2O_2 was monitored, concentrations as high as 5 ppb were observed.

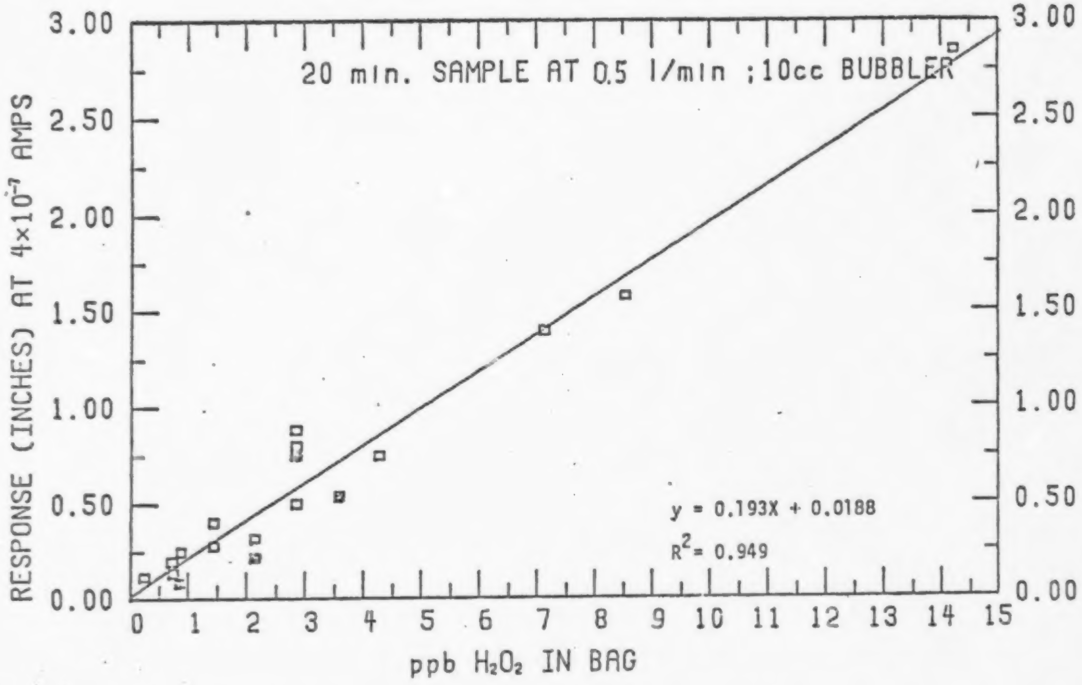

Figure 15. Response of H_2O_2 instrument to standard concentrations of H_2O_2 in dry air.

APPENDIX C

MAGNETIC TAPE FORMAT

The experimental data sets are written on the tape as separate character files. The tape is unlabeled, 1600 bpi, with a logical record length of 80 bytes (cardimage), and a block size of 6400 (i.e., 80 cardimages per block). The character code is IBM EBCDIC.

Each run file is divided into logical sections. The end of each logical section is marked by the occurrance of five nines in columes one to five (i.e., 99999).

The first logical section is usually a documentation section that includes the run date, type run, initial conditions and comments. Some early runs do not include documentation.

The next section is the continuous data. The first record contains the names of the species in the same fields as the data. Data from the two sides are interleaved, usually one record occurring for each side. The time is designated by a field that has two digits for each subfield; year, month, day, hour, minute, second. The two sides are designated by an R or B in column 10. This section is terminated by five nines in columns one to five.

Additional sections are used, as needed, to provide other data. Each section starts with a record of names and is followed by numerical data. Each section ends with five nines.

Nitrogen-containing species and ozone data are in ppm; hydrocarbon data (including organic products) are in ppm C; PAN data are in ppmV prior to 1980 and are in ppbV after 1980. Temperature and dewpoint are in Fahrenheit. Total solar radiation data are in cal-cm^{-2}-min^{-1}; UV radiation data are in millical-cm^{-2}-min^{-1}.

Table C.1 A Partial Listing of a Magnetic Tape File Showing Logical Divisions

```
DATE: JUNE 15, 1980

TYPE: ALPHA-PINENE IN BOTH SIDES

INITIAL CONDITIONS  PPM(C)
          RED       BLUE
NO        0.169     0.177                              Documentation
NO2       0.044     0.042                                 Section
NOX       0.213     0.219
A-PINENE  1.22      0.80

TIME OF SUNRISE     5:54
INITIAL TEMP (F)    59.8
MAX TEMP (F)        96.0 (ESTIMATED FROM RALEIGH LCD)

COMMENTS:  DATA IN THESE RUNS HAVE NOT BEEN COMPLETELY VERIFIED
AND ARE SUBJECT TO CHANGE.
THE COMPUTER WENT DOWN AROUND 12:30.  THERE IS NO AFTERNOON TSR,
TEMP, OR DEW POINT DATA.  THE NOX AND O3 DATA ARE IN TWO PARTS.

SYMBOLS AND UNITS OF HYDROCARBONS AND PRODUCT COMPOUNDS:
COMPOUND        SYMBOL       UNITS
A-PINENE        APINEN       PPMC
FORMALDEHYDE    FORM         PPMC
CO              CO           PPMC
PAN             PAN          PPBV
99999                                                  Terminator
                   NO          NO2          O3         Species Names
80 615 446 B       0.0051      0.0054       0.0158
80 615 450 R       0.0052      0.0050       0.0194
80 615 454 B       0.0048      0.0049       0.0165
80 615 458 R       0.0046      0.0050       0.0169       Data
80 615 5 2 B       0.0048      0.0244       0.0089
80 615 5 6 R       0.1669      0.0190       0.0003
80 615 510 B       0.1752      0.0168       0.0003
80 615 514 R       0.1659      0.0213      -0.0001
80 615 518 B       0.1765      0.0463       0.0002
80 615 522 R       0.1688      0.0443       0.0004
80 615 526 B       0.1775      0.0405       0.0000
80 615 530 R       0.1692      0.0450       0.0000
80 615 534 B       0.1759      0.0423       0.0001
80 615 538 R       0.1685      0.0445       0.0002
80 615 542 B       0.1763      0.0424       0.0002
80 615 546 R       0.1677      0.0450       0.0004
80 615 550 B       0.1756      0.0425      -0.0001
80 615 554 R       0.1681      0.0448       0.0002
80 615 558 B       0.1749      0.0418       0.0002
80 615 6 2 R       0.1675      0.0453       0.0005
80 615 6 6 B       0.1749      0.0420       0.0002
80 615 610 R       0.1676      0.0458       0.0004
 .   .   . .         .           .            .
 .   .   . .         .           .            .
 .   .   . .         .           .            .
```

Table C.1 (continued) A Partial Listing of a Magnetic Tape File

```
8006150730 R        1.1700
8006150800 B        0.7000                        Data
8006150900 B        0.5700
8006150930 R        0.7700
8006151000 B        0.3800
8006151030 R        0.2700
8006151100 B        0.2200
8006151130 R        0.1400
8006151200 B        0.0400
----------------------------------------------------------------
99999                                           Terminator
----------------------------------------------------------------
                    FORM                        Names
----------------------------------------------------------------
8006150745 R        0.0050
8006150757 R        0.0060
8006150803 B        0.0080
8006150813 B        0.0090
8006150835 R        0.0090
8006150850 R        0.0110
8006150900 B        0.0090                        Data
8006150922 B        0.0150
8006150940 R        0.0260
8006150948 R        0.0310
8006151010 B        0.0260
8006151021 B        0.0300
8006151033 R        0.0470
8006151050 R        0.0540
8006151100 B        0.0370
8006151122 B        0.0380
8006151138 R        0.0660
----------------------------------------------------------------
99999                                           Terminator
----------------------------------------------------------------
                    CO                          Names
----------------------------------------------------------------
8006150605 B        0.4000
8006150620 B        0.4000
8006150635 R        0.3880
8006150650 R        0.3750
8006150705 B        0.3880                        Data
8006150720 B        0.4000
8006150735 R        0.3630
8006150750 R        0.3750
8006150805 B        0.4250
8006150820 B        0.4000
8006150835 R        0.3630
8006150850 R        0.3500
8006150905 B        0.4000
8006150935 R        0.3630
8006150950 R        0.3880
8006151005 B        0.4250
8006151020 B        0.4000
8006151035 R        0.4000
8006151050 R        0.4000
8006151105 B        0.4000
----------------------------------------------------------------
```

APPENDIX D

MICROFICHE FORMAT

Each microfiche holds 265 pages of computer output arranged as 24 columns of 15 pages. Text is read down the first column and then down the second column and so forth. The microfiches are numbered sequentially and each fiche has row and column markers. The first fiche is an index listing similar to Table 4, listing the fiche number, the column number, and the row letter at which the listing from each run begins.

Two types of listings are given: the first 50 runs have an expanded format including line-printer plots of the data; the remaining 70 runs are magnetic tape images without plots. The magnetic tape image format is described in Appendix C. The expanded format listing is similar to the magnetic tape format; because of its formatting, however, it is easier to read. It usually begins with a DOCUMENTATION section, followed by a RED and BLUE listing of the continuous data every four minutes, and finally by the listings of hydrocarbon data. Some early runs do not have a documentation section.